UNIVERSITY OF LONDON

A HIGH-RESOLUTION RECORD OF MID-HOLOCENE CLIMATE CHANGE FROM DISS MERE, UK.

by

Ian Bailey

Thesis submitted in fulfilment of the requirements for the degree of Doctor of Philosophy

Department of Earth Sciences
University College London

March 2005

ProQuest LLC
789 East Eisenhower Parkway
P.O. Box 1346
Ann Arbor, MI 48106-1346

Abstract

Given that recent anomalous positive values in the North Atlantic Oscillation (NAO) may be related to anthropogenic forcing, the need exists to document more fully NAO evolution in palaeoclimate records. To this end, this thesis investigates whether NAO-type variability can be identified in biochemical varves of mid- to late-Holocene age from a lake sediment sequence in Diss Mere, UK.

The varved record was examined using a number of cutting-edge technologies, with an emphasis placed on the time-series analysis approach to determine spectral properties of high-resolution palaeo-environmental time-series constructed from laminae-thickness measurements (a palaeoproductivity indicator) and XRF core-scanning for inter-annual records, principally, of elemental Ca-abundance, a proxy for summer temperature. For comparison, a low-resolution record of organic carbon burial was taken to record change in winter temperature. The in-situ chemical, biological and clastic constituents of individual varves were also examined using SEM-BSEI to investigate the annual cycle of sedimentation and variety of varve-fabric types.

The results indicate that varve deposition is characterised by statistically significant interannual and bidecadal cycles that correspond to periodicities found in instrumental and other proxy records of the NAO. A shift from interannual to bidecadal cycles after 4000 Cal. BP is coincident with a rapid transition at Diss towards decreased seasonality during the late-Holocene that is also reflected in a distinct change in varve character and phytoplankton dynamics. This appears comparable, if not analogous, to the evolution of the modern NAO where a dominance of decadal variability since the 1950s is coincident with a tendency towards an NAO positive. It is hypothesised that change at 4000 Cal. BP and seasonality cycles thereafter have implications for the degree of longer-term predictability that may exist in the mean state of the NAO due to forcing by solar activity and orbital precession.

CONTENTS

FIGURES

TABLES

Acknowledgements

I would like to acknowledge the following: Sylvia Peglar and Steve Boreham for provision of a lot of the core material used in this study. To Steve, again, for allowing me use of the Godwin Laboratory's coring equipment and for discussions concerning the origin of Diss Mere. Thanks are due to the Environmental Change Research Group at University College London, especially Ric Batterbee and Ewan Shilland, for the lending of boats, coring platform, Livingstone corer and guidance in field sampling techniques. I would like to thank the following people for their generosity in what were sometimes very cold East Anglian field-trips: Steve Boreham, Ewan Shilland, Heather Cheshire, Rupert Green, Michael Green, Alexandra Nederbragt, Juergen Thurow and Luke Wooller. Luke provided expertise in global positioning satellite techniques; GPS equipment was loaned from the Vulcanology Group at the Open University.

I am grateful to Alan Kemp at Southampton Oceanography Centre for the use of their SEM and I am indebted to Richard Pearce for his expertise regarding SEM Backscatter Electron Imaging. I also thank Sandra Nederbragt for her help with spectral analysis and Ian Wood for running samples for XRD analysis.

Thanks are offered to Frank Lamy and Ursula Röhl and all those at the IODP Bremen core repository for their technical guidance in the use of the XRF Corescanner. My stay in Bremen was financed by a Palaeostudies grant, Contract No.: HPRI-CT-2001-0124. Also, special thanks are reserved for my supervisor Juergen Thurow. Finally, I would like to thank Heather, Rupert and Adrian for listening to my countless stories, ideas and 'interesting facts' concerning Diss Mere. Without your friendship, knowledge and driving skills, I wouldn't have got very far.

This PhD was supported by NERC studentship NER/S/A/2000/03967.

A high-resolution record of Mid-Holocene climate change from Diss Mere, UK.

1. Introduction

This chapter presents the rationale and objectives for this study, and a summary of relevant previous work.

1.1. Rationale

This thesis considers the potential for palaeoclimate studies of biogenic (organic) varved sediment of mid-Holocene age (2500 to 5000 Cal. BP) from Diss Mere, a hardwater lake located in central East Anglia, UK (Fig. 1.1). Studies of lacustrine varves are important as they contain highest-resolution records of regional climate change that are useful to address natural climate variability at a spatial- and temporal-scale that is relevant to human societies. It should be a major aim to elaborate such information along transects throughout Europe, cf. the European Lake Drilling Programme (Zolitschka & Negendank, 1999). Improvements in the overall database, especially in northern Europe, are crucial for understanding the regional impacts of the North Atlantic climate system, for example, the North Atlantic Oscillation (NAO).

The NAO is the dominant mode of winter climate variability in the North Atlantic region, controlling, for example, regional trends in surface winds, temperature and precipitation over Europe and North America (Wallace & Gutzler, 1981; Moses *et al.*, 1987; Deser & Blackmon, 1993; Hurrell, 1995; Rogers, 1990; Ulbrich & Christof, 1999; Perry, 2000). It has far reaching socio-economic impacts (Koslowski & Loewe, 1994, 1999; Fromentin & Planquem, 1996; Kettlewell *et al.*, 1999). Records of the NAO, kept since 1874, are characterised by increased spectral power around periods of 20 and 7-8 years (Rogers, 1984; Hurrell & van Loon, 1997; Benner, 1999) and reconstructions of the NAO based on palaeoenvironmental data (such as, tree-ring chronologies, ice accumulation in Greenland and documentary data) as far back as 1400 A.D.

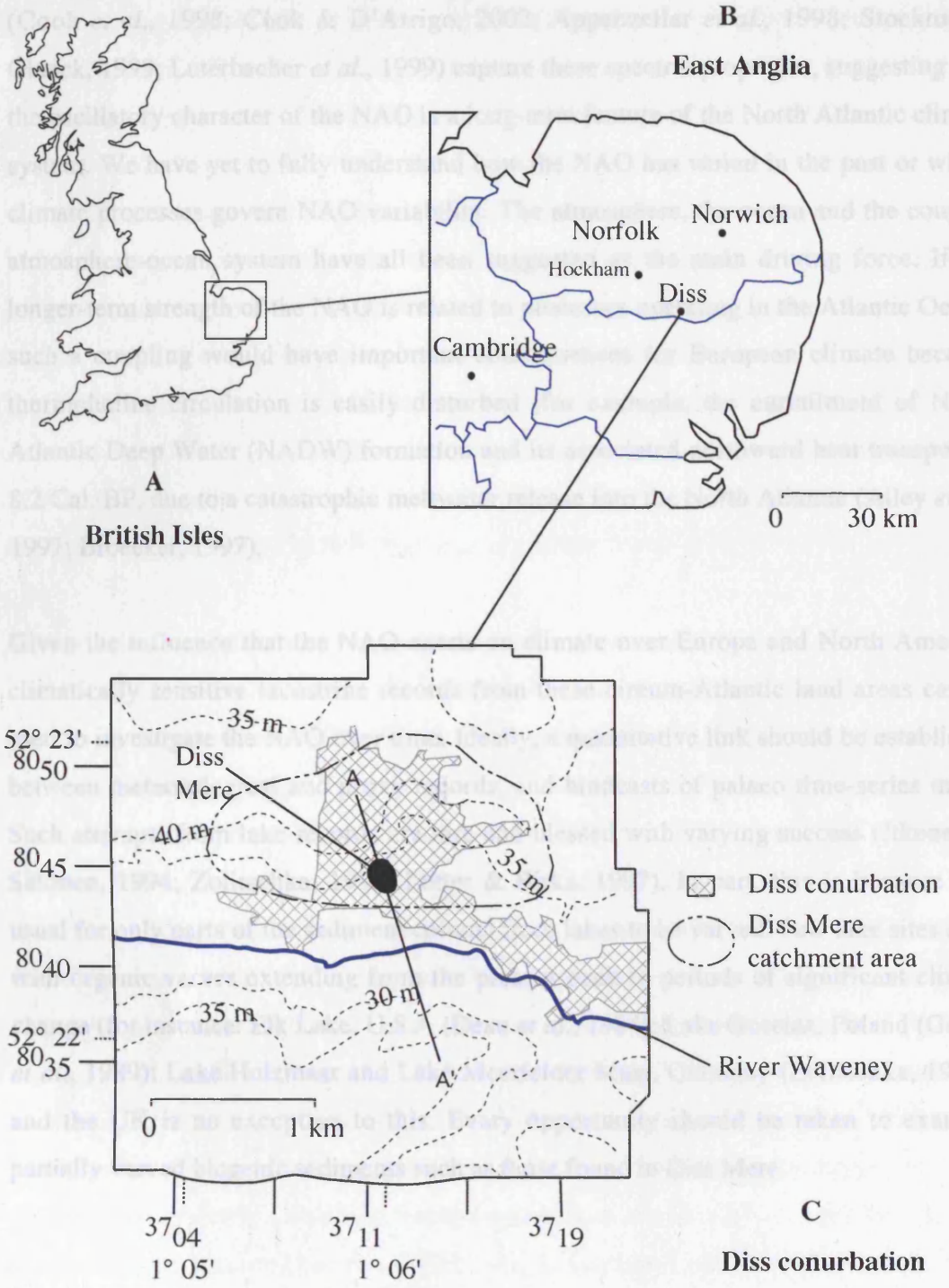

Fig. 1.1: Maps showing (A) location of East Anglia on the eastern side of Britain where the landmass crossed by the prevailing westerlies is broadest making its climate more continental than the rest of the British Isles; (B) location of Diss Mere within central East Anglia; (C) Diss Mere in the town of Diss and its likely catchment area.

(Cook *et al.*, 1998; Cook & D'Arrigo, 2002; Appenzeller *et al.*, 1998; Stockton & Glueck, 1999; Luterbacher *et al.*, 1999) capture these spectral properties, suggesting that the oscillatory character of the NAO is a long-term feature of the North Atlantic climate system. We have yet to fully understand how the NAO has varied in the past or which climate processes govern NAO variability. The atmosphere, the ocean and the coupled atmosphere-ocean system have all been suggested as the main driving force. If the longer-term strength of the NAO is related to processes operating in the Atlantic Ocean, such a coupling would have important consequences for European climate because thermohaline circulation is easily disturbed (for example, the curtailment of North Atlantic Deep Water (NADW) formation and its associated northward heat transport at 8.2 Cal. BP, due to a catastrophic meltwater release into the North Atlantic (Alley *et al.*, 1997; Broecker, 1997).

Given the influence that the NAO exerts on climate over Europe and North America, climatically sensitive lacustrine records from these circum-Atlantic land areas can be used to investigate the NAO over time. Ideally, a quantitative link should be established between meteorological and proxy records, and hindcasts of palaeo time-series made. Such attempts from lake records are rare and blessed with varying success (Itkonen & Salonen, 1994; Zolitschka, 1996; Lotter & Birks, 1997). In part, this is because it is usual for only parts of the sediment column from lakes to be varved. Few lake sites exist with organic varves extending from the present back to periods of significant climate change (for instance: Elk Lake, U.S.A (Dean *et al.*, 1984); Lake Gosciaz, Poland (Goslar *et al.*, 1989); Lake Holzmaar and Lake Meerfelder Maar, Germany (Zolitschka, 1998)) and the UK is no exception to this. Every opportunity should be taken to examine partially varved biogenic sediments such as those found in Diss Mere.

1.2. Previous work

Changes in varve composition, that is, in calcite and organic matter burial, offer a potentially valuable, high-resolution sedimentary record of environmental and climatic change (Kelts & Talbot, 1990). The potential of Diss Mere's laminated sediment to

preserve a high-resolution proxy climate record has been highlighted by a number of palaeolimnological studies, and basic data on sediment lithology, geochemistry, palynology (Peglar *et al.*, 1984; Peglar *et al.*, 1989; Peglar, 1993a, 1993b) and diatom content (Fritz, 1989) are available. Approximately 17 m of profundal sediment has been described, containing two intervals of calcareous organic-rich muds typical of Holocene sediment found in other hard-water lakes (Lotter 1989; Dean, 2002). Approximately 3 m of these muds are biochemically laminated consisting of regular couplets of a basal dark organic-rich and overlying pale carbonate lamina. Analysis of the individual lamina for their basic chemistry and biological (fossil pollen and chrysophyte) content demonstrates their seasonal nature, and that the couplets are varves (Peglar *et al.*, 1984). The contained pollen shows that the varves span approximately 3,000 years, covering the period 2500 to 5500 Cal. BP (Peglar *et al.*, 1989).

A literature search focusing on biogenic varves reveals that laminae similar to those found in Diss Mere have been described in Holocene sediments from a number of northern hemisphere lakes (O'Sullivan, 1983; Anderson *et al.*, 1985; Anderson & Dean, 1988; Zolitschka, 1996). These studies are mostly from North America, principal examples being carbonate-gyttja varves from Elk Lake, Minnesota (Bradbury *et al.*, 1993) and those from Fayetteville Green Lake, Cayuga Lake and Seneca Lake in New York State (Ludlam, 1967, 1969; Brunskill & Ludlam, 1969). Increasing numbers, however, have been discovered and investigated in Europe, for instance, Lake Baldeggersee, Lake Soppensee and Lake Zürich in Switzerland (Kelts & Hsü, 1978; Wehrli *et. al*, 1997; Lotter *et al.*, 1997a; Lotter *et al.*, 1997b; Lotter, 1989; Livingstone & Hadjas, 2001); the German volcanic lake, Lake Holzmaar (Zolitschka, 1992; 1996; 1998) and Mediterranean lakes, Lago Grande Di Monticchio, Southern Italy (Zolitschka & Negendank, 1996). Relatively few examples have been described from the UK, *e.g.* those from the glaciated region of East Anglia, Lopham Little Fen, Quidenham Mere (Tallentire, 1953; Horne, 1999) and Hockham Mere (Bennett, 1986).

A number of the investigations cited above have identified climate relevant periodicities using high-resolution time-series of lamina thickness (Renberg *et al.*, 1984; Anderson,

1992, 1993; Zolitschka 1992, 1996, 1998; Zolitschka *et. al.*, 2000; Vos *et. al*, 1997; Livingstone & Hadjas, 2001, Dean *et al.*, 2002b), geochemistry and mineralogy (Dean, 2002), and microfossils such as diatoms (Bradbury *et al.*, 2002). Results indicate that solar radiation is an important control on biogenic lacustrine sedimentation. A limited number of palaeoclimate studies report climate cycles similar to those described from modern indices of the NAO (Rogers, 1984; Hurrell & van Loon, 1997), *e.g.* Pliocene varves in Villarroya Basin, Spain (Muñoz *et al.*, 2002), late Pleistocene varves in Lake Albano, central Italy (Chondrogianni *et al.*, 1996) and recent varves in Loch Ness, Scotland (Cooper *et al.*, 2000). An increasing number of studies have shown that extreme events in the NAO may be linked to solar phenomena. These include, for instance, energetic solar eruptions, eruptive phases in the 11-yr sunspot cycle, and zero phases and extremes in the solar motion cycles (Landscheidt, 1990; Svensmark & Friis-Christensen, 1997; Svensmark, 1998; Bucha & Bucha, 1998; Marsh & Svensmark, 2000; Boberg & Lundstedt, 2002; Kodera, 2002, Thejll *et al.*, 2003). Traditionally, the NAO has been considered as a free internal oscillation of the climate system that is not subject to external forcing. These studies however, highlight the possibility that both the NAO and solar forcing are in some way linked.

1.3. Objectives of this study.

The main objective of this study was to determine whether NAO-type climate variability and its temporal evolution can be identified in biochemically varved lake sediment from the mid-Holocene. Variation in lamina thickness, for instance, reflects variation in seasonal primary productivity. Because productivity can vary with climate, time-series analysis may reveal the impact of the NAO on Diss Mere at interannual to interdecadal timescales. Varve counting provides a significant improvement to the tentative chronology provided by Peglar *et al.* (1989) for the period under study. An annually derived chronology for the mid-Holocene in East Anglia has important implications for the timing of regional palynological events, *e.g.* the *Tilia* decline in Britain. Study of the sediment fabric using scanning electron microscopy, principally, backscattered electron imagery (BSEI) will identify seasonal sediment fluxes and diatom seasonal succession

can provide independent confirmation of the annual nature of Diss Mere's laminae (as first described by Peglar *et al.*, 1984). The ecology of the diatoms in different lamina types also provides information about lake surface water processes and these diatom data, together with the detailed laminae analyses, provide an improved understanding of seasonal depositional processes operating in a northern hemisphere mid-latitude lake.

2. Physical setting

This chapter provides the physical background for the remainder of the thesis. First, the location and origin of Diss Mere are discussed. A summary is given of the lake basin hydrogeology and hydrography, and the climate of East Anglia is described.

2.1 Study site

Diss Mere is situated in the town of Diss in the heart of East Anglia (31 N 37116 80450; Fig 1.1). Diss is surrounded by rich farmland and has been established as an active market town and agricultural centre since Anglo-Saxon times (~500 AD). The lake has a surface area of 0.032 km^2, with a roughly oval outline and a maximum water depth of about 6 m. The lake is closely bordered by land rising to the west, north and east and has only a small catchment (~1.5 km^2). It has virtually no surface inflow or outflow.

2.2 Origin of Diss Mere

The lake sits in the northern margin of the Waveney Valley, an east-west trending buried glacial channel (BGC) that follows the course of former glacial meltwaters (Woodland, 1970), carved out of Upper Chalk during the Anglian glaciation (~450,000 yrs ago). It contains some of the most substantial developments of outwash silty clays and subordinate sand and gravel (~50 m at its thickest) deposited during the Lowestoft phase of glaciation. The geology in which the lake sits is complicated. The Lowestoft Till, which is responsible for the subdued and broad plateau landscape characteristic of the region, forms the slope to the north and the remainder of the depression is encircled by alluvium and peat deposits associated with the meandering River Waveney. Construction of a stratigraphic cross-section, trending north-south through Diss Mere and the Waveney Valley (using British Geological Survey 1:50 000 map (Sheet 175, 1986) and borehole data (Environment Agency, UK 2001) shows that at depth, lake sediment is in contact with the BGC sediment and Chalk (Fig. 2.1).

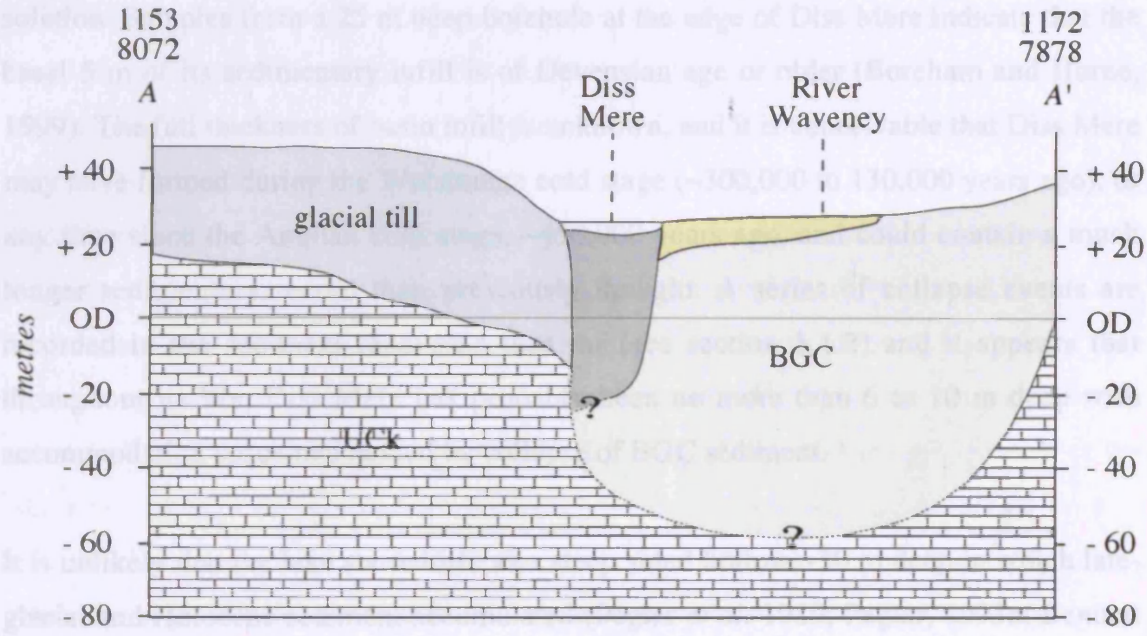

Fig. 2.1: Cartoon of stratigraphic cross-section N-S through Diss Mere and the Waveney Buried Glacial Channel (BCG).
UCk = Upper Chalk. Horizontal scale 1 : 20,000. Vertical scale x 15.

The geological and geomorphological setting described is consistent with the collapse of BGC sediment into Chalk solution cavities along the base of the steeply dipping contact between the channel infill and Chalk bedrock (Boreham & Horne, 1999). The formation of the majority of hollows and embayments in East Anglia and Fenland has been attributed to the most recent period of backwearing and other thermokarst processes in the late Devensian (last cold stage) (West, 1991). The late Devensian is cited as a time of high water-level in East Anglia (West, 1991; Boreham & Horne, 1999) and the combination of a cold-climate and a high water-table makes for enhanced Chalk bedrock solution. Samples from a 25 m deep borehole at the edge of Diss Mere indicate that the basal 5 m of its sedimentary infill is of Devensian age or older (Boreham and Horne, 1999). The full thickness of basin infill is unknown, and it is conceivable that Diss Mere may have formed during the Wolstonian cold stage (~300,000 to 130,000 years ago), or any time since the Anglian cold stage, ~450,000 years ago, and could contain a much longer sedimentary record than previously thought. A series of collapse events are recorded in the sediment recovered thus far (see section 5.1.2) and it appears that throughout its life, Diss Mere has probably been no more than 6 to 10 m deep with accommodation space maintained by collapse of BGC sediment.

It is unlikely that the lake started life as a steep sided hollow ~30 m deep in which late-glacial and Holocene sediment accumulated (Peglar *et al.* 1989; Peglar, 1993a; Bennett *et al.*, 1990). Sparks (1971) suggests that the dense jointing patterns and low physical strength of Chalk bedrock would limit the size of solution-collapse hollows. Sperling *et al.* (1977) and Edmonds (1983) note that solution hollows usually occur where thin deposits overlie Chalk bedrock, as caverns are more stable in that they grow to a greater size before collapsing (Thomas, 1954). However, it is unlikely that the relatively young and unconsolidated BGC sands and gravels would be capable of forming a roof stable enough to allow extensive cavern development beneath the BGC (cf. Thomas, 1954). Indeed, borehole collapse is a serious problem for engineers sinking water-wells into BGCs in East Anglia, because the infill can be fine-grained, uncemented and runs freely. In addition, it is probable that any deep hole situated in south-facing slope of the Waveney Valley during the Devensian Late Glacial would have been subject to intense

periglacial processes and infilled rapidly. The only other large-scale Chalk solution hollow described in the UK is from Slade Oak Lane, Buckinghamshire (Gibbard *et al.*, 1986). Here a 500 m wide and ~35 m deep hollow has apparently developed because a thin cover of Palaeogene sediments of sufficient induration provided a stable roof for the development of a large cavern in chalk bedrock during the Anglian. In contrast to Diss Mere's sediments, the majority of its thick infill was the product of solifluction processes and accumulated under cold climate conditions (during the late Anglian and early Wolstonian). Several other features in the Waveney Valley, Lopham Fen [TM 055 800], Royden Fen [TM 100 797] and Bressingham Fen [TM 065 803], may also have evolved out of subsidence and Chalk dissolution. A resistivity survey of Lopham Fen implies that it forms part of a large depression (Simon Wood, *pers. comm.*). Sediment cores from Little Lopham Fen (Tallantire, 1953) [TM 0425 7940] bear a striking resemblance to the profundal stratigraphy of Diss Mere described here (section 5.1.2) and provide evidence of a series of collapse events throughout the Late Glacial and Holocene (West, *pers. comm.*). No studies have directly attempted to explain why intermittent solution is focused at these locations, although this may be connected to the complex interaction of the hydrology of the Waveney Valley and change in strike of the Chalk bedrock.

A zone of high transmissivity exists along the base of the BGC in the Waveney Valley (Simon Wood, *pers. comm.*). Woodland (1946) and Ineson (1962) suggest that this might be connected to preferential solution along secondary fissures in the Chalk during longer-term natural circulation of groundwater. High permeability has also been shown in the region to be concentrated in the Chalk where it sits above -10 m OD (Foster & Robertson, 1977). The fact that boreholes on the edge of the BGC yield poor drawdown characteristics suggests that this zone of enhanced Chalk permeability has been eroded during BGC formation (Foster & Robertson, 1977). By implication, it has been suggested that the development of high permeability along the base of the BGC must in part pre-date BGC formation. Rhoades & Sinacori (1941) have demonstrated that permeability enhancement tends to occur via solution in both confined and unconfined Chalk aquifers due to topography, for example, along river valleys. Evidence that the

secondary solution fissures are usually concentrated at the water table or within the zone of seasonal water-table fluctuation is also provided by Foster & Milton (1974) and Owen & Robinson (1978). The distribution of outwash deposits in the Waveney Valley suggests that its drainage system was an important pathway for meltwaters at the close of the Anglian stage. It is plausible that a zone of high permeability may have first developed in the proto-Waveney Valley along the line of sub-glacial melt waters before the confining strata of the BGC were laid down, a theory similar to that postulated by Morel (1980) for the Chalk aquifer in the Upper Thames Valley. Rhoades & Sinacori (1941) assume that prior to fissure development Chalk behaves as a perfectly homogeneous and isotropic medium. In reality, fissure connectivity in chalk is highly anisotropic, due to both structural and lithological circumstances and the change in strike of the Upper Chalk in this area may have aided preferential solution of Chalk.

2.3 The Modern Basin

2.3.1 Basin hydrogeology

No studies have been undertaken on the hydrology of Diss Mere. However, we can state that Diss Mere is a freshwater, temperate, hardwater lake. It sits at an elevation of 69 m, and is located 7 km east of a major drainage divide (source of both the River Waveney and Little Ouse). Diss Mere's location is somewhat anomalous as the topographic contours do not reveal it to be part of any obvious surface water system and it is unclear how much modern surface drainage enters the lake. The water level in the lake correlates well with the semi-confined potentiometric head in the Chalk (*pers. comm.* Simon Wood) and the contribution from groundwater is probably large. However, it is not certain whether the lake's hydraulic continuity is principally with the BGC lithologies, or if it is fed by the Chalk. If hydraulic continuity is principally with granular sand and gravel lithologies the hydraulic response is likely to be well dampened. From pumping test data (Feather Factory Bore, 1978 [TM 1148 7955]), there seems to be very little evidence of direct connection between the lake and drift aquifer, and the Chalk. The cone of influence for the Feather Factory Bore extends strongly east-west on all the tests

and the shallow monitoring bores nearby respond to recharge signals but nothing else (Simon Wood, *pers. comm.*). The lake water chemistry is characterised by high conductivity (582 $\mu S\ cm^{-1}$), high alkalinity (3.86 meq l^{-1}) and high concentration of nutrients (total phosphorus, 300-μg^{-1}). The chemical composition of groundwater from the Chalk at Moore Nursery borehole, Bressingham (1978) (Table 2.1), which is about 3 km west of Diss, is characteristic of ground water in the region. The salinity (conductivity) of the lake water is about nine-tenths that of ground water from this locality, which suggests that, on average, about only one tenth of the lake's water results from direct precipitation and runoff from soils, sources that are more dilute than groundwater. Given the composition of the local bedrock and groundwater analyses from the Moore Nursery borehole, the water of Diss Mere is likely to be a dilute solution of calcium bicarbonate. Calcium appears to be the dominant cation, and alkalinity will be almost entirely bicarbonate. Measurable traces of iron and manganese were probably taken up by water infiltrating the drift.

Table 2.1: Typical analyses of groundwater from the Chalk in the Diss region (from Environment Agency, Ipswich Office, Suffolk, 1978)

Site	Moore nursery, Bressingham [TM 0650 8080]
Electrical conductivity ($\mu S\ cm^{-1}$)	621
Alkalinity as $CaCO_3$ (mg/l)	310
Potassium (mg/l)	3.7
Sodium (mg/l)	21
Dissolved P (mg/l)	0.2
Chloride (mg/l)	24
Total Iron (mg/l)	1.39
Total Manganese (mg/l)	0.1

2.3.2 Basin hydrography

Fig. 2.2 shows the bathymetry of the lake and Table 2.2 lists characteristic hydrographical parameters. The results of the bathymetric survey show that the lake has a maximum depth of 6.05 m, and a volume of 0.0016 km^3. The effective catchment area for surface drainage to the lake is 1.5 km^2, which is small relative to the lake surface area (0.032 km^2). Today, just under half the catchment is covered by urban development, the remainder is used for agriculture. The large volume of Diss Mere in relation to its relatively small watershed means that water-column mixing (that is, light and nutrient availability) is the dominant control on limnology, and not catchment processes such as terrestrial runoff. Today, the lake is meromictic - that is, it is permanently stratified - and rarely experiences complete water-column overturn. Meromictic lakes are best described as two lakes, the one overlying the other, but kept apart by a strong density gradient. Circulation occurs in the upper lake, the mixolimnion, down to its false bottom at the level of the density gradient at the chemocline. The underlying stagnant lake is called the monimolimnion. It has no contact with the overlying mixolimnion or atmospheric oxygen. A special feature of meromictic lakes is that, usually, stratified communities of blue-green bacteria are permanently associated with the chemocline.

Table 2.2: Characteristic hydrological parameters for Diss Mere, 2004 (this study)

Lake parameters	
Elevation	69 m above sea level
Average depth	3.9 m
Maximum depth	6.05 m
Lake volume	0.0016 km^3
Lake surface (L)	0.032 km^2
Catchment area (C)	1.5 km^2
Ratio z (L/C)	0.021
Estimated residence time	100 to 200-years

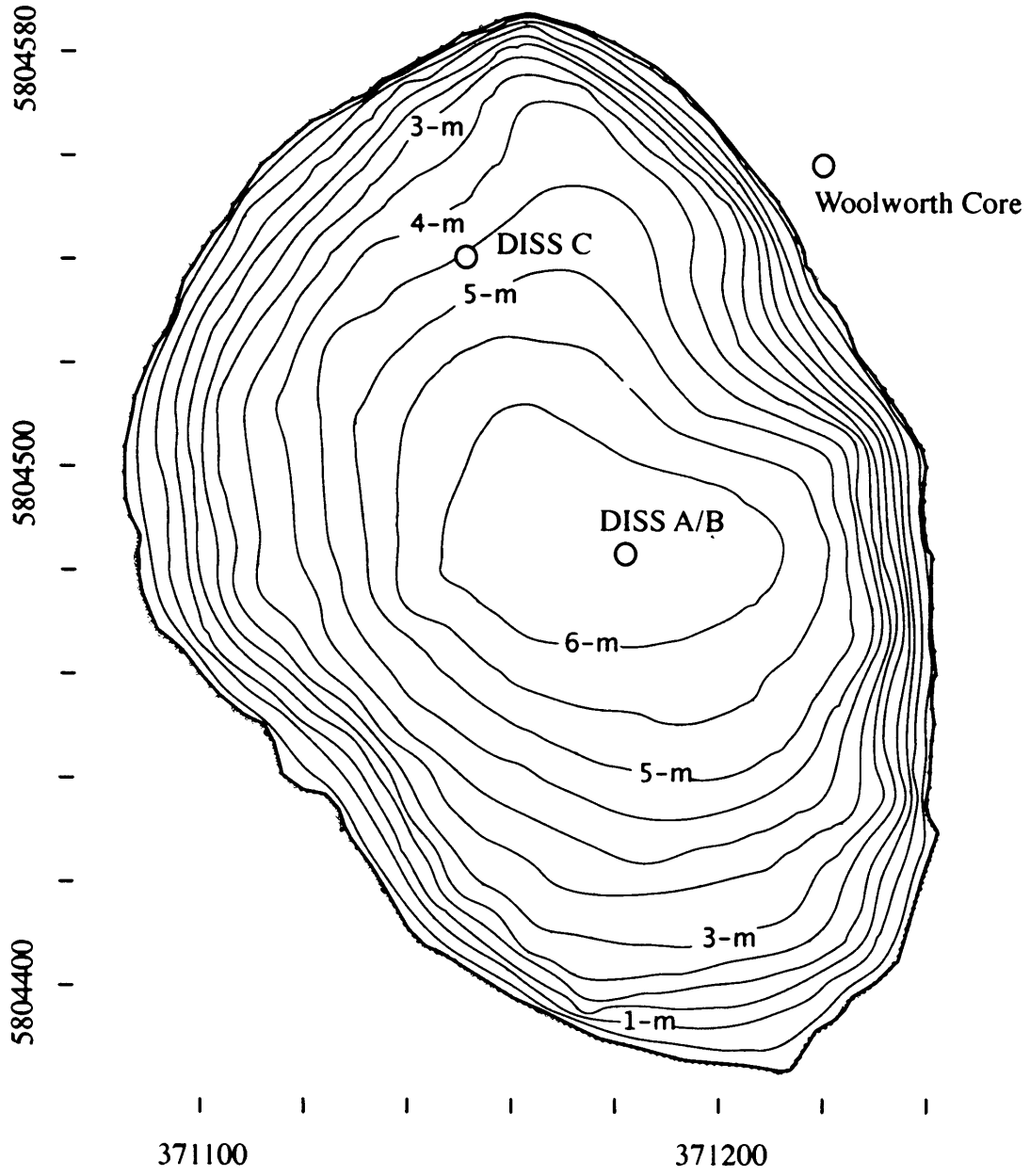

Fig. 2.2: Bathymetric map of Diss Mere with coring sites. The bathymetry was constructed from over 270 depth measurements taken using a weighted piece of rope at regular 5 m intervals over several traverses of the lake. The location of each measurement was evaluated using Global Positioning Satellite (GPS) values, processed relative to simultaneously collected data from the Ordnance Survey's UK network (http://www.gps.gov.uk/), which gave a precision for the individual XY GPS points in the centimetre range. Using the software package Surfer, the dataset was gridded using a standard krigging method. Grid references are in UTM coordinates, zone 31 north. The green diamonds are the lake edge (dense where measured, sparse where inferred), red crosses are bathymetric measurements.

Fig. 2.3 shows some of the features of meromixis. Meromixis is most likely to occur in lakes that are small, unusually deep and/or protected from the wind. Walker and Likens (1975) used relative depth as an index for the potential of such morphometric meromixis. Relative depth is the maximum lake depth expressed as a percentage of the mean diameter. They found that the relative depth typically is between 2 and 10% in lakes that are meromictic due to morphometric factors. Currently, Diss Mere is afforded some protection from the wind by the surrounding topography. With a relative depth of 3.5%, Diss Mere is favourable for meromixis. Density stratification has most likely been strengthened by the historical discharge of salts into the lake since the founding of the town of Diss. Given the lake's evident stratification and its depth, the residence time of its water is estimated to be 100-200 years (Simon Wood, *pers. comm.).*

2.4. Carbon cycle

Hard waters, like those in Diss Mere, precipitate calcium carbonate, mostly as low magnesium carbonate ($CaCO_3$) during summer. The solubility of calcite crystals in water can be influenced by changes in pH, temperature and the concentrations of various inorganic and organic substances. Calcite precipitation occurs in response to lowered solubility of $CaCO_3$. This is caused by increased activity of CO_3^{2-} resulting from decreased concentration of dissolved CO^{2-} primarily due to phytoplankton uptake during photosynthesis and/or seasonal temperature increase, for instance, as evidenced in seasonal studies of hard-water lakes in America (Megard, 1968; Brunskill, 1969; Dean & Megard, 1993), and Switzerland (Stabel 1986; Gruber *et al.* 2000). Kelts & Hsü (1978) provide a summary of these conditions. These studies have shown that, although surface waters tend to be relatively supersaturated with respect to calcite all year round, carbonate saturation increases as much as fourfold from spring through summer with maxima commonly in June and July (*e.g.* Megard, 1968; Brunskill, 1969; Dean & Megard, 1993; Gruber *et al.*, 2000; Dittrich & Koschel, 2002). One to three periods of calcite precipitation occur (Dittrich & Koschel, 2002). This pattern often results in slow

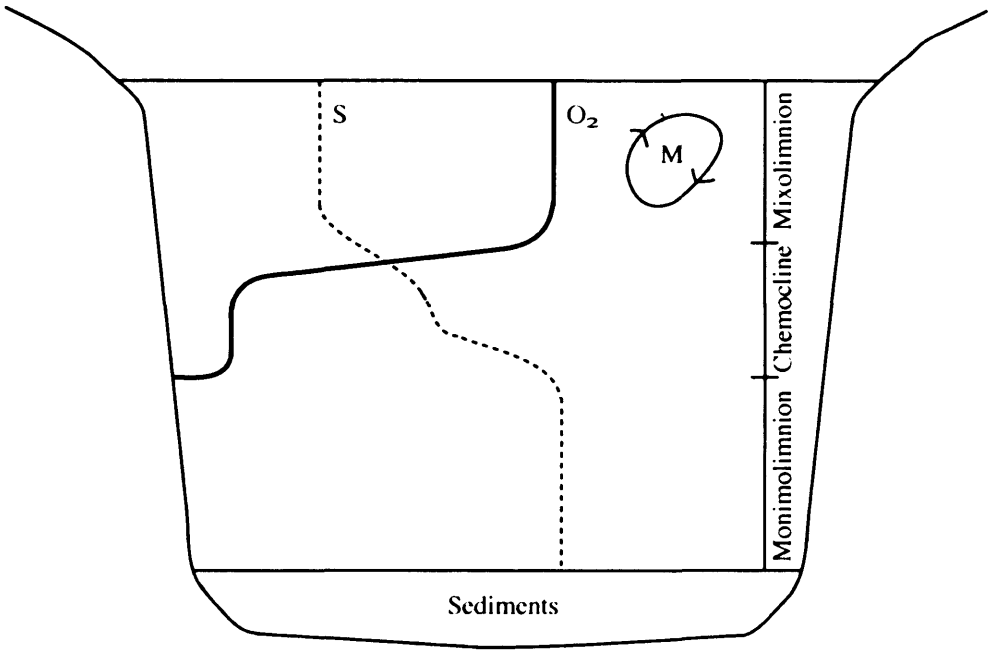

Fig 2.3: The main features of meromictic lakes. O2 = dissolved oxygen; S = salinity; M = wind driven mixing. Mixolimnion, Chemocline and Monolimnion are equivalent terms to epilimnion, metalimnion (thermocline) and hypolimnion of holomictic lakes (those that mix at least once a year).

and regular growth of calcite during spring-overturn when diatom populations dominate, and rapid crystallisation of many uniformly small (micritic) crystals in mid-summer when thermal stratification, and consequently algal stratification, result in increased cyanobacteria (blue-green algae) activity (cf. Folk, 1974). A mid-summer peak in supersaturation is mediated by the high photosynthetic activity of green and blue-green algae because they create a high pH microenvironment around their cells and act as numerous nuclei for rapid precipitation of calcite (Hartley *et al.*, 1995; Mullins, 1998; Yates & Robbins, 1998; Bradbury, 2002; Dean, 2002; Dittrich *et al.*, 2004). Higher $CaCO_3$ concentrations in sediments is therefore interpreted to be a result of warmer summers, which induce earlier seasonal stratification, decrease the solubility of calcite and lengthen the time of photosynthetic activity (Silliman *et al.*, 1996; Anderson *et al*, 1997; Mullins, 1998; Meyers 2002).

A model advanced by Koschel (1997) predicts a variety of grain-morphologies under different conditions of chemical saturation, but also highlights the importance of impurity absorption on calcite production (Fig. 2.4). For example, an increase in nutrient concentration and lake trophic status does not necessarily result in increased calcite deposition. Koschel (1997) states that although increased calcite deposition is recorded from oligotrophic through slightly eutrophic stratified lakes, further increase in lake eutrophication retards calcite burial. High eutrophic level, and hence high concentration of dissolved nutrients, *e.g.* phosphorus, is therefore often characterised by low calcite precipitation (Stabel, 1986; Dittrich & Koschel, 2002). This supports the argument that dissolved phosphorus is able to inhibit calcite precipitation (House, 1987) resulting in a 'run-away eutrophication' effect. Another possible interaction between phosphorus and calcite is its co-precipitation with calcite. This process is considered by many to be an important natural impairer of eutrophication in lakes due to phosphorus reduction and increase in the sedimentation rates (House, 1990; Hartley *et al.*, 1995). Co-maxima for calcite and phosphorus in lake sediments have been observed in a number of lakes

a) Dendritic growth - under very high supersaturation, especially in mesotrophic and slightly eutropic lakes

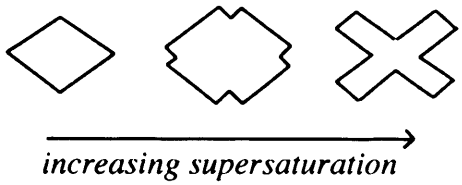

increasing supersaturation

b) Growth with non-preferred adsorption - in eutrophic lakes / or slow-growth in meso/eutrophic lakes

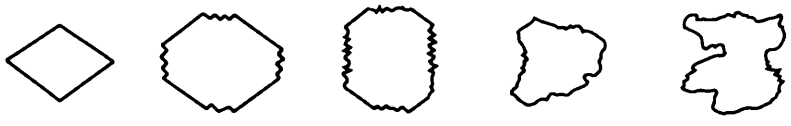

increasing absorption

c) Growth with preferred adsorption - in slightly eutrophic lakes

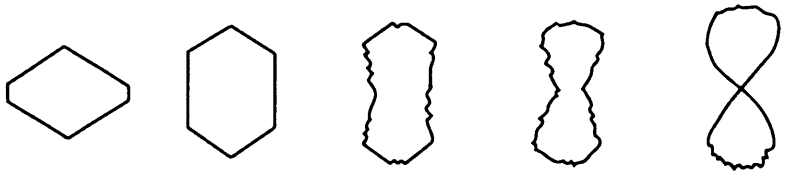

increasing absorption

Fig. 2.4: Morphological dependence of CaCO on supersaturation and adsorption of impurities (Koschel, 1997).

(Groleau *et al.*, 1999; Elk Lake, Dittrich & Koschel, 2002). It is likely, though, that the majority of co-precipitated phosphorus will not remain buried as it is common for calcite to be dissolved in anoxic CO_2 rich bottom waters.

Finally, the amount of calcite ultimately buried in lake sediments is not solely dependent on surface production. For example, Dean (1999) demonstrates that in seasonally stratified lakes eutrophication can result in decreased calcite burial. Hardwater lakes in Minnesota show that CO_2 produced by decomposition of high organic carbon flux (approximately greater than ~12%) lowers the pH of anoxic pore waters. Apparently if more than ~12% organic carbon is buried, most of the calcite that reaches the sediment-water interface is dissolved. Hence, despite an increase in surface water calcite production, the higher rain of organic carbon to the lake bottom waters results in decreased carbonate burial. The importance of dissolution in both the water column and sediments themselves is highlighted by Ramisch *et al.* (1999) and Müller *et al.* (2003). Dissolution of calcite crystals is thought to depend on surface area and residence time in the water column. In addition, the oxygenation state of the bottom waters and sediment pore-waters is considered important. Anaerobic decomposition of organic carbon, for example, creates alkalinity and inhibits dissolution.

2.5 Climate

2.5.1. East Anglian climate

The position of Diss, on the leeward side of the British Isles, inland and furthest away from the maritime influence of the Atlantic Ocean, means that it experiences larger temperature extremes and lower rainfall and therefore a more 'continental' climate than the surrounding coastal and western regions of Great Britain. According to the 'continentality' index of Conrad (1946), a scale from 1 to 100 based on the annual range of average temperature and the latitude of the site in question, East Anglia is one of the most continental regions in the British Isles (index rating of 11-13). For example, the annual range of monthly mean temperature reaches 15 °C in East Anglia, compared to

9°C in the extreme oceanity of areas exposed to the Atlantic Ocean, for example, the Hebrides and Orkneys. Coldest winter spells are usually the result of northerly or easterly airflow, making mild winters a product of westerlies. Cool summers tend to be produced by westerly or northerly airflows whilst southerly or easterly airflow results in warm summer episodes. The average rainfall over East Anglia is relatively low, with 600-700 mm per year. Rainfall occurs on about 150-180 days of the year (Lamb, 1987). There is no strong seasonality to the annual cycle of rainfall, although its maximum is during summer and autumn. A significant proportion of this rainfall is associated with convective thunderstorms. On average 20 days a year are witness to such events - amongst the highest number of thunderstorms in the UK - and they tend to occur between May and August.

2.5.2. The North Atlantic Oscillation

The patterns of heat and precipitation described above are largely controlled by the North Atlantic Oscillation. The NAO refers to a large-scale north-south oscillation in atmospheric mass between the North Atlantic subtropical high at the Azores and subpolar low centred around Iceland. Although the NAO is evident throughout the year (cf. Rogers, 1990), it is most pronounced during winter and indices of the NAO are defined as the difference between normalized mean winter (December-March) sea-level pressure (SLP) anomalies at, *e.g.*, Stykkisholmur, Iceland and Ponta Delgada in the Azores (*e.g.* Rogers 1984). The SLP record at Ponta Delgada begins in 1894, but more recently Hurrell (1995) and then Jones *et al.* (1997) used alternative weather station measurements for seasonal SLP's (south-west Iceland and Gibraltar, respectively) to extended the record back to 1821. It is one of the longest meteorological records available. During periods of enhanced pressure-difference the NAO is said to be in a positive phase (see Fig. 2.5). Because air flows counter clockwise around low pressure and clockwise around high pressure in the northern hemisphere, during a positive phase, stronger than average westerly winds deliver increased heat and precipitation across the mid-latitudes to northern Europe with a decrease in activity to the south. Extreme NAO conditions occur when there is a reversal of the pressure gradient between the two

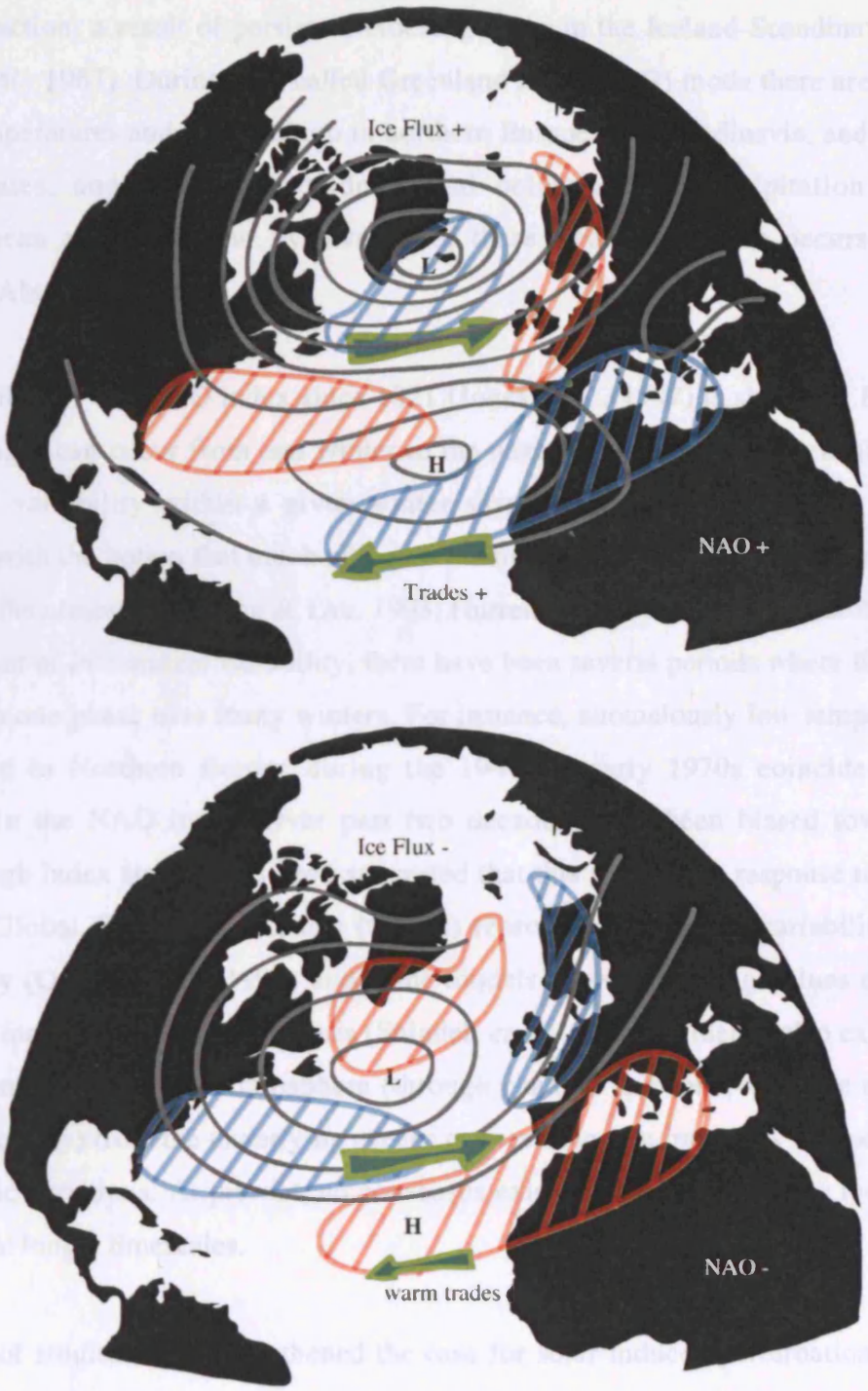

Figure 2.5: Cartoon illustrating NAO extremes. a) 'NAO +ive' where high surface pressure in the subtropical Azores and low surface-pressure in region of Iceland results in above normal temperatures and precipitation (red hatched areas) in north Europe and Scandinavia. b) at times of 'NAO -ive' a reversal in surface-pressure conditions results in anomalous coldness and below-normal precipitation (blue hatched areas) in the same regions.

centres of action; a result of persistent blocking highs in the Iceland-Scandinavia area (Moses *et al.*, 1987). During a so-called Greenland Below (GB) mode there are above-normal temperatures and precipitation in northern Europe and Scandinavia, and eastern United States, and anomalous coldness and below-normal precipitation in the Mediterranean and Greenland. A reversal of these weather patterns occurs during Greenland Above (GA) mode.

The variability of the NAO index since 1821 (Jones *et al.*, 1997) is shown in Fig. 2.6. Large changes can occur from one winter to the next, and there is also a considerable amount of variability within a given winter season (Hurrell *et al.*, 2003). This is consistent with the notion that much of the variability in the NAO arises from processes internal to the atmosphere (Ting & Lau, 1993; Hurrell, 2000). However, in addition to a large amount of interannual variability, there have been several periods where the NAO persisted in one phase over many winters. For instance, anomalously low temperatures experienced in Northern Europe during the 1940s to early 1970s coincide with a downturn in the NAO index. Over past two decades NAO been biased toward its positive, high index state; it has been suggested that this might be a response to global warming. Global Circulation Models (GCMs) reproduce NAO-type variability quite successfully (Osborn *et al.*, 1999) and some models show increasing values of NAO index with increasing greenhouse gases (Shindell *et al.*, 1999). Evidence also exists that forcing from the overlying stratosphere (through changes in ozone, volcanic aerosols and solar activity) from the underlying oceans can result in low frequency dampening of tropospheric variations. At present, no consensus exists on the relative roles they play, especially at longer timescales.

A number of studies have strengthened the case for solar-induced perturbations being propagated downward from the stratosphere to the troposphere. NAO extremes have been linked to geomagnetic activity (Bucha & Bucha, 1998), cosmic rays and Earth's cloud cover (Svensmark & Friis-Christensen, 1997; Svensmark, 1998; Marsh & Svensmark, 2000; Carlow *et al.* 2002). Links have been established between the geomagnetic index and sea-level pressures, and between geomagnetic activity and

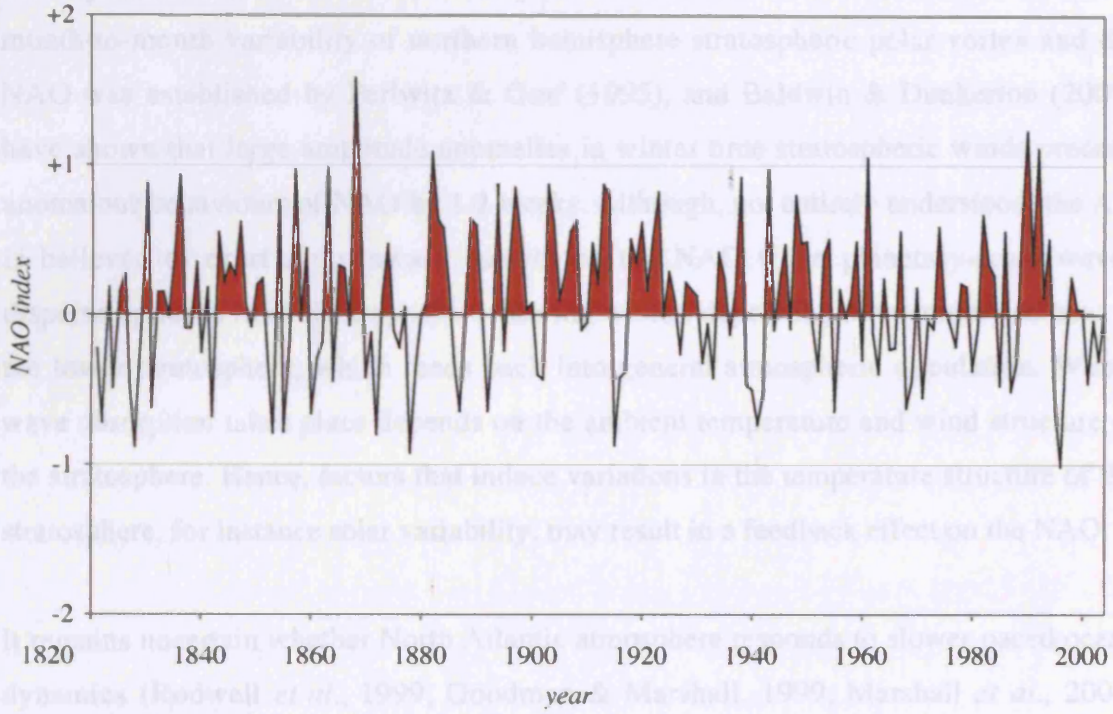

Figure 2.6: The North Atlantic oscillation index, AD 1821-2004, derived from pressure differences between Reykjavik, SW Iceland and Gibraltar, Azores. Area infilled red above values of zero denotes positive phase of NAO. Data for this index were taken from Jones et al. (1997).

stratospheric geopotential heights (surfaces of constant gravitational potential) (Hartley *et al.*, 1998; van Loon & Labitzke, 2000; Carlow *et al.*, 2002; Thejll *et al.*, 2003). Changes in geopotential height modulate the strength of winter polar vortex, the stratospheric winds. Changes in polar vortex are characterised by a seesaw in mass between the Arctic and the mid-latitudes. Termed the Arctic Oscillation (AO), its winter signature is similar in appearance to NAO anomalies and time-series of both stratosphere AO and the NAO are nearly identical. A statistical connection between the month-to-month variability of northern hemisphere stratospheric polar vortex and the NAO was established by Perlwitz & Graf (1995), and Baldwin & Dunkerton (2001) have shown that large amplitude anomalies in winter time stratospheric winds precede anomalous behaviours of NAO by 1-2 weeks. Although, not entirely understood, the AO is believed to exert a downward control on the NAO when planetary-scale waves disperse upwards from the troposphere during winter, depositing momentum and heat in the lower stratosphere, which feeds back into general atmospheric circulation. Where wave absorption takes place depends on the ambient temperature and wind structure of the stratosphere. Hence, factors that induce variations in the temperature structure of the stratosphere, for instance solar variability, may result in a feedback effect on the NAO.

It remains uncertain whether North Atlantic atmosphere responds to slower paced ocean dynamics (Rodwell *et al.*, 1999; Goodman & Marshall, 1999; Marshall *et al.*, 2001; Ferreira, 2001) such as anomalies in sea-surface temperature (SST), deep-water formation, Gulf Stream strength, and sea ice. The key question is the sensitivity of mid-latitude atmosphere, away from surface, to changes in ocean parameters. Theoretical studies suggest that NAO can interact with heat advection in the North Atlantic to produce anomalies that propagate north and east with longer time scales. It has been observed, for example, that winter SST anomalies from the western subtropical gyre, spread eastward along the path of the gulf stream with a transit time of a decade (Sutton & Allen, 1997). When forced by both Atlantic Basin and globally varying SST anomalies, Global Atmospheric Climate models (AGCM) reproduce realistic NAO variability including over half of the observed strong upward trend over past 30 years. (Visbeck *et al.*, 2002; Rodwell *et al.*, 1999). The relative importance of extratropical and

tropical SST anomalies on NAO variability is still unresolved (Venzke *et al.*, 1999; Sutton *et al.*, 2001; Peng *et al.*, 2002). The possibility of remote forcing of the NAO from tropical oceans is discussed by Xie & Tanimoto (1998), Venzke *et al.* (1999), and Sutton *et al.* (2001) who argue that changes in the meridonial SST gradient across the equator affects tropical Atlantic rainfall and potentially influences North Atlantic mid-latitude circulation. Tropical Indian Ocean forcing of the NAO on long (multidecadal) timescales has been modelled by Hoerling *et al.* (2001) and Sutton & Hodson (2003). It is not clear, however, from such studies if tropical forcing at such timescales is secondary to extratropical north Atlantic forcing itself. The impact of ENSO on the NAO is uncertain, although most evidence suggests the effects are small. Studies which highlight ENSO forcing presumably require an indirect link through the direct impact of ENSO on tropical north Atlantic SSTs (Saravanan & Chang, 2000; Chiang *et al.*, 2000).

3. Methods

3.1 Introduction

This chapter describes the techniques used in both the recovery and analysis of Diss Mere's laminated sediment for palaeoclimate records. First, it describes the procedures used to core Diss Mere. Then, it covers a variety of invasive and non-invasive sampling techniques used to construct highest-resolution climate-proxy time-series from lamina geochemical and physical properties. Finally, it describes the time-series analysis methodology used to discern climate-relevant periodicities in the palaeoclimate data.

3.2 Livingstone Piston Coring

A modified Livingstone piston corer (described in detail by Wright, 1967) was used to recover the sediment used for this study. This coring technique is hand-operated and samples the sediment as several consecutive one-metre cores; it is in contrast to those techniques that are driven into the sediment by weights and momentum or operated pneumatically, sampling sediment as a monolith (*e.g.* Kullenberg, 1947; Mackereth, 1958). The latter were deemed unsuitable for the recovery of Diss Mere's Holocene infill owing to its unusual thickness of ~17 m (Peglar *et al.*, 1989). Initially, coring efforts were carried out in the northern reaches of the Mere in the summer of 2001 (Fig. 2.2). From a raft constructed from two inflatable boats fastened together with a wooden platform, a 5.3-m water column was cased from the water surface to several metres into the sediment. This formed a moon pool through which coring took place. Depths were measured with the coring extension rods and relative to the water surface. Sediment from 5.3-15.3 m was recovered, Further penetration was found to be impossible though, given the purchase available from the coring platform used. Immediately following extrusion, the cores were wrapped in thin plastic, aluminium foil, and thick plastic sheets and stored in dark cold storage at 5°C. In addition, an overlapping sequence, cored from the central region of Diss Mere by Sylvia Peglar in 1980, was provided by the Department of Geography, University of Cambridge. Cores from this site span depths of 10-24 m. They were cored using the same technique described above through a 6.5-m

water column, but with a more stable platform. Throughout the remainder of this thesis stratigraphic depths refer to composite depths in metres below the lake-water surface (unless otherwise stated, *e.g.* as cored depth in metres below the lake water surface [mblw]). To compare composite depths to coring depths see Appendix I.

3.3 Techniques for the study of Diss Mere's laminated sediment

A wide range of laboratory techniques have been employed to facilitate environmental reconstructions. These techniques include a number of relatively new and progressive methods, such as SEM Back Scatter Electron Imaging (SEM-BSEI, see Dean *et al.*, 1999) and geochemical X-ray Fluorescence core scanning (Corescanner Texel, see Jansen *et al.*, 1998) as well as more traditional analyses, *e.g.* X-ray diffraction (XRD) and carbon content determinations, *e.g.* LECO carbon-analyser.

As a substantial part of the sediment record at Diss Mere is varved, not only does it preserve a seasonal record of sedimentation, but perhaps more importantly, it provides annual time calibration of rates and timing of environmental change. It has been possible, therefore, not only to use measurements of consecutive varve thickness as an annual record of autochthonous primary productivity, but also varve counting to calibrate high resolution XRF elemental concentrations, *e.g.*, elemental Ca counts per second (cps) every 2-mm, here a proxy for summer temperature to elucidate the changing nature of interannual and longer timescale environmental variability in the North Atlantic region, *e.g.* the NAO.

The most continuously varved and well-preserved sediment in Diss Mere was retrieved between 15.09 and 16.74 m composite depth (see section 5.1.1.). This interval records the East Anglian decline in *Tilia* pollen and its top corresponds to the base of pollen zone DMP 7a (Peglar *et al.*, 1989) where a decline in tree pollen percentages can be correlated to a regional-scale land clearance that is radiocarbon dated at Hockham Mere (Bennett, 1983; see section 3.3.3). This interval therefore offers the best opportunity to place a record of highest-resolution North Atlantic climate change within the calendrical

timeframe of the Holocene epoch. Although varved sediment was also recovered below 16.74 m composite depth (below 16.99 m coring depth), uncertainties in the nature of the composite stratigraphy, the independent chronology and also coring artefacts below this depth, have made its use as a highest-resolution record of climate change problematic (see section 5.1.1.). Consequently, this study focused on constructing time-series of varve thickness and XRF core scanning for 2-mm resolution records of elemental abundance within the interval 15.09-16.74 m. In addition, discrete samples were collected every 3 cm from the entire varved interval (15.09-17.79 m) to assess the evolution of carbon burial dynamics (organic carbon vs. inorganic carbon burial) and to determine sediment mineralogy via X-ray diffraction. SEM-Back Scatter Electron Imaging (BSEI) of the in-situ varve fabric from the interval 15.53-16.20 m was carried out to prove the annual nature of Diss Mere's varves and to evaluate change in seasonal water column processes. This interval was considered to be of most value as it covers a significant change in carbon burial dynamics recorded at 16 m depth (see section 5.2.). Table 3.1 summarises the laboratory analyses performed and core intervals and sampling resolution used.

3.3.1 Scanning Electron Microscopy (SEM)

SEM Backscatter Electron Imaging (BSEI) is used here to a) place laminae deposition in the context of seasonal water-column processes, ultimately leading to an understanding of how their physical attributes may be used to extract seasonal climate proxies, and b) confirm the varved nature of biogenic laminated sediment. These aims were achieved specifically by looking at the sediment microstructure and its phytoplankton remains. For lakes where most of the sedimentary components are autochothonous - that is, produced in the lake - the annual pattern can be determined from seasonal faunal succession. In the past, this has been achieved through, for instance, comparison of sediment core to modern sediment-trap data (Brunskill, 1969; Ludlam 1969; Kelts & Hsü, 1978; Nuhfer *et al.*, 1993; Alefs & Müller, 1999), and light microscope study of tape-peels and thin sections (Simola, 1977; 1979; 1984; Lotter, 1989; Card, 1997). SEM-based sediment fabric studies are used here because they are capable of resolving

individual laminae less than 100-μm thick (*e.g.* Kemp *et al.*, 1999; Dean *et al.*, 1999; 2001).

Table 3.1: Summary of laboratory analyses used in this study.

Laboratory analysis	Core interval (in m, composite depth)	Sampling resolution	Rationale
XRF CoreScanner (elemental Ca, Fe, Sr)	15.09-16.74 m	every 2 mm	interannual-resolution climate proxies recorded in elemental abundances.
	All cores, 10-18.5 m coring depth	every 1 cm	to aid stratigraphic correlation
SEM BSEI	15.53-16.20 m	Overlapping 15 x 1 x 2 cm sediment slabs.	confirm varved nature of Diss Mere's varves.
			evaluate deposition in terms of seasonal water column processes across significant change in carbon burial dynamics at 16 m depth.
LECO carbon analysis	15.09-17.79 m	every 3 cm	to assess carbon burial dynamics during varve deposition (organic carbon vs. carbonate carbon burial).
X-ray diffraction	15.03-17.79 m	8 samples	to determine varve mineraology.

Although the majority of phytoplankton that contribute to primary productivity are not preserved in the sedimentary record, seasonal cycles can still be discerned in laminated sediment by analysis of, for instance, the remains of diatoms and green algae. In many temperate lakes, laminae are composed of diatom frustules deposited during periods of spring and autumn water-column mixing (Reynolds, 1980; 1984) and micrite carbonate, biogenically precipitated during the period of summer biological production, dominated largely by green algae and cyanobacteria populations (Brunskill, 1969; Padisák *et al.*, 1998). Consequently, the diatom fraction of the total phytoplankton biomass varies

seasonally and is lowest in mid-summer whilst the remains of green algae are confined to carbonate layers (Shapiro & Pfannkuch 1973; Kelts & Hsü, 1978; Klemer & Barko 1991; Padisák, 1998, 2003). Taxonomic identification is notoriously difficult (Birks, 1994). However, relatively few species of dominant phytoplankton occur in a given lake (Kilham *et al.*, 1996) and ecological preferences are increasingly better constrained (Berglund, 1986). It is beyond the scope of this study to provide detailed taxonomic recognition of all phytoplankton preserved in Diss Mere's sediments. The low-resolution diatom and fossil pigment stratigraphy for Diss Mere constructed by Fritz (1989; see Fig. 4.1) has been used here and only patterns of the phytoplankton components preserved in the majority of laminae were considered.

3.3.1.1 Backscatter electron imagery (BSEI)

Backscattered electrons are the result of collisions between beam electrons and atoms within the specimen (Goldstein *et al.*, 1981). The atomic number of the target determines the number of backscattered electrons generated. The detector reconstructs this information on a photograph as image brightness. It is not necessary to use standards to check for drift in machine readings as image brightness is not used in this study to measure a change in parameter with time, for instance, as used in the construction of greyscale time-series, but to highlight differences in lithology within any given varve year. Grains such as carbonate and quartz tend to have the highest high atomic numbers in lake sediment, and produce brighter images than organic matter and the carbon-based resin, which have low atomic numbers. Laminae containing phytoplankton, typically diatoms in lake sediments, have high porosity and appear dark on photographs as their frustules are filled by the resin.

3.3.1.2 Preparation of thin-sections for SEM analysis

Thin-sections were prepared for SEM analysis by Dr. Richard Pearce, of Southampton Oceanography Centre from sediment sampled using a sediment slab-cutter at University College London (for method see Schimmelmann *et al.*, 1990). Sediment was cut in 15

cm long slabs each with several centimetres overlap. Sediment blocks were cut from these slabs using a scalpel. Unlike with indurated rocks, it was not so straightforward to prepare thin-sections from Diss Mere's wet, unconsolidated sediments. In order to preserve the sediment fabric, pore-fluids needed to be removed before the sample was resin-impregnated. This was achieved by passive fluid displacement (chemical dehydration) and resin embedding using a method described by Kemp *et al.* (1998). The method is outlined in Appendix I. Chemical dehydration has been demonstrated by Pike & Kemp (1996) to be a superior technique to vacuum drying and resin-impregnation methods as it stops the sediment fabric drying out and cracking. Preparation of thin sections from the resultant resin blocks was undertaken using a standard method (as used for saw-cut rock samples, for instance) but with an oil-based lubricant. The thin sections were highly polished using a range of grits down to 1 μm. Finally, the thin sections were carbon-coated before being analysed in the SEM.

Twenty-three thin sections were prepared from core DISS A-6 from 15.66-16.37 mblw, the equivalent of 15.53-16.20 m in the composite stratigraphy (see Appendix III for guidance to polished thin section codes and coring depth). The varved sediment that documents the change in carbon burial dynamics at 16 m is considerably better preserved in core DISS A-6 than the cored material used in the composite stratigraphy (*i.e.* core DISS B-6; see section 5.1.1.). Core DISS A-6, however, was not made available to this project before geochemical analyses were performed and consequently, it could not be included in the spliced record. Low resolution BSEI was used to provide base maps for more detailed imagery of lamina composition. Subsamples of sediment were prepared for standard SEM and smear slide analysis to facilitate identification of microfossil components. Phytoplankton identification was carried out in collaboration with Professor Sheri Fritz, University of Nebraska, and Dr. Carl Sayer, Environmental Change Research Centre at University College London. All significant taxa were identified to at least generic level.

3.3.2 Climate proxy records

Due to the poor analogy that modern biogeochemical processes acting in Diss Mere provide to past (prehistoric) conditions (see section 2.3.2) the results of SEM-BSEI analysis (see section 5.3) and underlying assumptions about biogeochemical cycling in hard-water lacustrine settings (see sections 2.4 and 4.3), has been used to validate the climate and palaeoproductivity proxies generated in this study. For example, the thickness of comparable biogenic varve segments from successive years, which SEM-BSEI analysis demonstrates to contain siliceous cells of diatoms, are taken to be related to diatom productivity. Also, the SEM study has shown that the thickness of carbonate varve segments are related to productivity changes in late-spring through summer when the water column is oversaturated with respect to calcite and precipitates carbonate, due to removal of CO_2 in response to seasonal warming of surface waters, lake stratification and phytoplankton photosynthesis. By extension high-resolution records of elemental Ca, which records variation in calcium carbonate, are taken as a proxy for summer temperature. OM burial is used here as a proxy for changes in winter temperature. Sediment trap studies in analogous varved hardwater lakes show that most of the OM that is preserved in sediments comes from populations of diatoms that settle rapidly and escape oxidation in the epilimnion (Dean, 1999). Owing to strong correlation that exists between winter air temperature and the relative abundance of diatoms that make up the spring phytoplankton peak, increased OM burial is hypothesised to reflect a milder winters at Diss (see section 4.3). Finally, Elemental Fe, which shows a close association with sulphur and is therefore primarily incorporated into pyrite, is taken to record changes in the degree of water column anoxia and is therefore also related to changes in productivity.

3.3.2.1 X-ray Fluorescence (XRF) Core Scanning

The XRF Corescanner (Jansen *et al.*, 1998; Röhl & Abrams, 2000) at the University of Bremen was used to determine the chemical element composition of the split core segments. The XRF Corescanner can measure elemental concentrations from 100% down to ppm levels on wet, freshly split cores. Although a freshly split core is not an

ideal sample for XRF analysis, which certainly makes the resultant data semi-quantitative at best, this system has important advantages. First, a very high resolution can be achieved rapidly, so that nearly continuous records can be produced in a short time. Secondly, the system is non-destructive, protecting the sediment fabric for further investigation. Finally, it provides data about the actual composition of the sediment, in contrast to tools such as natural gamma-ray and colour-loggers that produce data depending on a combination of sediment properties. The general method and calibration procedures for the XRF system are discussed comprehensively by Jansen *et al.* (1998). In summary, the whole system is computer-operated, allowing for precise positioning of measurements. The core is moved by a stepper motor relative to the measurement unit (X-ray source, and detector) which is lowered onto a core surface covered by a foil during analysis. The analyses are performed at predetermined positions and counting times. The acquired XRF spectrum for each measurement was processed by the KEVEX™ software Toolbox©. Environmental background subtraction, sum-peak and escape-peak correction (to remove sum [pile-up] peaks and account for detector escape), deconvolution (necessary for determining net intensities if two spectral lines of characteristic X-rays overlap), and peak integration (to quantify elemental abundances) are applied. The resultant data are essentially element intensities in counts per second (cps). The system allows the analysis of the elements K, Ca, Ti, Mn, Fe, Cu, and Sr. Statistically significant counts for elemental Ca, Fe and Sr were collected from the Diss Mere cores at 1 cm intervals over a 1 cm^2 area from cores collected at 10-18.5 m coring depth and for selected laminated cores at 2 mm intervals over a 2 mm^2 area. Although K, Ti, Mn and Cu measurements were also obtained, counts at the selected counting time were too low to be interpreted.

3.3.2.2 Carbon LECO analyser and X-ray diffraction.

Samples of laminated sediment were collected every 3 cm for analyses of geochemistry and mineralogy. Each sample was dried and homogenised for analysis of total and inorganic-carbon. Eight of the sediment samples were used to characterise bulk mineralogy from conventional X-ray diffraction (XRD) using Ni-filtered, Co-Kα

radiation using a standard method. Owing to equipment failure, two samples had to be run using Cu-Kα radiation. This change in X-ray wavelength resulted in a shift of characteristic peaks for the minerals identified for several samples. Oriented glass slides were prepared from the same samples in an attempt to identify the overall contribution of clay minerals to sediment composition. No attempt was made to separate the <2 μm sediment fraction. To demonstrate that low percentages of clay minerals were still detectable using this method, one sample was re-run after being spiked with 2% kaolin (English China Clay standard). XRD analysis was performed by Dr. Ian Wood from the Department of Earth Sciences, University College London, whereas slide preparation and interpretation of the results were carried out by myself.

Total carbon (TC) was determined with a LECO carbon analyser housed at the Wolfson Laboratory, University College London. Total organic carbon (TOC) was determined in the same manner after an aliquot of the sample was acidified to remove carbonate minerals. TOC was multiplied by 2.13 to estimate organic matter (OM) content (Dean, 1974). Carbonate carbon (CC) was taken as the difference between TC and TOC. This was multiplied by 8.33 to obtain an estimate of $CaCO_3$ carbon content (the ratio of the molar mass of $CaCO_3$ to CC in calcium carbonate; Dean, 1974).

As the laminated sediment contains very little terrigenous material, it was possible to make an estimate of the biogenic silica content. This was made by assuming that the sediment is made up by three main components: OM, $CaCO_3$ and silica. An estimate of silica content was therefore made using the measured percentages of OM and $CaCO_3$ using the following formula.

$$\text{Biogenic silica\%} = 100 - (\text{OM wt. \%} + CaCO_3 \text{ wt.\%}) \qquad (3.1)$$

3.3.2.3 Varve-segment thickness measurements

Varve-segment thicknesses were measured on low magnitude BSEI images (see section 3.3.1.1). Because of the large number of pixels per millimetre (191), these images

allowed for an accurate constraint of segment thickness. Boundaries between segments were judged by eye and perpendicular distances between them measured and recorded using Object Image 2.10, a Macintosh public domain image program (an extended version of the image processing program 'NIH Image', http://simon.bio.uva.nl/object-image.html). Total varve thickness and carbonate varve segment thickness were determined (Fig. 3.1). The final value was taken as the average of five measurements per layer undertaken (from the thickest and thinnest portion of each segment, plus at three other equally spaced positions) by the same operator. Biogenic varve segment thickness was taken as the difference between the two average measurements from each varve. By careful measurement of the initial core sample, and comparison with the length of the polished thin sections, the effects of vertical distortion due to resin embedding was quantified. Thickness measurements were corrected by multiplying values by the ratio between thin section and equivalent sediment core length.

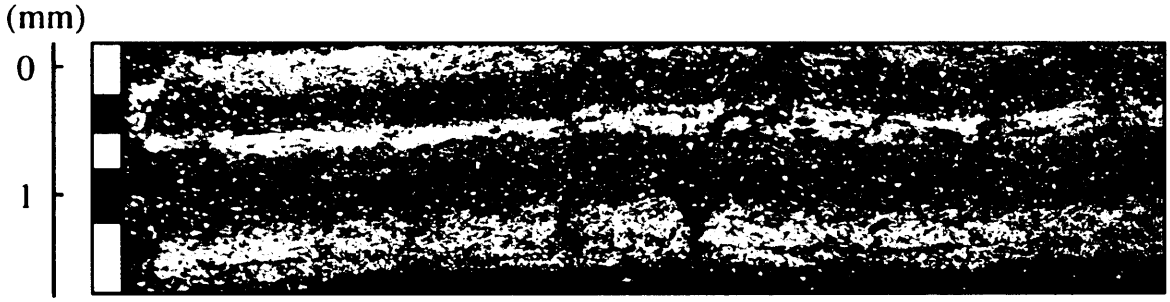

Fig. 3.1: Total varve thickness (red dashed line) and carbonate varve segment thickness (green dashed line, also white filled boxes). Biogenic varve segment thickness (black filled boxes) was taken as the difference between the two average measurements from each varve. Short horizontal black lines donate visually determined varve segment boundaries.

3.3.3 Chronology

A chronology for this study has been provided by varve counts calibrated to the calendrical timescale (Calendar years BP; hereafter referred to as Cal. BP) through correlation of Diss Mere's pollen stratigraphy to other radiocarbon dated regional pollen

stratigraphies. Obtaining radiocarbon dates for Diss Mere itself is fraught with difficulties. For example, the calcareous nature of the sediment renders it unsuitable for radiocarbon dating. The probable large incorporation of 'old carbon' from the surrounding till sediments, principally from ground-water sources, would result in dates that are too old. The dating of terrestrial plant macrofossils, which fix carbon from the atmosphere, would negate this problem. Unfortunately, none suitable could be recovered from the cores. In order to build up an age model, it was therefore necessary to use dates derived from an age model based on the East Anglia regional pollen stratigraphy.

The correlation of pollen sequences for chronological purposes is underlain by the assumption that biostratigraphic boundaries, such as pollen marker horizons are time-parallel, and can therefore be regarded as isochronous. The tendency for pollen zones to be time-transgressive however, is problematic. Whether due to diachronous anthropogenic or climatic influences, such homotaxial errors are accentuated over increasingly larger geographical separations. At Diss, the transition from laminated to homogeneous sediment at 15.09 m contains pollen that records widespread and extensive forest clearance and conversion of cleared land to grassland (*Pm-1*, see Fig. 3.2 [Peglar *et al.*, 1989]). This trend is found in a variety of pollen records from East Anglia and it is fortunate that its timing can be determined from two close-bounding radiocarbon dates at Hockham Mere, a lake only <20-km due north-west of Diss (1980 ± 50 and 2660 ± 50 ^{14}C yrs. BP at 2σ [Bennett, 1983]). Considering the close proximity of Hockham to Diss (see Fig. 1) the timing of this region-wide land clearance is hypothesized here to be synchronous at least on the timescale of several human generations and most likely to have occurred at both sites within the error associated with calibrating Hockham Mere's radiocarbon dates to the calendrical timescale over the time-period concerned (at 2σ, the range on the bounding calendar ages is several hundred years; see, section 5.2.1).

Figure 3.3 illustrates how the ^{14}C timescale varies against a chronology of calendar years in the time period concerned. Fortunately, the radiocarbon dates that bound late-Holocene land clearance at Hockham Mere do not correspond to the plateaux in ^{14}C

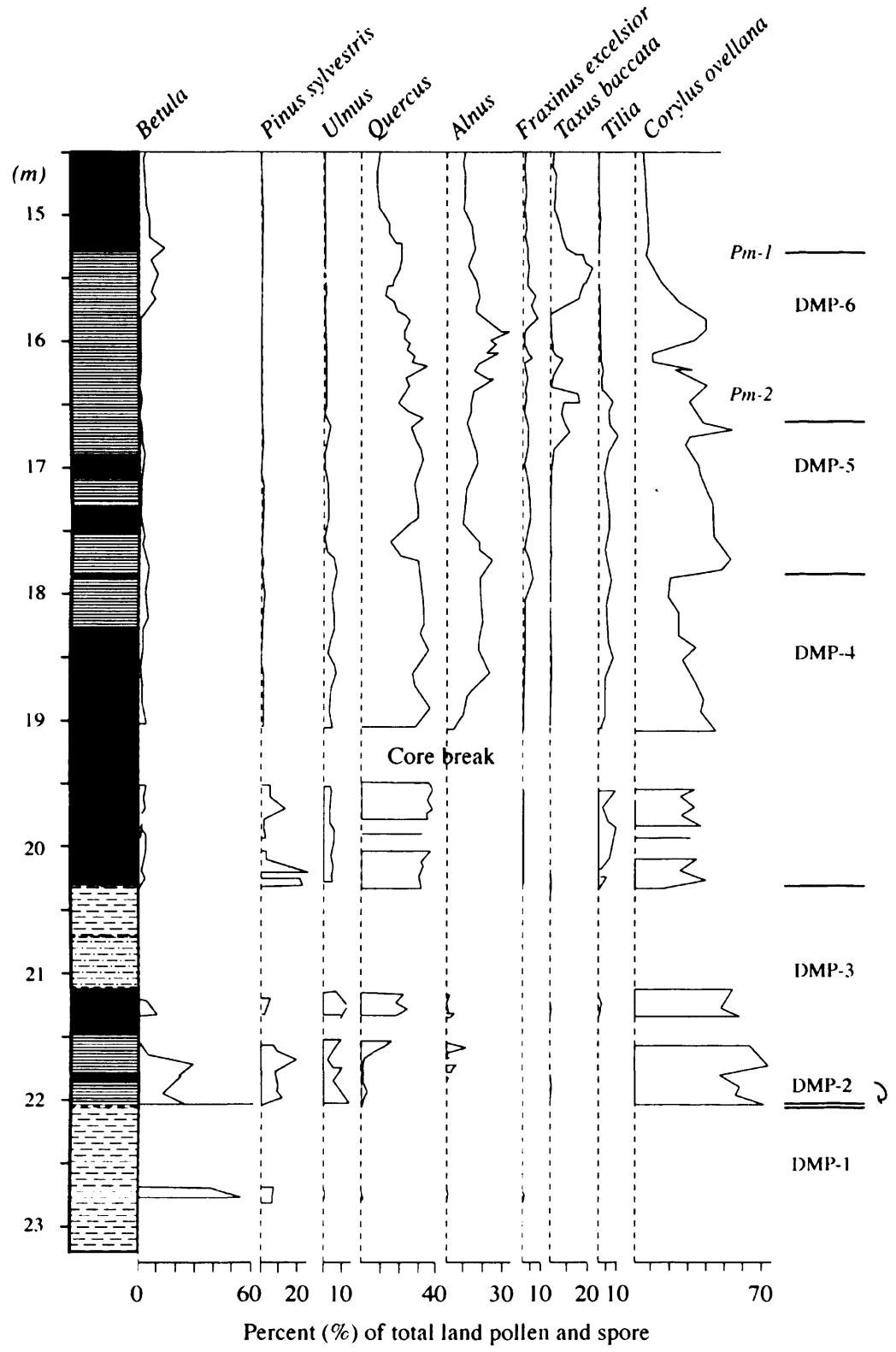

Fig. 3.2: Diss Mere summary pollen diagram. Adapted from Peglar *et al.* (1989). *Pm-1* & *Pm-2* refer to pollen markers used for correlation with pollen record of Hockham Mere; see text for details.

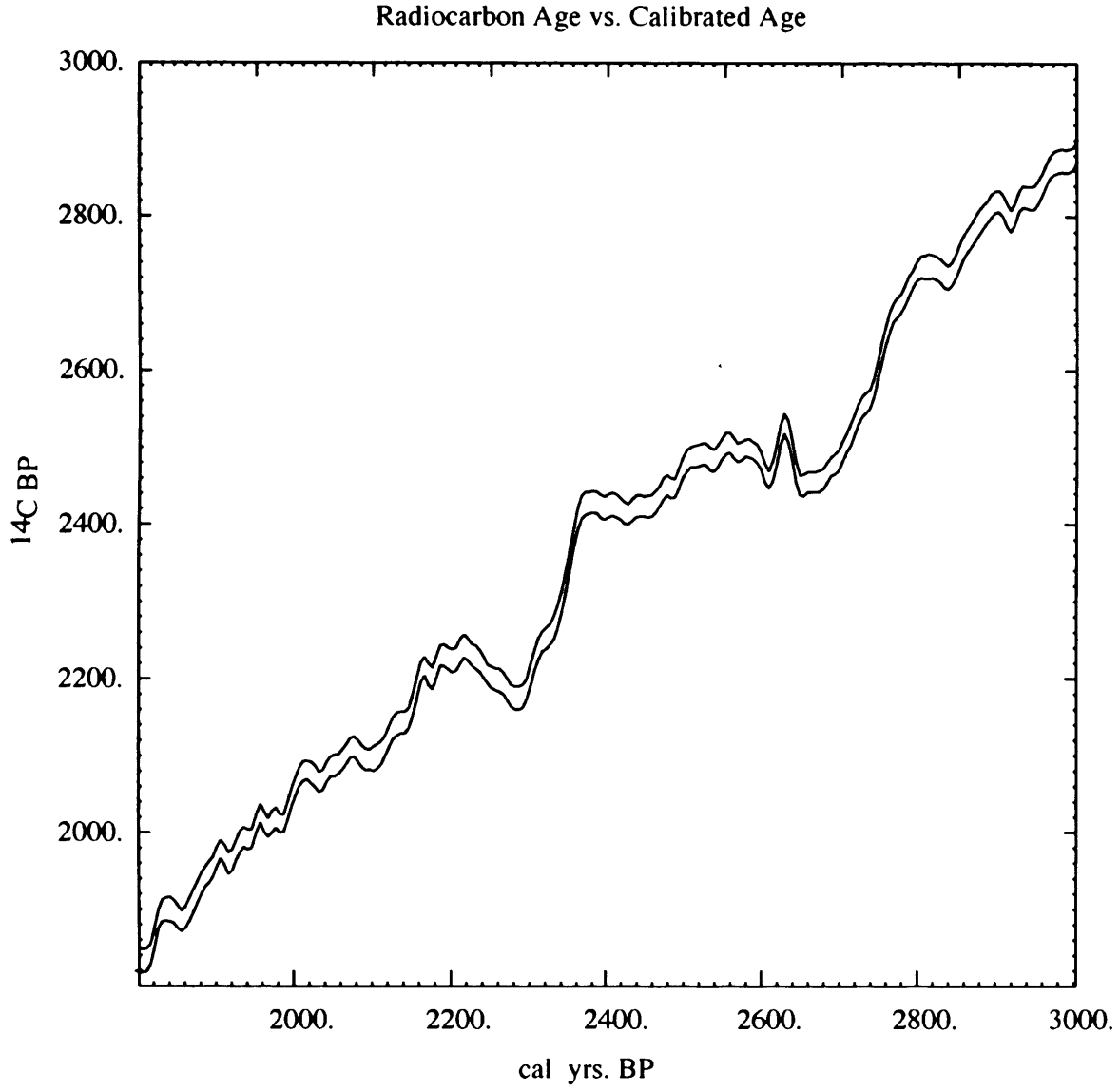

Fig. 3.3: IntCal04 calibration curve with 1-standard deviation envelope for period 1800-3000 14C BP.

atmospheric production between *ca.* 2350 to 2700 Cal. yrs. BP. Hence, calibrated radiocarbon dates at 1980 and 2660 ± 50 ^{14}C yrs BP, when the 2σ confidence limit is taken into account, result in calendrical ages with significantly less range. In this study, Hockham Mere's radiocarbon dates were calibrated to the calendar timescale with the IntCal04 calibration curve (Reimer *et al.* 2004) using the age calibration software package, CALIB 5.0.1. The timing of land-clearance at Diss was then determined through sedimentation-rate extrapolation across *Pm-1* using the age range between the bounding calibrated radiocarbon dates.

Varve counts were used to calibrate geochemical depth-series (15.09-16.74 m) in the time-domain. Varves were counted in a similar fashion to Sprowl (1993) and Anderson (1993). The main varved interval was divided into 22 counting zones, the boundaries of which occurring at the most prominent sedimentary horizons used in correlation between overlapping cores. Counts were carried out by eye on enlarged digital images of the varved sediment using Object Image 2.10. Object Image allows the user to place 'graphical objects' on a transparent layer, superimposed on the original images. Such objects can be used as counting markers forming a digital record of the location and number of laminae in a core photographic-archive. Three counts were made from each counting zone and the overlapping cores provided two-fold redundancy for most zones. Counts were not performed on images of DISS C varved cores. This was due to the lack of composite stratigraphy and the more disturbed nature of, and therefore lack of continuity in, the varved fabric in sediment cores from this hole. The benefit of multiple counts being carried out by the same analyst, as opposed to replicate counts by different analysts (known as independent multiple counting), is that the varve concept remains the same, *i.e.* what groupings of laminae constitute one year of sedimentation. The highest count from each counting zone was used to determine the number of varves present. It is considered here that counting too few varves is more likely than counting too many, and errors are expected to be biased on the low side. For example, identification of subannual sets of laminae is problematic when assessing the thinnest carbonate laminae which can be left obscured or undistinguished sedimentologically or 'smeared out' on the split core surface by the cleaning process prior to core digitisation. In addition,

redundancy in the varve counting permits an evaluation of the precision of the varve counts. The variance among the multiple counts from common intervals in different cores is taken as a measure of the counting precision. Thus, two standard deviations from the mean estimates the limits of 95% confidence on the precision of the counts. Intervals with less than two-fold redundancy are assigned the highest variance from a bordering interval. Sedimentation-rates (in mm/yr) were calculated for the composite stratigraphy at a continuous 2 mm scale between 15.09-16.55 m, the sediment for which high-resolution (2 mm) XRF geochemical data was available. This was achieved by dividing each 2 mm segment by the number of varves contained within it (Fig. 3.4). This data was used to interpolate sedimentation-rates for counting gaps. Such gaps represent missing material or varved material which was thoroughly obscured or ambiguously defined.

3.3.4 Analysis of climate time series

Fourier analysis was used to test for the presence of regular cycles in both time-series of varve thickness and XRF elemental abundance. It follows the premise that any time-series, regardless of its data values, can be fully approximated by a sum of a suite of sine and cosine waves of different wavelengths. In its most basic form, the method tests how well a series of cosine waves with variable frequencies can be fitted to the data. High variance is found for a particular frequency if a cycle with that wavelength is strongly present in the data. For each frequency, a measure of the strength of the oscillation at that frequency is obtained by looking at the variance or power (amplitude squared, s^2) of the appropriate sinusoid. A plot of power against frequency up to the Nyquist frequency is called a periodogram. The statistical property of such power spectra is very well understood (Jenkyns & Watts, 1968) allowing for tests of significance. The highest frequency that can be sampled is half the number of observations in the time-series, known as the Nyquist frequency. For example, the maximum frequency resolvable in a time-series with annual resolution, *e.g.* varve thickness, is 0.5, which has a period of 2 years (period = 1/f). In other words, the shortest cycle in the data that can be detected has one cycle every two data points, the minimum number of observations needed to

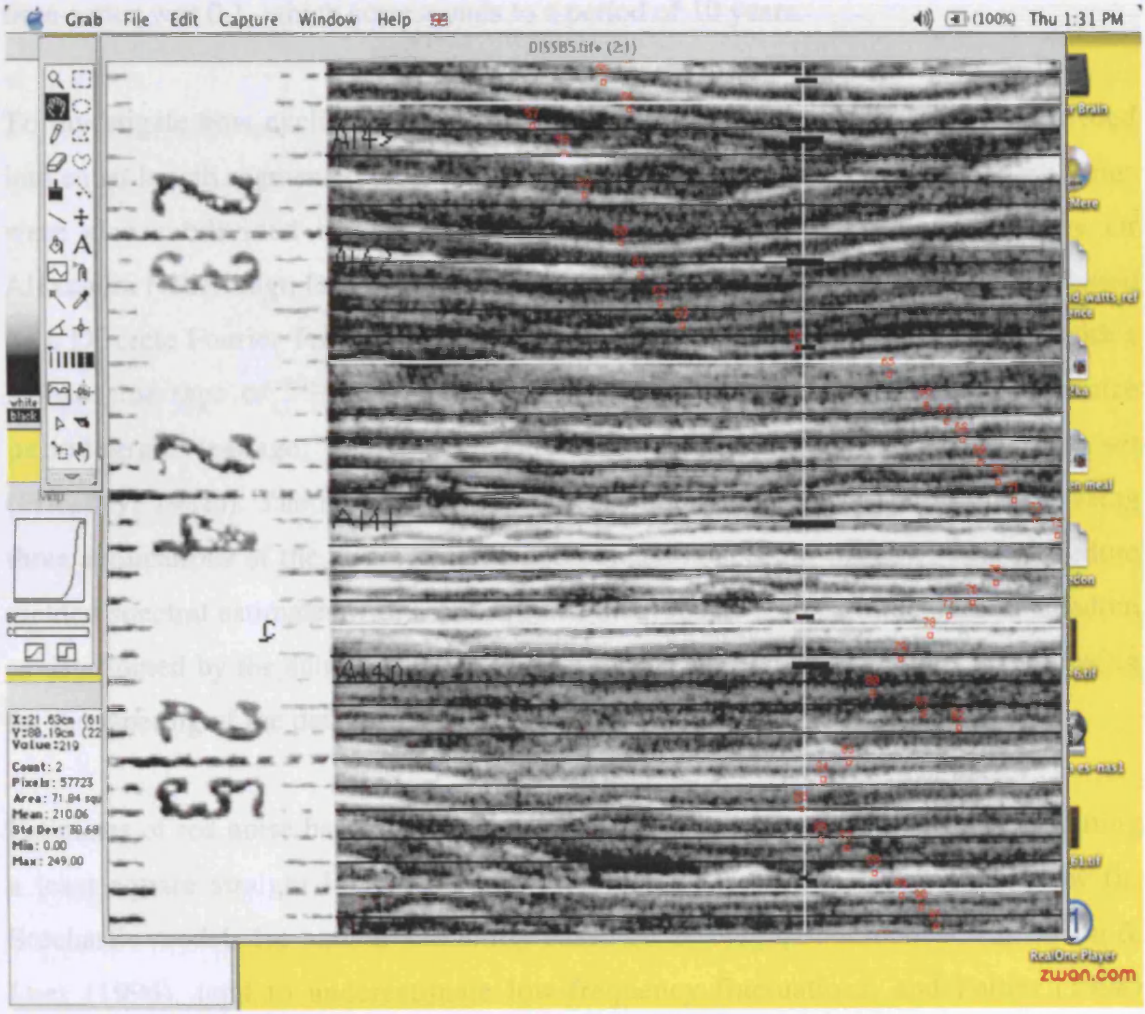

Fig. 3.4: Varve counting using Object Image 2.10 a Macintosh public domain image program. Red numbers are 'graphical objects', superimposed on the original core image. Such objects can be used as counting markers forming a digital record of the location and number of laminae in a core photographic-archive.

define a waveform. In the time-domain, XRF data were not sampled evenly. It was necessary to resample such time-series at 5-year intervals using linear integration so that data points were equally spaced. Consequently, the highest frequency resolvable in these time-series was 0.1, which corresponds to a period of 10 years.

To investigate how cyclicity changed with time, varve thickness data were subdivided into equal length segments, ~100-year time-series with 50 year overlap. XRF time-series were also subdivided into three segments. Power spectra were calculated by Dr Alexandra Nederbragt, Department of Earth Sciences, University College London, based on a Discrete Fourier Transform (DFT; Davies, 1986) of linearly detrended data with a split-cosine tape of 5% applied to both ends of the record (designed to minimize periodogram leakage, *i.e.* spectral side lobes caused by the ends of the data set (Priestley, 1981)). The spectral estimates were obtained from the periodogram using three applications of the discrete, three-point Hanning spectral window. This procedure yielded spectral estimates with a chi-squared distribution with eight degrees of freedom as determined by the sum of squares of the final spectral window weights and allowing for the tapering of the data.

Estimates of red noise background spectrum from the periodograms are made by fitting a least square straight line to log-log plots of power spectra, *i.e.* a power law fit. Stochastic models for natural variability based on autoregressive models, *e.g.* Mann & Lees (1996), tend to underestimate low-frequency fluctuations, and Peltier (1998) demonstrates that natural variability in climate can be better modelled using a power law model. Using the calculated background noise as the null hypothesis, peaks in the spectrum were tested against the background distribution to see if they qualified as significantly different at the 95% level.

4. Phytoplankton stratigraphy and ecology of Diss Mere's varves

4.1. Introduction

This chapter presents a summary of Diss Mere's known diatom and fossil pigment stratigraphies. Published ecological preferences of the major taxa preserved from comparable hardwater lakes are also discussed. This information is used to interpret both the changes in phytoplankton succession from SEM data and to help validate climate proxy records generated in this study.

4.2. Diatom and fossil pigment content of Diss Mere's varved sediment

The published diatom and fossil pigment stratigraphies for Diss Mere's varves (Fritz *et al.* 1989) are shown in Fig. 4.1. They reveal that below 16.24 m moderate to high fossil pigment concentrations of the caroteniods, oscillaxanthin and myxoxanthophyll, indicate that a mixed assemblage flora of blue-green cyanobacteria dominated the phytoplankton community at this time and restricted the growth of diatom populations to *Cyclotella* species. Given the moderate to high concentrations of blue-green pigments, and the varved sediments, lake trophic status is inferred to be mesotrophic, a lake with moderate nutrient concentrations, which are primarily utilised by cyanobacteria that out-compete diatoms. Above 16.24 m, a marked reduction in fossilised caroteniod concentrations suggests that cyanobacteria became less important as primary producers. A rapid increase in the cell numbers of the diatom species *Cyclotella ocellata* and *Stephanodiscus* spp. indicates that the lake became more eutrophic.

4.3. Phytoplankton ecology

No modern studies of seasonal phytoplankton succession in Diss Mere's water-column exist, and given a discernable human influence on the lake, processes acting today should be considered a poor analogy to past (prehistoric) conditions. The ecological information about the taxa was provided by the publications listed in Table 4.1. These are based on studies of modern phytoplankton succession in comparable temperate

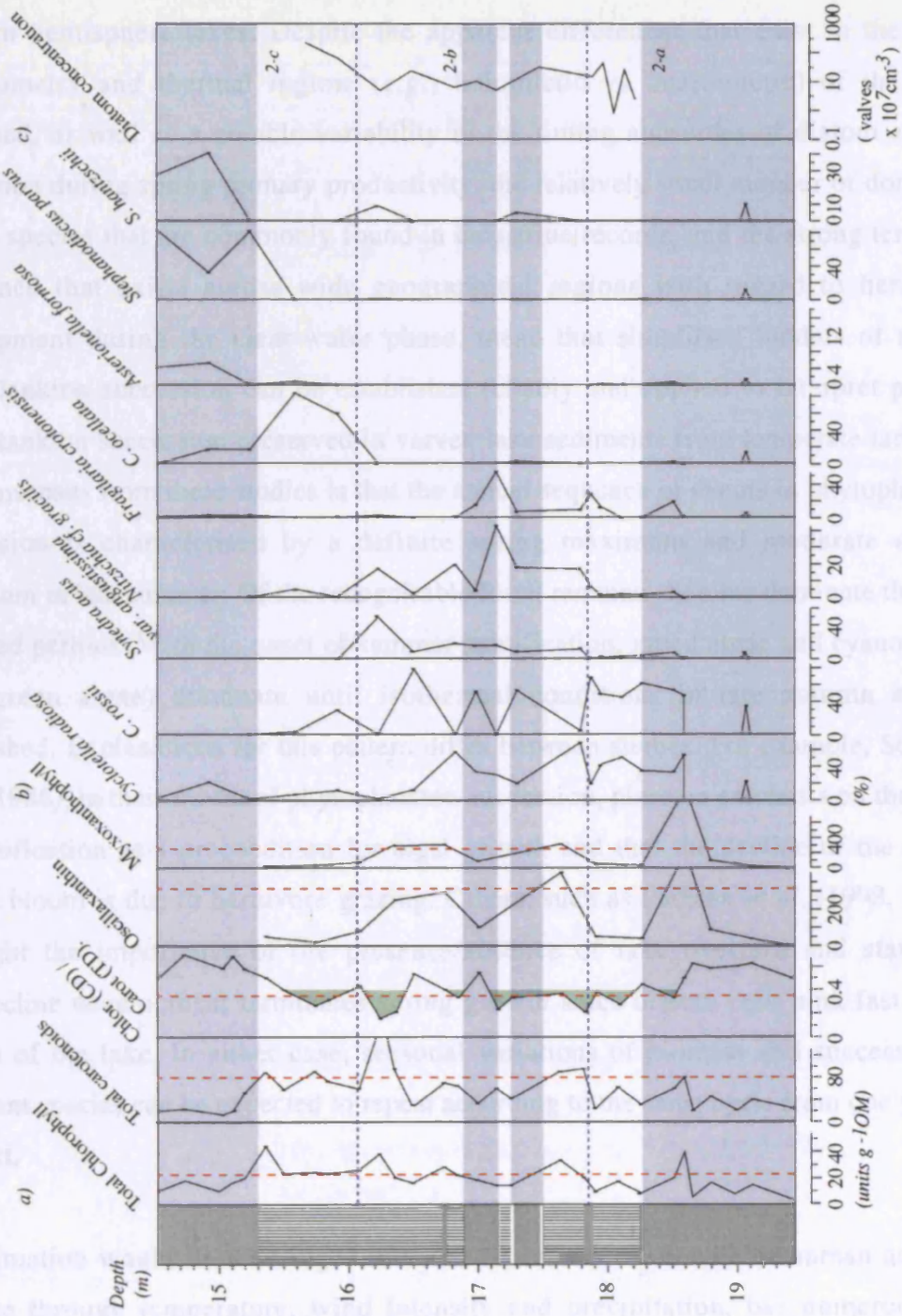

Fig. 4.1: Plots of a) fossil sedimentary pigments as absorbance units per gram organic matter b) relative abundance of major diatom taxa and c) diatom valve concentration against stratigraphic depth in the varved and associated homogeneous intervals of Diss Mere. Short-dashed horizontal lines delimit diatom zones as according to Fritz (1989). Short-dashed vertical lines denote the average values for the various fossil pigments. The grey filled regions on CD/TC plot delimits ratios indicative of sedimenting organic pigments in an anoxic environment. Data is reproduced with the kind permission of Fritz (1989).

northern hemisphere lakes. Despite the apparent differences that exist in the basin morphometry and thermal regime (*e.g.*, holomictic vs. meromictic) of the lakes examined, as well as a notable variability in the timing and order of diatom species succession during spring primary productivity, the relatively small number of dominant diatom species that are commonly found in lacustrine records, and the strong temporal coherence that exists across wide geographical regions with regard to herbivore development during the clear-water phase, mean that simplified models of annual phytoplankton succession can be established reliably and applied to interpret palaeo-phytoplankton succession preserved in varved lake sediments from temperate latitudes. The consensus from these studies is that the annual sequence of events in phytoplankton succession is characterised by a definite spring maximum and moderate second maximum in late summer. Of the recognisable fossil remains, diatoms dominate the non-stratified periods. With the onset of summer stratification, green algae and cyanophytes (blue-green algae) dominate until isothermal conditions in late autumn are re-established. Explanations for this pattern differ between studies. For example, Sommer *et al.* (1986), in their model of phytoplankton succession, place an emphasis on the onset of stratification as a precondition for algal growth and that the decline of the spring diatom bloom is due to herbivore grazing. Others, such as Padisák *et al.* (1998, 2003), highlight the importance of the presence/absence of lake overturn and state that thermocline development terminates spring growth since diatom cells sink fast to the bottom of the lake. In either case, seasonal variations of biomass and succession of dominant species can be expected to repeat according to the same cycle from one year to the next.

This situation would be unchanged without the effects of climate or human activity. Climate through temperature, wind intensity and precipitation, has numerous and complex indirect effects on lakes. It influences nutrient concentration, via the catchment through changes in vegetation, surface run-off and ground water flow, or the timing and duration of both thermal stratification and water column overturn. At timescales most pertinent to humans, catchments like Diss Mere's - that is, relatively small and fed predominantly by groundwater seepage - play only a limited role in lake water

Table 4.1: Studies with information on phytoplankton ecology/seasonal succession

Survey type	Region	Study
Seasonal plankton hauls	Lakes of Yellowstone and Grand Teton National Park, Wyoming USA	Kilham *et al.*, 1996 Interlandi *et al.*, 1999
Sediments / plankton hauls	Laurentian Great Lakes, USA. *e.g.*Lake Michigan, Lake Huron, Lake Superior, Lake Erie, Lake Ontario	Stoermer *et al.*, 1993; Stoermer *et al.*, 1996 Stoermer, 1978; Stoermer & Yang 1970; Stoermer & Ladewski, 1976; Tilman, 1981.
Sediments/ sediment traps	Elk Lake, Minnesota, USA	Bradbury, 1988; Bradbury *et al.*, 2002. Nuhfer *et al.*, 1993.
Sediments	Upper Klamath Lake, Oregon	Bradbury *et al.*, 2004.
Seasonal plankton hauls	Eau Galle Reservoir, Spring Valley, Wisconsin	Klemer & Barko, 1991.
Sediments	Lake Holzmaar, West Eifel region, Germany	Baier *et al.*, 2004; Bruchmann and Negendank, 2004.
Seasonal plankton hauls	Lake Stechlin, Germany	Padisák *et al.*, 1998; Padisák *et al.* 2003.
Seasonal plankton hauls	Baltic Lake District, northeastern Germany (60 lakes)	Schlegel *et al.*, 1998.
Seasonal plankton hauls	Massif Central, France (25 lakes)	Rioual, 2000; Rioual *et al.*, 2001.
Sediments	Lake Soppensee & Baldeggersee, Switzerland	Lotter, 1989; 1998.
Plankton hauls	Wide range of freshwater bodies in Netherlands	van Dam *et al.*, 1994
Seasonal plankton hauls	Lake Peipsi, Estonia Lake Yaskhan, Turkmenia	Nõges, 1997
Plankton hauls	Cross Mere, UK	Reynolds, 1973; 1976.
Plankton hauls	S.E. England ponds, UK.	Bennion, 1994.

chemistry. Instead, the relative interplay of thermal stratification and water column overturn is more important. For example, increased wind energy promotes increased mixing and the delivery of hypolimnetic nutrient-rich water to the surface. Development of spring blooms is typically during late February to March but can range from as early as January, to as late as May (cf. Padisák *et al.*, 2003). Spring blooms are also influenced by the presence, absence and duration of winter ice-cover (Padisák *et al.*, 2003). If prolonged ice-cover exists, inverse stratification will develop and may result in pronounced winter diatom productivity as well (Kilham, 1990). Summer stratification also is enhanced with increased summer temperature. This inhibits water column mixing, the 'clear-water phase', reducing the number of spring diatom blooms. To avoid overexposure to light, the main location of primary production may shift from the surface to the thermocline, thus influencing species composition (Anderson, 1995), *e.g.* populations of *Cyclotella* sink to a deeper zone with more equitable light and nutrient conditions. A number of studies have shown that delayed or early breakdown of stratification results in marked variation in species composition (Reynolds & Bellinger, 1992). Amongst the many effects of climate on lakes, significant summer cooling might be expected to result in a shift from lakes characterized by permanent stratification (*i.e.*, meromictic lakes) to those characterized by periods of water-column overturn (*i.e.*, holomicitc lakes) (Porter *et al.*, 1996).

A growing number of studies have demonstrated that in circum-Atlantic regions meteorological conditions during winter, *e.g.*, due to the NAO, play a significant role in phytoplankton dynamics; Ottersen *et al.* (2002) reviews many of these efforts. Whilst the link between the NAO and winds is only strong during winter, the link between the NAO and the thermal structure of lakes however, may carry over through to the spring and summer. This is because warming of lake waters during winter is shown to influence the intensity of spring mixing intensity and the degree by which nutrients, that accumulate in the hypolimnion and sediments during the productive season, are recycled back to the surface waters (Straile et al., 2003) and the spring plankton population dynamics of herbivores (Straile, 2000; Anneville et al., 2002). In large and deep temperate lakes mild winters are shown to restrict winter mixing and nutrient

replenishment (Straile *et al.*, 2003). Straile & Adrian (2000) note that during and after mild winters spring water temperatures and late-winter/spring biovolumes at Müggelsee, a small, shallow lake in north-eastern Germany, increase more rapidly than at Lake Constance, a large, deep lake in Switzerland. The response of phytoplankton to the NAO therefore, in part, appears to depend on lake depth. They attributed large biovolumes in shallower lakes to a restriction in, or a lack of, ice development during warmer winters, observing the most pronounced diatom blooms during years with no ice cover when increased turbulence favoured diatom growth. Similar conclusions were drawn by Gertin & Adrian (2000) who show that at Lake Müggelsee during the warm winter period 1988-1998, phytoplankton developed about one month earlier than in the preceding cool period 1979-1987, with a higher phytoplankton biomass recorded in early spring. Diss Mere, with an average depth of 3.9 m is probably more comparable to Lake Müggelsee than a deep lake such as Lake Constance and during the mid- to late-Holocene when a seasonal ice-cover was likely a prominent feature of Diss Mere, milder winters probably also resulted in increased spring diatom primary productivity and subsequent OM burial owing to an early break up or absence of ice-cover.

At Lake Erken in Sweden, Weyhenmeyer *et al.* (1999) linked an earlier timing of the spring phytoplankton peak (resulting in an extension of the phytoplankton growing season) and increased relative abundance of diatoms during this period to an earlier timing of ice break-up and increased values of the NAO index over the last 45 years. Whilst they found that the timing of ice-break up was best correlated to the whole winter period (December through March), species composition was better correlated with the 'seasonal NAO index' (December through February). This indicates, apparently, that species composition at time of the spring peak in April to May is already determined during the period December through February. Weyhenmeyer *et al.* (1999) suggest this may occur because spring phytoplankton develop slowly in cold waters with productivity intensifying as soon as light and sufficient warmth are available.

4.3.1. Ecology and seasonal succession of major phytoplankton

The following section provides a summary of studies (Tab. 4.1) with information on the ecology and seasonal succession of those phytoplankton found in Diss Mere's varved sediment

Cyclotella radiosa (Fig. 4.2, *a*) has been shown to bloom from early to late summer in Lake Holzmaar, Germany (Baier *et al.*, 2004). This is in agreement with Stoermer & Yang (1970) and Stoermer (1978). *Cyclotella radiosa* is found to be a dominant component of the summer phytoplankton assemblage in Lakes Superior and Huron (Stoermer *et al.*, 1993). *C. radiosa* is associated with decreased nutrient supply, but according to van Dam *et al.* (1994) it blooms under higher nutrient concentrations. It may therefore reflect a range of trophic conditions from oligotrophic to mesotrophic. Stoermer & Ladewski (1976) suggest that high concentrations of *C. radiosa* coincide with a warmer climate.

Cyclotella ocellata (Fig. 4.2, *b*) has an ambiguous ecology, occurring in oligotrophic to eutrophic conditions (Wunsam *et al.*, 1995; Lotter *et al.*, 1998; Rioual, 2000; Brüchmann & Negendank, 2004). It is the dominant component in the stratified waters from late spring to summer in a number of lakes, *e.g.* Lake Erie, Lewis Lake Upper Kalmath Lake, Oregon and the Great Lakes, USA (Yellowstone region; Kilham *et al.*, 1996; Bradbury, 2004). It has also been found in weakly stratified, eutrophic lakes (Wunsam, *et al.*, 1995; Lotter *et al.*, 1998). Lake Balaton, in Hungary, from which the type material of *C. ocellata* comes, is typical of such an environment.

Cyclotella rossii (Fig. 4.2, *c*) is little referred to in the literature. It forms part of the *rossii–tripartita–comensis* complex. Like many other small *Cyclotella* species, *C. comensis*, for example, is regarded by many as a typical summer stratifying diatom (Crumpton & Wetzel, 1982) and has been used to reconstruct past summer temperature from Alpine lakes (Hausmann & Lotter, 2001).

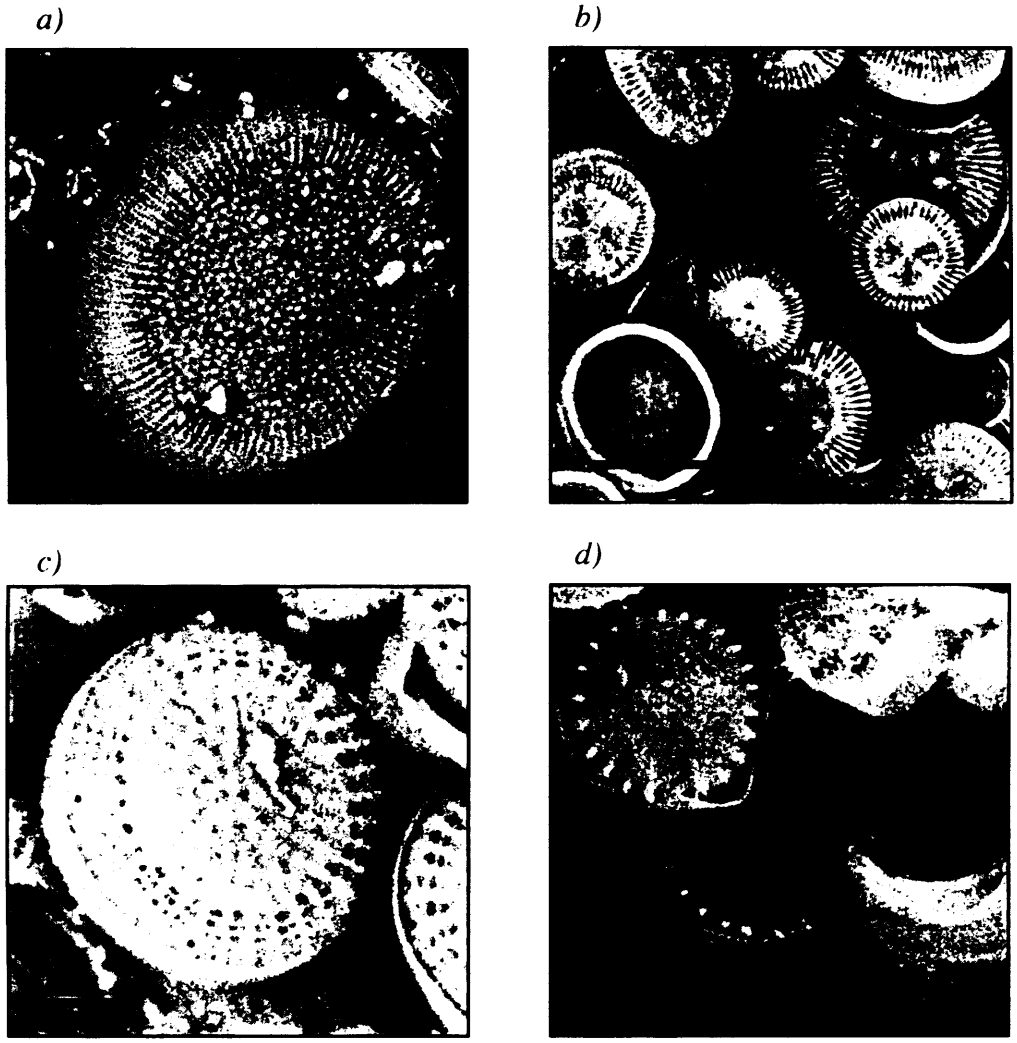

Fig. 4.2: SEM topographic images of major phytoplankton in varved sediments of Diss Mere. a) Cyclotella radiosa. . b) Cylotella ocellata c) Cyclotella rossii. d) Stephanodiscus parvus.

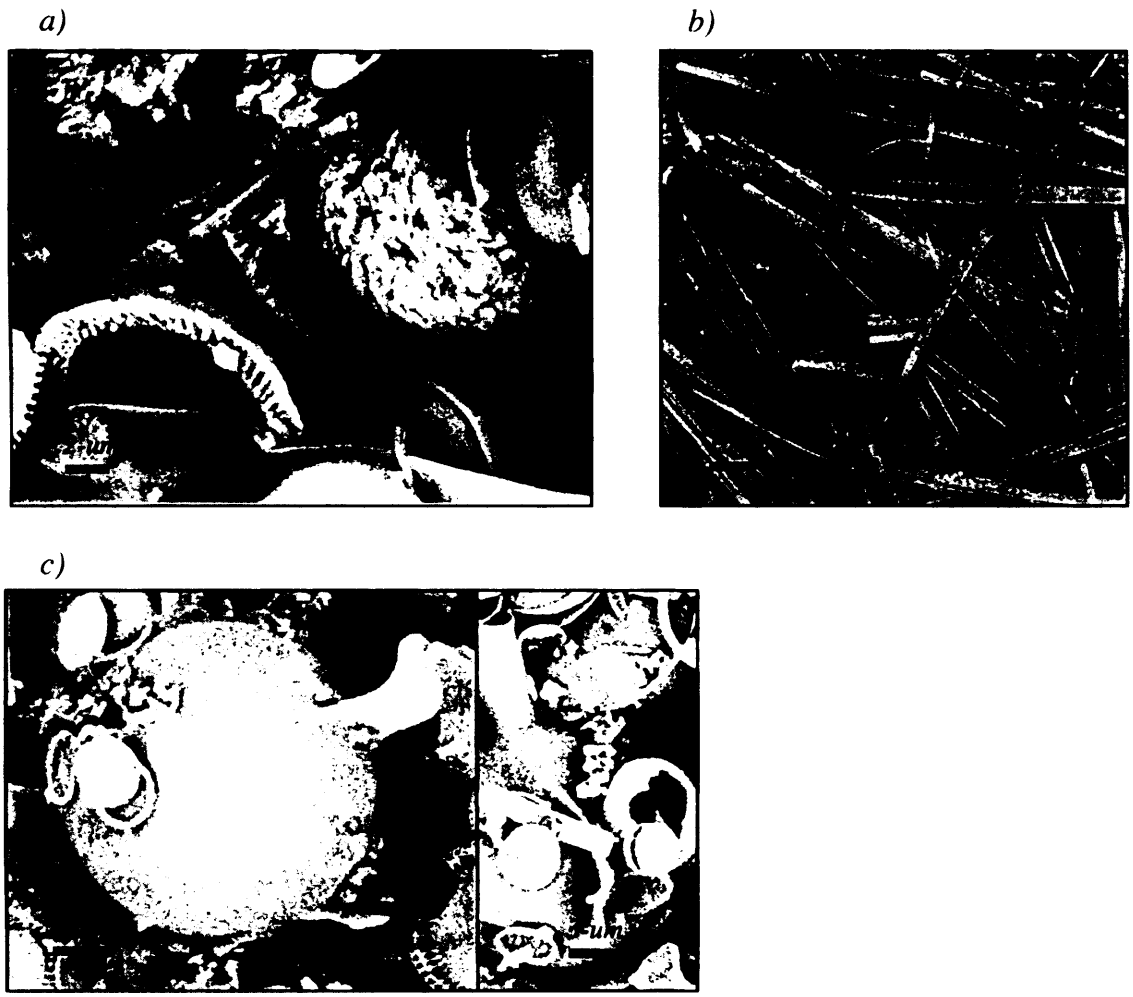

Fig. 4.3: SEM topographic images of major phytoplankton in varved sediments of Diss Mere. a) Phacotus lenticularis. b) Synedra acus var. angustissima and Synedra nanna. c) Chrysophyte cysts.

Stephanodiscus parvus (Fig. 4.2, *d*) shows a significant response to nitrate and silica and is the dominant species when water temperature is just a few degrees above freezing (Rioual, 2000). This is consistent with known ecology that these species are low light and spring blooming (Foy & Gibson, 1993). It has been found in nutrient-rich waters (Bennion 1994; Wunsam & Schmidt, 1995). Rioual (2000) shows that *S. parvus* is optimum in oligo-mesotrophic or mesotrophic conditions in lakes of the Massif Central, France. Similar results were also obtained in North America by Hall & Smol (1992) and Reavie *et al.* (1995).

Synedra acus var. *angustissima* and *S. nana* (Fig, 4.3. *b*) show ecological preference for meso-eutrophic waters (Rioual, 2000; Nõges, 1997 Lake, Yaskhan). Both have maximum development in spring overturn in a number of Swiss, German and American lakes (Lotter 1989). Of all diatoms studied, *S. acus* is the best competitor for phosphorus (Tilman 1981; Kilham 1984) and a poor competitor for silica; it therefore grows best when Si is not limiting and is a high Si:P species, *i.e.* it occurs during spring overturn.

Chrysophytes (golden brown algae) (Fig. 4.3, *c*) represent a predominantly planktonic group of algae found in oligotrophic lakes. The systematics, ecology, and physiology of the Chrysophyceae have been reviewed by a number of authors (the most principal being, Smol, 1988). They are identified in lake sediments by the production of a siliceous resting stage known as a stratospore and the shedding of scales from their vegetative cells. Peglar *et al.* (1984) find that chrysophyte cysts occur in Diss Mere with higher frequency in organic-rich laminae. They are likely to be formed after the peak of the Chrysophyceae crop and although the timing of this is species-dependent (Simola, 1977), they are mostly deposited at the start of autumn (Tippett 1964, Batterbee, 1981; Starmach, 1985).

Phacotus lenticularis (Fig. 4.3, *a*) development normally starts in early summer, immediately after the clear-water phase, and ends at the beginning of autumn. Mass abundances are typically recorded in July and August. It is capable of producing high cell concentrations in eutrophic to polytrophic conditions, but shows its highest densities

in eutrophic waters. *Phacotus* spp. are found in all waters of the lake, including the anoxic hypolimnion. The records of *Phacotus* spp. appear increasingly regular in the plankton lists of waters whose trophic degree begins to increase from a mesotrophic to a slightly eutrophic state. Lake Zurich and Lake Constance at the end of the 19th century and the beginning of the 20th century showed no evidence of *Phacotus* spp.. However, its subsequent appearance can to be linked to eutrophication of these lakes. Concentration of phosphorus does not appear to have any real limiting effect on the growth of *Phacotus* as populations appear to use micro-habitats of excrements of zooplankton (Bergquist & Carpenter, 1986). *Phacotus* could also obtain nutrients by passing through the digestive tract of zooplankters (Porter, 1973). It is thought that ingested cells leave the intestine of grazers intact because of their calcite lorica. Their resistance to summer grazers may, in part, explain their summer abundance.

5. Results and interpretation

In this chapter, sedimentary logs of the piston cores are presented and macro-scale primary and secondary sedimentary features are described. The mineralogy and geochemistry of the varved sediments are also reported. Next varve microtexture and phytoplankton succession are examined and their depositional significance discussed. Finally, constructed palaeoclimate and palaeoproductivity proxies are examined for dominant periodicities.

5.1. Core description and correlation

The reader is referred to Appendix IV for detailed descriptions of sediment cores from holes DISS A, B & C. Simplified logs of these cores and correlations between them are shown in Fig. 5.1 (see Fig. 5.2 for key to logs).

5.1.1. Core disturbance

The piston cores are mostly undisturbed, although, the top few centimetres of some cores were disrupted (e.g. water-logged sediment in DISS A-6, at 16.50-16.54 mblw; upbowed laminae in DISS A-6, at 16.54-16.60 mblw, DISS B-7, at 17.09-17.14 dblw, Fig. 5.3), or composed of sediment 'chippings' that sit in erosive contact with sediment core below (DISS A-8b, at 0 to 10-cm Fig. 5.4). In addition, disturbance to sediment fabric made correlations of laminated core difficult between 16.99-18.50 mblw, as for example, DISS A-8a, where physical jarring of the core barrel during sediment drives caused a loss of fine structure blurring layer contacts and DISS A-8b, where sediment between 17.64-18.01 mblw has been considerably thickened by micro-folding (Fig. 5.5), *e.g.*, contorted, upbowed and occasionally overturned. McCoy (1985) and Ruddiman *et al.* (1987) attribute such features seen in DSDP cores to anomalously accelerated upward motion of the piston-head during drives, stretching and upbowing sediment in the process and/or the piston being pulled to the top of the core barrel during retrieval, following only a partial stroke of the core barrel.

5. Results and interpretation

In this chapter, sedimentary logs of the piston cores are presented and macro-scale primary and secondary sedimentary features are described. The mineralogy and geochemistry of the varved sediments are also reported. Next varve microtexture and phytoplankton succession are examined and their depositional significance discussed. Finally, constructed palaeoclimate and palaeoproductivity proxies are examined for dominant periodicities.

5.1. Core description and correlation

The reader is referred to Appendix IV for detailed descriptions of sediment cores from holes DISS A, B & C. Simplified logs of these cores and correlations between them are shown in Fig. 5.1 (see Fig. 5.2 for key to logs).

5.1.1. Core disturbance

The piston cores are mostly undisturbed, although, the top few centimetres of some cores were disrupted (e.g. water-logged sediment in DISS A-6, at 16.50-16.54 mblw; upbowed laminae in DISS A-6, at 16.54-16.60 mblw, DISS B-7, at 17.09-17.14 dblw, Fig. 5.3), or composed of sediment 'chippings' that sit in erosive contact with sediment core below (DISS A-8b, at 0 to 10-cm Fig. 5.4). In addition, disturbance to sediment fabric made correlations of laminated core difficult between 16.99-18.50 mblw, as for example, DISS A-8a, where physical jarring of the core barrel during sediment drives caused a loss of fine structure blurring layer contacts and DISS A-8b, where sediment between 17.64-18.01 mblw has been considerably thickened by micro-folding (Fig. 5.5), *e.g.*, contorted, upbowed and occasionally overturned. McCoy (1985) and Ruddiman *et al.* (1987) attribute such features seen in DSDP cores to anomalously accelerated upward motion of the piston-head during drives, stretching and upbowing sediment in the process and/or the piston being pulled to the top of the core barrel during retrieval, following only a partial stroke of the core barrel.

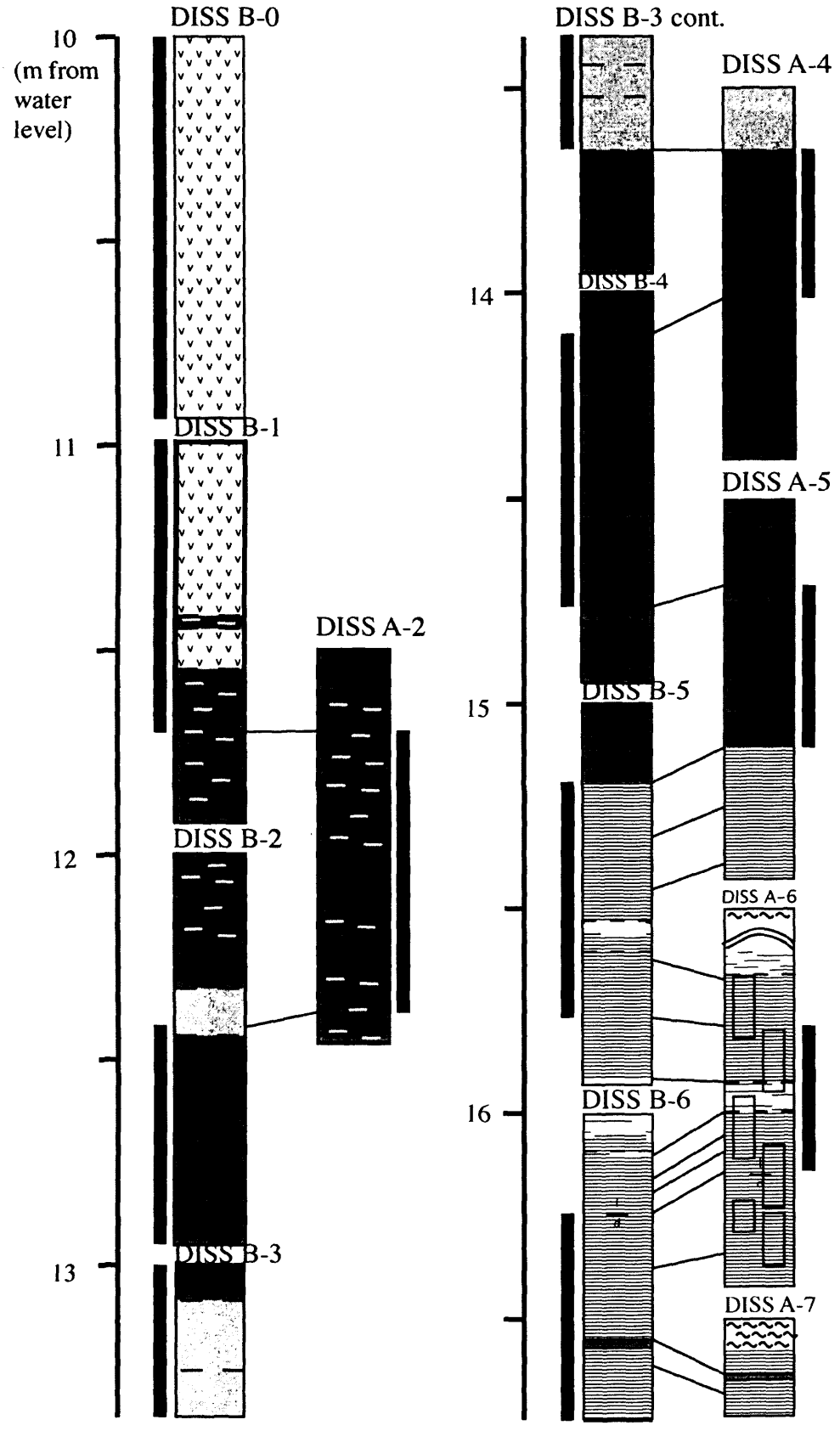

Fig. 5.1: Stratigraphic logs of piston cores.

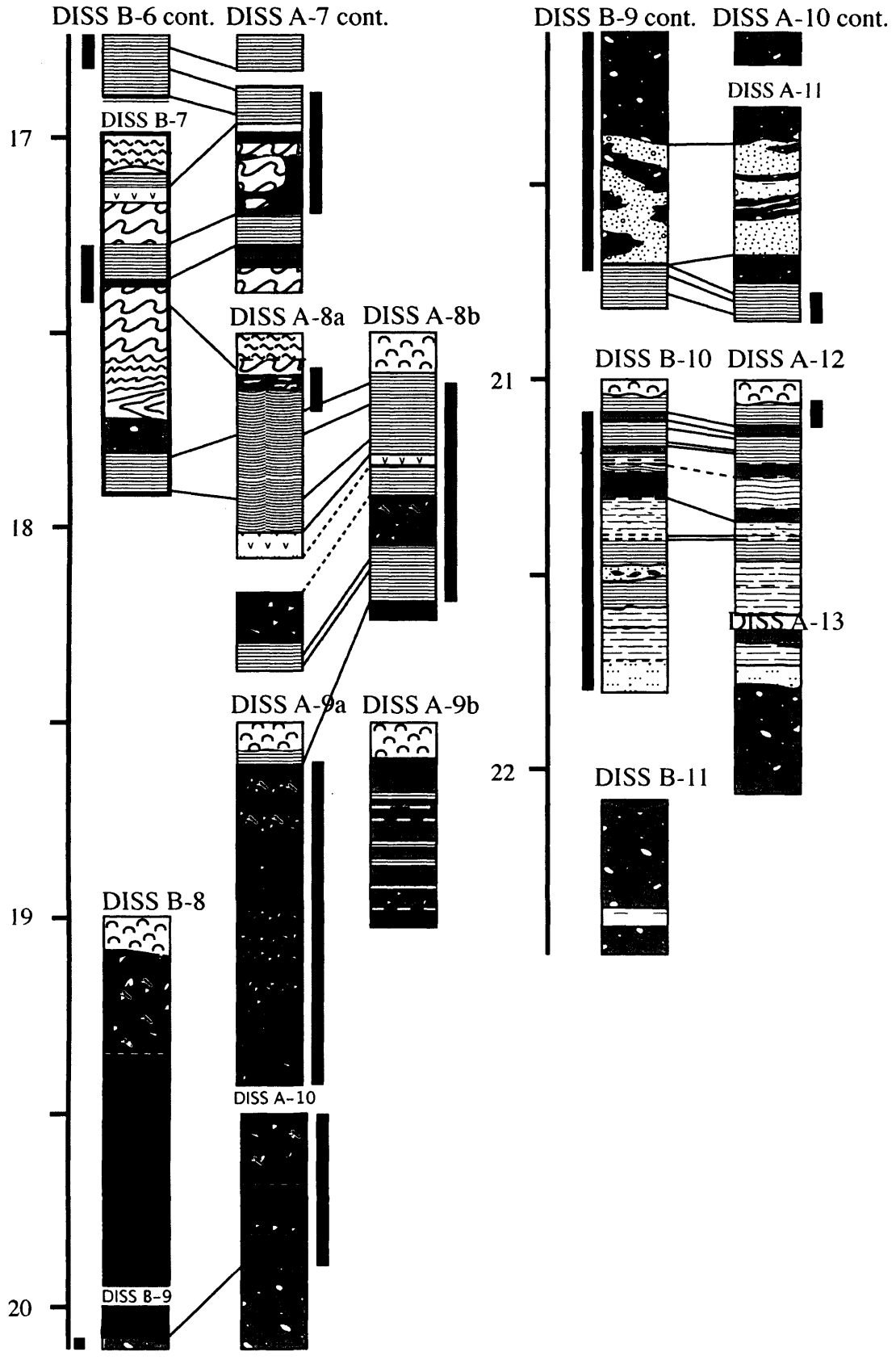

Fig. 5.1 (cont.): Stratigraphic logs of piston cores.

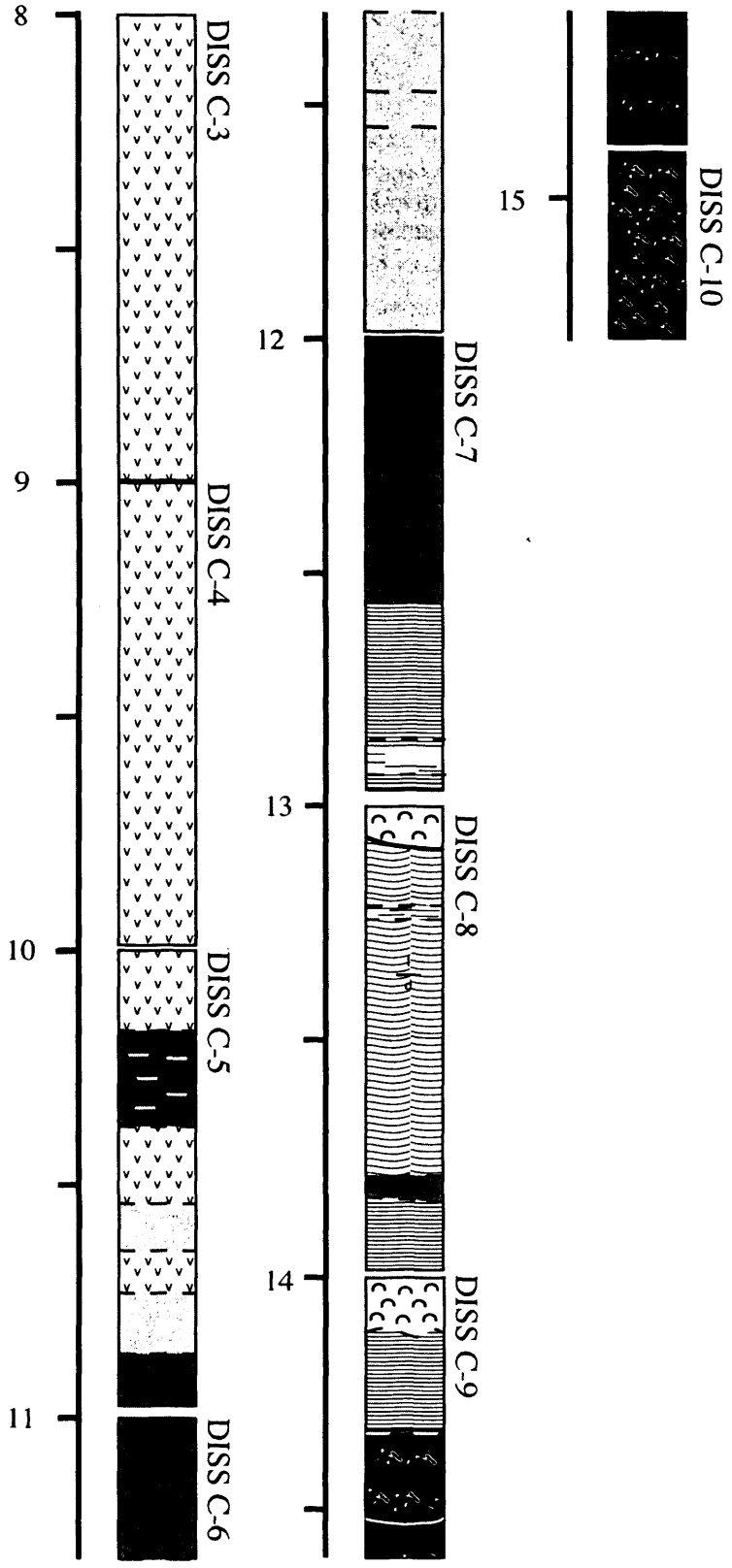

Fig. 5.1 (cont.): Stratigraphic logs of piston cores.

Livingstone piston cores, Diss Mere.

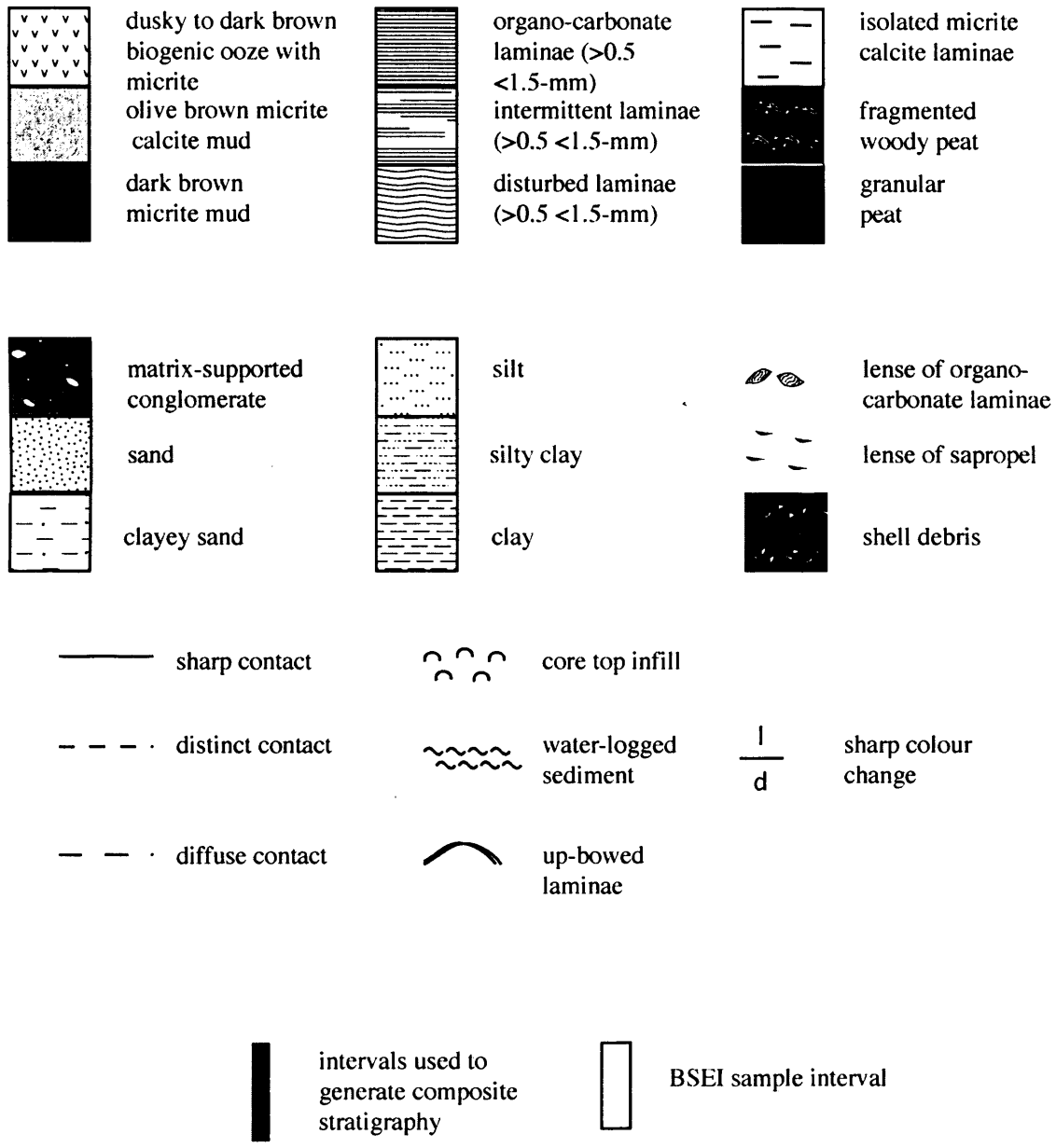

Fig. 5.2: Key to stratigraphic logs.

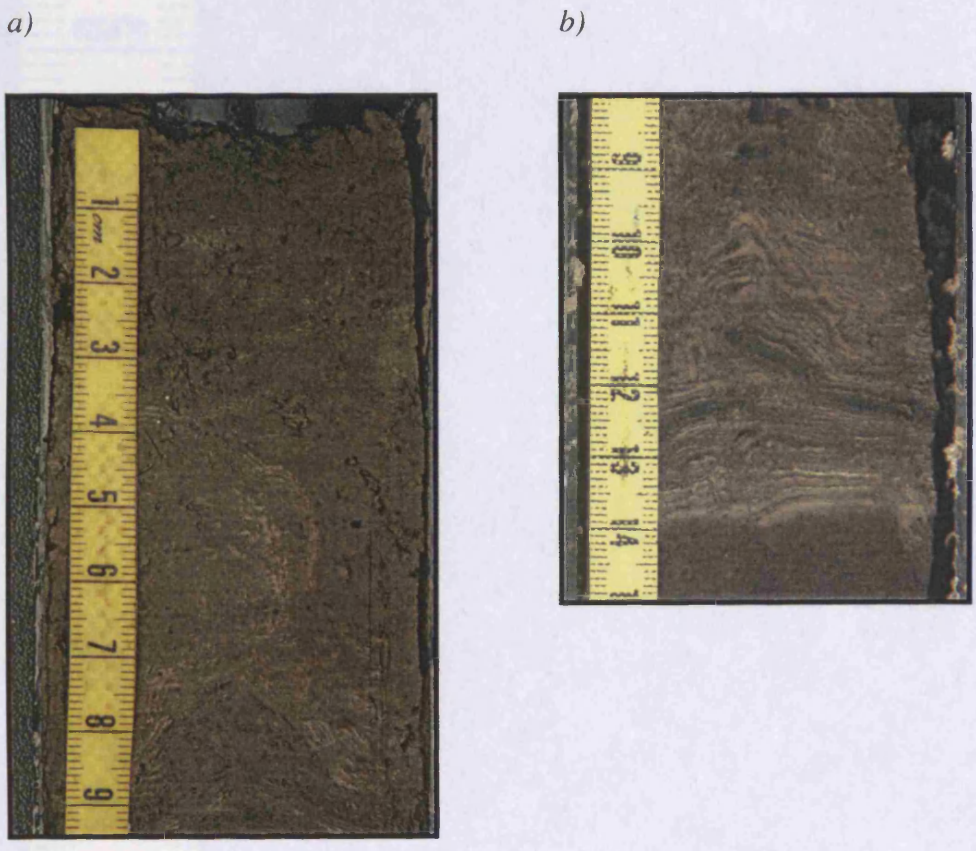

Fig. 5.3: a) Destruction of sediment fabric due to water logging in DISS A-6 between 0 to 4-cm. Upbowed laminae at 4 to 9.5-cm. b) Upbowed laminae in DISSB-7 at 9.5 to 14-cm.

Fig. 5.4: Sediment chippings sit in erosive contact with sediment core below in DISS A-8b.

a)

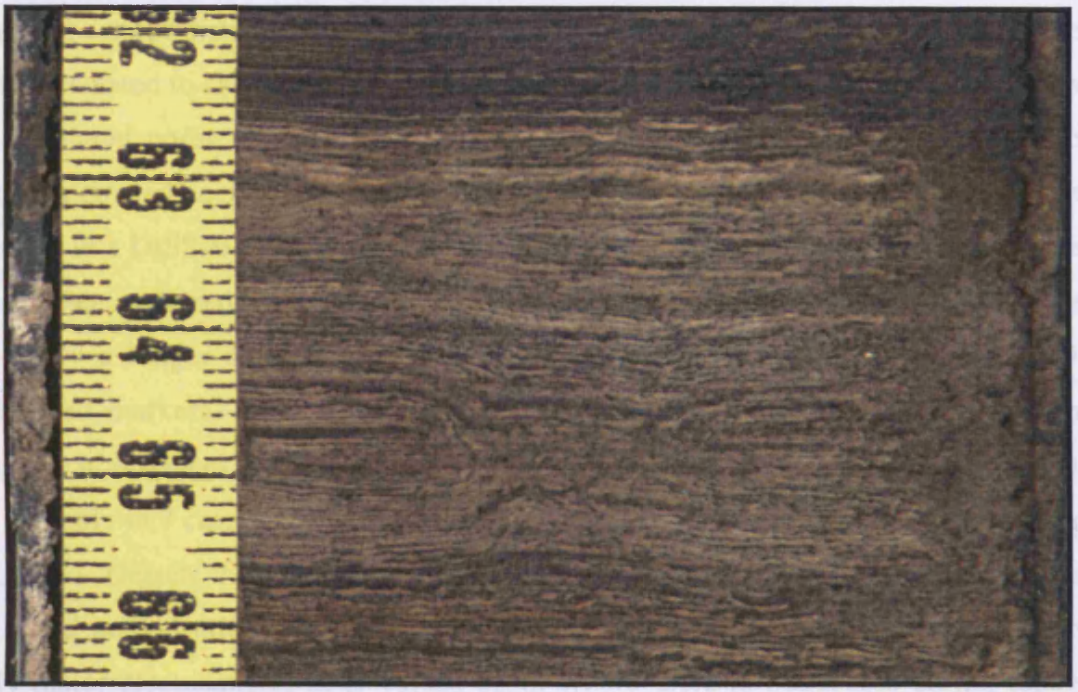

b)

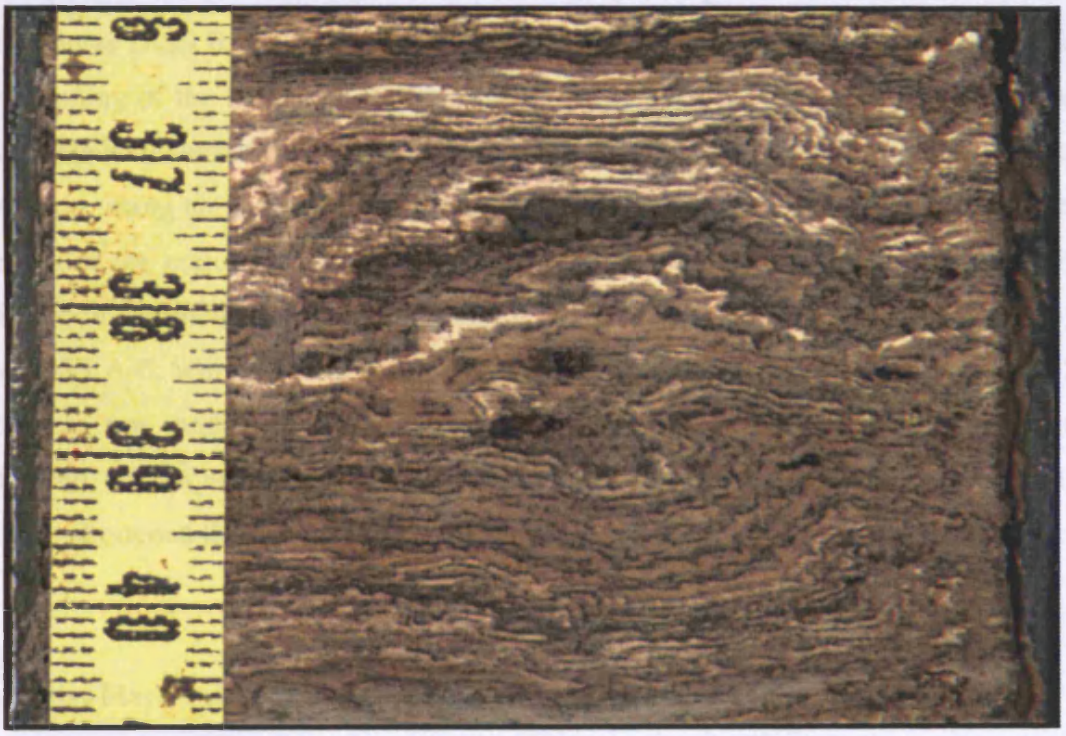

Fig. 5.5: a) Loss of fine structure to laminated fabric in DISS A-8a due to physical jarring of core barrel.
b) Micro-folding of laminated fabric thickens interval in DISS A-8b.

The presence of millimetre-scale laminations affords an opportunity to assess the degree of coring-related disturbance. Following the procedure of Lotter *et al.* (1997a), *Q*-values were calculated to assess discrepancies in thickness between individual marker horizons in correlated cores between 15-17 mblw. This was done by dividing the distance between two adjacent markers in a DISS-A core by the distance between the same markers in a DISS-B core (see Fig. 5.6). The results are shown in Fig. 5.7. Here, values <1 indicate more sediment between the same markers in DISS B cores, whereas values >1 imply a longer distance between markers in DISS A cores. From a total of 94 correlated markers, 54 *Q*-values (57.5%) have values <1, *i.e.* suggesting that the majority of distances are longer between markers in hole DISS B. 33 *Q*-values (35%) are >1 and only in 7 cases (7.5%) are the distances between markers identical in both cores, *i.e.* $Q = 1$. Despite the absence of constant *Q*-values, the majority of *Q*-values are close to 1, and no real difference exists between the majority of correlated thicknesses. The only major discrepancies in *Q*-values occur where there is noticeable coring-related disturbance to the sediment fabric, *e.g.*, the high (>1.5) *Q*–values for markers D55 to D59 in cores DISS B-6 and DISS A-6 are a coring artefact that can be attributed to mid-core thinning of the laminated fabric in DISS B-6. Given the lack of significant visual coring-related disturbance, and that the cores were recovered with only ~10 m horizontal separation, using an identical set-up, the slight differences in vertical distance between markers in the majority of these cores are of primary origin, that is, due to spatial variation in sedimentation-rate, and generally are not coring artefacts. Unfortunately, core DISS A-6, which represents undeformed sediment fabric between markers D55-D59, was not made available to this project before geochemical analyses were performed. Consequently, it was not used in the generation of a composite stratigraphy. This has shortened the composite stratigraphy by ~7 cm.

5.1.2. Diss Mere's stratigraphy

The spliced core of Diss Mere's profundal infill is shown in Fig. 5.8. It contains eleven metres of sediment, here, divided into seven Lithozones (A-G), comparable to the

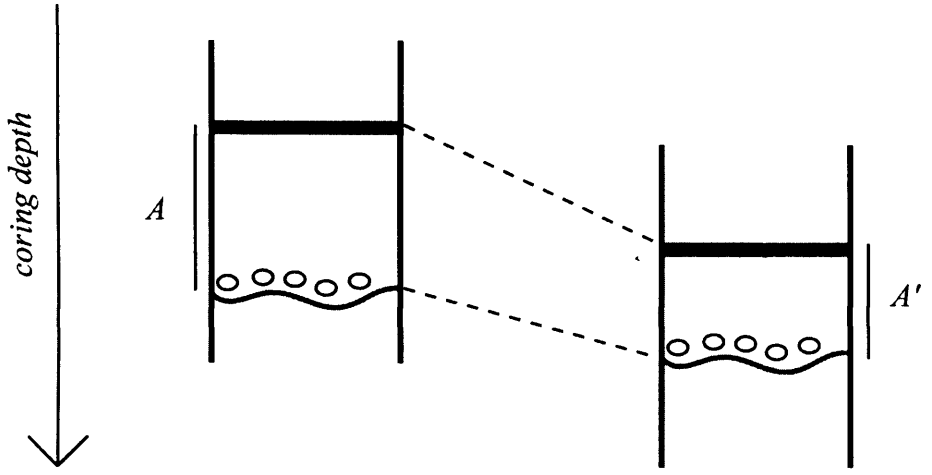

$$\textit{Q value} = \frac{A}{A'}$$

when ..... $A' < A$, $Q = > 1$

..... $A' > A$, $Q = < 1$

..... $A' = A$, $Q = 1$

Fig. 5.6: Cartoon illustrating how Q-values given in Fig. 5.7 are calculated as the ratio of the vertical separation between two adjacent markers horizons from correlated cores.

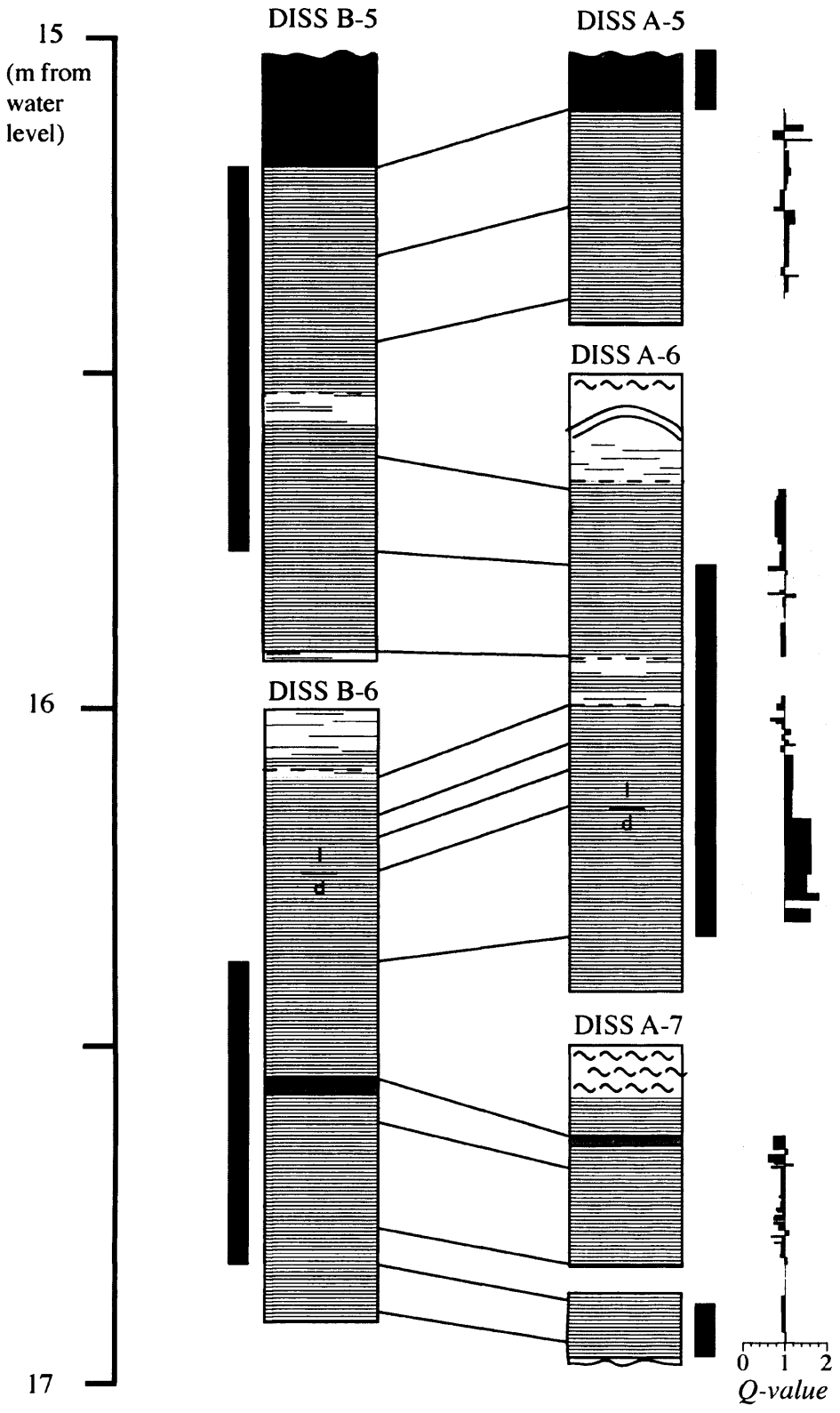

Fig. 5.7: Q-values representing relative difference between two stratigraphic makers in adjacent cores (for details see text).

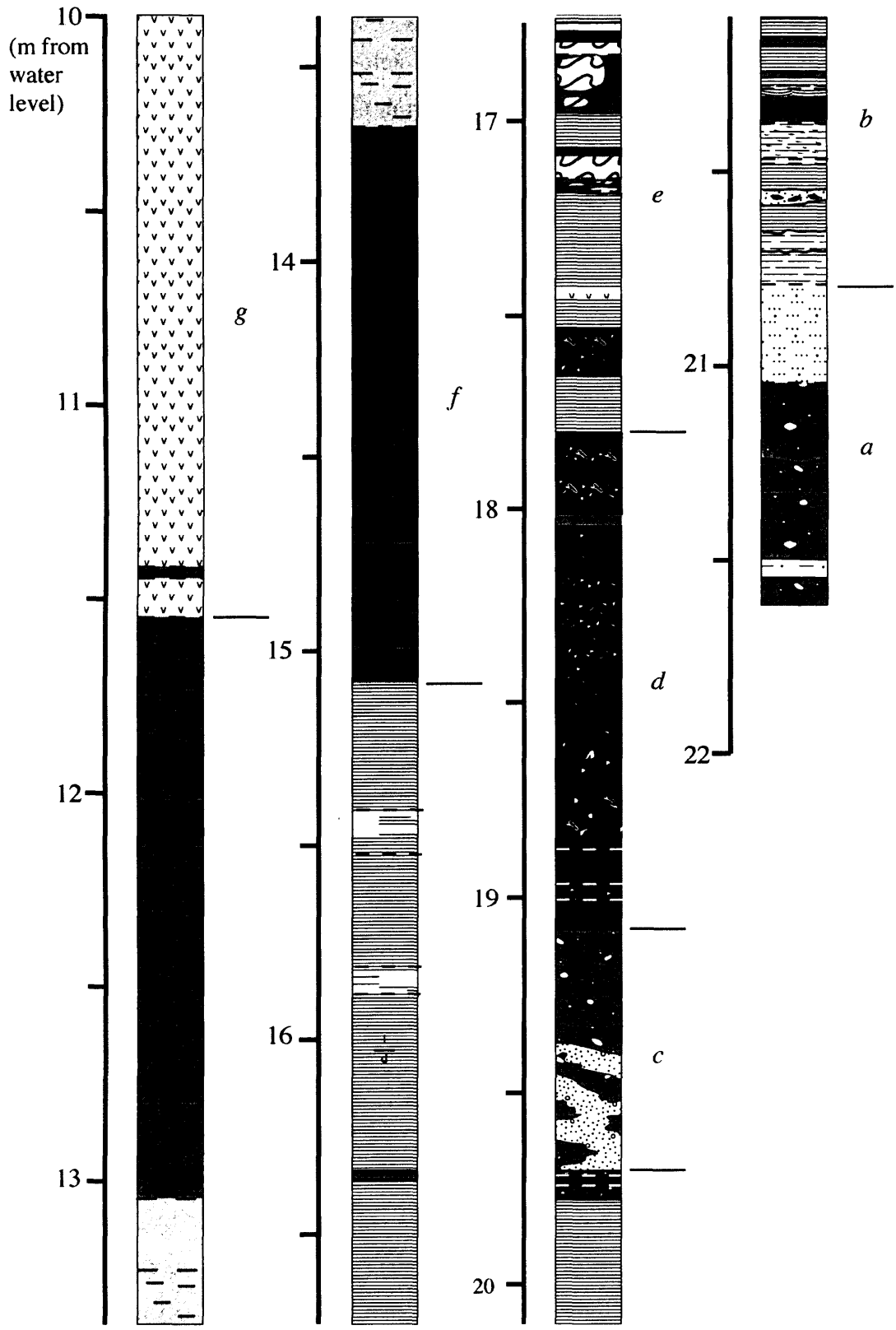

Fig. 5.8: Composite stratigraphy for DISS A/B. Key to lithostratigraphy given in Fig. 5.2.

stratigraphy reported by Peglar *et al.* (1989). The sequence is characterised by two minerogenic/organic sediment cycles (Lithozones A/B and C/D-G). Minerogenic sediment (Lithozones A and C) is composed of plastically folded matrix-supported conglomerates and quartzo-calcareous clays and sands, similar in character to the Fenland 'Crowland Bed' (Fig. 5.9; Booth, 1982; Gozzard, 1982). In each case, the upper transition to organic-rich sediment is sharp; both contacts are probably depositional hiatus. The lower minerogenic series (Lithozone A) passes directly into laminated organic muds (lithozone B, 19.78-20.82 m). The upper minerogenic series (Lithozone C) is succeeded by a thick interval of fragmented granular to woody peat (1.27 m) containing abundant horizons of the gastropods *Valvata cristata* and *Bithynia tentaculata.* This in turn, lies in sharp contact with a second series of varved muds (Lithozone E, cf. 15.09-17.78 m). The remainder of the sequence (Lithozones F & G) is composed of structurally homogeneous very organic-rich muds (>20% amorphous organic matter, *i.e.* lake-gyttja), with occasional parallel micrite carbonate laminae horizons (*e.g.*, Fig. 5.10). Their structure and composition are a product of hyper-eutrophication of the lake's waters from the Iron Age (~ 2500 Cal. BP), a direct result of a series of changes in land-use and agricultural practices culminating in the founding of the town of Diss (cf. Wiseman *et al.*, 1798; Peglar *et al.*, 1989).

Varved sediments (Lithozones B and E) are composed of sub-millimetre and millimetre-scale alternations between light micrite calcite-rich muds and dark diatomaceous organic-rich muds. Alternate bundling of thicker and thinner laminae is manifested in centimetre-scale colour banding (*e.g.* Fig 5.11). The laminated sediment fabric is discussed in detail in Section 5.3. The continuity of laminae is disrupted by dark centimetre-scale slump deposits composed of calcareous mud (*e.g.*, 16.34-16.36 m, Fig. 5.12), centimetre- to decimetre-scale fragmented, granular peats, and bioturbation (*e.g.*, intermittently laminated horizons, cf. 15.44-15.50 m, Fig. 5.13). The continuity of the varved sediment of Lithozone B is also disrupted by centimetre- to decimetre-scale horizons of quartzo-calcareous silty-sands and silty-clays, containing semi-indurated, millimetre-scale 'rip-up' clasts of varved sediment (Fig. 5.14), as well as marked

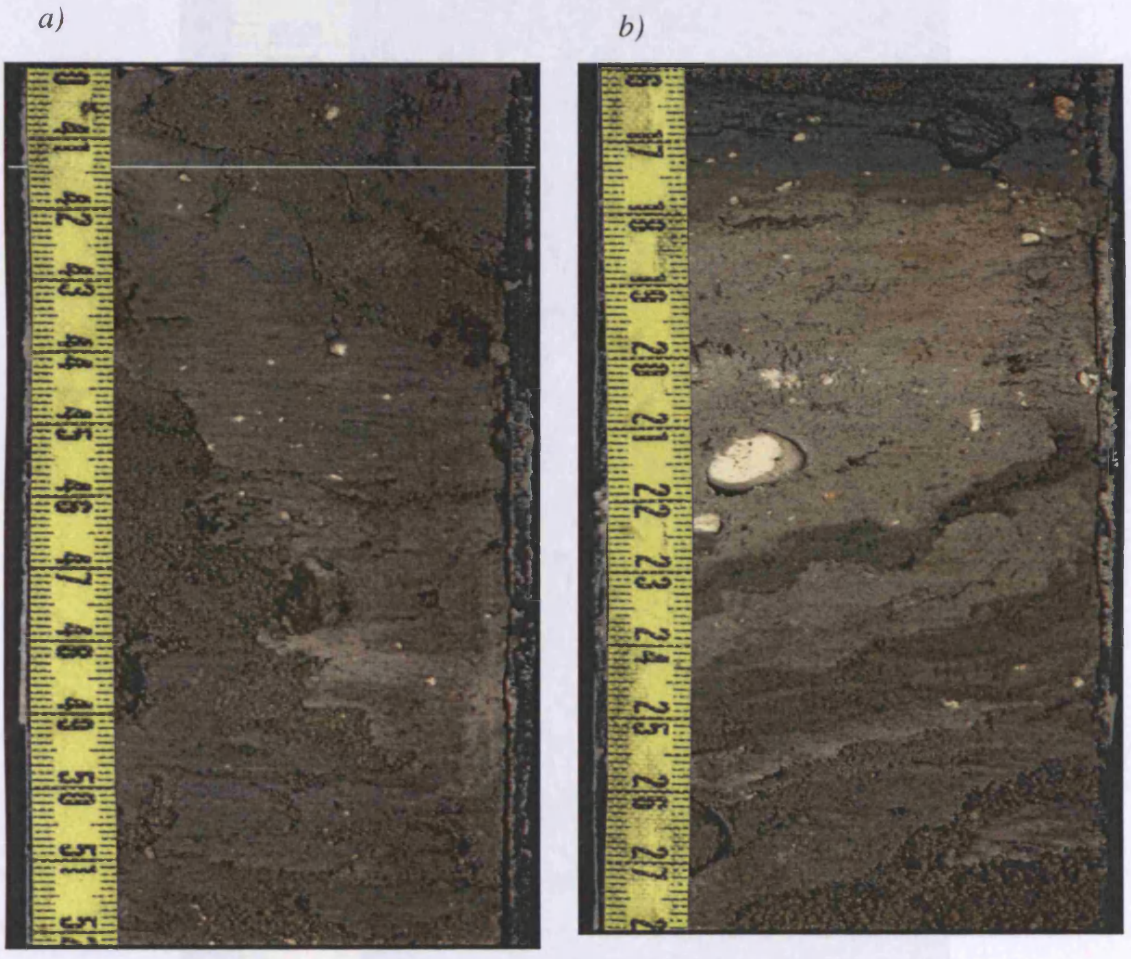

Fig. 5.9: 'Crowland Bed' deposit in a) DISS B-9 b) DISS A-11.

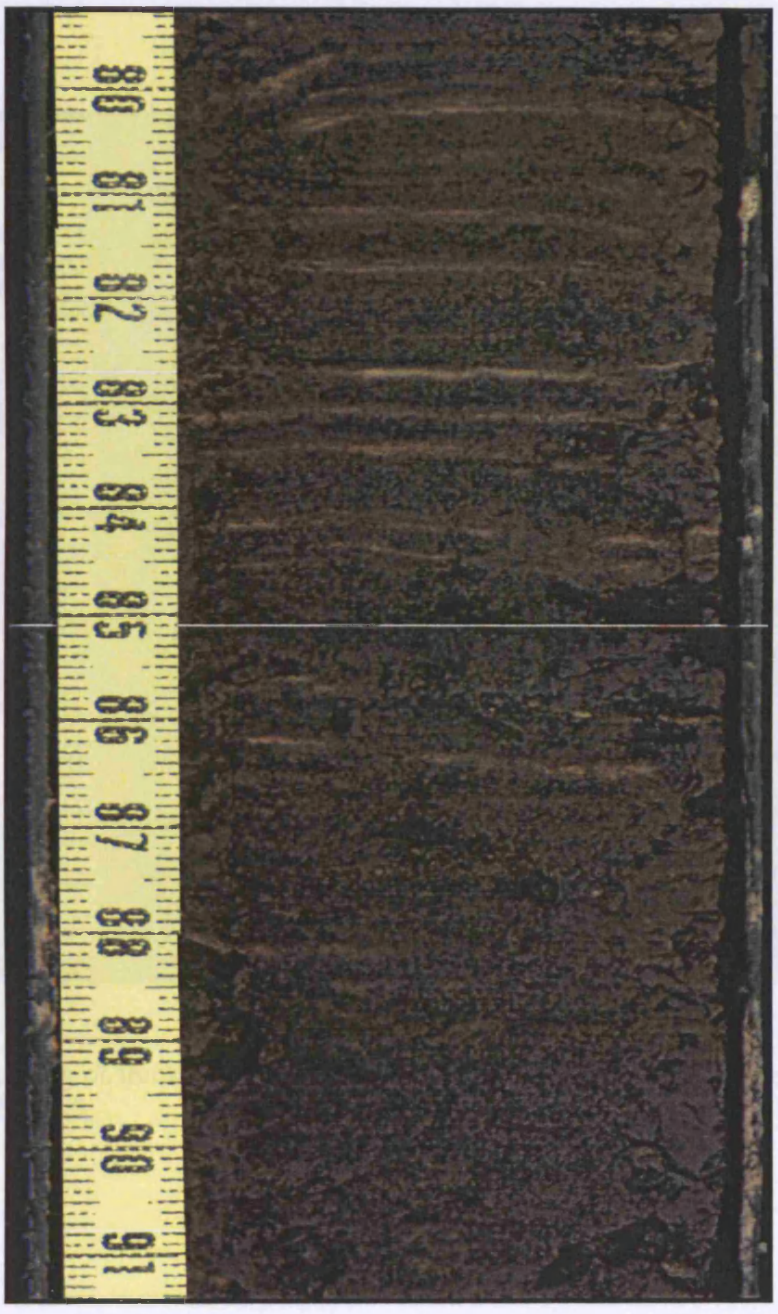

Fig. 5.10: Interval with parallel micrite carbonate laminae, core DISS B-1.

Fig. 5.11: Bundling of thicker and thinner varves manifested as centimetre-scale colour banding in DISS B-5.

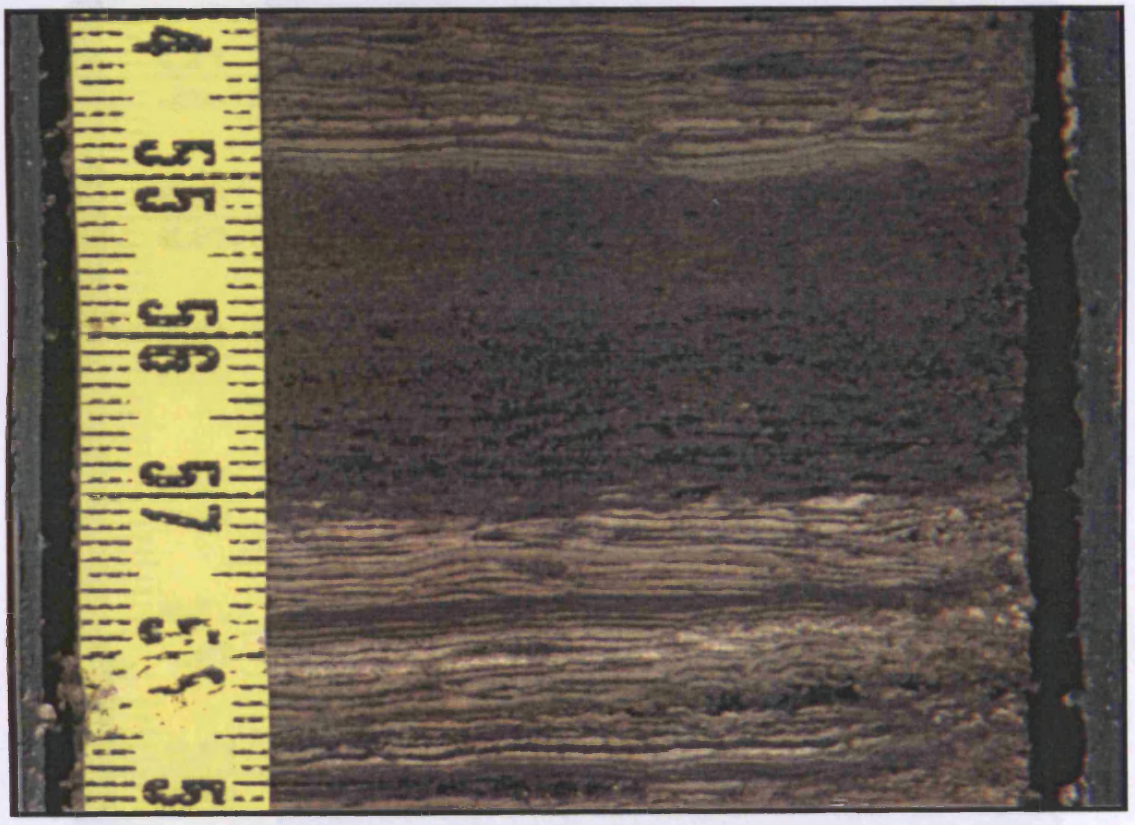

Fig. 5.12: Slump deposit disrupting continuity of laminated fabric in DISS B-6.

Fig. 5.13: Bioturbated laminated sediment in DISS B-5.

a)

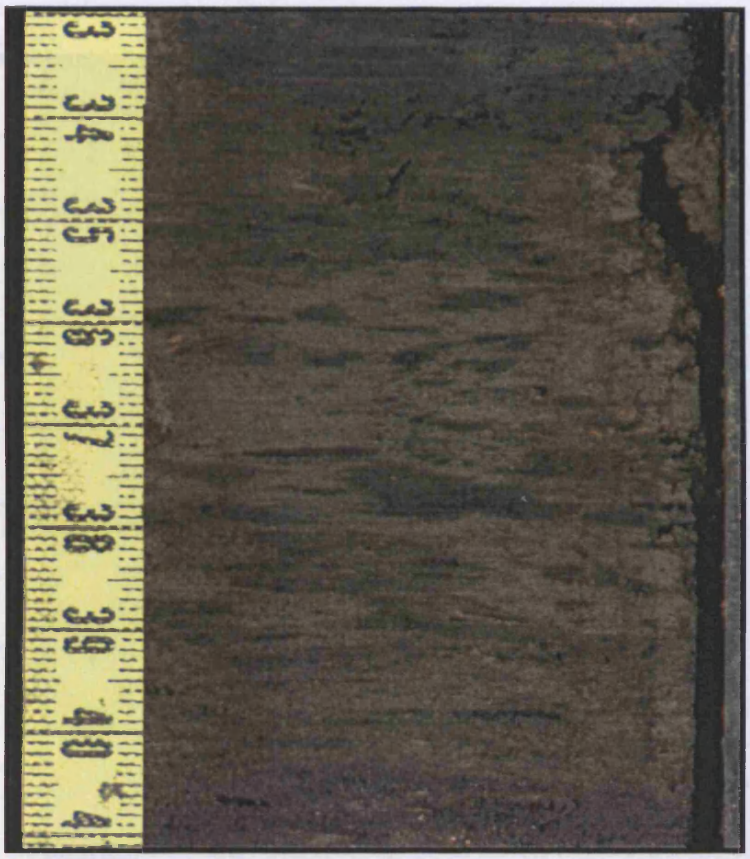

b)

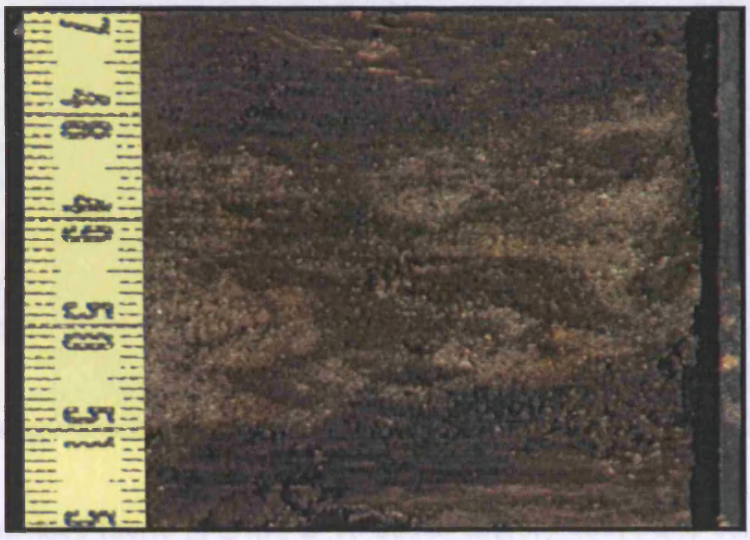

Fig. 5.14: DISS B-10 a) Gray silty-clay containing dark sapropel lenses. b) Olive brown silty-sand containing lenses of laminated micrite calcite mud.

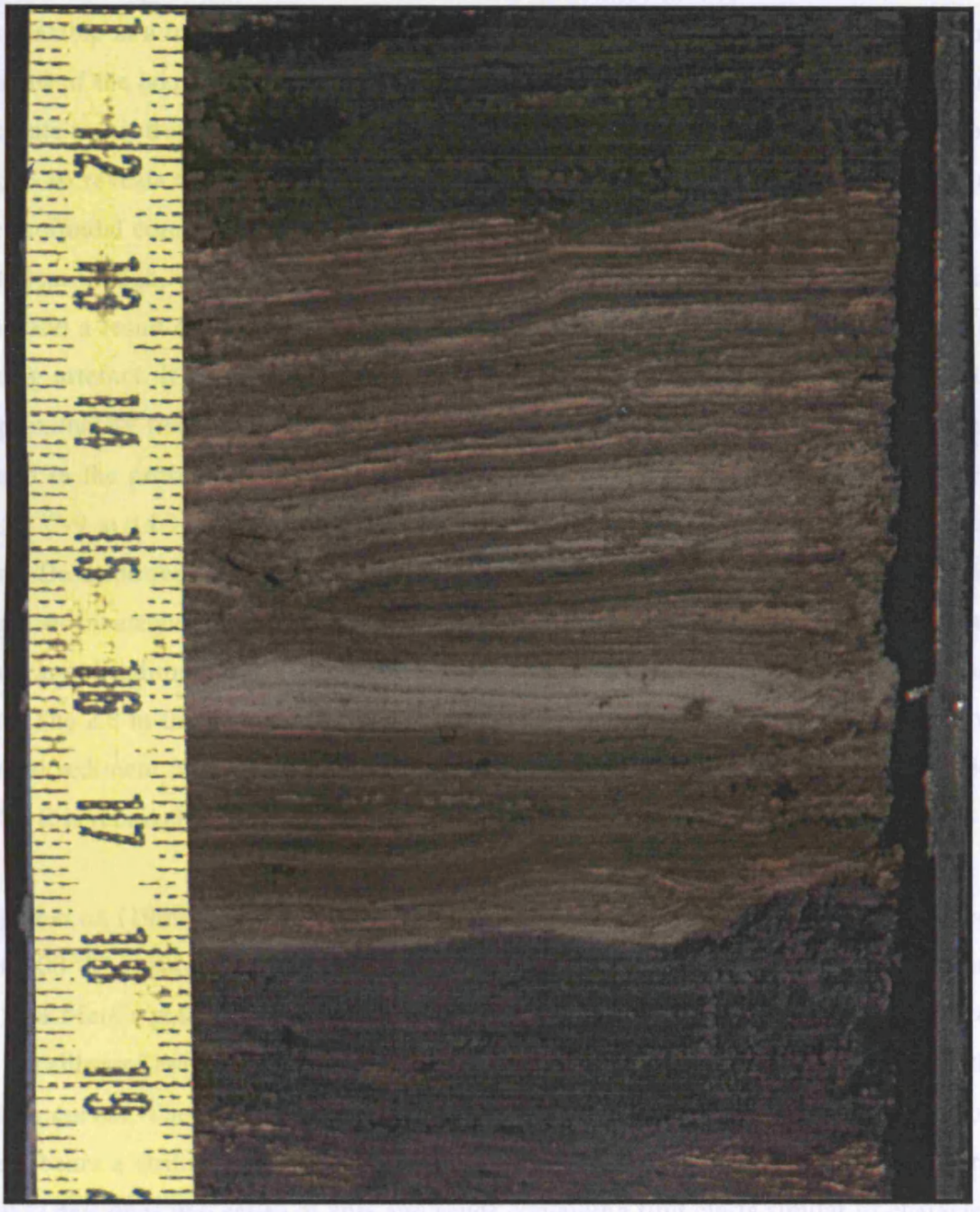

Fig. 5.15: Laminated fabric of DISS B-10 bound sharply above and below by organic slump deposits. Marked truncation at 18-cm and within laminated horizon.

truncation (Fig. 5.15). A visual comparison of the profundal stratigraphy to sediment cores from hole DISS C reveal that the majority of the profundal sediment profile is correlatable at a millimetre- to centimetre-scale across more than 70 m to the northern reaches of the lake (Fig. 5.16). The loss of overlapping cores from this hole restricts an accurate reconstruction of stratigraphic thickness at this location. However, inspection of Fig. 5.16 reveals that the vertical distance between the majority of marker horizons in the profundal core are noticeably larger than their equivalents in the northern core. It is not clear though, whether an apparent reduced sedimentation in the north of the lake is real, and a result of sediment focusing (Lehman, 1975; Davis *et al.*, 1984) or simply a coring artefact. It is noteworthy that the main laminated interval in hole DISS C sits approximately two and a half metres higher in the stratigraphy than the same interval found in the profundal core (Fig. 5.7). In addition, a significant hiatus exists in core DISS C-9 at 14.3 mblw, represented by over one metre of sediment in the profundal core. Descriptions of sediment samples recovered from the Woolworth Core (private engineer investigation, not shown here) on the north-eastern flank of the lake confirms that varved sediment also occurs at a depth of 13 m in the north-eastern margin of the lake. The 2.8 m-thick laminated interval found here is more comparable to the 2.7 m of varved sediment found in the profundal core, implying that the hiatus found in the hole DISS C is relatively localised.

Peglar *et al.* (1989) propose that the base of Diss Mere's 11 metre record was deposited >10,000 ^{14}C yrs. ago (see Fig. 5.17, b); this chronology was established by comparison of Diss Mere's pollen stratigraphy to East Anglia's regional pollen curve, age-calibrated by uncalibrated radiocarbon dates of non-calcareous sediments from other lake sites with pollen curves. The succession at Lopham Little Fen, a small fossil lake 8 km west of Diss, bears a striking resemblance to the stratigraphy found in Diss Mere. Tallantire (1953) describes two series of silts and sands containing flint clasts similar in character to the minerogenic sediment of Lithozones A & C, each overlain by 'organic lake' muds. On stratigraphic and fossil pollen grounds, he attributed the base of the sequence to the Older Dryas-Allerød-Younger Dryas climate oscillation. At Diss, a Late-Glacial age for pollen zones DMP 2 and 3 seems improbable on the basis of the known regional

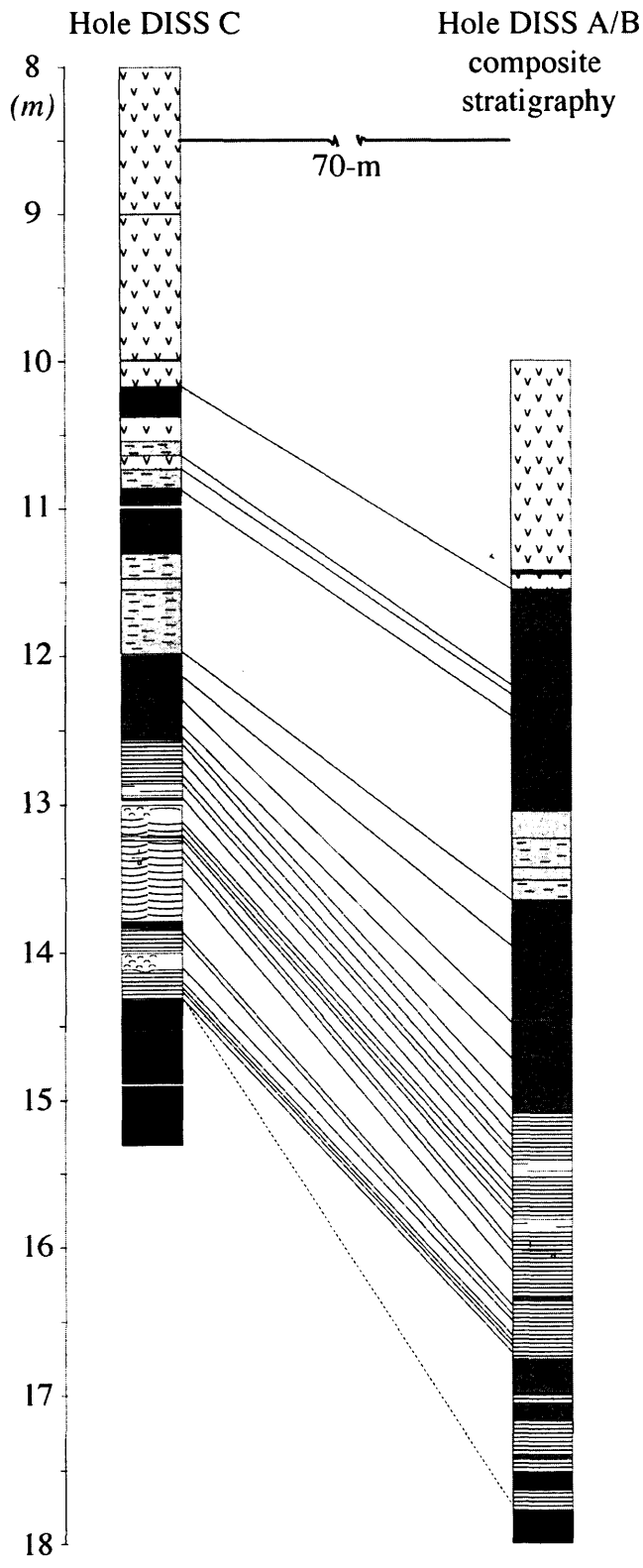

Fig. 5.16: 70-m correlation across lake between holes DISS C and DISS A/B. Key to lithostratigraphy given in Fig. 5.2.

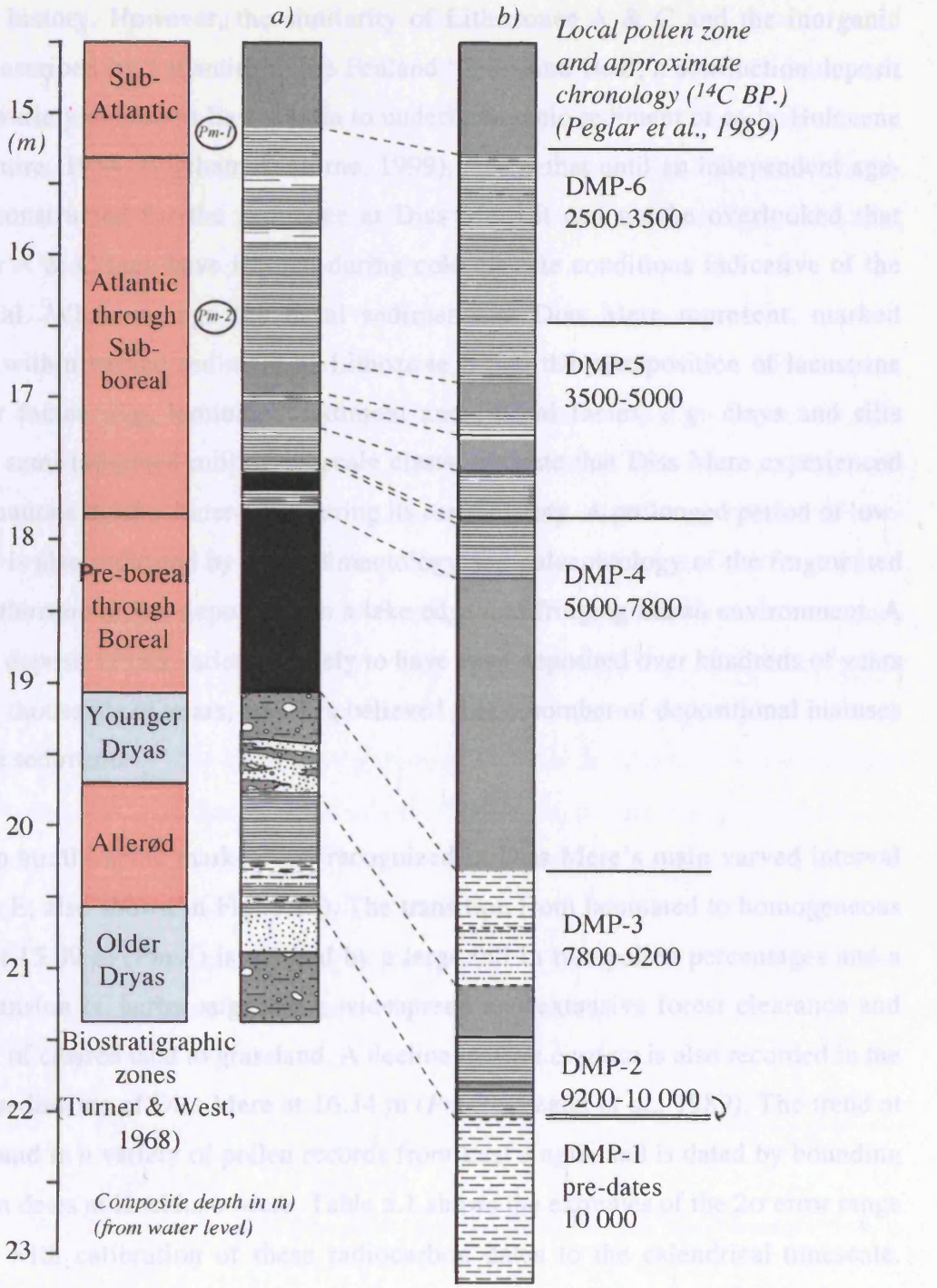

Fig. 5.17: Correlation of two profundal cores from Diss Mere. a) Stratigraphy from this study with reintrepretation of age-model mainly on stratigraphic grounds b) stratigraphy of Peglar et al. (1989) with age-model based on correlation of Local Pollen record with other radiometrically dated East Anglian pollen records. Circled codes, Pm-1 & Pm-2 refer to the stratigrahpic location of two pollen markers (see text for explanation). Key to lithostratigraphy given in Fig. 5.2.

vegetation history. However, the similarity of Lithozones A & C and the inorganic sediment described by Tallantire to the Fenland 'Crowland Bed', a solifluction deposit found at a variety of sites in East Anglia to underlie organic sediment of early-Holocene age (Tallantire, 1954; Boreham & Horne, 1999), means that until an independent age-model is constructed for the sequence at Diss Mere it can not be overlooked that Lithozones A & C may have formed during cold climate conditions indicative of the Late-Glacial. Whatever age the basal sediments at Diss Mere represent, marked truncation within varved sediment of Lithozone B and the juxtaposition of lacustrine deep-water facies, *e.g.* laminated sediment and littoral facies, *e.g.* clays and silts containing semi-indurated millimetre-scale clasts, indicate that Diss Mere experienced rapid fluctuations in lake-water level during its early-history. A prolonged period of low-lake levels is also indicated by the sedimentology and palaeontology of the fragmented peats in Lithozone D, *i.e.* deposition in a lake edge and fringing marsh environment. A ~1 m thick deposit of this variety is likely to have been deposited over hundreds of years rather than thousands of years, and it is believed that a number of depositional hiatuses exist in this sediment.

Two pollen stratigraphic markers are recognized in Diss Mere's main varved interval (Lithozone E; also shown in Fig. 5.17). The transition from laminated to homogeneous sediment at 15.09 m (*Pm-1*) is marked by a large fall in tree pollen percentages and a major expansion of herbs, suggesting widespread and extensive forest clearance and conversion of cleared land to grassland. A decline in *Tilia cordata* is also recorded in the profundal sediments of Diss Mere at 16.34 m (*Pm-2*) (Peglar *et al.*, 1989). The trend at *Pm-1* is found in a variety of pollen records from East Anglia and is dated by bounding radiocarbon dates at Hockham Mere. Table 5.1 shows the extremes of the 2σ error range associated with calibration of these radiocarbon dates to the calendrical timescale. Sedimentation-rate extrapolation using the age range between the bounding calibrated dates suggests that region-wide land clearance is first detected in the sediments of Hockham Mere from the Iron Age at 2480 Cal. B.P. The error range associated with the bounding calendar dates is *ca.* 200 years (at 2σ). Considering the close proximity of Hockham to Diss (~20-km due north-west), the timing of this major region-wide land

clearance is likely to be well within the error associated with the conversion of radiocarbon dates to the calendrical timescale over the time-period concerned. Although, the above dates are considered as open to revision by, *e.g.* by direct radiocarbon dating of suitable material from Diss Mere, the strong correlation of elemental Ca concentration from this interval to the residual ^{14}C record (Stuiver *et al.*, 1998) indicates that the chronology is broadly correct (see Section 5.4).

Tilia spp. pollen frequencies decline in East Anglia from about 5000 Cal. BP onwards, consistent with cooling climate after the mid-postglacial thermal optimum. Human influence was probably a more important factor than climate and Turner (1962) has shown that the *Tilia* spp. decline was not a synchronous event, but rather occurred at different times at different sites. Hockham Mere dates the *Tilia* spp. decline at 3640-3900 Cal. BP (2σ [Bennett, 1983]). Age extrapolation down-sequence with varve counts from Lithozone E indicates a significantly earlier timing of 4495 Cal. BP for the decline in *Tilia* spp. pollen in Diss Mere's catchment area. If both dates are taken as reasonable indicators of the timing *Tilia* decline at different localities in East Anglia, they further demonstrate the potential diachronous nature of regional pollen stratigraphies due to human activity.

Table 5.1. Radiocarbon dates bounding region-wide land clearance, *Pm-1*, at Hockham Mere and their equivalent calendrical ages.

Sample	Depth (cm)	^{14}C age yr. BP (1σ)	95.4% (2σ) Cal. age ranges BP	Relative area under distribution
Q-2224	257.5-262.5	1980 ± 50	1820-2060	1.0
Q-2223	289.5-262.5	2660 ± 50	2720-2870	1.0

nb. depth at which Hockham Mere pollen stratigraphy first records region-wide land clearance (*Pm-1*) is 280 cm.

5.2. Geochemistry and mineralogy of laminated sediments of Lithozone E.

The geochemical profile of the laminated muds (Figs. 5.18 & 5.19) is dominated by elemental Ca; for the given count-time, the X-ray detector received five and a half times

more fluorescent radiation characteristic of elemental Ca than the next most abundant element, Fe. Elemental Ca and Sr show a highly significant positive correlation (*r*, 0.807, n= 255; cf. *C*, in Fig. 5.20), whereas elemental Ca (plus Sr) and the redox sensitive element Fe, show no significant covariance (*r*, -0.095; -0.108 for Sr and Fe-counts, n=255; cf. *D*, in Fig. 5.20). Identifying the mineral residences of Ca and Sr from the XRD analysis was relatively straightforward. The majority of both have been incorporated into low Mg-calcite (the dominant peak in X-ray diffractograms, see Figs. 5.21 through 5.23). This is, by far, the most common carbonate mineral in hardwater lakes (Dean & Megard, 1993). The presence of significant peaks for pyrite below 16 m in X-ray diffractograms and the close correlation of elemental Fe and OM below 16 m suggests that most Fe is incorporated into iron-sulphides (FeS & FeS_2) and is associated with organic matter, probably as organic complexes. Peglar *et al.* (1984), who report a close association between Fe and S in Diss Mere's laminae, support this conclusion. Scanning electron micrographs show no evidence for laminae of oxyhydroxide gels (see Section 5.3). Although iron oxyhydroxides cannot be detected by XRD, the persistent observation of pyrite in organic-rich laminae in such images throughout Lithozone E suggests that most iron oxide would have been reduced to pyrite by hydrogen sulphide. The relatively high concentration of pyrite would also preclude iron phosphate oxides as a potential mineral residence for elemental Fe (Holmer & Storkholm, 2001). Above 16 m, the decline in elemental Fe-cps probably indicates a decrease in sulphate reduction. For comparison, the rich black colour of the sediments at the top of Lithozone G and throughout lithozone H is probably due to significant deposition of iron sulphides. This is reflected by high counts for elemental Fe (see figure 5.18) and is most likely an artefact of wastewater run-off, rich in sulphate, from the town of Diss (see Wiseman *et al.*, 1798).

Results of measurements of calcium carbonate ($CaCO_3$) and organic matter (OM) confirm that the laminated sediments are carbonate-rich, with up to 89 wt% $CaCO_3$ (mean content of 69.2%). Mean content of organic matter is 12.6 wt%. Carbonate carbon content shows a strong correlation with the Ca-counts (*r*, +0.68, n = 85), demonstrating

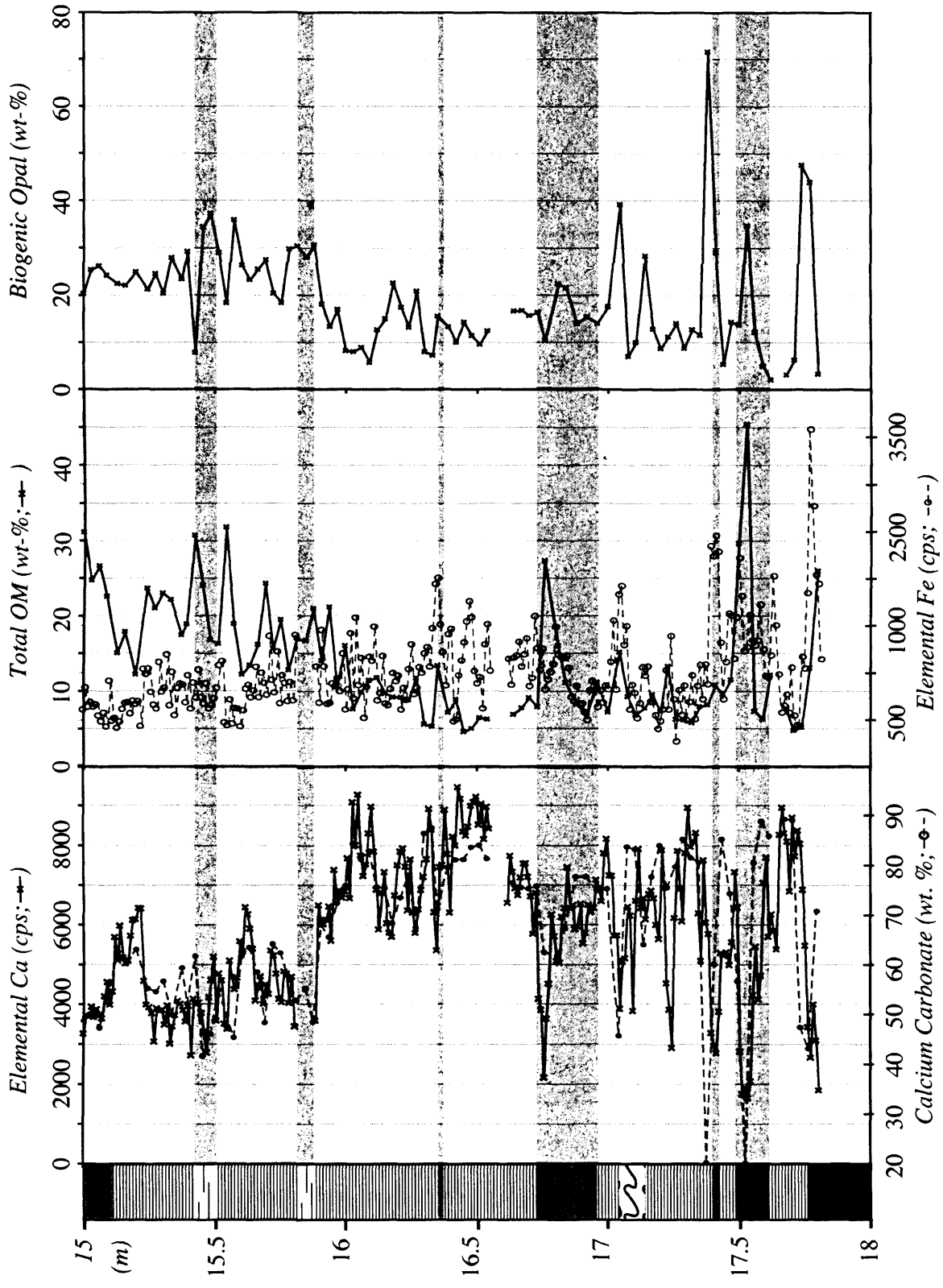

Fig. 5.18: Plots of XRF determined elemental abundance for Ca, Fe together with weight percent CC, OC and Opal. Key to lithostratigraphy given in Fig. 5.2.

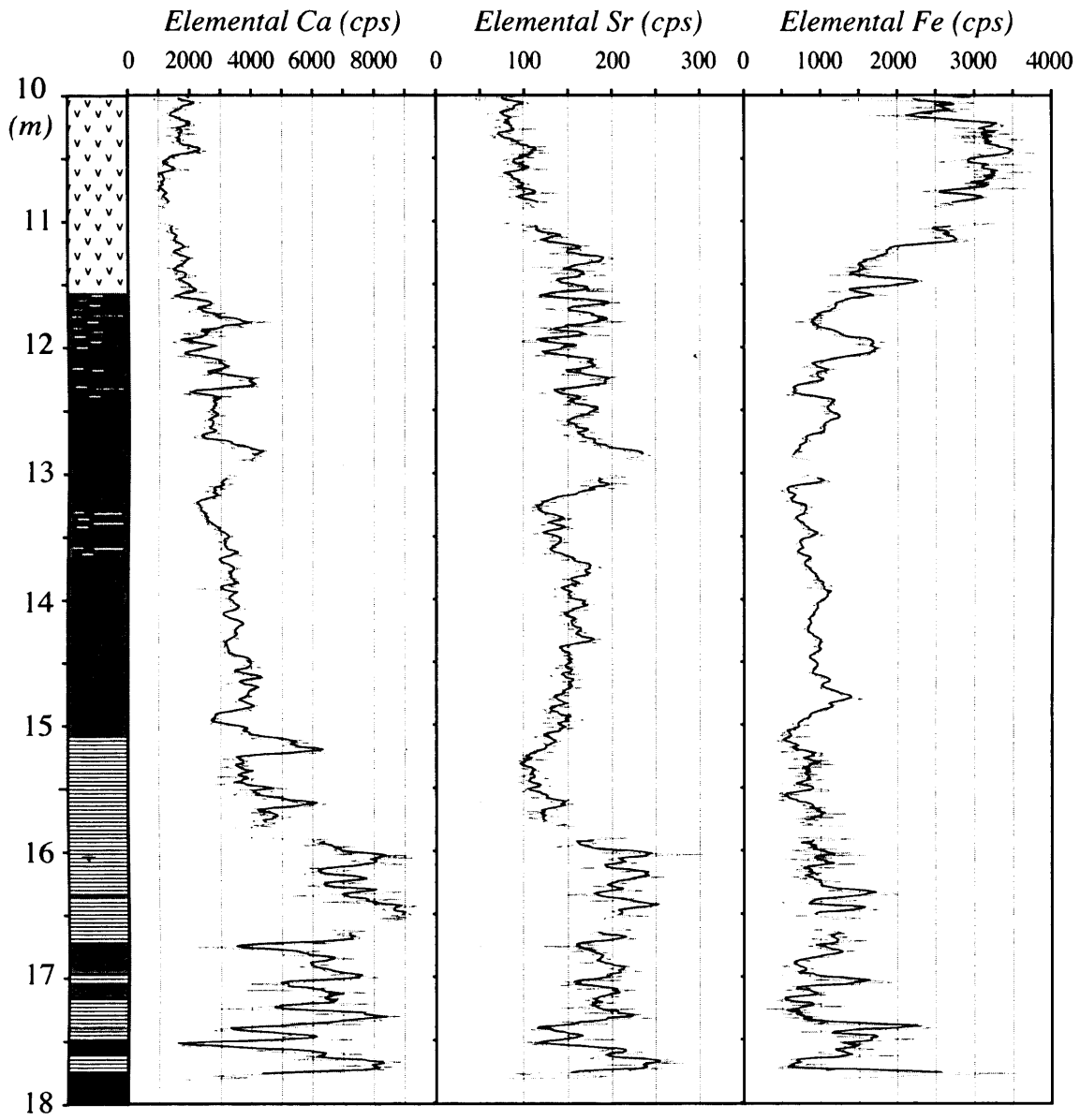

Fig. 5.19: XRF elemental concentration for Ca, Sr and Fe for Lithozones E through G. Key to lithostratigraphy given in Fig. 5.2.

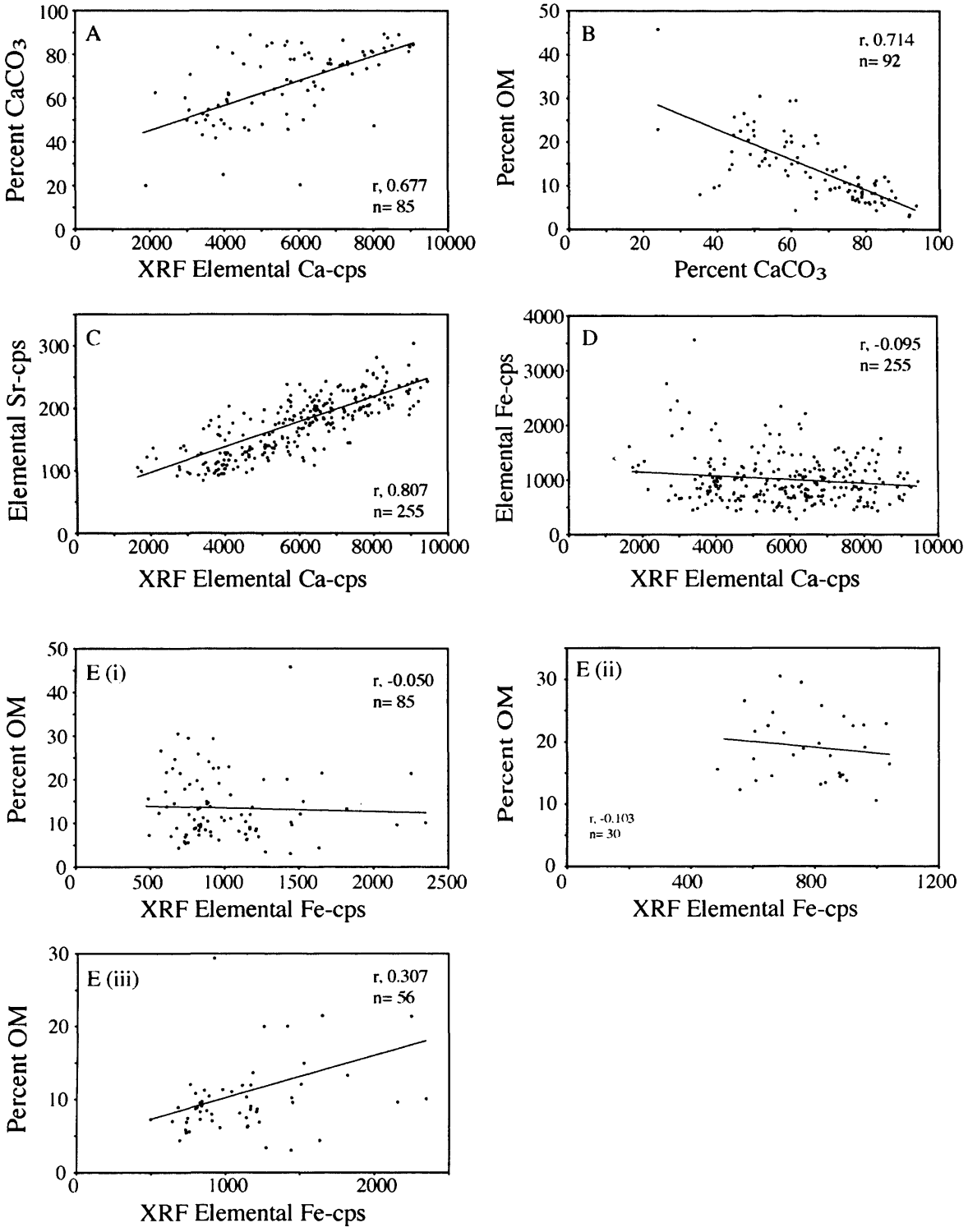

Fig. 5.20: A through E cross plots showing geochemical relationships.

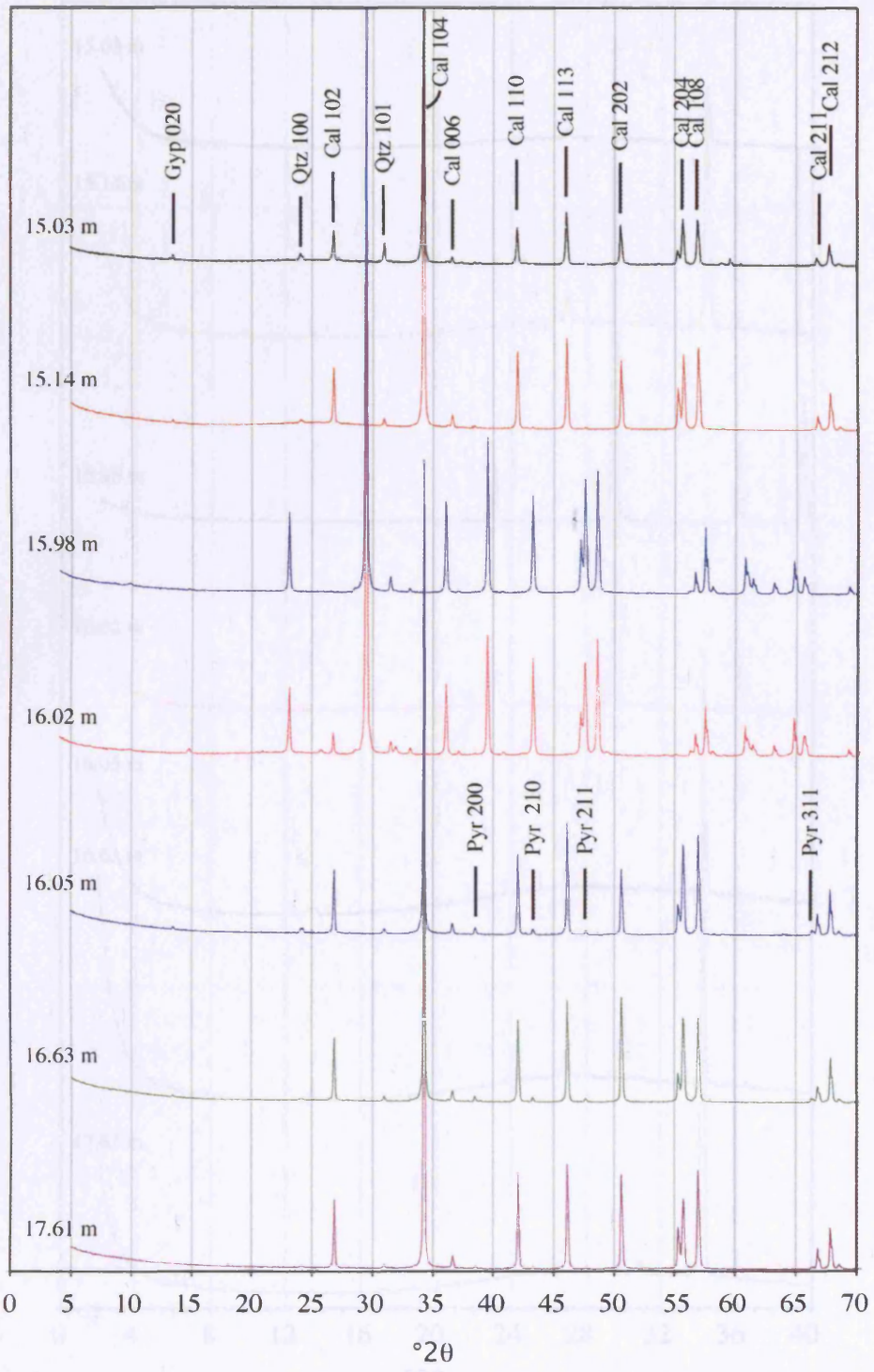

Fig. 5.21: X-ray diffraction patterns for the top, intermediate and bottom of the sediment. Depths are from composite stratigraphy. Identified peaks are for the 'hkl' planes of calcite (Cal), quartz (Qtz), and pyrite (Pyr). No substantial variation in mineralogy has been evidenced by XRD down core. Note shift in peaks for major mineralogy in samples, 15.98 m and 16.02 m due to use of different X-ray source (see methodology, Section 3.3.2.2).

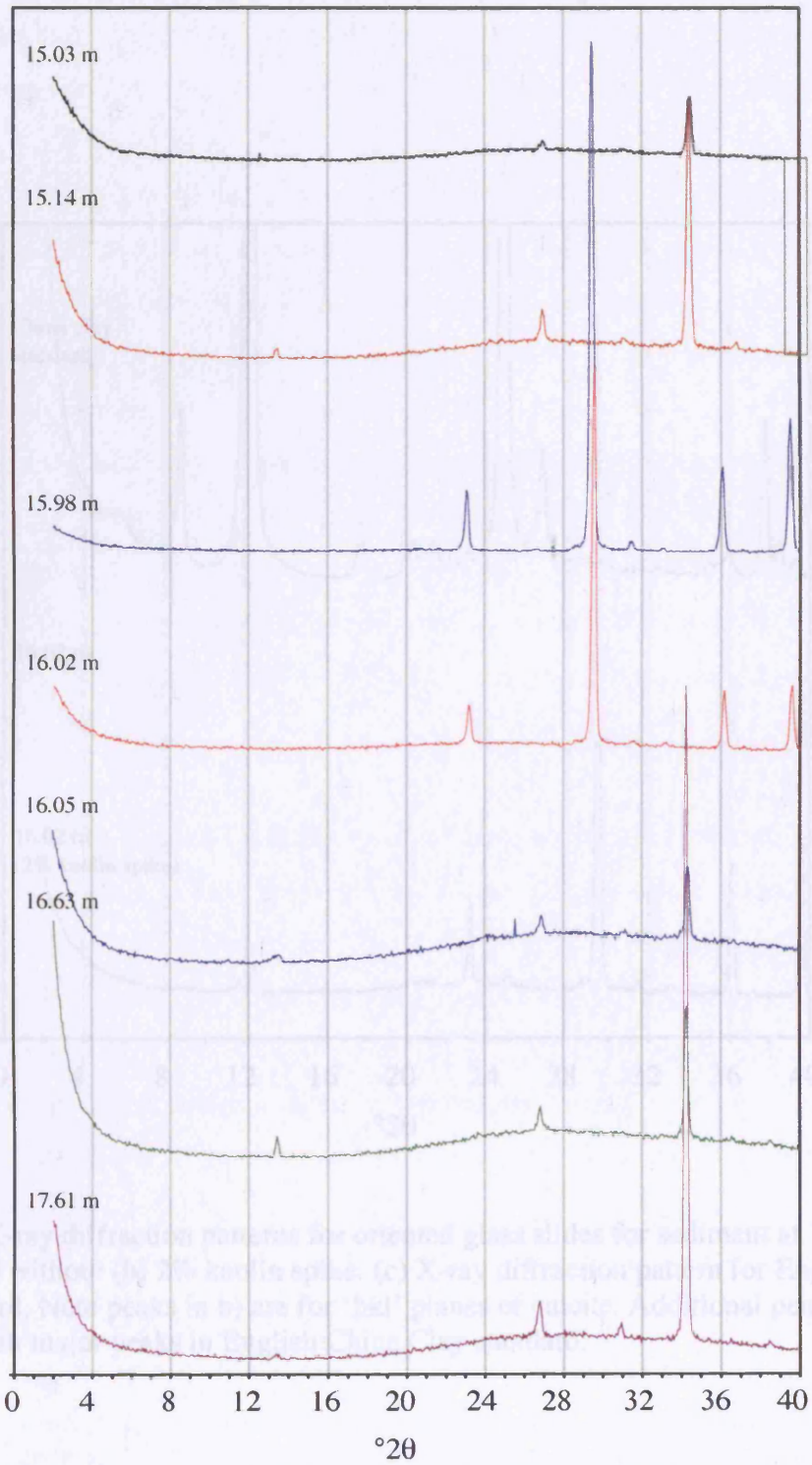

Fig. 5.22: X-ray diffraction patterns for the oriented glass slides for sediment from top, intermediate and bottom of the stratigraphy. Note shift in peaks for major mineralogy in samples, 15.98 m and 16.02 m due to use of different X-ray source (see methodology, Section 3.3.2.2). All major peaks result from Bragg diffraction on calcite 'hkl' planes. Small peaks around 13° 2q are due to post depositional gypsum.

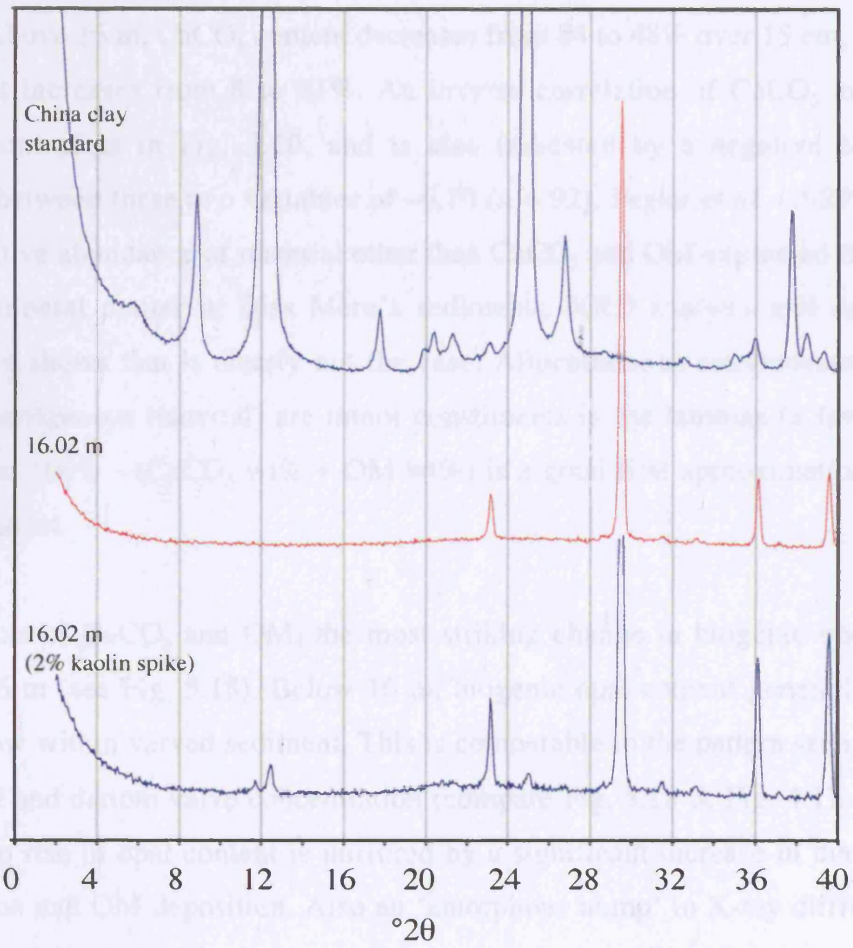

Fig. 5.23: X-ray diffraction patterns for oriented glass slides for sediment at 16.02 m, with (a) and without (b) 2% kaolin spike. (c) X-ray diffraction pattern for English China Clay standard. Note peaks in b) are for 'hkl' planes of calcite. Additional peaks in a) correlate with major peaks in English China Clay standard.

that Ca-counts are a useful approximation of high-resolution variation in carbonate concentration down-core. The most striking feature of the plots in Fig. 5.18 is the abrupt decrease in $CaCO_3$ burial and a concomitant increase in OM burial at 16 m. Laminated sediment deposited below 16 m has a mean $CaCO_3$ content of 76.7 wt% and less than 10 wt% OM. Above 16 m, $CaCO_3$ content decreases from 84 to 48% over 15 cm, whilst the OM content increases from 8 to 21%. An inverse correlation of $CaCO_3$ and OM is apparent from plots in Fig. 5.20, and is also indicated by a negative correlation coefficient between these two variables of –0.70 (n = 92). Peglar *et al.* (1989) assumed that the relative abundance of material other than $CaCO_3$ and OM expressed the amount of clastic mineral matter in Diss Mere's sediments. XRD analysis and smear-slide investigation shows that is clearly not the case. Allochthonous components (sand- to clay-sized terrigenous material) are minor constituents in the laminae (a few percent) and the sum, 100% - ($CaCO_3$ wt% + OM wt%) is a good first approximation for opal (diatom) content.

As with plots of $CaCO_3$ and OM, the most striking change in biogenic opal content occurs at 16 m (see Fig. 5.18). Below 16 m, biogenic opal content generally remains relatively low within varved sediment. This is comparable to the pattern seen in weight percent OM and diatom valve concentration (compare Fig. 5.18 & Fig. 4.1). Above 16 m, the sharp rise in opal content is mirrored by a significant increase in diatom valve concentration and OM deposition. Also an 'amorphous hump' in X-ray diffractograms centred around 20 to 30° 2θ records the presence of biogenic silica. This 'hump' is more prominent above 16 m. Finally, the change at 16 m is also reflected in the sediment by a sharp change in colour from reddish brown to cream brown varves (Fig. 5.8). Variation in weight percent is not solely a product of variable dilution of one component by another (that is, a consequence of the closed sum nature of percentage data). OM contents range from 4.7-31.7%, $CaCO_3$ contents range from 41.7-89.3% and opal contents range from 3.1-47.4%. The difference in OM is 27%, whereas the difference in $CaCO_3$ and opal is 47.3% and 44.3% respectively, so the inverse relation cannot be one of simple dilution of one or more components by another. Despite precise varve calibration, a lack of measured bulk densities for the sediment meant it was not possible

to calculate mass accumulation rates for each component. However, sedimentation rates determined from varve counting for the interval 15.09-16.55 m (Fig. 5.24) show little change in central tendency, for the most part varying between 0.4-1.0 mm/yr with two periods of increased sedimentation centred on 15.14 m and 16.16 m depth. Given a normal profile of increasing dry bulk density with depth (*i.e.*, due to compaction), the trend in sedimentation rates across 16 m suggests that the change in carbon accumulation at 16 m is absolute.

Calibration of varve counts to the calendrical timescale by regional pollen zones indicates that the significant change in carbon-burial occurred at ~4000 Cal. yrs BP and over a period of 220 years. Table 5.4 uses the codes given in Tables 5.2 and 5.3 to detail results of varve counts from each of the counting zones in the varved section from 15.09-16.74 m composite depth. Figure 5.25 shows an age-depth model for the interval concerned. Five counting gaps and their estimated counts are: between markers B & C, 6.5 mm, 10 yrs; between E & F, 75 mm, 110 yrs; between I & J, 111 mm, 159 yrs; between K & L for DISS A-6, 14 mm, 20 yrs, and for core DISS B-6 11 mm, 14 yrs; between T & U, 51 mm, 91 yrs. The total number of uncounted years in the chronology is thus 390, 14.3% of the varve chronology. The overall uncertainty in the varve counts as assessed from the variance among counts from common intervals is about 2% at the 95% confidence level. This is used as a conservative estimate of counting precision.

Sedimentation-rate shows variable covariance with elemental Ca (Table 5.5). Below 16 m, it exhibits a significant negative correlation at the 5% level (r, -0.770) and a significant positive correlation above this depth (r, +0.361). On the other hand, elemental Fe displays a consistent small, but significant antithetic relation throughout. The relatively few data for OM and biogenic opal wt% covering this interval makes any statistical correlation with sedimentation-rate meaningless. However, a visual inspection between the two sets of depth-series reveals a strong apparent degree of covariance below 16 m. Above this depth increased biogenic opal wt% correlates with decreased sedimentation. No apparent relationship, however, exists between sedimentation-rate and OM wt% burial above 16 m (Figs. 5.26 & 5.27).

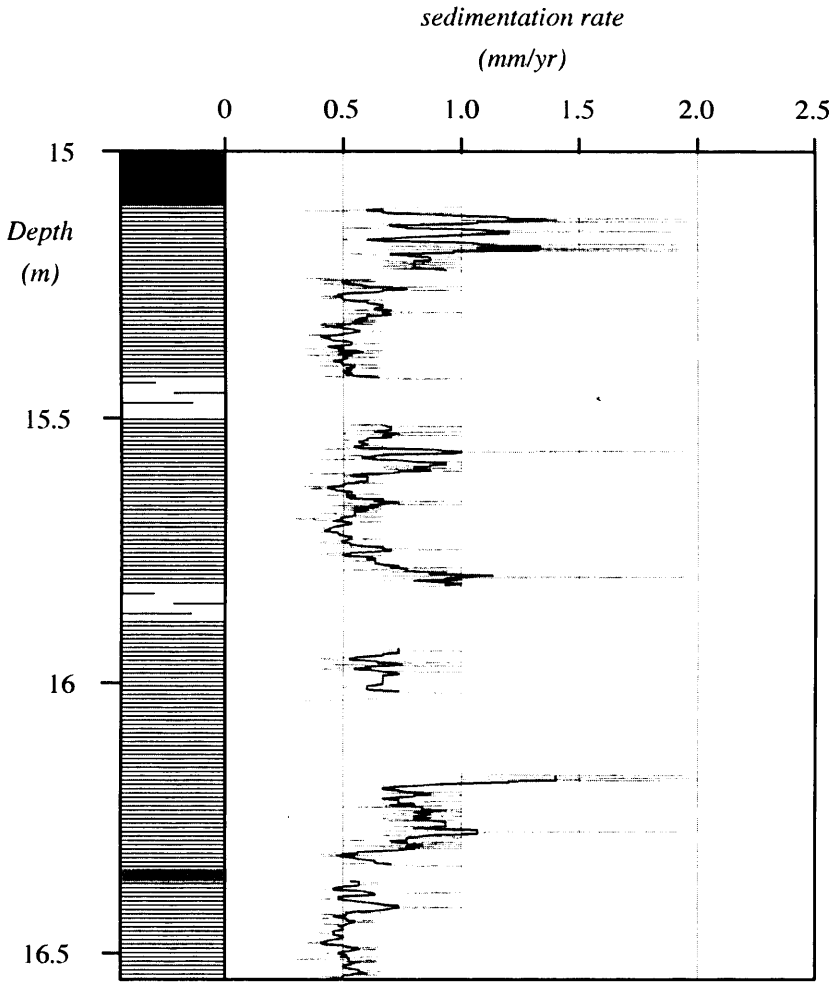

Fig. 5.24: 2 mm sedimentation rate (grey line) for 15.09-16.55 m composite depth. Black line shows 5-point moving average. Gap in data between ~16-16.2 m exists because the deformed nature of core DISS B-6, used to generate this potion of the composite splice, made it impossible to determine sedimentation rates at a 2 mm resolution (see text for details).

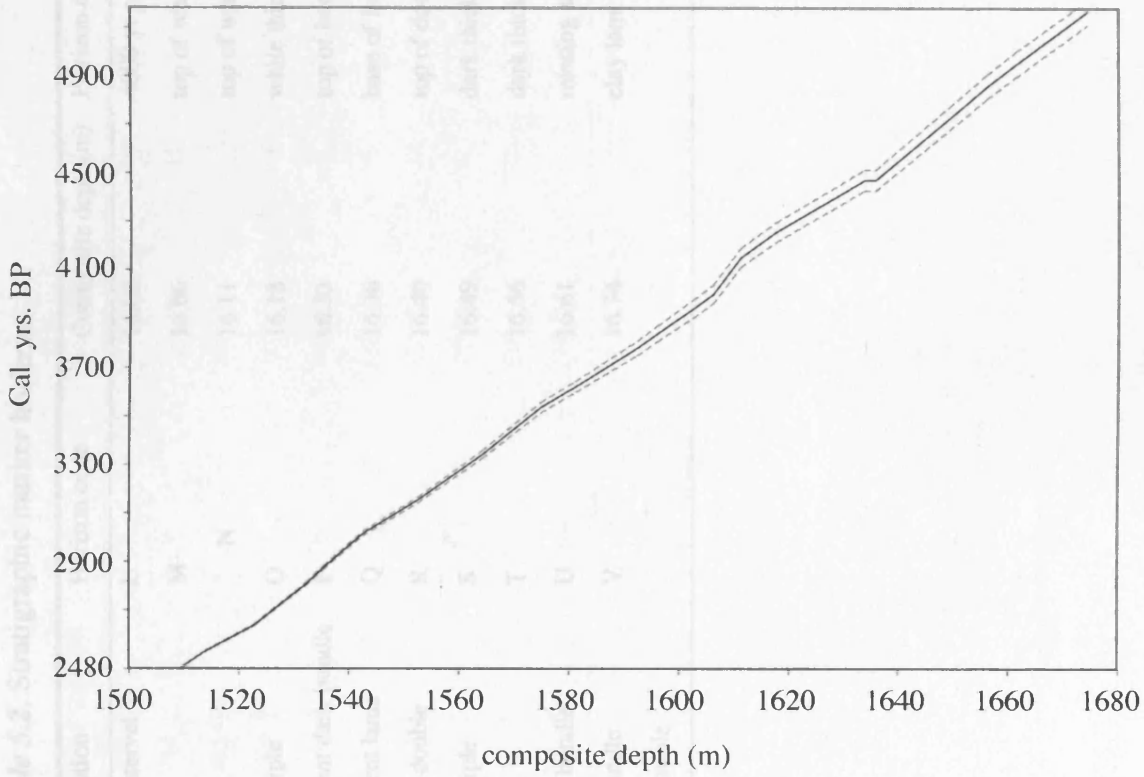

Fig. 5.25: Age-depth model for varved sediment between 15.09-16.74 m. Dashed lines delimit 95% confidence envelope for varve count precision.

Table 5.2. Stratigraphic marker horizons

Horizon code	Composite depth (m)	Horizon description	Horizon code	Composite depth(m)	Horizon description
TOP	15.09	top of varved interval	L	16.02	4000 yr colour change
A	15.14	top of 7 white	M	16.06	top of white double
B	15.23	single white	N	16.11	top of white triple
C	15.32	base of white triple	O	16.18	white thick lam
D	15.35	base of prominent dark bundle	P	16.33	top of homog. bed
E	15.46	top of intermittent lams	Q	16.36	base of homog. bed
F	15.56	prominent dark double	R	16.40	top of double white
G	15.64	base of white triple	S	16.49	dark thick lamina
H	15.75	base of 7 white	T	16.56	dark thick lamina
I	15.81	base of 5 white bundle	U	16.61	missing sediment
J	15.92	top of dark 3 bundle	V	16.74	clay lam
K	15.96	base of white double			

Table 5.3 Core segment identification codes

Code	Core segment	Code	Core segment	Code	core segment	Code	Core segment
a	DC-0	k	DC-10	u	DA-8b	ee	DB-3
b	DC-1	l	DA-0	v	DA-9a	ff	DB-4
c	DC-2	m	DA-1	w	DA-9b	gg	DB-5
d	DC-3	n	DA-2	x	DA-10	hh	DB-6
e	DC-4	o	DA-3	y	DA-11	ii	DB-7
f	DC-5	p	DA-4	z	DA-12	jj	DB-8
g	DC-6	q	DA-5	aa	DA-13	kk	DB-9
h	DC-7	r	DA-6	bb	DB-0	ll	DB-10
i	DC-8	s	DA-7	cc	DB-1	mm	DB-11
j	DC-9	t	DA-8a	dd	DB-2		

Table 5.4. Varve counts.

Varve Horizons	Composite Depth (cm)	C1	C2	C3	C4	C5	C6	Average counts	Max counts	n	Cumm max	Std dev.	% dev.	+at 95%	Cumm 95%
A	1513.9	72a	69a	73a	73d	70d	71d	71.3	73	6	73	1.63	2.29	3.27	3
B	1522.7	106a	107a	107a	107d	107d	107d	106.8	107	6	180	0.41	0.38	0.82	4
C	1532.2	169d@10	167d@10	168d@10				168.0	169	3	349	1.00	0.60	2.00	6
D	1535.4	68d	67d	66d				67.0	68	3	417	1.00	1.49	2.00	8
E	1542.6	141d	142d	141d				141.3	142	3	559	0.58	0.41	1.15	9
F	1552.6	137d@110	137d@110	139d@110				137.7	139	3	698	1.15	0.84	2.31	12
G	1564.2	183d	187d	183d	186b	187b	188b	185.7	188	6	886	2.16	1.16	4.32	16
H	1574.9	191d	191d	186d	192b	193b	192b	190.8	193	6	1079	2.48	1.30	4.97	21
I	1581.2	85d	86d	86d	85b	84b	86b	85.3	86	6	1165	0.82	0.96	1.63	22
J	1592.5	159b@	159b@	159b@				159.0	159	3	1324	0.00	0.00	0.00	22
K	1596.1	54b	55b	54b	57e	55e	54e	54.8	57	6	1381	1.17	2.13	2.34	25
L	1602.6	98b@20	98b@20	96b@20	103@14	100@14	100@14	99.2	103	6	1484	2.40	2.42	4.80	30
M	1606.2	57b	58b	59b				58.0	59	3	1543	1.00	1.72	2.00	32
N	1611.2	152b	152b	151b				151.7	152	3	1695	0.58	0.38	1.15	33
O	1617.7	104b	105b	104b				104.3	105	3	1800	0.58	0.55	1.15	34
P	1633.8	213e	213e	215e				213.7	215	3	2015	1.15	0.54	2.31	36
Q	1635.8	Event bed									2015				36
R	1640.3	84e	84e	83e				83.7	84	3	2099	0.58	0.69	1.15	37
S	1649.3	170e	172e	170e	168c	168c	168c	169.3	172	6	2271	1.63	0.96	3.27	41
T	1656.2	131e	128e	127e	129c	130c	129c	129.0	131	6	2402	1.41	1.10	2.83	43
U	1661.3	@91	@91	@91				91.0	91	6	2493		0.81	1.47	45
V	1674.2	216c	216c	213c				215.0	216	3	2709	1.73	0.81	3.46	48

@ = number of varves interpolated through a gap in the core/intermittently laminated sediment/disturbed fabric.

Table 5.5. Correlation coefficients between the elemental Ca and Fe profiles and sedimentation-rates for varved interval 15.09 to 16.74 m, lithozone *E*

	15.09- 16.74 m: n = 118	15.09- 16.03 m: n = 71	16.03- 16.74 m: n = 47
	sed. rate	sed. rate	sed. rate
Elemental Ca	-0.034*	0.261	-0.770
Elemental Fe	-0.197	-0.243	-0.231

All correlations significant at the 5% level, except*

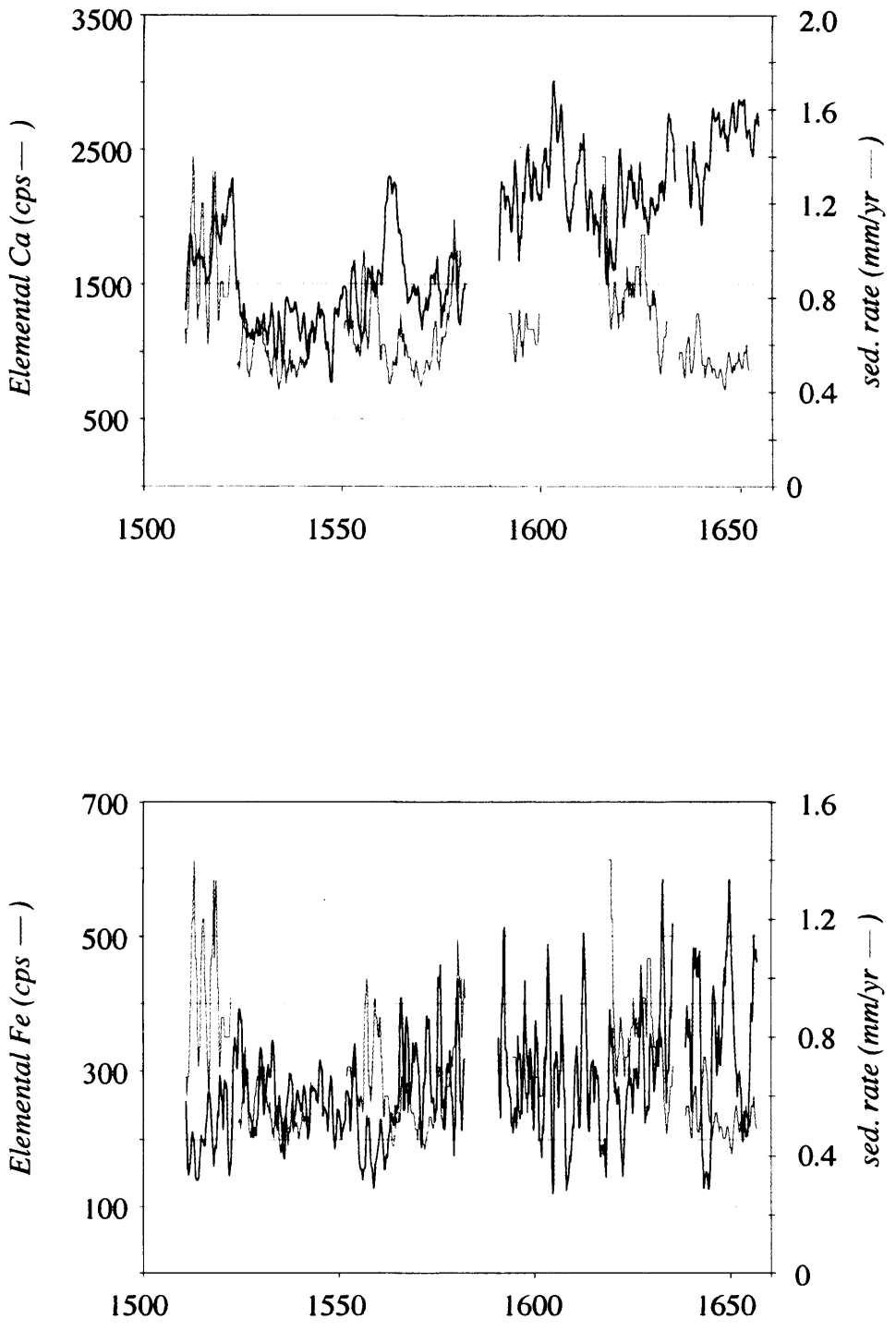

Fig. 5.26: Correlation plots of Elemental Ca and Fe against sedimentation rate.

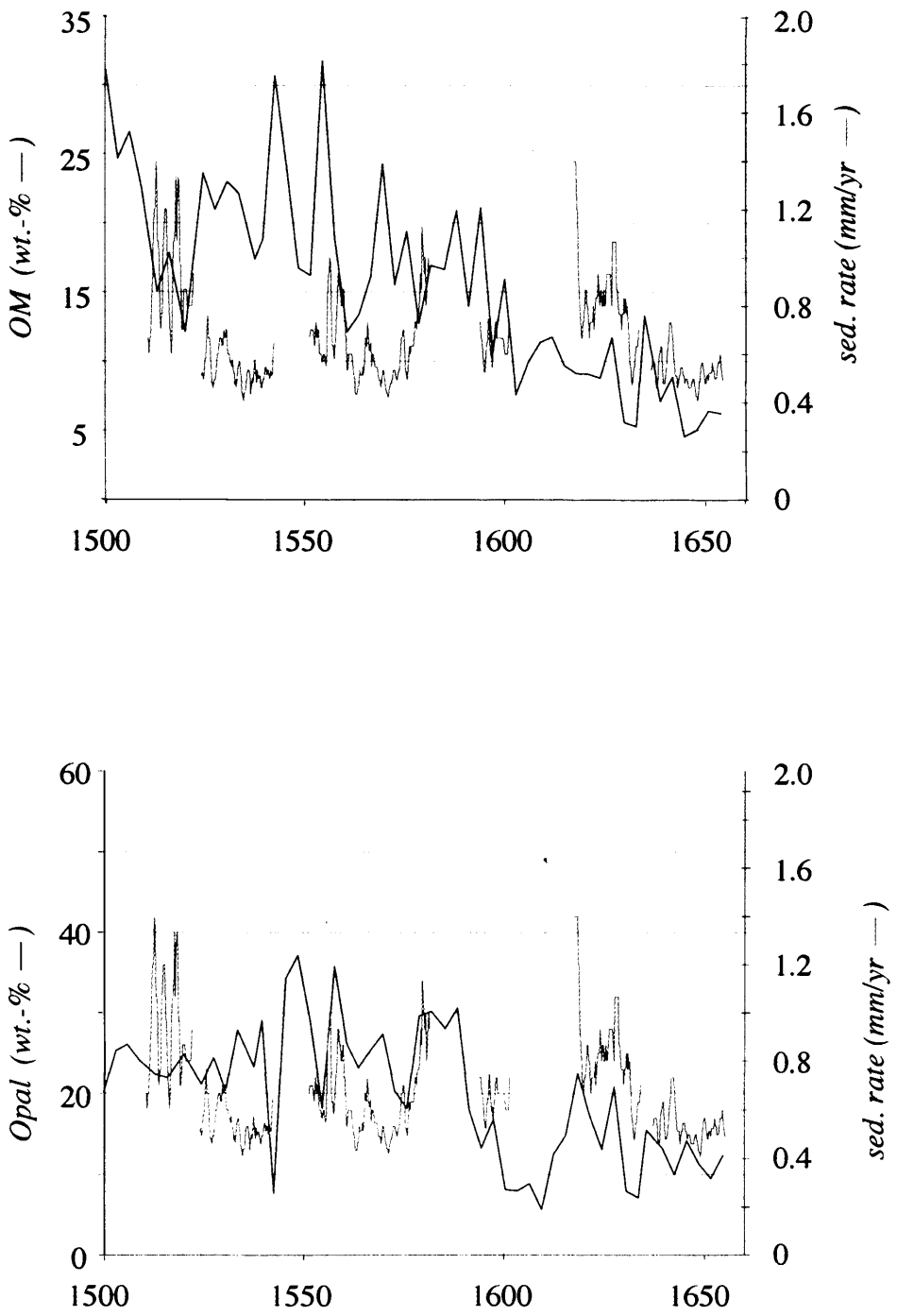

Fig. 5.27: Correlation plots of weight percent OM and Opal against sedimentation rate.

5.3. SEM Backscatter Electron Imaging

BSEI investigation of Diss Mere's varves has identified two lithologies: biogenic mud, deposited primarily during late winter and spring, and authigenic calcite mud, deposited during late spring through autumn. Each of these lithologies contains a range of lamina-types, comprising a variety of components and structures. This section reviews these laminae to construct changes in seasonal flux. Throughout this section, the reader is referred to Appendix XI for low-resolution BSEI base-maps of the petrographic thin sections (PTS) from core DISS A-6.

5.3.1. Low magnification SEMs

Figure 5.28 shows the location of PTS intervals investigated in core DISS A-6 (Figs. 5.29 through 5.32, hereinafter referred to as intervals *A* through *D*). The paler tones represent laminae with a relatively high average atomic number and, therefore, high backscatter coefficient; here typical of calcite grains, but also of quartz and pyrite. The darker tones represent a lower average atomic number, which here is the carbon-based epoxy resin filling the voids within porous diatom ooze or unstructured organic-matter. The varve cycle is clearly visible. The biogenic varve-segment comprises either darker, diatom ooze laminae or unstructured organic fine detritus laminae both ranging in thickness from 30 to 500 μm. The calcite varve segment (for the most part) is the relatively thicker layer which follows diatom ooze with a sharp lower contact. The boundary between the calcite varve segment and the following biogenic varve segment is also usually sharp, suggesting a distinct start to spring biological production. Measured thicknesses for the biogenic and calcite-diatom varve segments, as well as total varve thickness are shown in Fig. 5.33. Thickness of biogenic- and calcite-diatom varve segments shows low correlation between themselves. (r= 0.185 for PTS64-70, n = 322; 0.286 for PTS 72-86, n = 516). Below 16 m (varves 350 to 864), calcite-diatom varve segments are considerably thicker than biogenic varve segments. Above 16 m, calcite segments show a reduction in average thickness, and above varve 322, biogenic varve segments are noticeably thicker than their calcite-diatom counterparts.

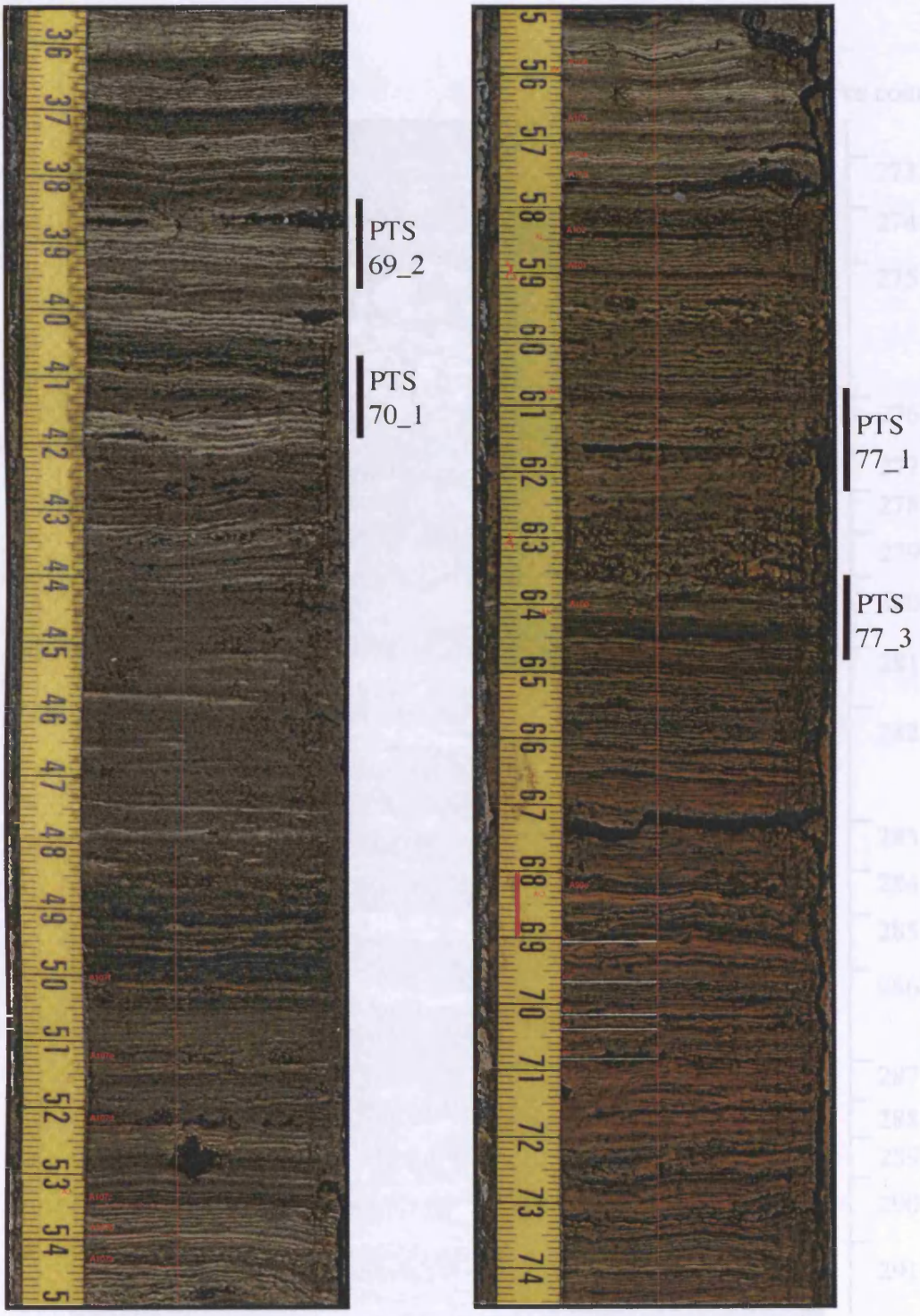

Fig. 5.28: PTS position for SEM-BSEI investigation in core DISS A-6.

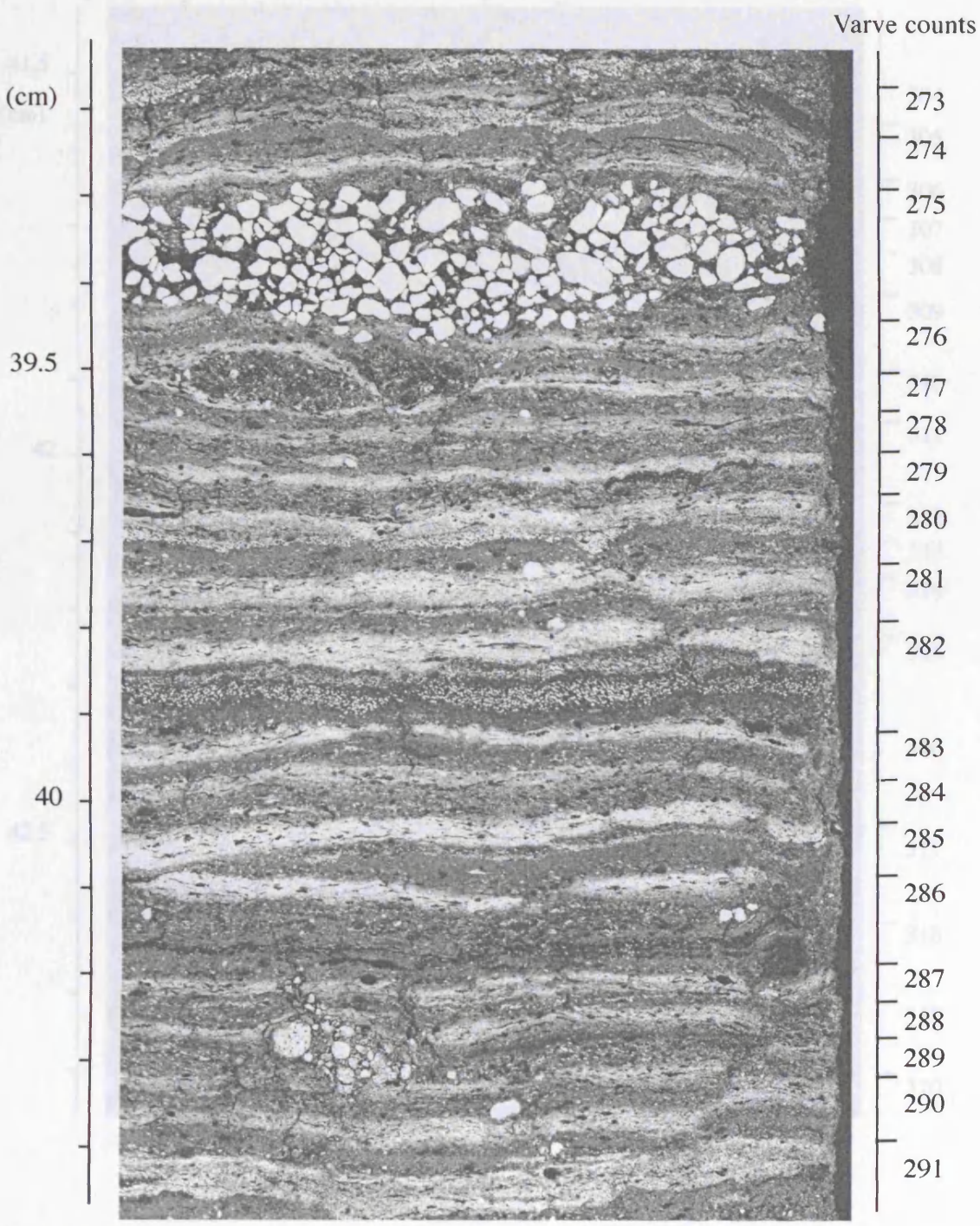

Fig. 5.29: Photo-mosaic for PTS69_2 with varve counts.

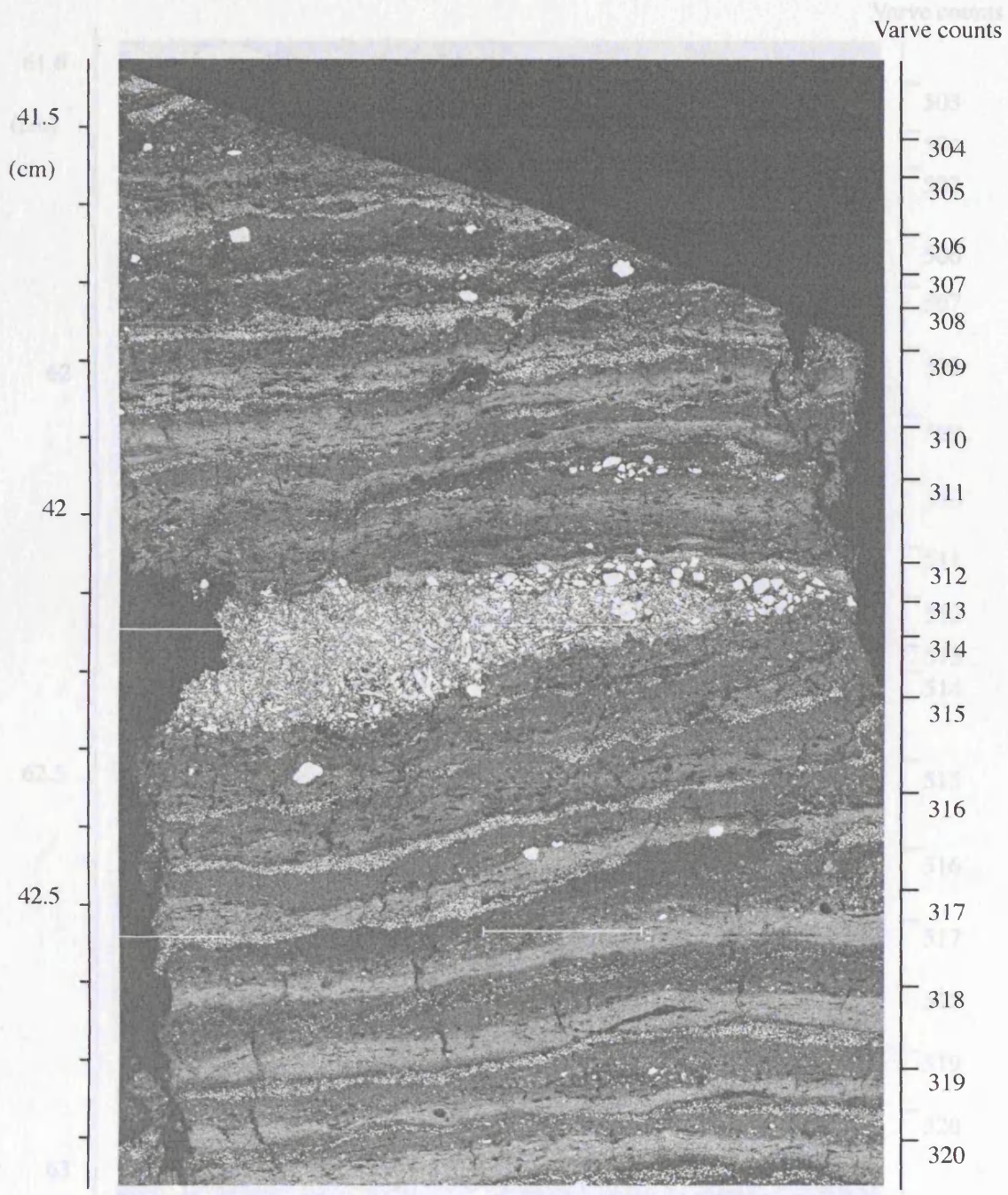

Fig. 5.30: Photo-mosaic for PTS70_1 with varve counts

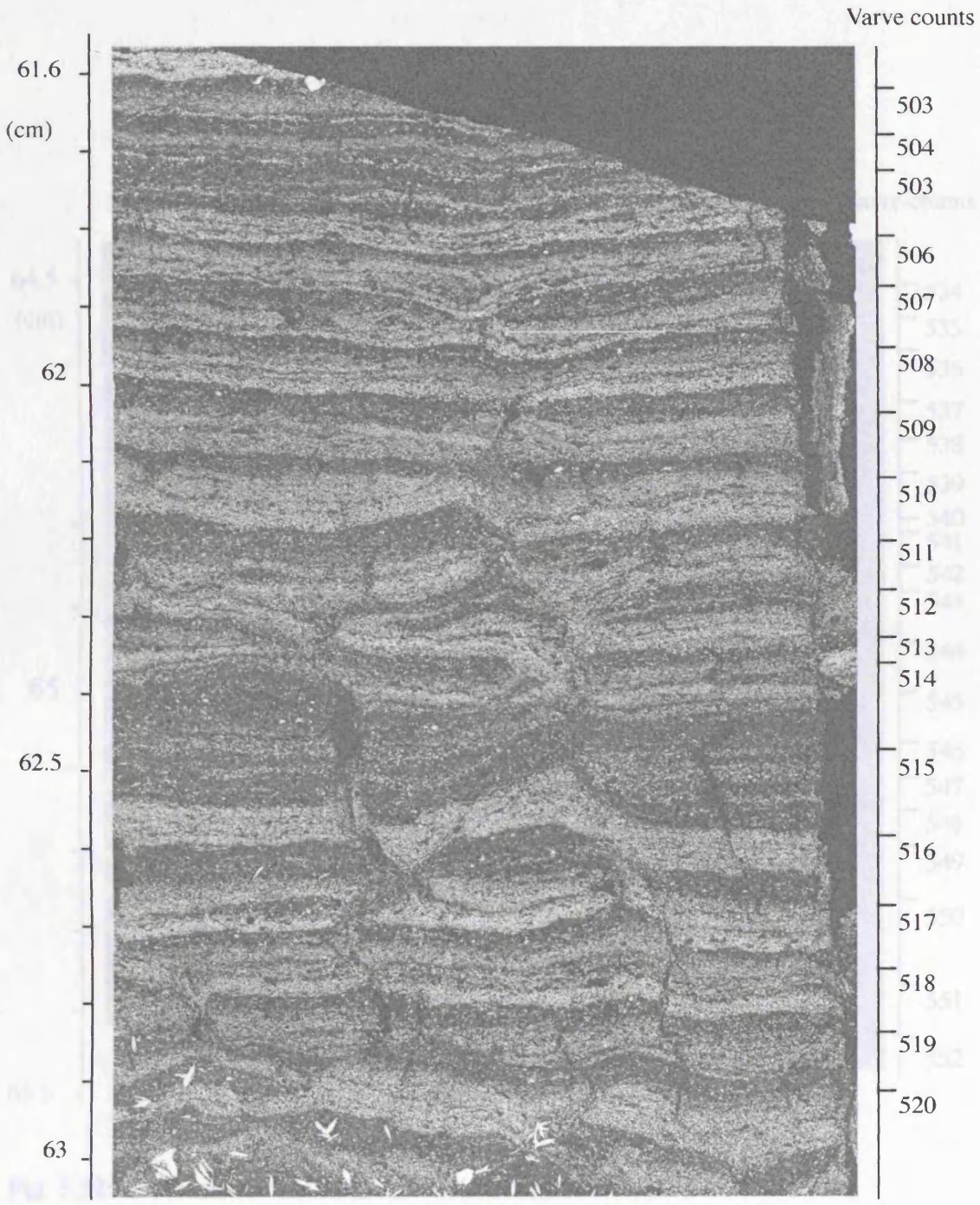

Fig. 5.31: Photo-mosaic for PTS77_1 with varve counts.

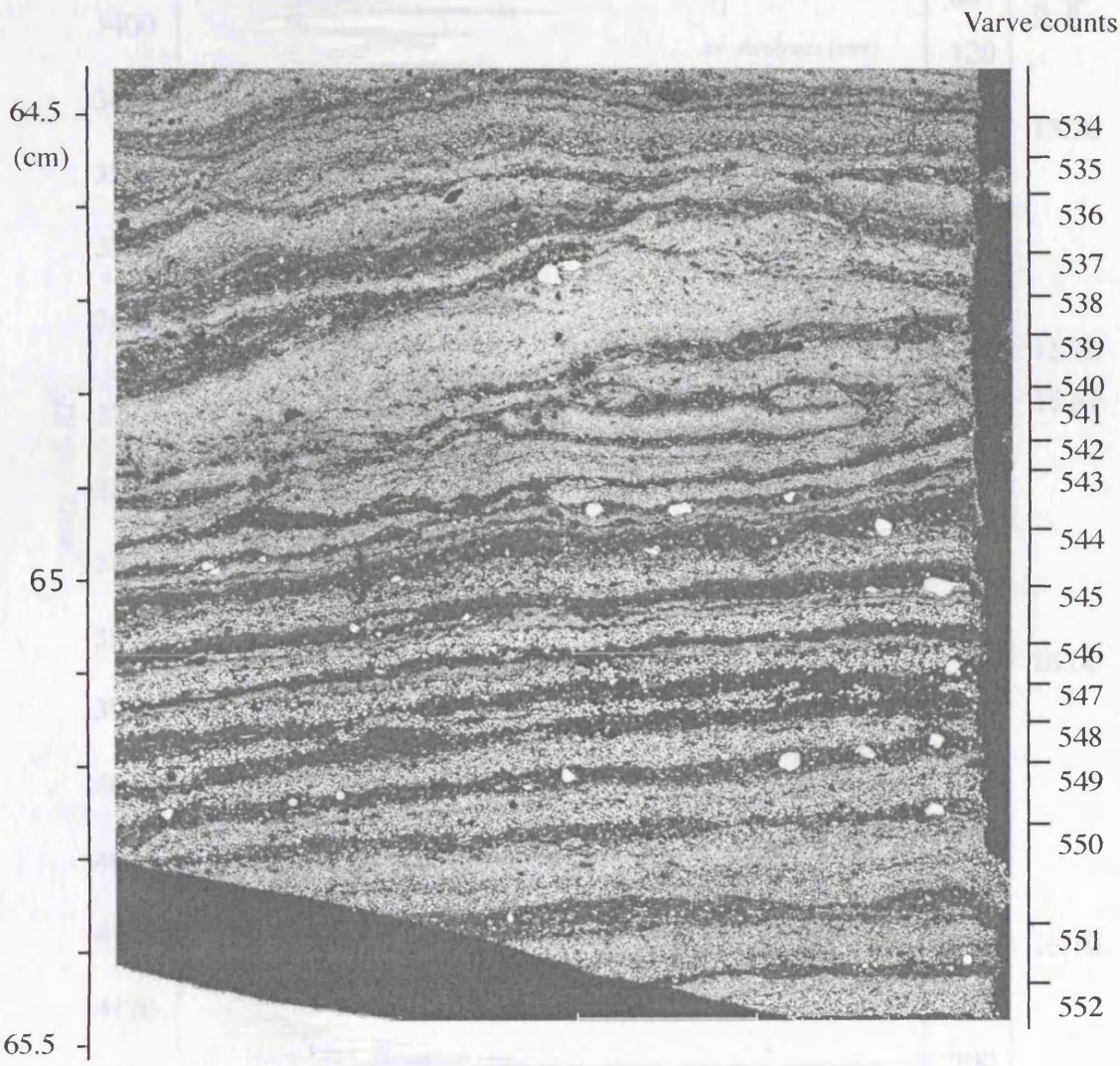

Fig. 5.32: Photo-mosaic for PTS77_3 with varve counts

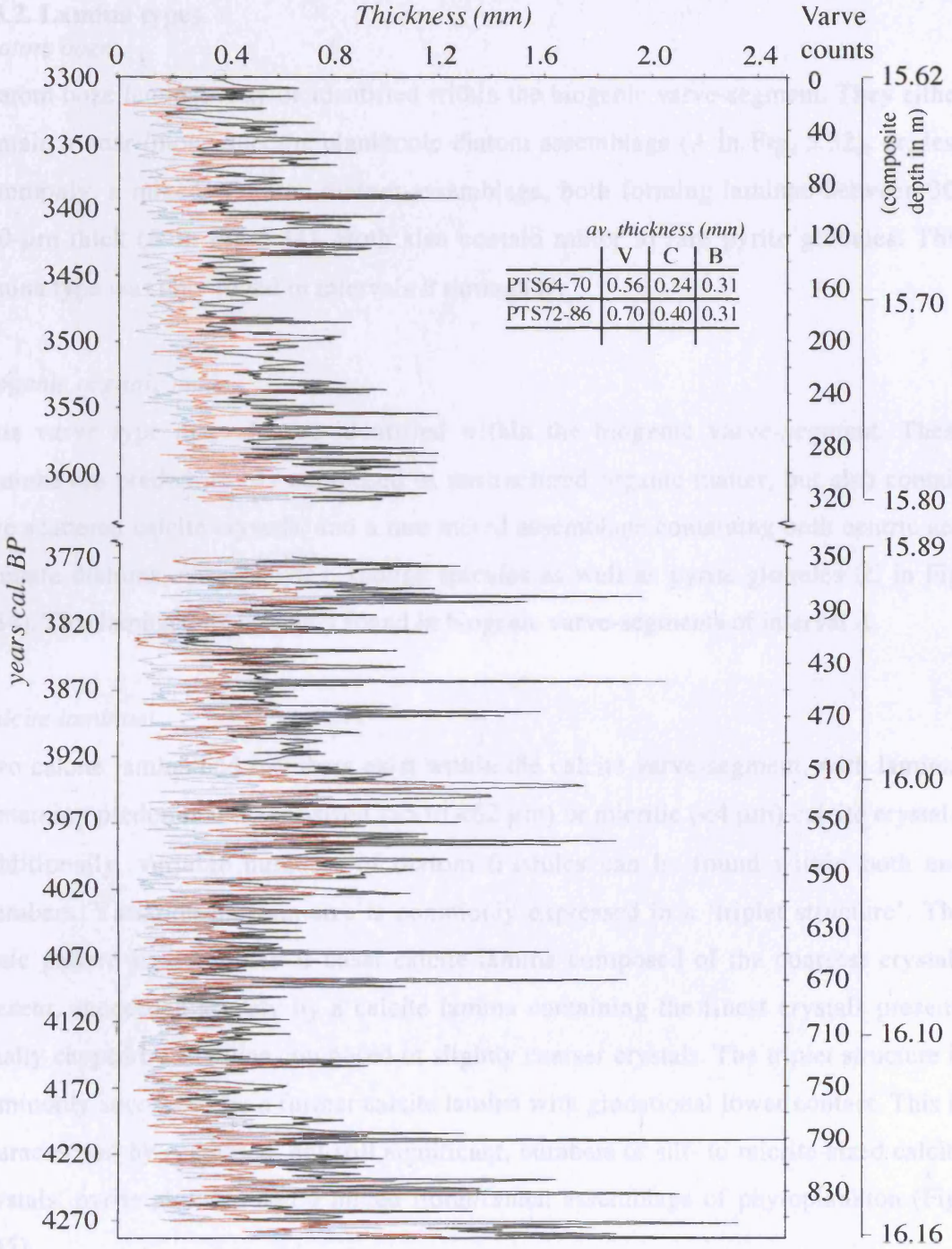

Fig 5.33: Plot of biogenic and calcite-diatom varve segment thickness as well as overall varve thickness in DISS A-6. Table insert details average thickness for varve (V), calcite-diatom (C), and biogenic (B) varve segments.

5.3.2. Lamina types

Diatom ooze

Diatom ooze laminae may be identified within the biogenic varve-segment. They either contain a near-/mono-specific planktonic diatom assemblage (*A* in Fig. 5.32), or, less commonly, a mixed plankton-diatom assemblage, both forming laminae between 30-300-μm thick (*B* in Fig 5.34). Both also contain minor to rare pyrite globules. This lamina type was only found in intervals *B* through *D*.

Biogenic organic mud

This varve type may also be identified within the biogenic varve-segment. These laminae are predominantly composed of unstructured organic matter, but also contain rare scattered calcite crystals, and a rare mixed assemblage containing both centric and pennate diatoms, chrysophytes, sponge spicules as well as pyrite-globules (*C* in Fig. 5.34). This lamina type was only found in biogenic varve-segments of interval *A*.

Calcite laminae

Two calcite lamina end members exist within the calcite varve-segment, with laminae containing predominantly silt-sized (>5 to <62 μm) or micritic (<4 μm) calcite crystals. Additionally, variable numbers of diatom frustules can be found within both end members. Variation in grain-size is commonly expressed in a 'triplet structure'. The basic pattern is as follows: a basal calcite lamina composed of the coarsest crystals present, succeeded sharply by a calcite lamina containing the finest crystals present; finally capped by a lamina composed of slightly coarser crystals. The triplet structure is commonly succeeded by a further calcite lamina with gradational lower contact. This is characterised by decreased, but still significant, numbers of silt- to micrite-sized calcite crystals, pyrite globules and a mixed floral/faunal assemblage of phytoplankton (Fig. 5.35).

Of the intervals investigated, calcite laminae were coarsest and always at least silt-sized in interval *A*. (Fig. 5.35). The largest calcite crystals were found in varve 544 (*i.e.* fine

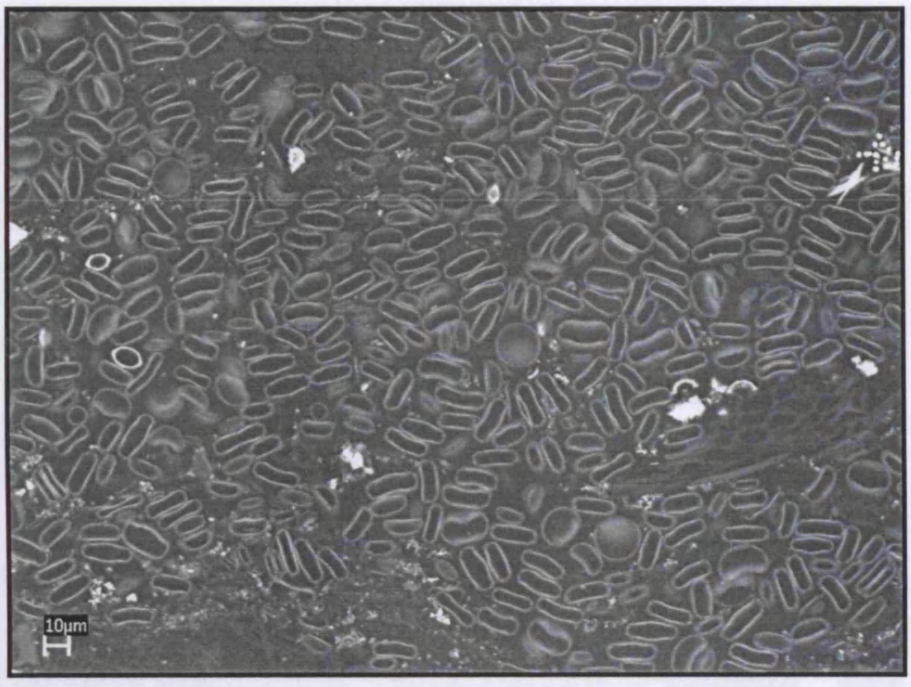

A) SEM-BSEI

A') SEM-topographic

Fig. 5.34: A: *Cyclotella radiosa/ocellata* diatom ooze

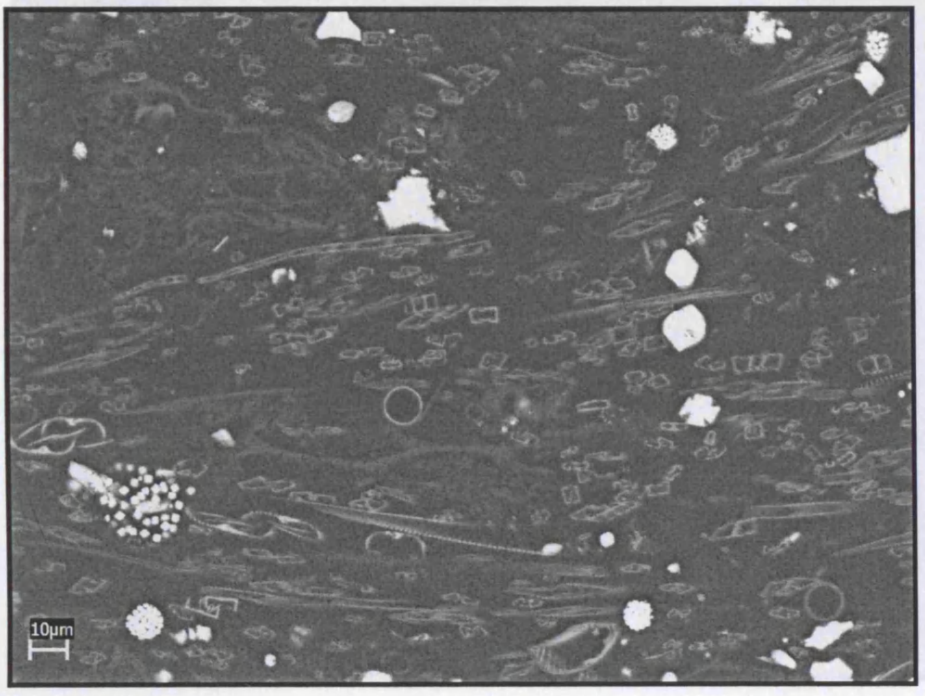

B) SEM-BSEI

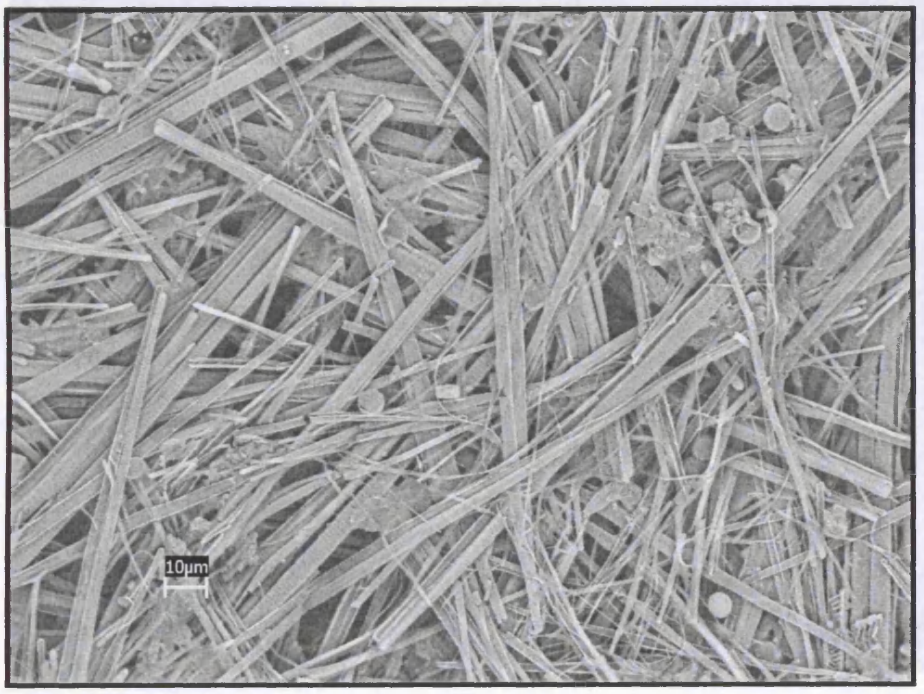

B') SEM-topographic

Fig. 5.34(cont.): B: *Synedra* spp. diatom ooze

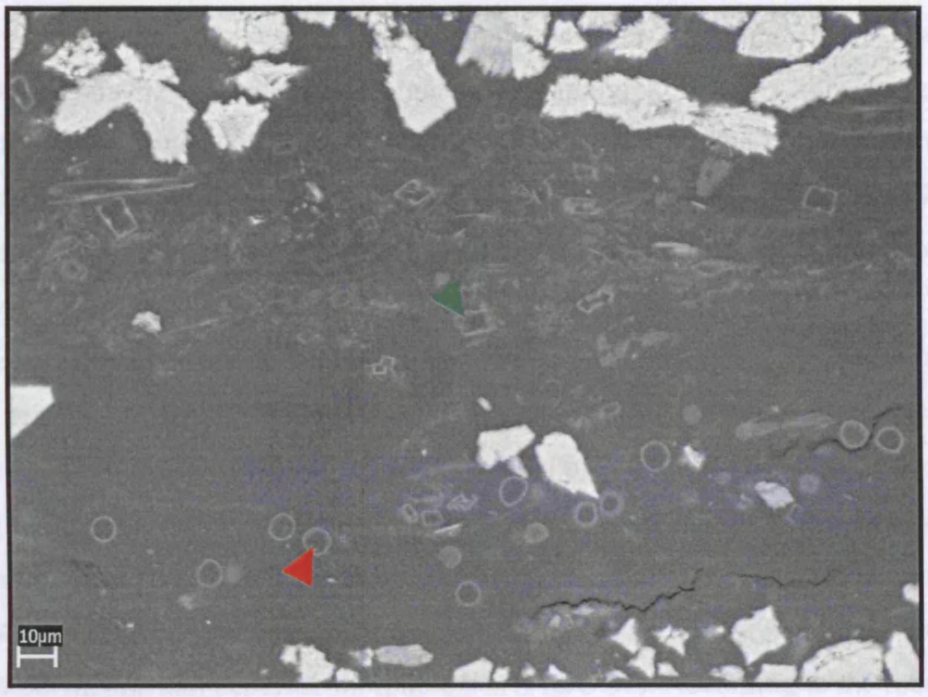

C) SEM-BSEI

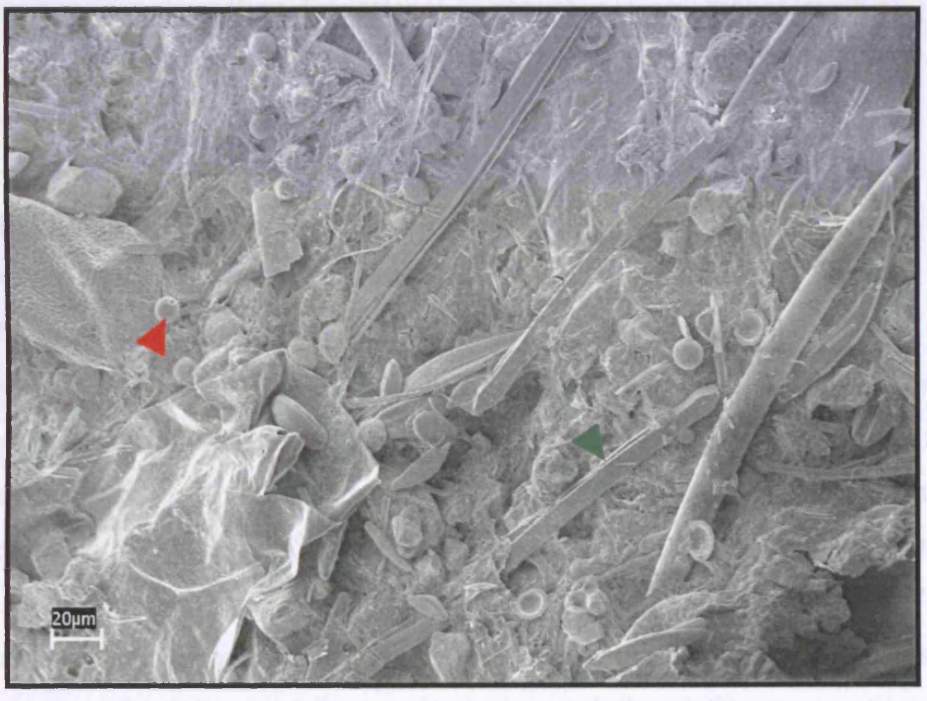

C') SEM-topographic

Fig. 5.34(cont.): C: Biogenic organic lamina of varve 544.

sand-sized polyhedral calcite grains ~90 μm in diameter, cf. *C* in Fig. 5.34). A sharp reduction in grain-size was recorded in intervals *B* through *D*. Initially, this change is sharp (cf. Fig 5.32) and coincident with the abrupt change in carbon-burial dynamics and shift in sediment colour from reddish-brown to cream-brown at 16 m depth (see Section 5.2). Calcite crystals in interval *B* are still silt-sized, but much finer than those recorded in interval *A*. Subsequent change in grain-size is gradual. The end product of the decrease is recorded in calcite laminae in intervals *C* and *D*. Here, the basal calcite laminae are still silt-sized, but the succeeding calcite laminae are micritic in nature, separated occasionally from the basal calcite lamina by a thin, ~30 μm diatom ooze lamina (*b*, varve 314, *iii*, Fig. 5.35). The change in grain-size is mirrored by a significant change in grain morphology. For example, below varve 546 calcite grains are more rhombohedral (Fig 5.36) whereas calcite grains in varves above this point possess more complex polyhedral and dendritic morphologies (Fig. 5.37). According to the models advanced by Folk (1974) and Koschel (1997), this morphological change indicates increasing impurity absorption, for instance of phosphorus, and higher levels of supersaturation in the waters from which they precipitated.

5.3.3. Phytoplankton succession within the varve

Below varve 543 there was no diatom ooze lamina. Instead, an organic mud lamina forms the biogenic varve-segment. This contains low to rare numbers of the centric diatoms *C. radiosa* and other unidentified large pennate diatoms, as well as Chrysophyceae cysts. The lattermost are usually, but not exclusively, found near its lower contact. Above varve 543 distinct diatom ooze laminae are preserved. The varve cycle begins with frustules of *S. acus var. angustisimma* and *S. nana.* (as in interval *B* and *D*), or predominantly *C. ocellata* but also some *C. radiosa* (as in interval *C* and *D*) or *S. parvus* (as in interval *D*).This may be followed by a bloom of *S. parvus* associated with the onset of calcite precipitation (as in interval *B* and *C*) or a continuation of decreasing numbers of the previous diatom bloom (as in interval *D*).

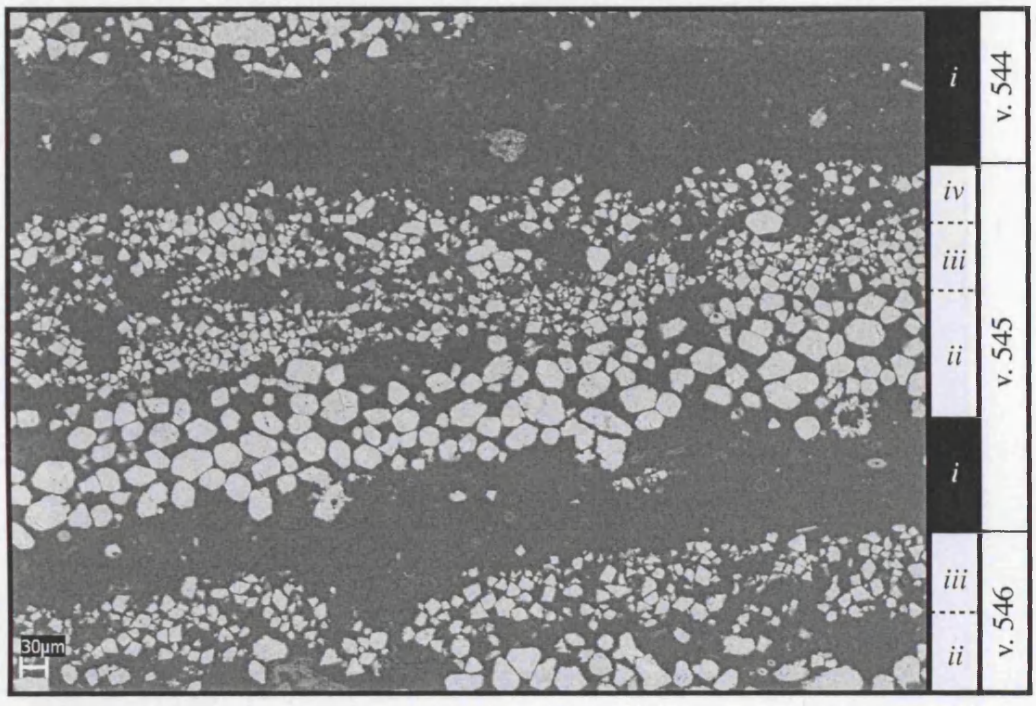

a)

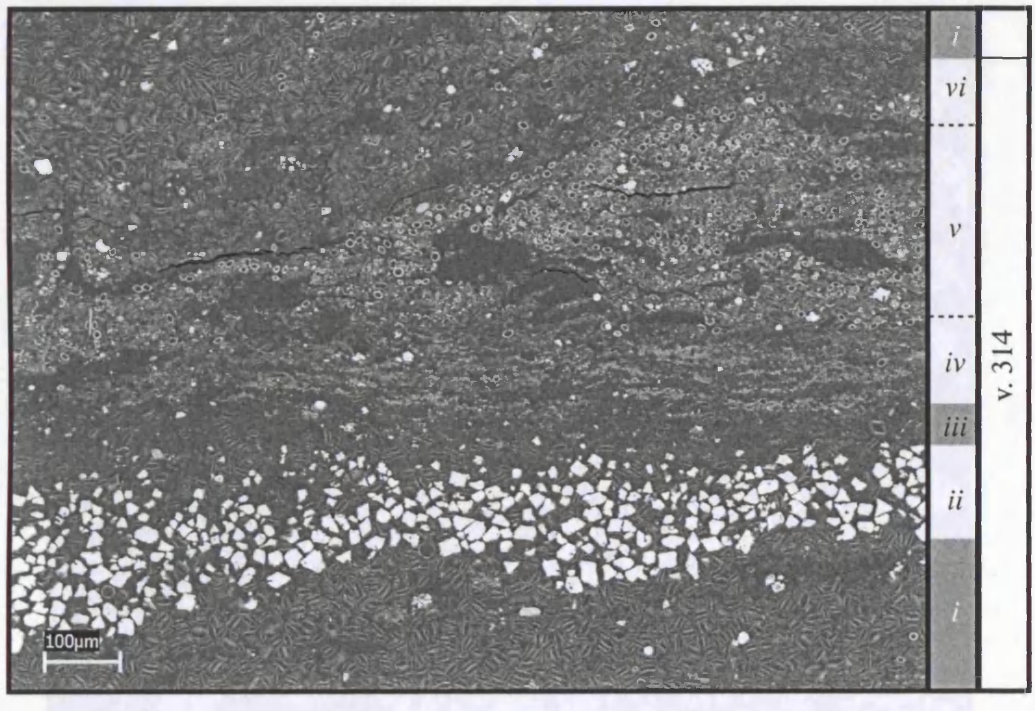

b)

Fig. 5.35: Calcite-diatom laminae (white filled boxes) in a) varve 545 of PTS77_3 and b) varve 314 in PTS70_1. Roman numerals indicate laminae number per varve. Black filled boxes donate biogenic organic mud lamina and grey filled boxes donate biogenic diatom ooze lamina.

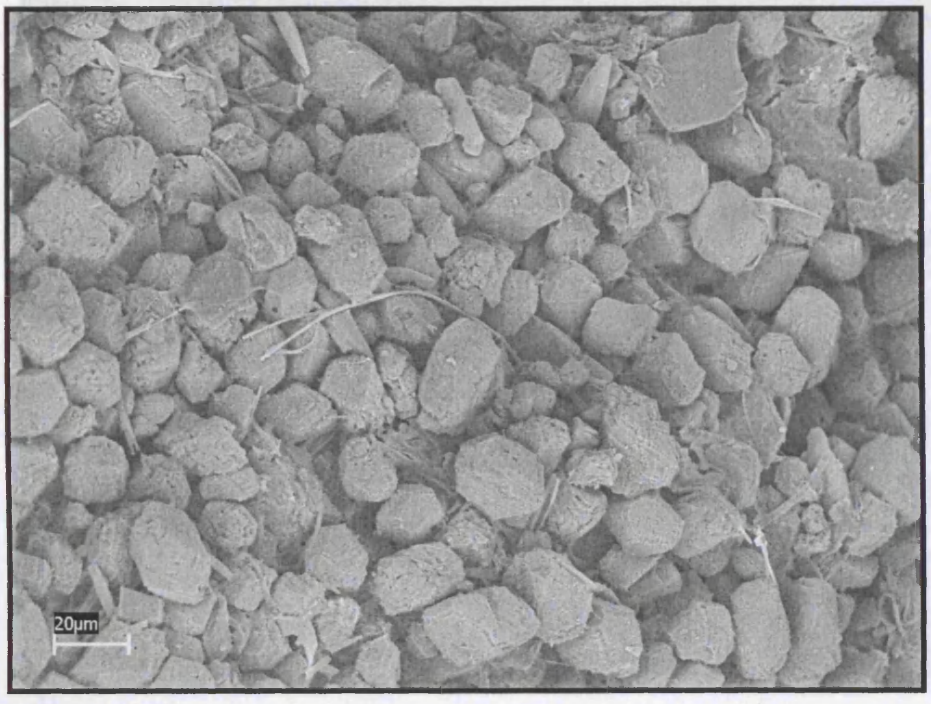

a)

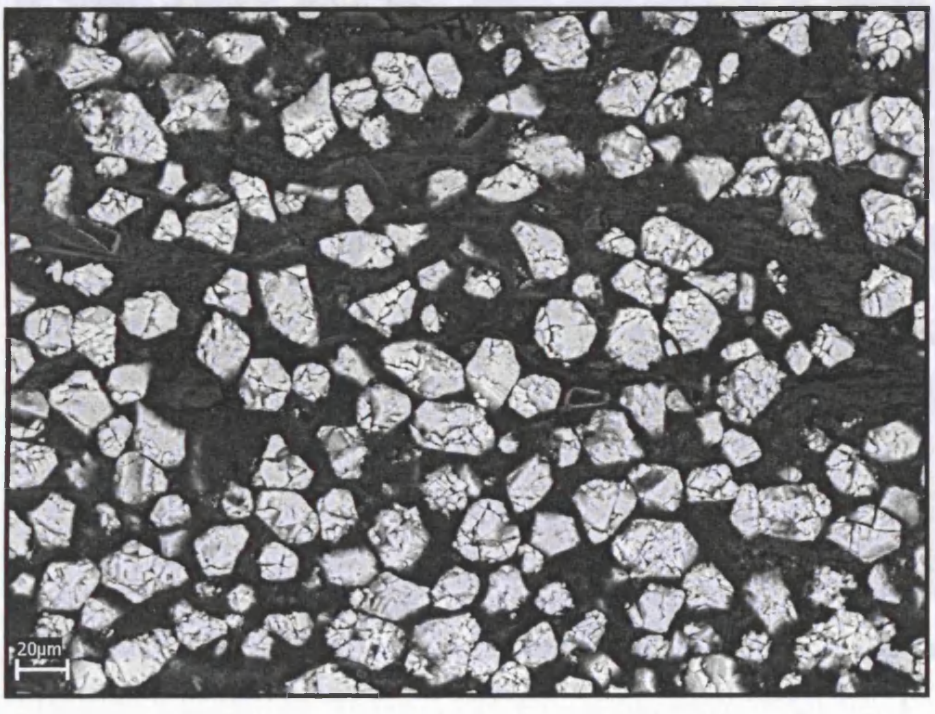

b)

Fig. 5.36: Calcite grain morphologies preserved below 4000 Cal. BP.
a) SEM topographic. b) SEM BSEI.

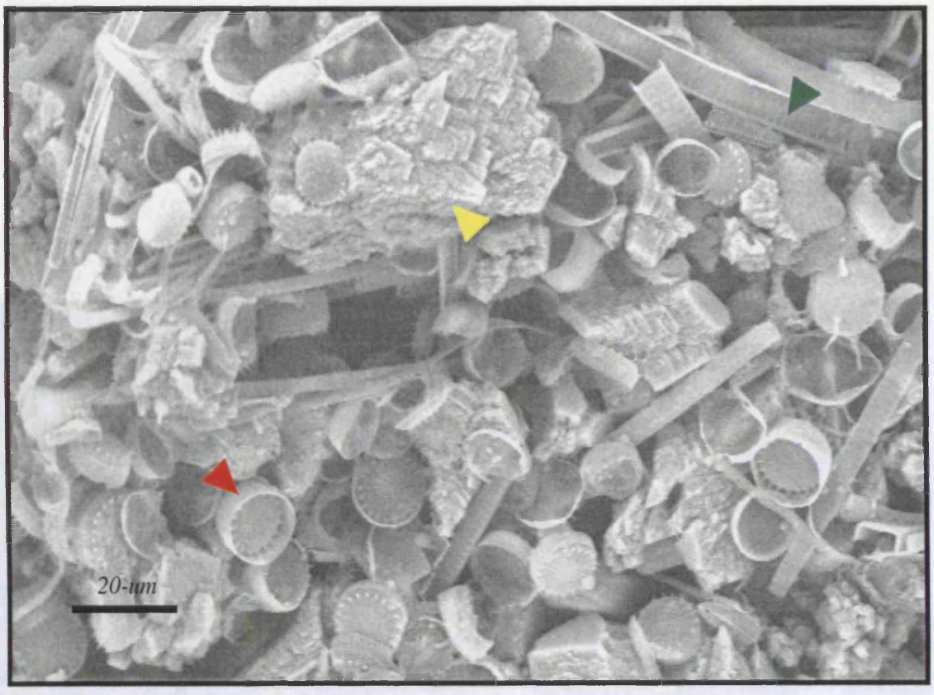

a)

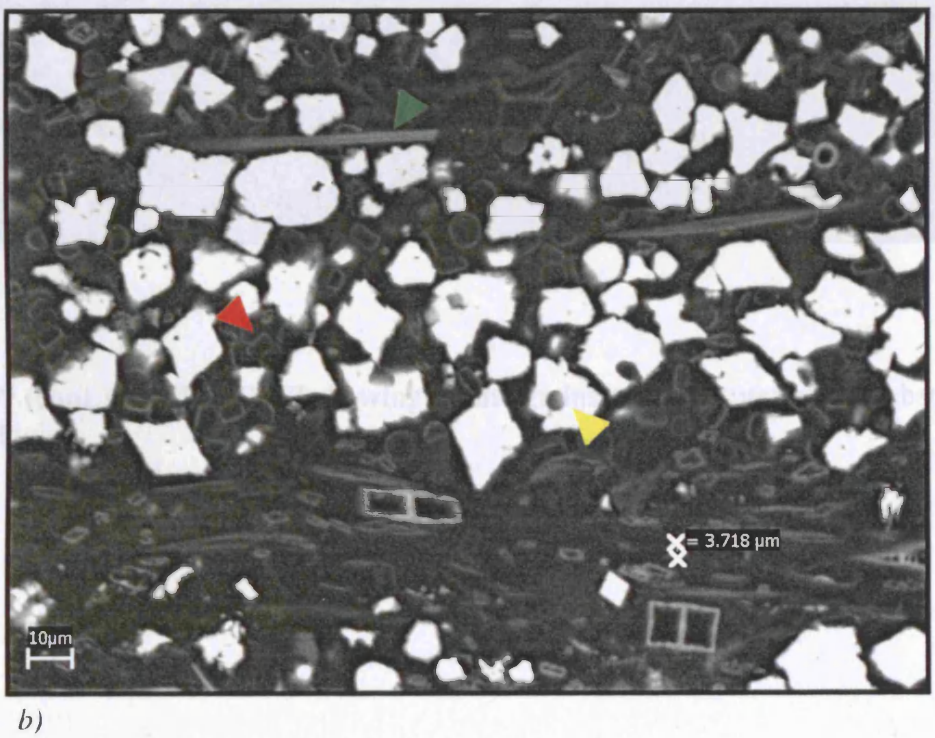

b)

Fig. 5.37: Calcite grain morphologies preserved above 4000 yrs BP. The green triangle picks out *Synedra* spp. frustule; red triangle shows *S. parvus* frustule and yellow triangle shows polymorphic calcite grain in a) SEM topographic and b) SEM-BSEI of spring calcite-diatom lamina.

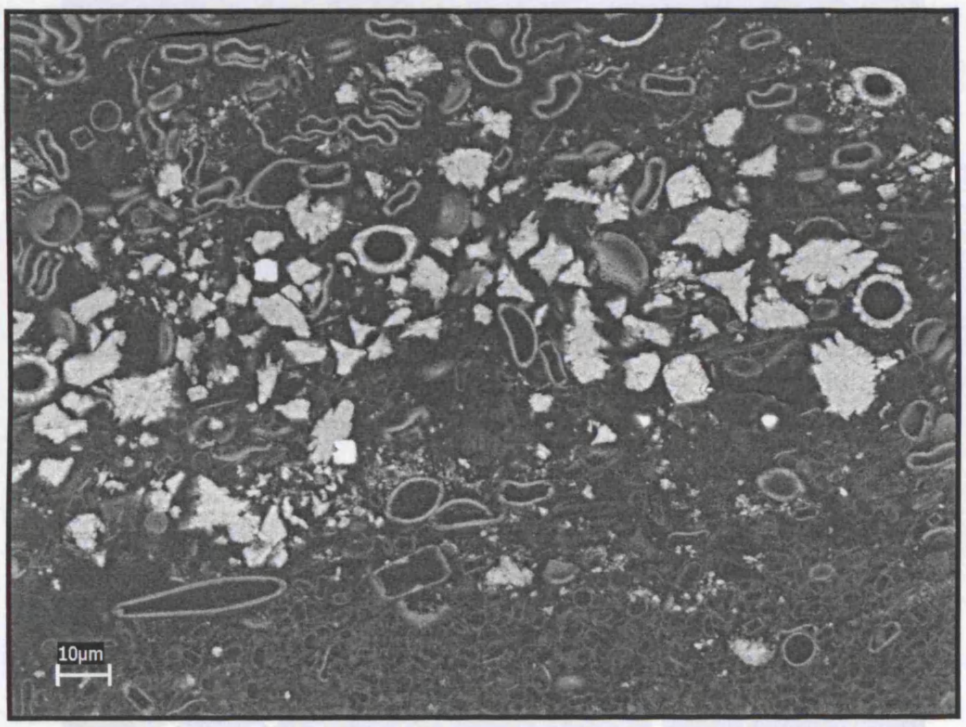

c)

Fig. 5.37 (cont.): c) SEM-BSEI showing calcite grains with non-preferential absorption morphologies.

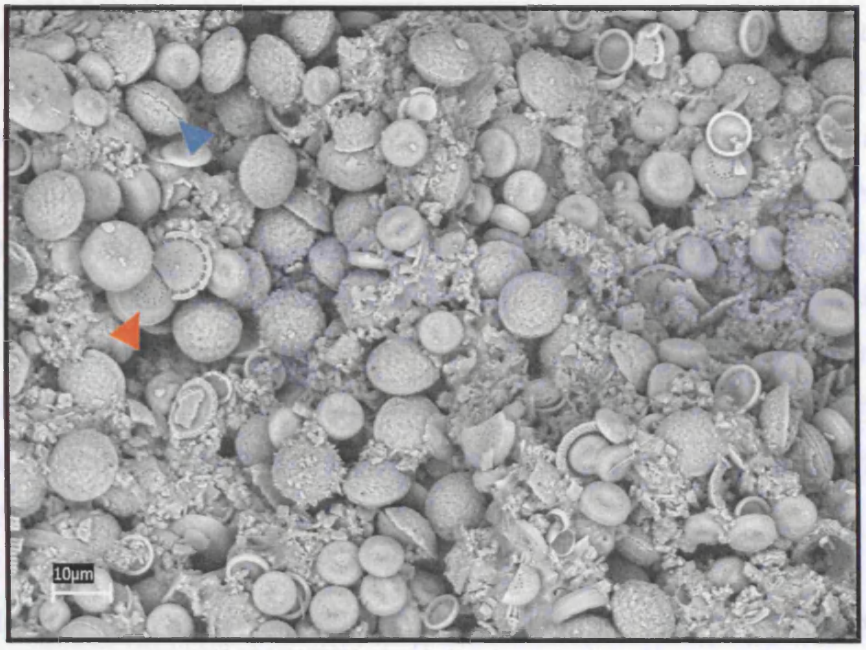

d)

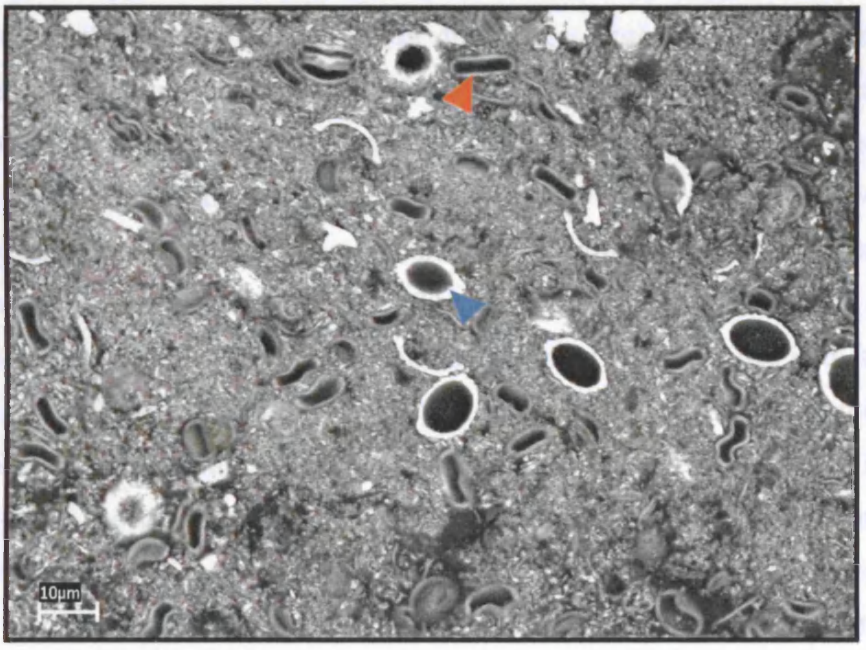

e)

Fig. 5.37 (cont.): The blue triangle picks out a 'bi-valved' *Phacotus lenticularis* calcite lorica whilst pink triangle picks out *C. radiosa* frustule in d) SEM topographic and e) SEM-BSEI of summer micrite calcite-diatom lamina.

The remaining calcite laminae are associated with varying numbers of the green algae *P. lenticularis* (*e.g.*, rare to minor in interval *A*, and minor through abundant in interval *B* through *D*) and rare to minor numbers of *C. ocellata* and *C. radiosa*. *Phacotus* spp. is the most dominant phytoplankton component in the uppermost calcite laminae of the 'triple-structure' in, for example, varves 505 and 314, and a significant component of the middle (micrite) laminae in for example, varve 281. *C. rossii* is preserved in significant numbers in the coarser micrite calcite laminae in interval *D* (*e.g.*, varve 282). Phytoplankton succession finishes in intervals *B* through *D* in a calcite lamina composed of a mixed assemblage flora/fauna of large pennate and centric diatoms, chrysophytes and sponge spicules.

The BSEI varved phytoplankton succession is similar to that reported from modern phycology studies of northern hemisphere temperate lakes (Section 4.3.1). It demonstrates the varved nature of Diss Mere's laminae. Below 16 m, diatom productivity is suppressed. Annual succession is therefore recognised by increased preservation of the summer production of green-alga *Phacotus* spp. in inorganically precipitated calcite laminae. This is followed by the preservation of chrysophyte cysts in the base of the overlying biogenic organic matter lamina deposited during the peak of Chrysophyceae crop at the start of autumn. Above 16 m, the vegetative period commonly begins with preservation of cold-water spring-blooming diatoms *Synedra acus/nana* and *S. parvus*. or *C. ocellata*. The close association of the onset of calcite precipitation either shortly after the first diatom bloom, or with a change in diatom flora, indicates that biological productivity played a significant role in inorganic calcite precipitation. Diatom numbers decline throughout the calcite lamina and increased preservation of the green alga *P. lenticularis* concentrated in either the middle or uppermost calcite lamina of the 'triple-structure' indicates inorganic precipitation continued to occur during mid to late summer. Where preserved, a mixed assemblage of centric and pennate diatoms, Chrysophytes and sponge spicules indicates that the top of the varve cycle was deposited during the autumn period of lake overturn. The sharp onset of the next spring diatom bloom suggests the sedimentation was markedly reduced in the lake during winter.

Changes in spring diatom succession are probably related to the timing and strength of spring circulation that controls the supply rates of principal nutrients, *e.g.*, silicon and phosphorus and the preferred light regime for photosynthesis. Spring blooms of *Stephanodiscus* spp. and *Synedra* spp. prosper when supply ratios of Si:P are very low and illumination restricted. Their preservation is therefore consistent with periods of more vigorous spring circulation. *Cyclotella* spp., due to their superior ability to compete for phosphorus in low concentrations, probably bloomed in spring when supply ratios of phosphorus diminished and light levels increased during periods of less vigorous overturn. Summer diatom blooms are likely to be smaller than spring blooms because of the onset of thermal stratification, nutrient limitation and increased herbivore grazing. The predominance of *Phacotus* spp. in summer laminae may provide further evidence that they can survive ingestion by summer grazers because of their calcite lorica. The dominance of green algae and, presumably, cyanobacteria during summer stratification, reflects their ability to utilize nutrients at depth just above the thermocline. Preservation of small numbers of *Cyclotella* spp. frustules in calcite laminae probably reflects their ability to sink to a deeper zone during summer stratification and compete for hypolimnetic nutrients as well. Diatom productivity during autumn appears suppressed relative to spring. This may indicate less vigorous autumnal lake overturn, or more likely, that nutrient supply had been exhausted by spring and summer productivity.

5.3.4. Changes over time in lake chemistry

The 'triplet-structure' evident in the calcite-laminae demonstrates that calcite precipitation occurred most years over three periods from spring to summer. Whilst calcite precipitation is clearly linked to seasonal warming of lake waters the tri-association of calcite laminae appears to be linked to the seasonal order of phytoplankton events; the first, commonly coarser-grained calcite laminae occurs with the first diatom bloom, or with a change in diatom flora in spring and the finer-grained second and third laminae are coincident with the preserved remains of the clear-water phase and therefore the timing of blue-green/green algae primary productivity. According to Folk (1974) and Koschel (1997), the coarser grain-size and more

rhomobohedral morphology of calcite crystals preserved below 16 m is indicative of slow growth of calcite in a meso-oligotrophic lake. The published diatom and fossil pigment stratigraphies for Diss Mere's varves (Fritz, 1989) also reveal that mesotrophic conditions persisted through much of this period. Mesotrophic conditions are explained by the moderate to high fossil pigment concentrations of the carotenoids oscillaxanthin and myxoxanthophyll. They indicate that a mixed assemblage flora of blue-green cyanobacteria dominated the phytoplankton community at this time restricting growth of diatom populations to low nutrient specialists, *e.g.*, *Cyclotella* spp. The latter is confirmed by the absence below 16 m of any diatom blooms in the BSEI phytoplankton succession. Sediment trap studies in analogous varved hardwater lakes show that most of the OM that is preserved in sediments comes from populations of diatoms that settle rapidly and escape oxidation in the epilimnion (Dean, 1999). Cyanobacteria are less important than diatoms in contributing to the ultimate accumulation of OM in profundal sediment, but are important for carbonate production (see Section 2.4 and Mullins *et al.*, 1998; Megard *et al.*, 1993). The prevalence of cyanobacteria and absence of diatom blooms would therefore account for the high concentrations of calcite and low amounts of OM and opal buried below 16 m. This scenario suggests that Diss Mere's waters experienced restricted water-column overturn during this period, with protracted or even perennial stratification, *i.e.*, meromixis. These conditions would be enhanced by warmer summers and/or colder winters (increased seasonality). Evidence of increased summer temperature is also indicated by relative prevalence amongst the restricted diatom population of the warm climate indicator, *Cyclotella radiosa* (see Fig. 4. 1 and Stoermer & Ladewski, 1976). Colder winters are indicated by the absence of significant diatom blooms, low numbers of diatoms cysts and a relatively low burial rate of OM (see section 4.3 and Fig 4.1). The dominance of blue-green algae would enhance bacterial reduction of sulphate and accounts for higher Fe-burial below 16 m. Permanent stratification would also result in anerobic decomposition of OM at the sediment water interface and in the sediment itself (Müller *et al.*, 2003). The resultant increase in pH does not cause calcite dissolution, as might be expected following aerobic decomposition, but results in calcite precipitation and an overall increase in observed grain-size.

Above 16 m, the reduction in calcite grain-size and increase in polymorphic and dendritic grain-morphologies is indicative of higher supersaturation due to lake eutrophication (Folk, 1974; Koschel, 1997). A marked reduction in fossilised carotenoid concentrations suggests that cyanobacteria became less important as primary producers. The preservation of multiple diatom blooms, especially of *Stephanodiscus* spp. and *Synedra* spp., but also *C. ocellata* as well as a significant increase in lorica of *P. lenticularis* confirms an increase in lake trophic status. A shift from cyanobacteria to diatom-dominated productivity can be explained by increased and more intense period of water-column overturn during spring (due to an earlier timing of ice break-up in spring or an absence of ice during winter) and more restricted summer stratification. These conditions might be enhanced by decreased summer temperature and milder winters (decreased seasonality). Increased spring overturn would have made available bottom-waters rich in nutrients, *e.g.*, phosphorous and silicon, promoting blooms of spring diatoms. Above 16 m, bioturbation, which disrupts the varved fabric at 15.44-15.50 m and 15.81-15.92 m depth (see Section 5.3), provides further evidence for both increased and cyclical variation in the degree of lake overturn. Increased presence of dissolved phosphorous in surface waters would have greatly inhibited the precipitation of calcite during spring and summer, and partly explains the rapid decrease in calcite burial above 16 m as well as the smaller grain-size. The concomitant increase in OM and opal burial is explained by increased diatom productivity (Megard, 1968; Dean, 1999). Seasonal regeneration of oxygen to Diss Mere's bottom waters would have promoted aerobic OM decomposition in the water column and sediments as well. The resultant decrease in pH would have promoted dissolution of calcite grains and may also have contributed to the rapid decrease in calcite burial, as well as the observed reduction in grain-size. The relative shallowness of Diss Mere, *i.e.*, only 6-8 m, means that dissolution in the water column was probably not that significant. Settling velocities for calcite crystals would have been in the order of hours and not days (Kelts & Hsü, 1978; table 9, page 317). It is clear that dissolution would have only played a significant role in sediment pore-waters, post-deposition.

5.4. Time-series and spectral analysis

Results of spectral analysis of varve thickness and elemental Ca and Fe time-series are shown in Figs. 5.40 through 5.42. Power law fit to log-log plots of power spectra and the resulting red noise background spectrum for each periodogram are shown in Figs. 5.36 through 5.39. Despite the low correlation between light and dark layers preliminary spectral analysis (results not shown here) indicated that no new information would be discerned by calculating power spectra for seasonal components. Consequently, only total varve thickness was considered for Discrete Fourier Transform (DFT) investigation. For varve thickness, each power spectrum corresponds to one of eleven overlapping 100 yr data segments denoted next to the time-series. DFT spectra for XRF data, represent power spectra calculated from three periods: 2480-3640, 3760-4510 and 4510-4880 Cal. BP.

For varve thickness data, peaks significant at the 95% confidence level were centred on, *i)* 20, *ii)* 8 to 7, *iii)* 5, *iv)* 3.6 and *v)* 2 to 3 yrs. Power at periods less than 10 years were most pronounced between ~3900-4300 Cal. BP (segments *H* to *P*). Overlapping power spectra demonstrate that this period contains temporally passive (*e.g.*, segments G, I, P) and active phases (*e.g.*, segments H, J through O) of cyclicity characterised by a degree of non-stationarity, *i.e.* a change in dominant wavelength with time. The persistent presence of cycles with a period of 20 yrs in segments *A* to *E* implies that the varve thickness data since ~3600 Cal. BP is stationary.

Aspects of the same regular cyclicity found in varve thickness data is seen in elemental Ca and Fe time-series. Elemental Fe data are characterised by cycles corresponding to periods of ~20 and 23-22 yrs. In addition, a number of multidecadal cycles were found with periods of, *i)* 84-75, *ii)* 44-37, *iii)* 30-25, and *iv)* 17.5 yrs. Only the period corresponding to 20 yrs is evident in all three segments investigated. Elemental Ca data is also characterised by cycles with periods of ~20 yrs (segments *A* & *C*), as well as

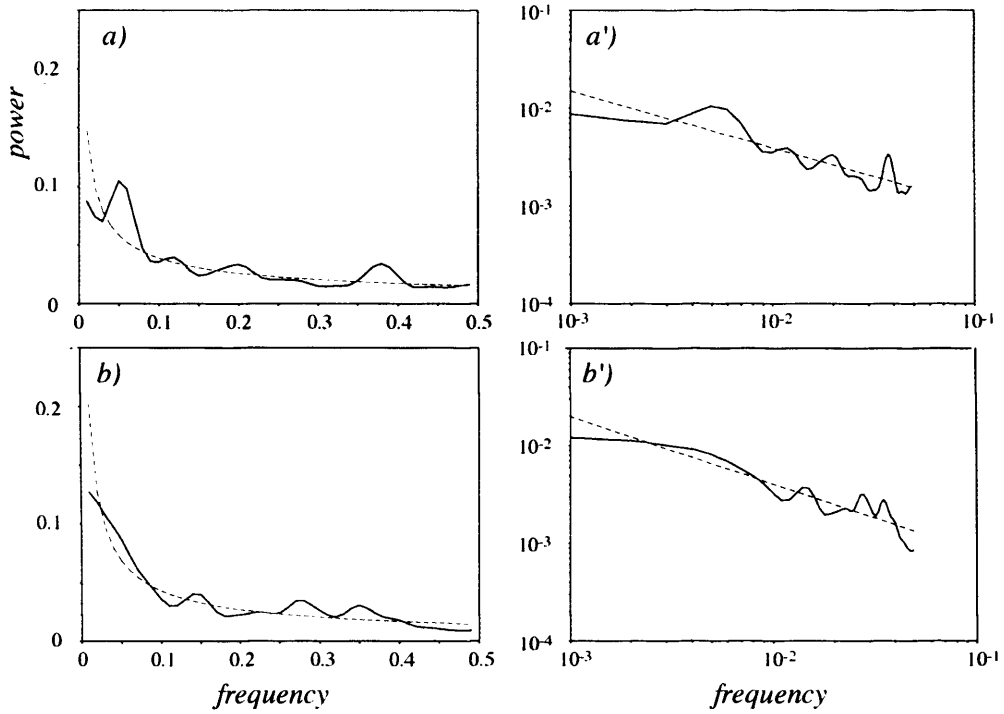

Fig. 5.38: Estimation of red noise background spectrum (red line) for power spectrum of varve thickness time-series from a) varves 1-322 & b) varves 350-864. Derived from fit of least square straight (blue) line to log-log plots (a' & b') of same power spectra.

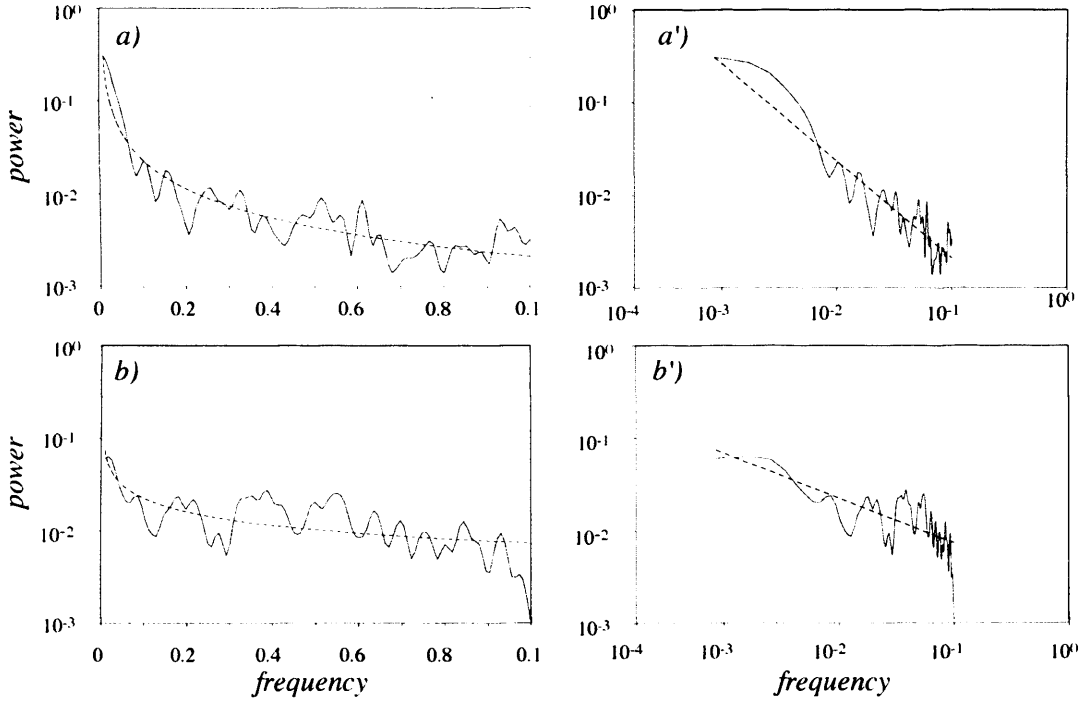

Fig. 5.39: Estimation of red noise background spectrum (red line) for power spectrum of a) Elemental Ca & b) Elemental Fe time-series data from 2500-3660 Cal BP using fit of least square straight (blue) lines to log-log plots (a' & b') of the same power spectra.

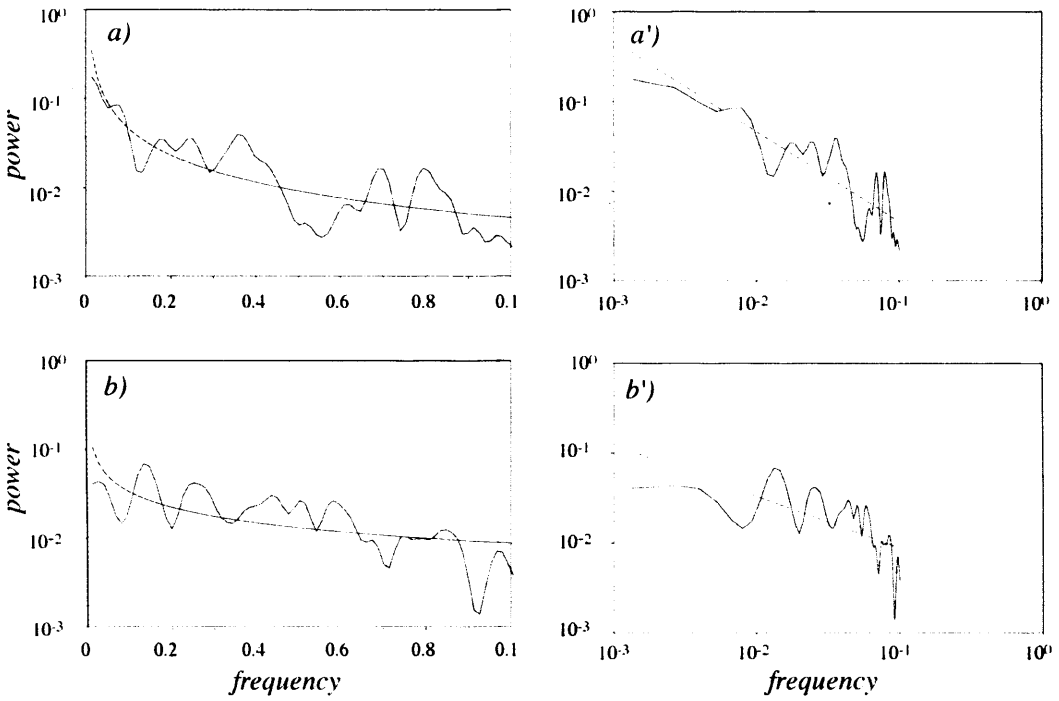

Fig. 5.40: Estimation of red noise background spectrum (red line) for power spectrum of a) Elemental Ca & b) Elemental Fe time-series data from 3770-4530 Cal. BP using fit of least square straight (blue) lines to log-log plots (a' & b') of the same power spectra.

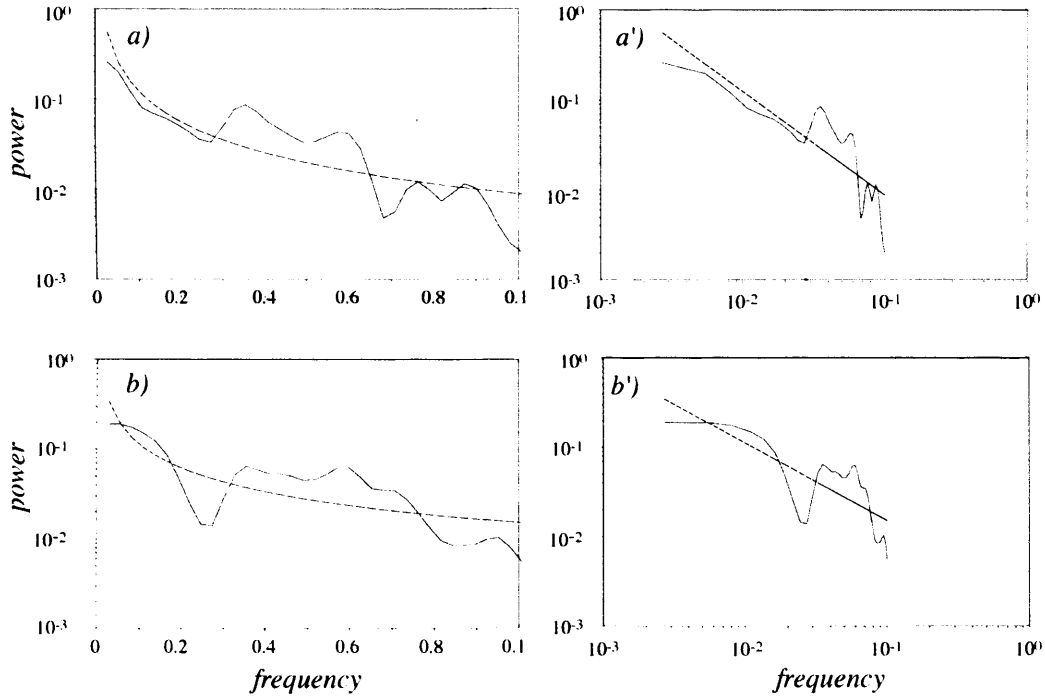

Fig. 5.41: Estimation of red noise background spectrum (red line) for power spectrum of a) Elemental Ca & b) Elemental Fe time-series data from 4530-4900 Cal. BP using fit of least square straight (blue) lines to log-log plots (a' & b') of the same power spectra.

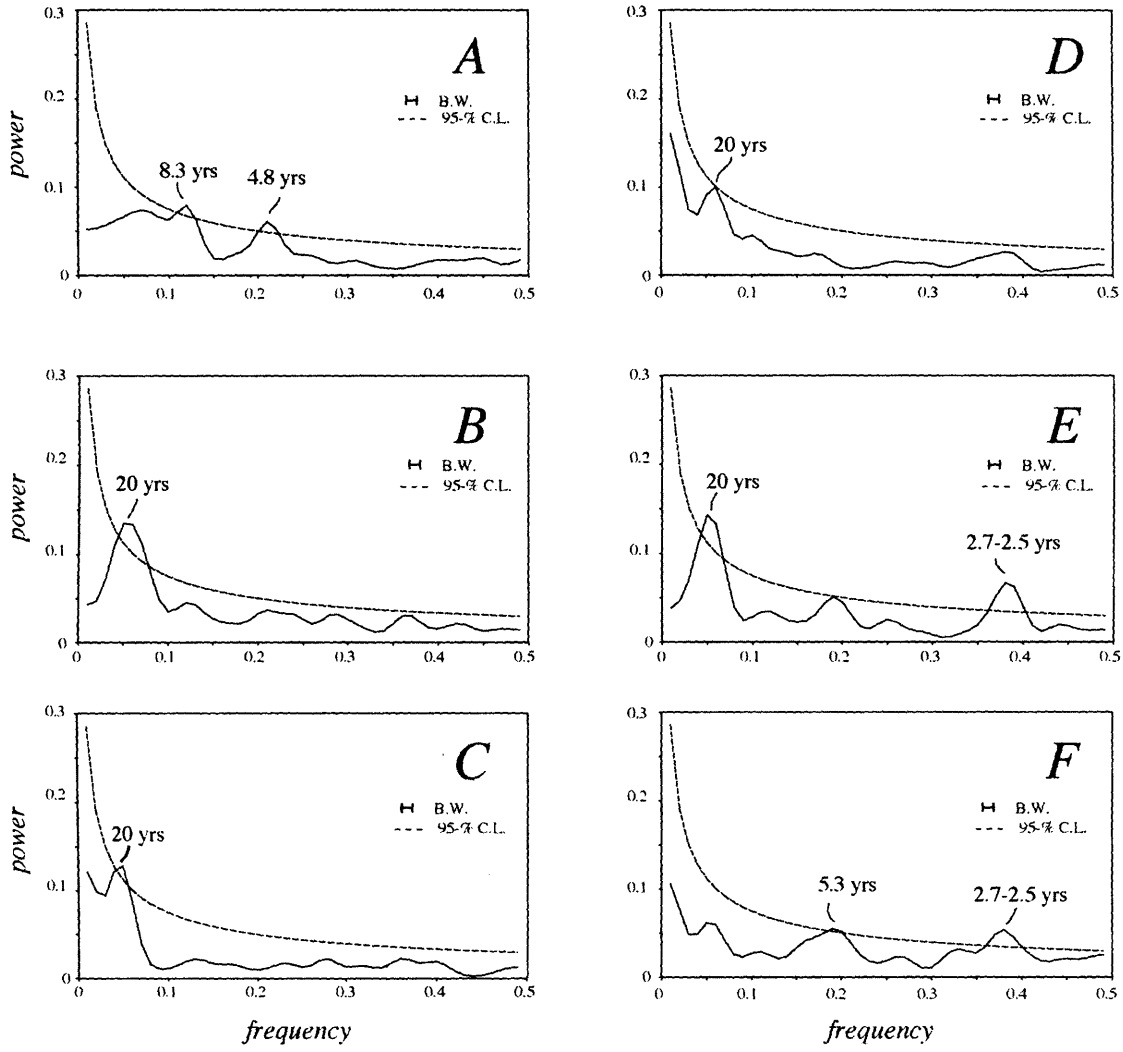

Fig. 5.42: Power spectra for varve thickness time series (varves 1 to 322).

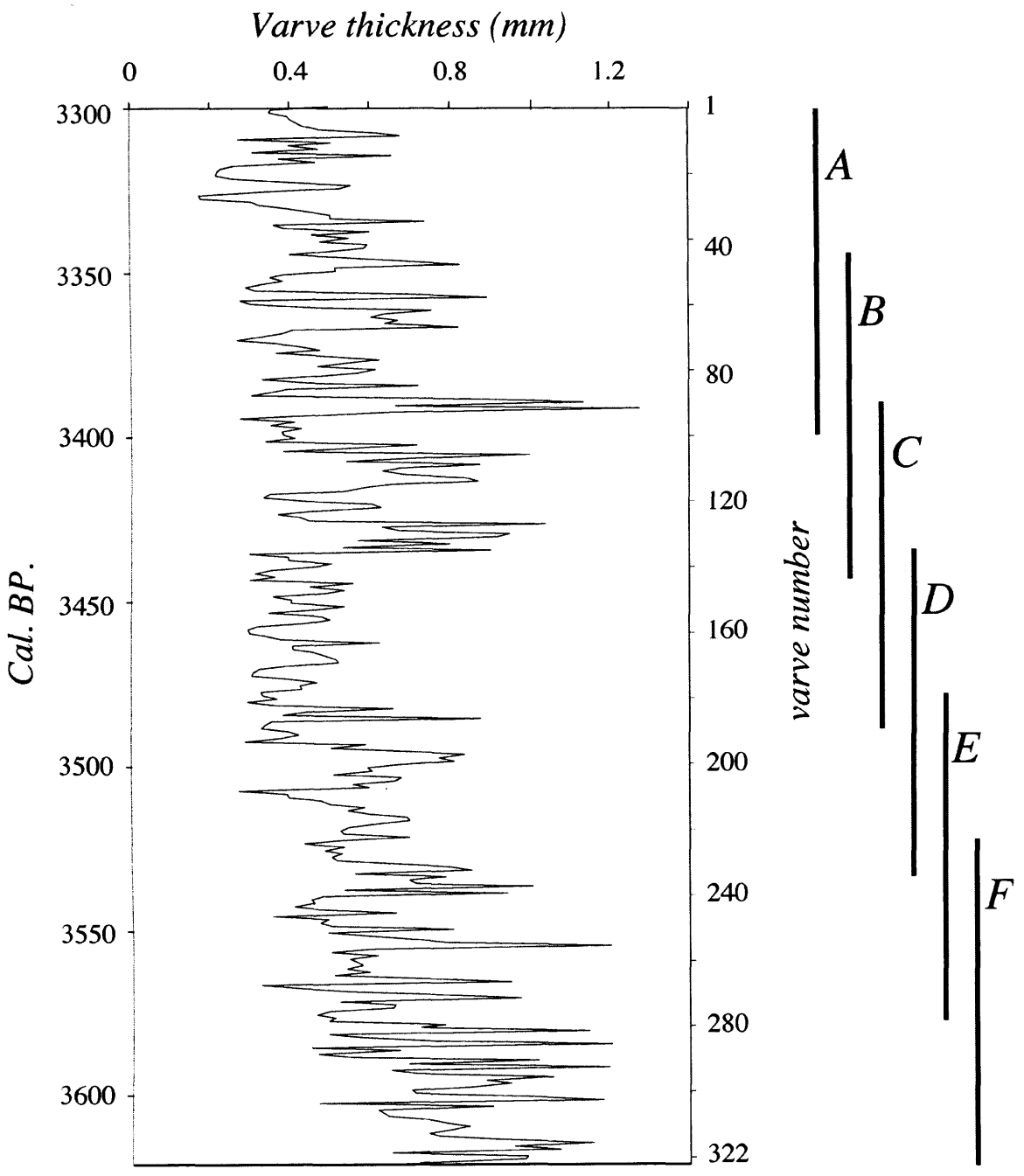

Fig. 5.42 (cont.): Varve thickness time-series (varves 1 to 322). Corresponds to 15.62-15.80 m (composite) depth

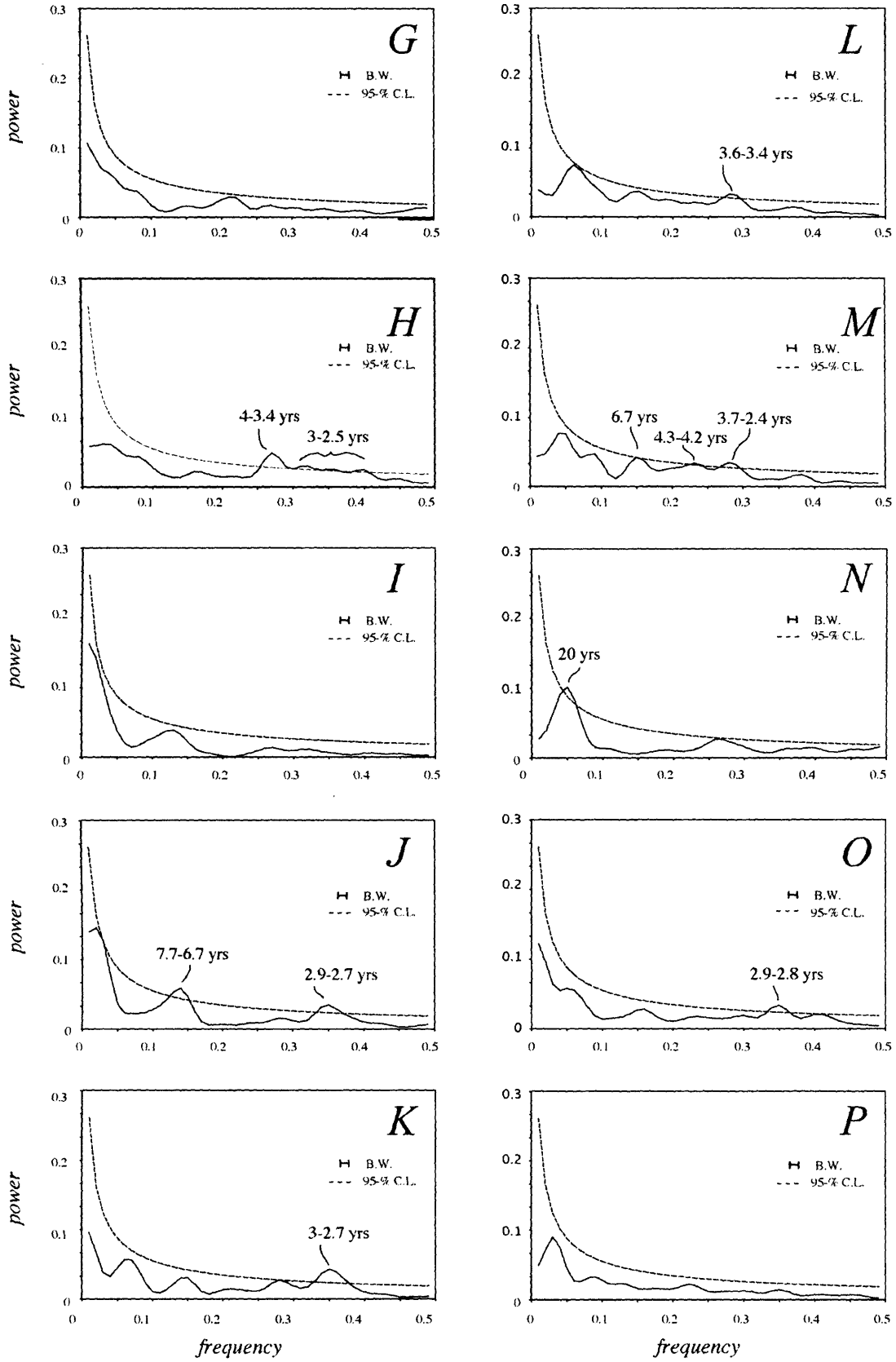

Fig. 5.43: Power spectra for varve thickness time series (varves 350 to 864).

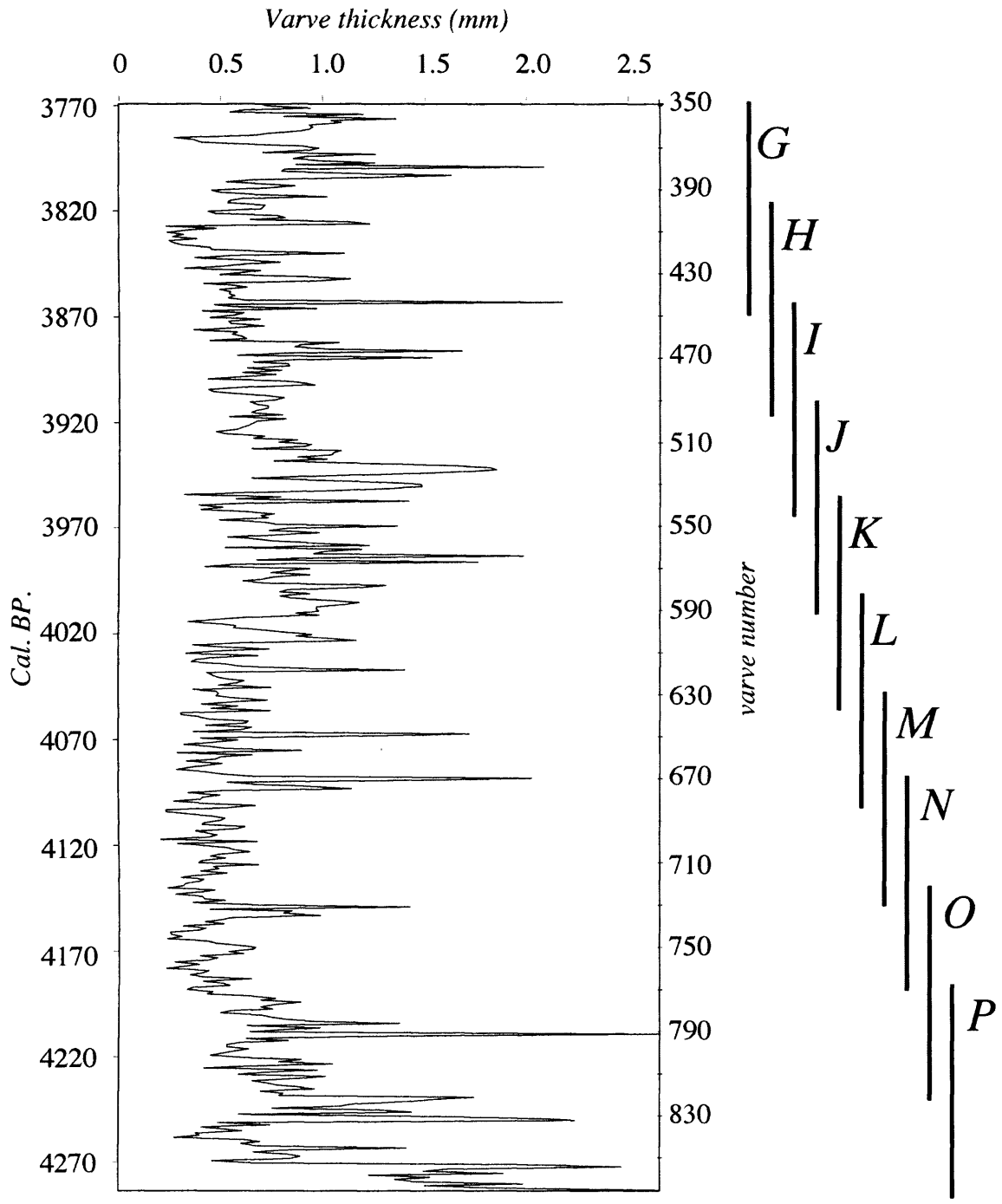

Fig. 5.43 (cont.): Varve thickness time-series (varves 350 to 864). Corresponds to 15.89-16.16 m (composite) depth.

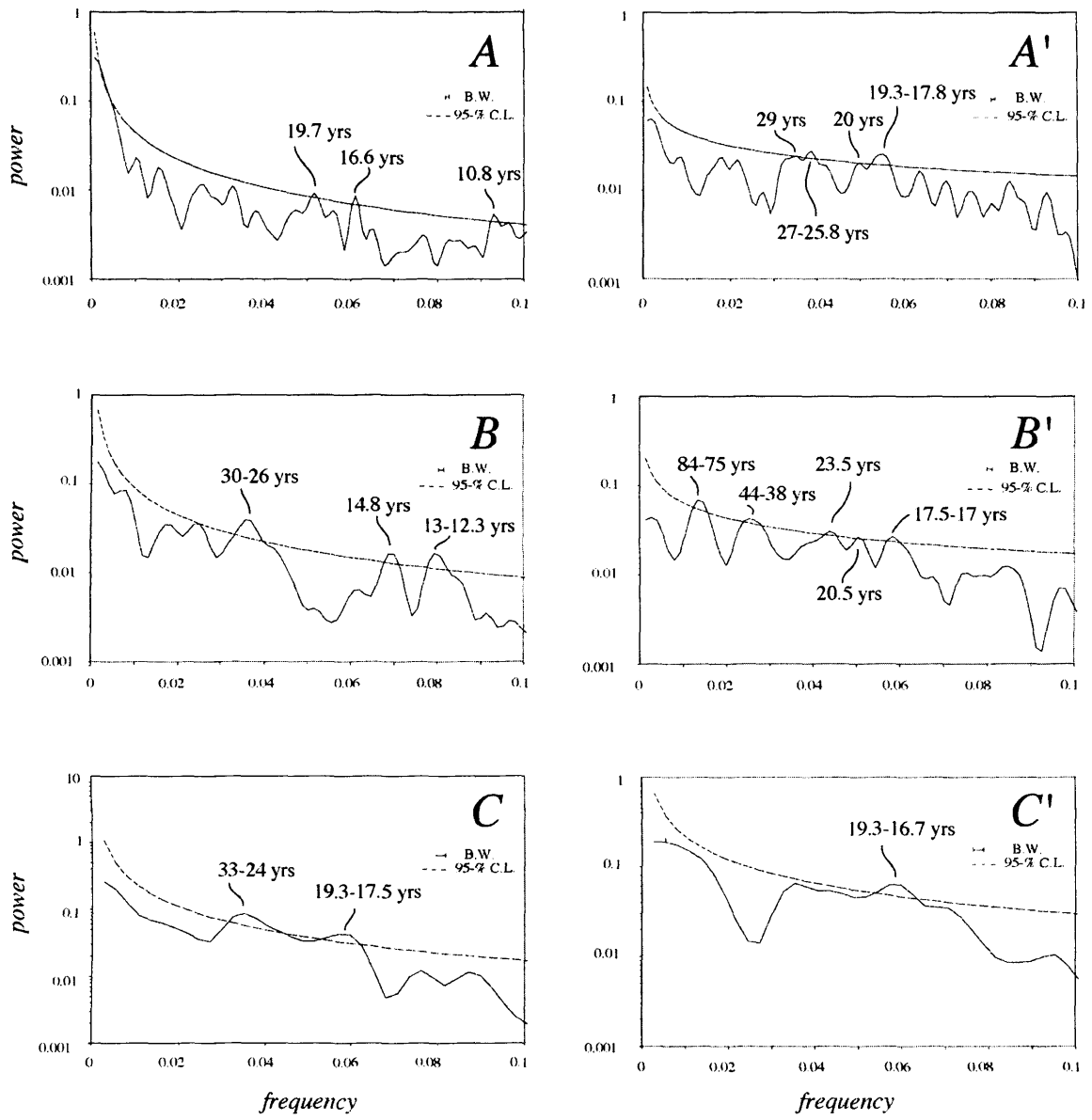

Fig. 5.44: Power spectra of XRF 2 mm Ca- (A through C) and Fe- (A' through C') elemental abundance from ~2500-4900 Cal. BP.

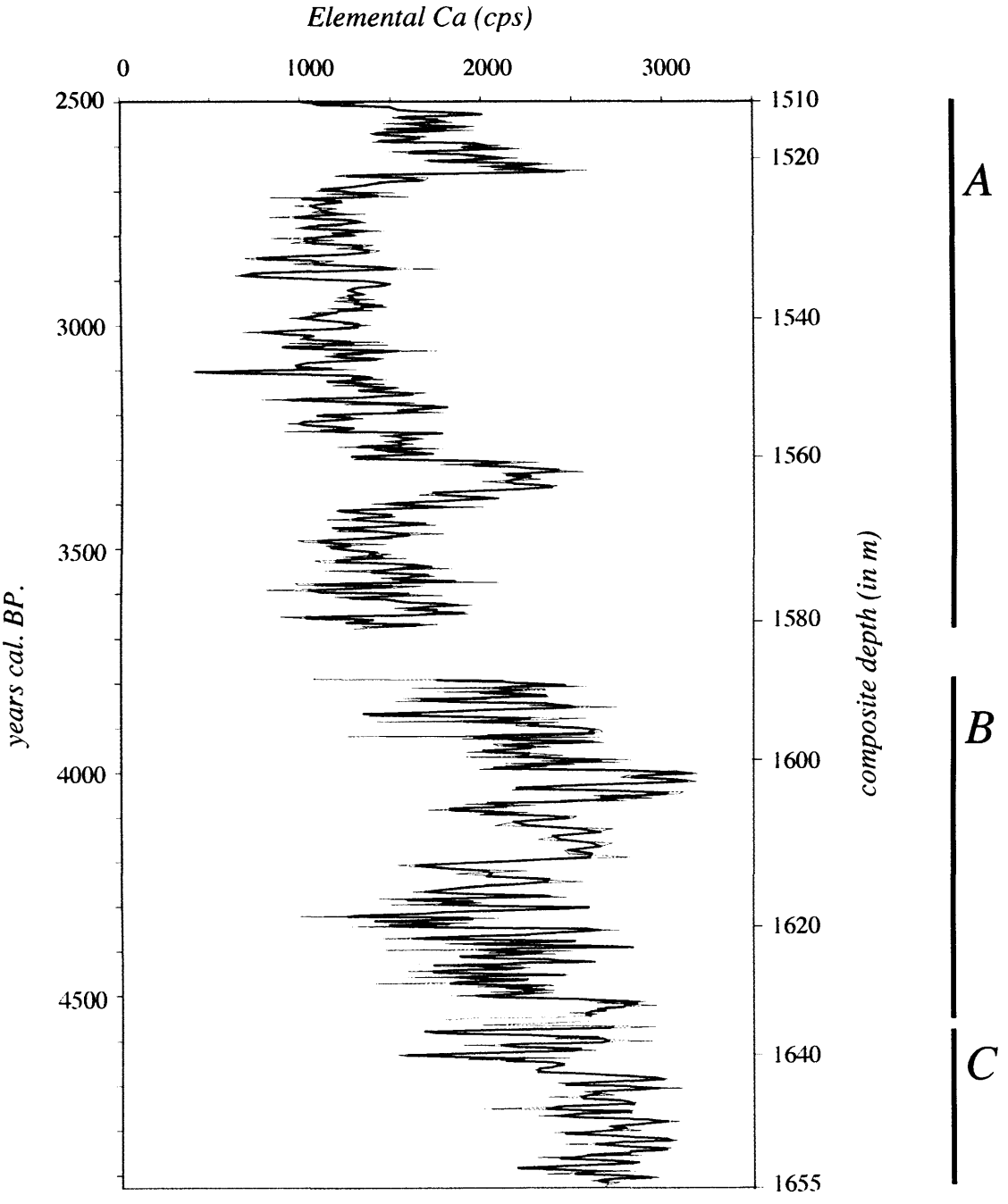

Fig. 5.44 (cont.): XRF 2 mm Ca-elemental abundance (blue line) from ~2500-4900 Cal. BP. Black line is 50 point moving average.

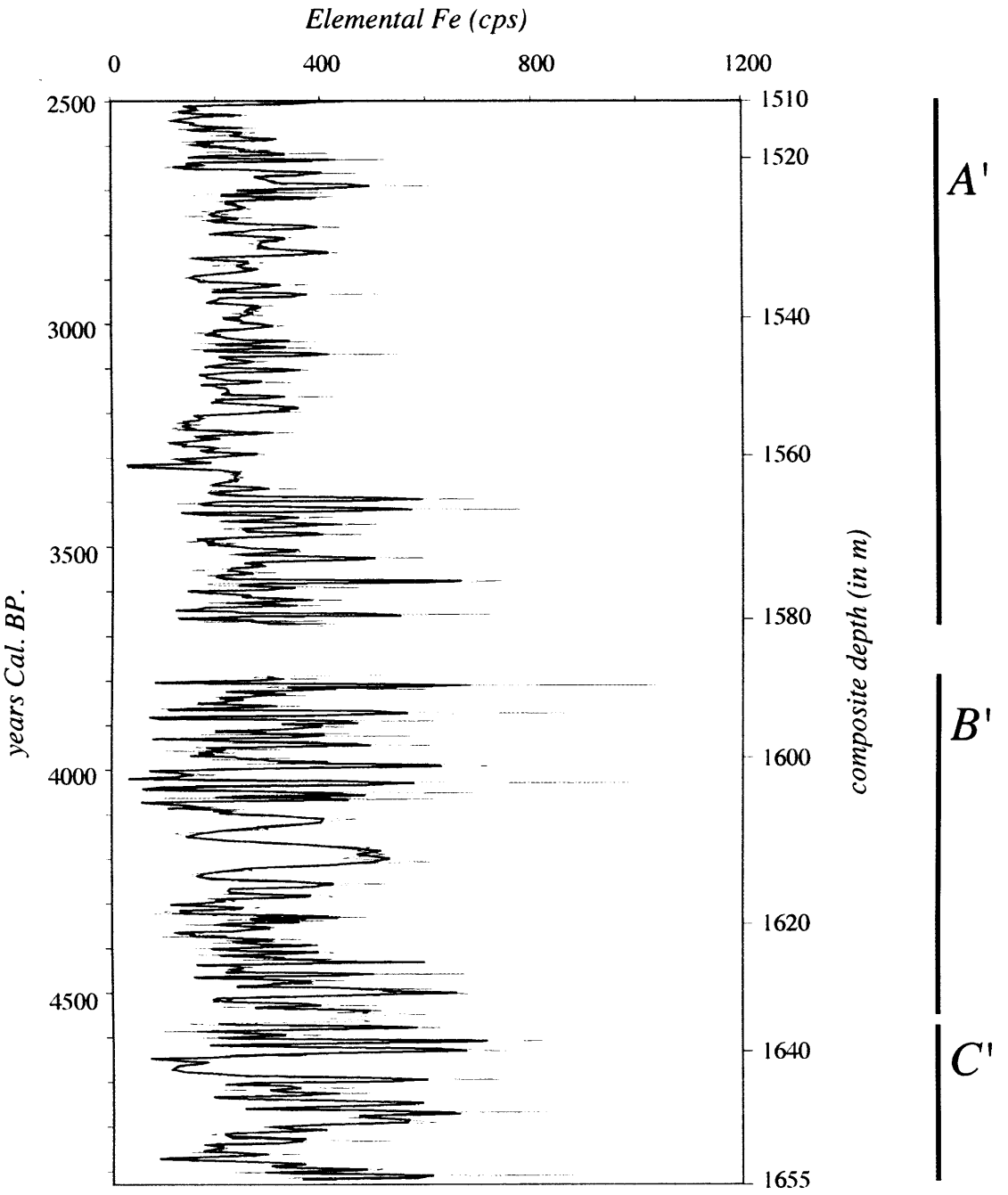

Fig. 5.44 (cont.): XRF 2 mm Fe-elemental abundance (red line) from ~2500-4900 Cal. BP. Black line is 50 point moving average

significant power at frequencies corresponding to 30-25 yrs (segments *B* & *C*). In addition, periods of 16.6, 15 to 14.5, 13-12 yrs, and 10.7, are also detected in the spectra.

The periodicities found at *i)* 20 yrs, *ii)* 7-8 yrs, *iii*) 5, *iv)* 3-4, and *v)* 2-3 yrs are similar to those reported from the power spectra of a number of proxy and instrumental winter NAO reconstructions, and Greatbatch (2000) and Wanner *et al.* (2001) review many of these efforts. Significant power at 25-20 yrs and 7-8 yrs is reported by Rogers (1984), Cook *et al.* (1998), and Mann (2002). Cook & D'Arrigo (2002) report find significant power at 7.7 yrs, 4 yrs, and 2-3 yrs; Schneider & Schönwiese (1989) also report significant spectral power at a 'quasi-biennial' timescale (2-3 yrs) in monthly NAO data. Spectral analysis of an NAO record constructed from modern Red Sea corals reveals strong interannual variability at 5-6 yrs (Felis *et al.*, 2000). The NAO index of Jones *et al.* (1997), analysed using the same techniques outlined in section 3.3.4, also reveals significant power at 7-8 and 2-3 yrs (Fig. 5.43).

Existence of periodicities at 44, 25 to 30 and 23-22, 10.7 yrs in XRF elemental time-series may provide further evidence of some solar-climate link. These peaks are close to periodicities attributed to solar activity in climate relevant time series, *e.g.* 40-50 yrs and 20-25 yrs in ^{10}Be concentrations in Greenland ice core (Beer et al, 1994) and in tree-ring data on radiocarbon production (Stuiver, 1983; Stuiver & Braziunas, 1993). A global 'solar forcing' of sedimentation at such timescales is borne out in a number of varved sedimentary lake records from a range of geological periods. Notably, amongst others, these are the Holocene sediments of Lake Soppenssee, Switzerland (Livingstone & Hadjas 2001), Elk Lake, Minnesota, (Anderson, 1992, 1993; Bradbury *et al.*, 2002, Dean *et al.*, 2002), and Lake Holzmaar, Germany (Zolitschka, 1992, Vos et al., 1997). Figure 5.44 shows the correlation of the elemental Ca time-series with the low-pass filtered INTCAL 98 atmospheric Δ^{14}C radiocarbon age calibration of Stuiver *et al.* (1998), a proxy for solar variability. To maximize cross-correlation, the elemental Ca curve was moved 35 yrs relative to the Δ^{14}C curve, a shift well within the dating error associated with the calendrical chronology generated for the Diss Mere record. This technique is justified as although the tree ring chronology is probably accurate to within a few

decades (Stuiver *et al.*, 1986) the tentative nature of the correlation of pollen zones from Diss Mere to Hockham Mere means that the varve chronology although internally consistent, may only be placed accurately in time to within a few centuries (see section 5.1.2). Although there are differences between the two time-series, elemental Ca variation bears a strong resemblance to atmospheric $\Delta^{14}C$ variation after ~4000 Cal. yrs. BP, especially on centennial- to multi-centennial-timescales ($r = 0.36$, $n = 118$; significant at 99.99% confidence level). Minima in ^{14}C production rate (enhanced solar activity) correspond to periods of reduced carbonate burial and, commonly enhanced organic matter burial (cooler summers/milder winters, decreased seasonality).

Because of the ubiquitousness of high-frequency noise in geophysical time series, one should be careful in interpreting peaks in annual time series at periods of <10 yrs. However, the repeated occurrence of strong periodicities (well above the 95% confidence limit) at 2-3 yrs and 4-6 yrs in the varve series, as well as the common occurrence of increased power in these cycles in a variety of modern and palaeoclimate time series, point towards some real underlying environmental control. Given that, at the 95% confidence level, there is a one-in-twenty chance that a peak in a power spectrum will be statistically significant by chance. For example, in the varve thickness data, of the 50 frequencies investigated, statistically speaking, '2.5 peaks' could appear significant at the 95% confidence level, but could potentially be due to random sedimentation processes. This is a serious limitation for the interpretation of these results. However, it is the subjective opinion of the author that, if a peak is consistently present throughout the power spectra investigated, then it is likely to represent some real periodic phenomenon. Consequently, the existence of periodicities at 44, 25-30 and 23-22, 10.7 yrs (the latter of which is close to the resolution of the XRF power spectra and is probably a function of aliasing of higher frequencies) are considered with caution.

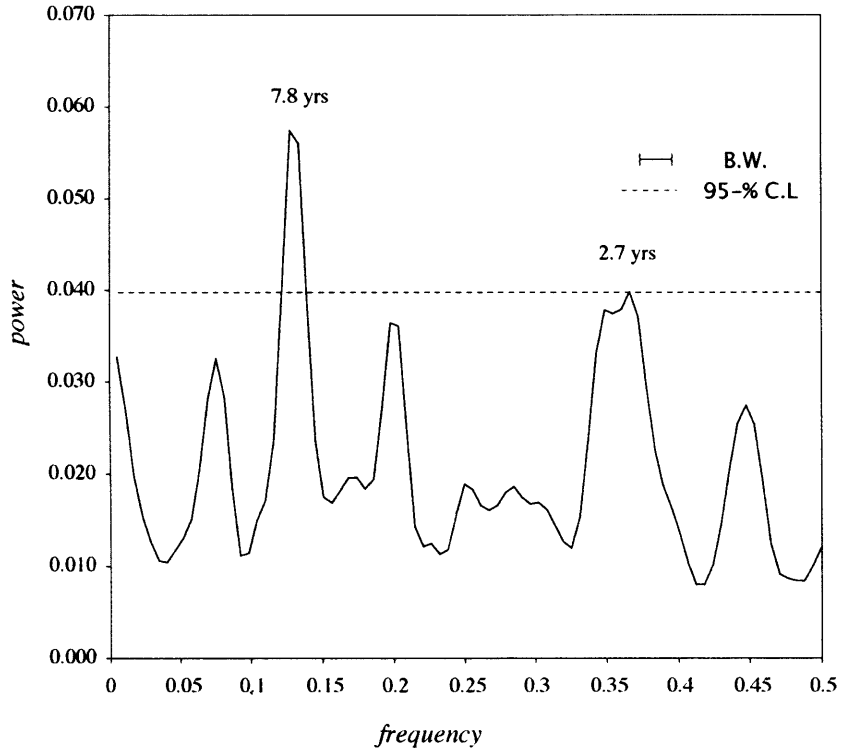

Fig. 5.45: TSA of NAO index of Jones et al., (1997).

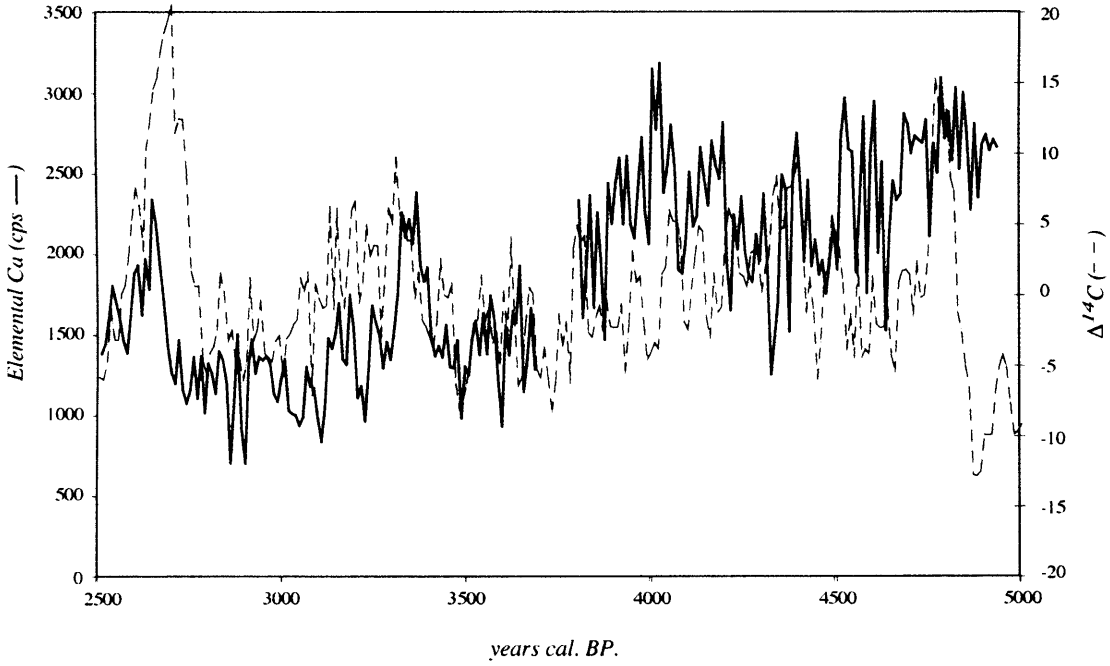

Fig. 5.46: Correlation between Δ14C of Stuiver (a low-pass filter was applied to the data to remove trends >1500 yr.) and time-series of XRF Ca-cps.

5.5. Environmental vs. cultural influences on Diss Mere sedimentation

A strong climate-sedimentation link at Diss Mere is indicated by the recognition of, and distinct evolution in, interannual to interdecadal climate relevant periodicities across the significant change in seasonality *ca.* 4000 Cal. yrs. BP, as well as apparent linear-response of seasonality cycles following this event at Diss to solar forcing on centennial-timescales. Given Diss Mere's lack of river input/output, its long residence time and small catchment area, it is unlikely that on such timescales, unless there is complete vegetation clearance (as seen at ~2500 Cal. yrs. BP, cf. Fig. 3.1, 15.28 m depth), catchment processes would have any significant or dominating control on nutrient cycling and lake sedimentation. It is internal limnological forcing driven by environmental variability that dominates change at Diss Mere on annual to centennial timescales, that is, the degree of lake stratification/overturn.

Diss Mere's catchment, though, has a long record of human settlement and the change in lake system state at *ca.* 4000 Cal. BP underlines the difficulty of separating the effects of climate change and human-induced land-use conversion on lake sedimentation at Diss Mere over longer timescales. The problem is that lake eutrophication, whether driven by environmental change or changes in human catchment practices, tends to leave an identical record in lake sediment geochemistry and only through the application of multi-proxy studies can the relative influences begin to be determined. Indeed, whilst the influence of climate on Diss Mere's record at ~4000 Cal. BP is clear, and confirmed by cross-reference with other circum-Atlantic palaeoclimate records (see section 6.2), the pollen, fossil pigment, and diatom stratigraphies indicate, however, that the carbon burial dynamics that record this change were also likely influenced by human activity. For comparison, Table 5.6 provides a summary of the major changes in sedimentology, palynology and phytoplankton dynamics over the time period concerned. It is clear that diatom and pollen evidence (Fritz, 1989 and Peglar *et al.*, 1989, respectively) demonstrate around this time that a large increase in the relative abundance of littoral diatoms and in sedimentary pigment concentration appear to correlate with a spike of barley pollen and the beginning of continuous curves of pollen taxa characteristic of open habitats. Fritz (1989) argues that small-scale deforestation resulted in changes in

Table 5.6: Summary table showing the timing of vegetation, phytoplankton and climate inferred events recorded in the mid- to late-Holocene varved interval at Diss Mere. Correlation of the Peglar et al. (1989) & Fritz (1989) stratigraphy to the record used here is based on inflections between CaCO3 and OM records from both stratigraphies and the recognition of a sharp change in sediment colour at 16.03 m (16.24 m in the Peglar et al. (1989) & Fritz (1989) record.

catchment nutrient cycling, which resulted in enhanced inputs of nutrients to the lake and hence elevated algal production. She reports an isolated 15% spike in barley pollen at 16.23 m. The stratigraphy used by Fritz (1989), Peglar *et al.* (1989) and Peglar (1993b) is based on coring depths and correlations of $CaCO_3$ between this record and the composite stratigraphy generated here are only as accurate as the resolution of the former (*i.e.* 8-4 cm). Despite this limitation sediment descriptions by Peglar (1993b) indicate that the spike in barley pollen is 1 cm above the sharp change in sediment colour recorded at 16.03 m in this study. Peglar (1993b) reports this evidence as a 16% spike in barley pollen 8 cm higher in their stratigraphy. Wherever this spike is preserved, it appears to occur after the initial sharp change in sediment colour and therefore change in central tendency in carbon burial rate. The expansion of open habitat and minor arable cultivation appears to have contributed to an initially natural euthropication of Diss Mere's waters may therefore reflect increased human migration to the region in a response to decreased seasonality. The sampling resolution of the pollen and diatom studies of Diss Mere's varves, however, is low (every 8-cm) and more detailed studies across this transition are required to determine the relative phasing of events.

5.6. Summary

In summary, this chapter presents evidence for the annual nature of Diss Mere's varves. During the mid- to late-Holocene their deposition is characterized by statistically significant cycles that are similar to periodicities attributed to modern day indices and proxy records of the NAO. A distinct evolution in NAO-type variability from interannual to multidecadal cycles occurs in tandem with a rapid reduction in seasonality from 4000 Cal. BP. A change in seasonality at Diss is manifested in lake eutrophication and recorded by a shift in carbon burial dynamics, a pronounced switch from cyanobacteria-dominated to diatom-dominated productivity and a change in the varve character. Following this event, seasonality cycles show a strong correlation with $\Delta^{14}C$ record from European tree rings. Enhanced solar radiation is correlated with reduced seasonality in East Anglia.

6. Discussion

In this chapter the significance of the NAO-type periodicities recorded in mid-Holocene annual accumulation rates from Diss Mere is investigated further and their evolution across the rapid transition in seasonality at 4000 Cal. BP is discussed. This Rapid Climate Change (RCC) is then compared to change during the Holocene in a number of other circum-Atlantic palaeoclimate records and inferences are drawn. Finally, the potential for solar forcing of the NAO is discussed.

6.1. NAO-type climate variability

The recognition of periods of 20 yrs, 7-8 yrs, 4-5 yrs, and 2-3 yrs in Diss Mere's varved record during the mid-Holocene implies that these oscillations, which are also recorded in instrumental and tree-ring proxy records of the NAO from the last millennium, are likely to have been consistent, long term features of the North Atlantic climate system. Here, NAO-type climate variability is recorded in sediment that is largely deposited during spring through summer. Given that the NAO is most pronounced in winter in the northern hemisphere, these findings may imply a significant memory effect of the winter NAO on primary productivity in terrestrial ecosystems during spring through summer. The physical mechanisms by which this may occur are not certain. However, they may, in part, be connected to the important influence that winter temperatures play on the timing, duration and strength of spring water-column overturn/summer stratification (see also section 4.3).

The evolution of the NAO during the mid-Holocene bears a striking resemblance to modern day features of the NAO on the following fronts:

a) Interannual NAO variability shows no preferred mode with a tendency to switch between dominant periodicities over time. This is consistent with the notion that highest frequency variability in the NAO is a product of processes intrinsic to the atmosphere.

b) The shift from interannual to multidecadal variability following the change in system state at 4000 Cal. BP is comparable to the evolution of the NAO over the 19th to 20th centuries. A switch from 'quasi-bennial' variance enhanced in the late 19th and early 20th centuries to 8-10 yr. variance over the latter half of the 20th century is coincident with bias towards a positive, high index state of the NAO (Hurrell & van Loon, 1997).

A positive NAO is associated with milder winters in the UK and consequently a reduction in seasonality over the annual cycle. To explore whether the RCC recorded at Diss at 4000 Cal. BP is a local manifestation of a much larger event that reflects such change a number of other circum-Atlantic Holocene palaeoclimate records were compared to the local signal from Diss. The proxy records used were selected because of their peer-reviewed association with a climate variable (such as temperature or rainfall), because they are reconstructions from regions known to be sensitive to NAO forcing and because they are radiocarbon dated (resulting in an error range much less than 500 yr). Because the NAO is predominantly a winter phenomenon, a deliberate bias was placed on the selection of records that reflect either winter or annual variability.

6.2. Comparison of circum-Atlantic palaeoclimate records

The results of this survey are shown in Figures 6.1 and 6.2. Although there is currently a lack of high-resolution seasonal records from both the Greenland and Mediterranean regions, the evidence presented suggests that from 4000 Cal. BP and likely until the present, milder and wetter winters across northern Europe and North America may form regional anomalies of opposite sign to increased aridity in Greenland and the Mediterranean. Increased flood frequency, for example, is recorded in British river deposits from 4000 Cal. BP (Macklin and Lewin, 2003) and abundant ancillary evidence exists for increased wetness over Britain during the late-Holocene from peat humification profiles (Hughes *et al.*, 2000; Barber *et al.*, 2003). Further a field, glacier advance is more common after 4000 Cal. BP. in western Norway (Nesje *et al.*, 2001) which is consistent with a tendency towards higher lake levels and increased winter

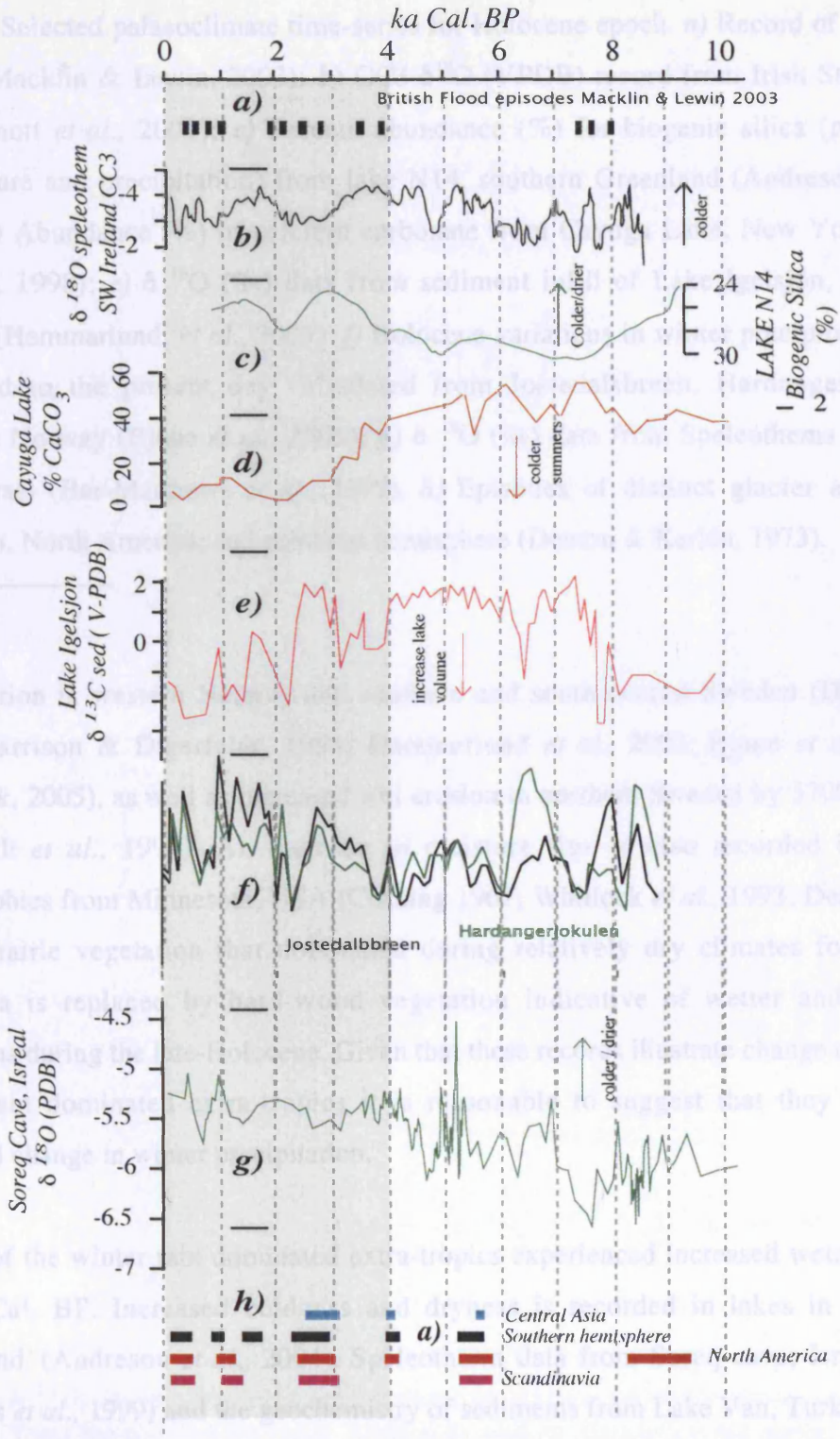

Fig. 6.1: (full description overleaf): Palaeoclimate time series for Holocene Epoch from Europe and North America and globally distributed glacier advance records

Fig. 6.1: Selected palaeoclimate time-series for Holocene epoch. ***a)*** Record of flooding in UK (Macklin & Lewin, 2003); ***b)*** CC3 $\delta^{18}O$ (VPDB) record from Irish Stalagmite (McDermott *et al.*, 2001); ***c)*** Percent abundance (%) for biogenic silica (proxy for temperature and precipitation) from lake N14, southern Greenland (Andresen, *et al.*, 2004); ***d)*** Abundance (%) of calcium carbonate from Cayuga Lake, New York, USA (Mullins, 1998); ***e)*** $\delta\ ^{18}O$ (‰) data from sediment infill of Lake Igelsjön, southern Sweden (Hammarlund, *et al.*, 2003); ***f)*** Holocene variations in winter precipitation in% compared to the present day calculated from Jostedalsbreen, Hardangerjøkulen, Southern Norway (Bjune *et al.*, 2005); ***g)*** $\delta\ ^{18}O$ (‰) data from Speleothems of Soreq cave, Israel (Bar-Matthews *et al.*, 1999). ***h)*** Episodes of distinct glacier advances: European, North America, and southern hemisphere (Denton & Karlén, 1973).

---

precipitation in western Norway and southern and south central Sweden (Digerfeldt, 1988; Harrison & Digerfeldt, 1993; Hammarlund *et al.*, 2003; Bjune *et al.*, 2005; Bargmark, 2005), as well as increased soil erosion in northern Sweden by 3700 Cal. BP (Snowball *et al.*, 1999). An increase in moisture flux is also recorded in pollen stratigraphies from Minnesota, USA (Cushing 1967; Whitlock *et al.*, 1993; Dean, 1999) where prairie vegetation that dominated during relatively dry climates for several millennia is replaced by hard-wood vegetation indicative of wetter and warmer conditions during the late-Holocene. Given that these records illustrate change across the winter-rain dominated extra-tropics it is reasonable to suggest that they reflect a profound change in winter precipitation.

Not all of the winter rain dominated extra-tropics experienced increased wetness from ~4000 Cal. BP. Increased coldness and dryness is recorded in lakes in southern Greenland (Andreson *et al.*, 2004). Speleotherm data from Soreq cave, Israel (Bar-Mathews *et al.*, 1999) and the geochemistry of sediments from Lake Van, Turkey (Wick *et al.*, 2003) suggest that from ~4000 Cal. BP the eastern Mediterranean is characterised by increased aridity. Further west, the palynology and palaeolimnology of a number of lakes in southern Spain, record this shift, although less precisely, from 4500-3500 Cal.

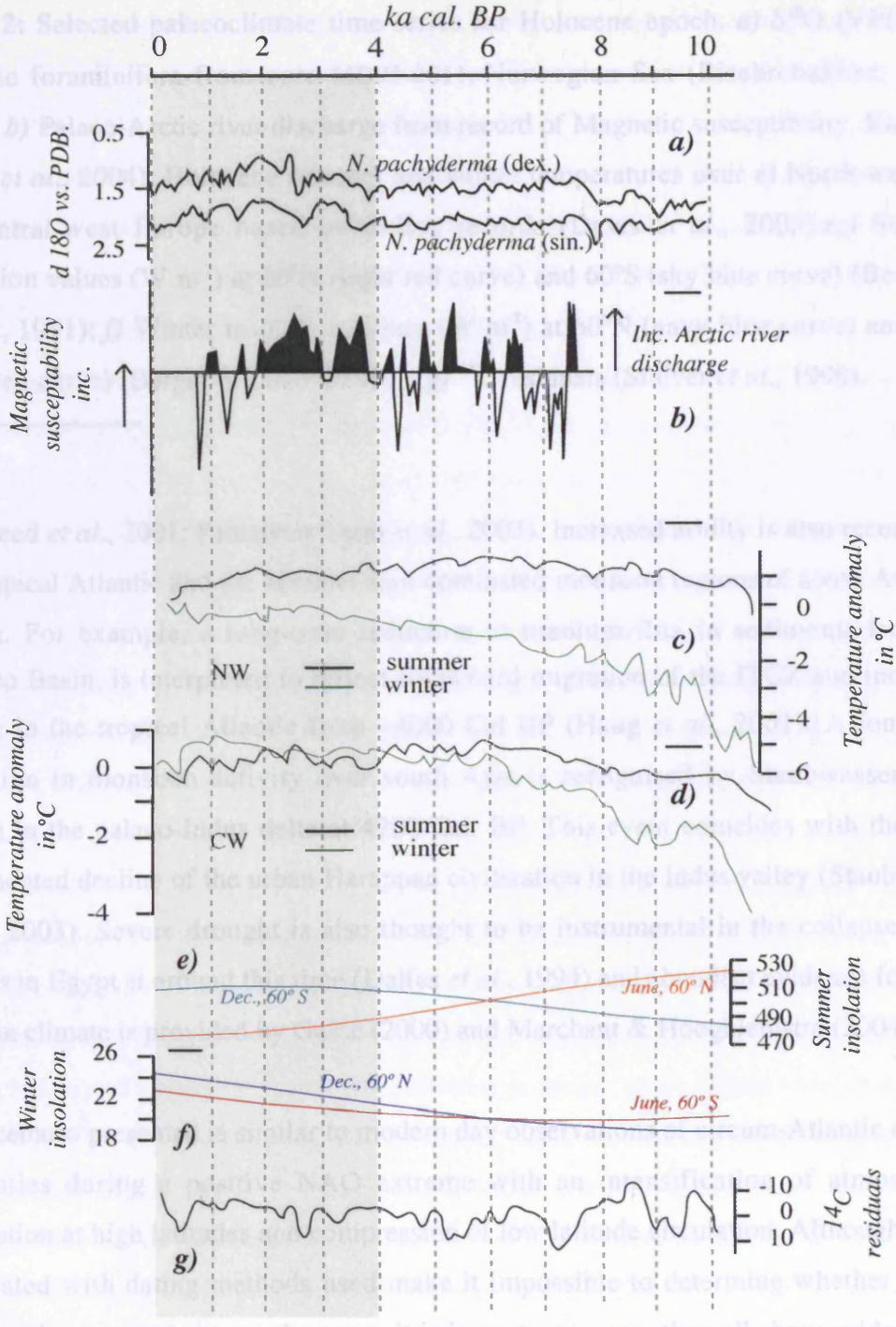

Fig. 6.2: (full description overleaf): Palaeoclimate time series for Holocene Epoch from Europe and the North Atlantic as well as climate forcing series.

Fig. 6.2: Selected palaeoclimate time-series for Holocene epoch. ***a)*** $\delta^{18}O$ (VPDB) in planktic foraminifera from core MD95-2011, Norwegian Sea (Risebrobakken, *et al.*, 2002); ***b)*** Palaeo-Arctic river discharge from record of Magnetic susceptibility, Kara Sea (Stein *et al.*, 2004); Holocene summer and winter temperatures over ***c)*** North-west and ***d)*** Central-west Europe based on pollen records (Davis *et al.*, 2003).***e;)*** Summer insolation values (W m^{-2}) at 60°N (light red curve) and 60°S (sky blue curve) (Berger & Loutre, 1991); ***f)*** Winter insolation values (W m^{-2}) at 60°N (navy blue curve) and 60°S (dark red curve) (Berger & Loutre, 1991); ***g)*** ^{14}C residuals (Stuiver *et al.*, 1998).

BP (Reed *et al.*, 2001; Pantaléon-Cano *et al.*, 2003). Increased aridity is also recorded in the tropical Atlantic and the summer-rain dominated monsoon regions of south Asia and Africa. For example, a long-term reduction in titanium flux in sediments from the Cariaco Basin, is interpreted to reflect southward migration of the ITCZ and increased aridity in the tropical Atlantic from ~4000 Cal BP (Haug *et al.*, 2001). A long-term reduction in monsoon activity over south Asia is recognised by Staubwasser *et al.* (2003) in the palaeo-Indus delta at 4200 Cal. BP. This event coincides with the well-documented decline of the urban Harappan civilization in the Indus valley (Staubwasser *et al.*, 2003). Severe drought is also thought to be instrumental in the collapse urban centres in Egypt at around this time (Dalfes *et al.*, 1994) and abundant evidence for a dry African climate is provided by Gasse (2000) and Marchant & Hooghiemstra (2004).

The scenario presented is similar to modern day observations of circum-Atlantic climate anomalies during a positive NAO extreme with an intensification of atmospheric circulation at high latitudes and compression of low latitude circulation. Although errors associated with dating methods used make it impossible to determine whether all the changes documented are synchronous, it is important to note they all show evidence for a long-term reorganisation of climate that persists throughout the late-Holocene. The uncertainty, though, that is found in the exact phase relationships that exist between records, is problematic and until a larger network of annually resolved climate records is established, *e.g.* through lacustrine varve studies and dendrochronology, the

interpretations made here will remain hypothetical and open to testing. Certainly, at ~4000 Cal. BP, it can be hypothesised that climate records from circum-Atlantic landmasses reflect an antiphase relationship in humidity between Greenland (Mediterranean) and northwest Europe (North America). However, most palaeoclimate reconstructions are biased towards inferences of mean summer temperature. Given the scope of proxy records available, it is difficult, if not currently possible, to determine whether this relationship holds up for winter heat distribution. Where annual mean temperature records exist - for instance, the record CC3 from southwest Ireland, which infers annual temperature change from $\delta^{18}O$ (‰) from speleothem data (McDermott *et al.,* 2001) - an antiphase relation exists between increased warmth in Ireland and increased coldness and aridity in Greenland from ~4000-2500 Cal. BP (for instance the lake N14 record; Andresen *et al.,* 2004). Whilst the south Greenland lake N14 record shows a downturn in annual temperature at ~4000 Cal. BP, the Holocene winter precipitation curves for Josteldalsbreen, Hardangerjøkulen and northern Folgefonna in Norway, indicate increased milder (warmer) and wetter winters from this time (Nesje *et al.*, 2001; Bjune *et al.,* 2005). Highest winter temperatures are observed in the late- to mid-Holocene in western Europe, based on pollen data (Davis *et al.,* 2003) and off northwest Africa, from subtropical SST anomalies (deMenocal *et al.,* 2000). Globally, glacier readvance is more frequent after ~4000 Cal. BP (Denton and Karlen, 1973) which is consistent with increased winter precipitation during milder winter months. In the marine realm increased magnetic susceptibility values from Kara Shelf Sea sediments record enhanced Arctic river discharge during more humid conditions from 4000-2500 Cal. BP (Stein *et al.,* 2004). Temperature reconstructions from subsurface dwelling microfossils (Risebrobakken *et al.*, 2003) and IRD data (Moros *et al.*, 2004) from the Norwegian Sea confirm this region was warmer and its climate more unstable after ~4000 Cal. BP. Moros *et al.* (2004) interpret decreased ice-rafting in marine core MD95-2011 from the Norwegian Sea with a poleward advance of the relatively warm North Atlantic Current. Increased ice-rafting recorded in sediments recovered from the East Greenland Shelf by Jennings *et al.,* (2002) after 4000 Cal. BP reflect a stronger East Greenland Current (ECG). In the scenario presented here, a stronger ECG would have

been driven by prevailing northerlies that deliver relatively cold and dry weather to the Greenland region during more positive phases of the NAO.

What is responsible for a late-Holocene reorganization in climate recorded in so many circum-Atlantic climate proxy records at ~4000 Cal. BP? Moros *et al.* (2004) note, that a reduction in seasonality may force mean annual temperatures to rise in the northern North Atlantic region leading to strong meridonial atmospheric circulation, a northward shift in the Atlantic jet stream and increased moisture transport over northern Europe and north America. Southward migration of ITCZ would be consistent with such a scenario and may explain the extreme aridity recorded at ~4000 Cal. BP through reduction of monsoon conditions across Africa and south Asia (Hodell *et al.*, 2001). A variety of climate records highlight a centennial-scale anomaly at 4200 Cal. BP characterised by high-latitude cooling/wetness and low latitude aridity (Bond *et al.*, 2001; Mayewski *et al.*, 2004). Some authors envisage this event to be one of a number of cold spells recurring on millennial timescales (Bond *et al.*, 1997; Bond *et al.*, 2001). This event is commonly linked with increased IRD (Bond *et al.*, 1997) and reduced North Atlantic Deep Water (Bianchi and McCave, 1999), said to be forced by changes in solar variability (reduced solar radiation), as documented by increased cosmogenic isotopes in tree-ring and ice-core data (Bond *et al.*, 2001). Superficially, Diss Mere's record of summer temperature across ~4000 Cal. BP, within the dating error, can be fitted into a pattern of high-latitude cooling at 4200 Cal. BP. A number of other terrestrial records from Europe and the USA record this change and it appears that when summer temperature declines at ~4000 Cal. BP it remains relatively low until modern industrial times (*e.g.*, Mullins *et al.*, 1999; Heiri *et al.*, 2003; Wurth *et al.*, 2004; Bjune *et al.*, 2005). It is hypothesized, therefore, that the shift recorded in Diss Mere at this time is not connected to millennial-scale variability in solar radiation, but is related to the Holocene decay in orbital summer insolation. A late-Holocene decline in summer temperature is only part of the story, and with the recognition of a late-Holocene shift in seasonality also due to milder winters, it would be erroneous to reconcile all anomalies in terrestrial climate proxy records around this time to a centennial-scale 4200 Cal. BP event proposed to be driven by changes in solar output.

Instead, we postulate in accordance with Morros *et al.* (2004), that variability on orbital timescales may be responsible for a reduction in seasonality and predominance of positive phases of the NAO since ~4000 Cal. BP. Felis *et al.* (2004) highlight that the NAO may play an important role in modulating patterns of seasonality in the Northern Hemisphere on orbital timescales. Using short seasonally resolved proxy records from corals in the Red Sea and simulations with a coupled atmosphere-ocean circulation model they show that climate variability at 3000 Cal. BP displays a tendency towards a positive phase of the NAO. Increased winter temperatures and decreased seasonality in the North Atlantic region after ~4000 Cal. BP may therefore indicate that a climate threshold was crossed in response to increasing winter insolation and decreasing summer insolation. A gradual change in insolation, however, does not fully explain the rapidity of climate change recorded at Diss Mere and other sites across the globe, or the marked persistence in multidecadal cycles following this event. Although, beyond the scope of this thesis, complex, non-linear interactions in the ocean-atmosphere system need to be invoked to explain this change.

An increased influence of northern winter insolation during late Holocene increases the potential of a strong impact of Southern Ocean changes on the northern North Atlantic climate (Mayewski *et al.*, 1997). Consequently, the impact of climate change at ~4000 Cal. BP may have been magnified by oceanic feedbacks associated with changes in tropical SSTs and ENSO strength. Ocean-Atmosphere models reveal long-term changes in moisture balance and ENSO strength. These appear to be related to orbitally driven changes in the seasonal cycle of solar radiation with an increase in ENSO activity from the mid-Holocene (Clement *et al.*, 2000). An association of tropical-wide warm SSTs with the recent positive NAO phase (Hoerling *et al.*, 2001) highlights the potential for tropical Atlantic forcing of lower frequency NAO variability. Variations in tropical SSTs can be large and occur on interannual to decadal time scales. A remote tropical Atlantic forcing of extratropical atmospheric circulation over the North Atlantic may therefore have driven change in extratropical SSTs that, in turn, fed back into the atmosphere to cause bidecadal oscillations in temperature and precipitation that are

reflected in NAO-type cycles observed in Diss Mere following 4000 Cal. BP.

6.3. Solar forcing of the NAO?

The good visual agreement and relatively high coefficient for cross correlation obtained between the interannual elemental Ca record at Diss Mere and atmospheric $\Delta^{14}C$ variation, a proxy for solar activity during the Holocene (Stuvier *et al.*, 1998) for the interval 2500 to 3700 Cal BP (Fig. 5.46, section 5.4), may reveal important insights into the relationship between solar variability and the NAO. It appears that a high index state of the NAO, which we associated here with decreased seasonality (cooler summers and warmer winters), coincides with enhanced solar flux (^{14}C minima) and a low index state of the NAO is coincident with decreased solar activity (^{14}C maxima). Our results support the findings of Shindell *et al.* (2001) who use GCM experiments to demonstrate that a decrease in solar irradiance correlates with regional temperature anomalies that resemble a more negative phase of the of the NAO. The fact that summer temperature appears to show increased coherence with ^{14}C variability on centennial- and multi-centennial-scales may indicate an increased importance of solar forcing on North Atlantic climate on longer timescales. Conversely, the lack of visual coherence at interannual- to interdecadal-timescales implies that highest frequency variability in the NAO is a product of the internal non-linear dynamics of the atmosphere.

Despite the poor spatial and temporal coverage of Holocene climate records from circum-Atlantic landmasses, a significant amount of additional data appear to indicate that reduced solar forcing is associated with regional anomalies indicative of a low index state of the NAO. For example, dry periods interpreted from lacustrine records of Mg/Ca ratios in ostracode shells in the Great Plains of North America (Yu and Ito 2002) and a record $\delta^{18}O$ in stalagmites from northern Europe (Niggemann *et al.*, 2003) appear to correlate with solar minima. Ocean sediments show a distinct temperature dipole anomaly during the Maunder Minimum between cooling surface waters in the Sargasso Sea and warming Atlantic temperatures north of 44°C (Keigwin and Pickart, 1999), consistent with a low index NAO and in contrast to the uniform basin-wide cooling

argued by others (*e.g.*, Bond *et al.*, 2001). Instrumental data indicates that Middle East climate becomes wetter during a low index state of the NAO (Cullen *et al.*, 2002) and Holocene records of south Asian monsoon climate show that increased wetness is associated with solar minima as well (Staubwaser *et al.*, 2004). Verschuren *et al.* (2000) and Stager *et al.* (2005) report a strong correlation between solar variability over the past 1000 years and drought at Lake Naivasha and Lake Victoria, in Kenya, respectively. Here, periods of low solar output appear to correlate with periods of increased East African rainfall too. Negative phases of the NAO are associated with weakened meridional circulation. This is consistent with a northward migration of ITCZ and may explain increased wetness in these records.

The lack of similarity between the two records prior to ~4000 Cal. BP may be due to the existence then of a more complex carbonate – summer temperature relationship or a non-linear solar – summer temperature relationship. It is unlikely that a sampling or chronological artifact is responsible, as the varved stratigraphy between 16-16.65 m depth appears complete and devoid of any obvious breaks in sedimentation. Several other records show increased coherence with $\Delta^{14}C$ following ~4000 Cal. BP. For example, a record of south Asia monsoon climate from $\delta^{18}O$ in the palaeo-Indus delta (Staubwaser *et al.*, 2004) and $\delta^{18}O$ of stalagmites from the B7 cave in Iserlohn–Letmathe (Northern Rhenish Massif, NW Germany; Niggemann *et al.*, 2003) show significant correlations with the $\Delta^{14}C$ record from European tree rings only during the late-Holocene. It is not immediately obvious as to why this would be the case, however, this feature may indicate a more significant role of solar forcing in late-Holocene climate and may explain, in part, the widely recognised observation that climate variability became more regional and complex as the Holocene progressed (*e.g.* as first suggested by O'Brien *et al.*, 1995).

7. Conclusions and future work.

7.1 Conclusions

A high resolution study of the physical properties of, and depositional controls on, the Diss Mere varve series heralds a number of important conclusions, namely that,

a) the annual nature of biochemical varves can be demonstrated by SEM-BSE imaging of seasonal sediment fluxes and phytoplankton succession.
b) during the mid- to late-Holocene their deposition is characterised by statistically significant cycles acting on a variety of timescales, indicating that lake sedimentation at Diss is influenced by some cyclic external forcing mechanism(s).
c) periodicities of 20 yrs, 7-8 yrs, 4-5 yrs, and 2-3 yrs correspond to cycles found in modern instrumental and other proxy records of the NAO from the last millennia. Their recognition indicates that these cycles may have been persistent features of the North Atlantic climate system for at least since ~4500 Cal. BP.
d) a forced shift from interannual cycles with no preferred mode to persistent multi-decadal cycles after 4000 Cal. BP is coincident with a rapid transition towards decreased seasonality during the late-Holocene, as reflected in a change in sediment carbon burial and phytoplankton dynamics as well as a distinct change in varve character. This appears comparable, if not analogous, to the evolution of the NAO over the 19th to 20th centuries where a switch from interannual to decadal variability over the last half of the 20th century is coincident with a tendency towards a high index state of the NAO. Whereas the recent NAO positive phase is thought to be related to an increase in anthropogenic greenhouse gas concentrations, change at 4000 Cal BP is hypothesised to reflect a non-linear reaction of the climate system to a gradual convergence in orbitally controlled summer and winter insolation budgets.
e) following this event, seasonality cycles on centennial to multi-centennial timescales at Diss show a close correspondence to variations in solar variability, with a high (low) index state of the NAO, associated here with decreased (increased) seasonality, coinciding with enhanced (decreased) solar flux, corroborating the findings of a number of previous studies (for instance, Keigwin and Pickart, 1999;

Shindell *et al.*, 2001). Increased coherence of a number of climate records with solar activity following 4000 Cal. BP may indicate a more significant role for solar forcing in regional climate change during the late-Holocene, *i.e.*, as manifested in NAO-type dipole anomalies.

f) whilst the tendency for interannual variability to switch between dominant periodicities over time further highlights that highest frequency variability in the NAO is likely a consequence of unpredictable internal atmospheric processes, the above findings indicate that a degree of longer-term predictability in the mean state of the NAO may be possible due to its forcing by solar activity and changes in the Earth's orbital parameters.

Also of note are the important issues that varve counting has raised concerning the previously accepted duration of the period under study. The recognition that the interval 15.09-16.74 m represents deposition during 2480-5190 Cal. BP has implications for original interpretations of established fossil pollen and diatom stratigraphies for Diss Mere (Peglar *et al.*, 1989; Fritz *et al.*, 1989), *e.g.* the timing of *Tilia* decline (at ~4500 Cal. BP) in central East Anglia and of cultural influences on lake sedimentation at Diss. The analytical competence found in the XRF Corescanner as a means of generating high-resolution palaeoenvironmental time-series has also demonstrated the value of its application in lake sediment palaeoclimate studies. The XRF Corescanner is a non-destructive, fast and relatively inexpensive determinate of detailed core composition that negates many of the time-constraints and costs involved in analysing sediment core. The early stage acquisition of detailed sediment composition was important, not only to understand the full range of sedimentary components available for multi-proxy palaeoclimate/palaeolimnological reconstruction, but also to develop a clear understanding of sediment facies to guide further sampling strategies. For example, the protection that the XRF core scanning method affords to the sediment fabric allows for detailed in-situ laminae scale investigation via SEM-BSEI, as well as by a number of other sediment property determinations. An ultra-high resolution SEM study of seasonal sediment fluxes and phytoplankton seasonal succession has not only highlighted the power of SEM studies for recognising the annual nature of lacustrine varved sediment,

but also the significant contribution that such studies can make in the understanding of palaeo-seasonal depositional processes and ultimately how laminae attributes from successive years may be used as palaeoclimate/palaeoproductivity proxies. This latter point has particular relevance to lakes where, owing to the significant influence of human catchment-based activities on sedimentation, no modern-day comparison can be made between, *e.g.*, geochemical time-series and meteorological records.

7.2. Future work

This study demonstrates that whilst twentieth century NAO behavior may be considered unusual it is not necessarily unique within the timeframe of the Holocene. There is a need, therefore, to better constrain the evolution of multidecadal variability in the NAO beyond the chronological limits of its modern indicies. To this end, a study of highest frequency NAO-type change should be extended to regular time-windows throughout the remainder of Diss Mere's varved sequence and investigated in other annually laminated lacustrine sequences from regions sensitive to NAO forcing. For example, establishing the stratigraphic continuity and a reliable age-model for the entire varved section at Diss, especially that below 16.7-m, would help define the nature and evolution of the NAO over an unprecedented time-period during the early to late Holocene (from 2500 Cal. BP, potentially, as far back as ~7000 Cal. BP). Basic sediment descriptions from other East Anglian lakes, *e.g.* Quidenham Mere, Lopham Fen and Hockham Mere, highlight these sites as promising localities for the preservation of varved lake sediment during the Holocene. These records could be used to verify whether the local signal from Diss is indeed a manifestation of regional-scale anomalies that describe highest-frequency NAO behaviour; their integration may, therefore, serve to help establish the relative phasing of highest-frequency NAO variability further back in time.

In addition to multidecadal change, this study and an increasing number of other palaeorecords highlight that significant and periodic low-frequency components may exist in the evolution of the NAO (*e.g.*, Felis, *et al.* 2001; Moros *et al.*, 2004; Shindell *et al.* 2001; Noren *et al.*, 2003). In order to assess such claims the lack of spatial and temporal coverage of palaeorecords in many key regions should be addressed. Although

such attempts exist, *e.g.* N-S transects being established under the ASCRIBE (Atlantic Seaboard Climatic Reconstruction Including Bounding Errors) project, more coordinations are required amongst scientific communities if we are to understand how the NAO effects terrestrial environments on a variety of timescales. An emphasis should be placed on high-precision correlation between terrestrial records and marine counterparts from areas of high-sedimentation, as well as with the known pacing of potential forcing agents, *e.g.* records of solar variability. Given the inherent stratigraphic uncertainties that always exists with correlations of radiocarbon-dated sequences, multiple independent chronologies should be used to reduce uncertainty, *e.g.* by integrating radiocarbon dating, varve counting and tephra stratigraphies. The best opportunities are offered by palaeoclimate time-series constructed from tree rings and organic varved records. Not only do they provide an internally consistent annual chronometer with which to assess rates of environmental change, in theory, they also contain sufficient organic material to generate past records of atmospheric ^{14}C production, a proxy for solar variability. If these records are of sufficient resolution they can be correlated to master ^{14}C chronologies of known calendar age, and because the ^{14}C can be measured from the same record used to generate palaeoclimate time-series, actual relationships and potential phase lags that exist between solar forcing and climate change can be established. Finally, tree-ring and varved sediments perhaps offer the best opportunity to resolve highest resolution change in winter variability. An understanding of change in cold seasons is paramount if we are to fully understand the regional nature of climate change.

Appendix I. Composite depths (cdblw) vs. Coring depth (mblw)

cdblw	mblw	cdblw	mblw	cdblw	mblw
1000	1000	1046	1046	1092	1092
1001	1001	1047	1047	1093	1093
1002	1002	1048	1048	1094	1094
1003	1003	1049	1049	1095	1095
1004	1004	1050	1050	1096	1096
1005	1005	1051	1051	1097	1097
1006	1006	1052	1052	1098	1098
1007	1007	1053	1053	1099	1099
1008	1008	1054	1054	1100	1100
1009	1009	1055	1055	1101	1101
1010	1010	1056	1056	1102	1102
1011	1011	1057	1057	1103	1103
1012	1012	1058	1058	1104	1104
1013	1013	1059	1059	1105	1105
1014	1014	1060	1060	1106	1106
1015	1015	1061	1061	1107	1107
1016	1016	1062	1062	1108	1108
1017	1017	1063	1063	1109	1109
1018	1018	1064	1064	1110	1110
1019	1019	1065	1065	1111	1111
1020	1020	1066	1066	1112	1112
1021	1021	1067	1067	1113	1113
1022	1022	1068	1068	1114	1114
1023	1023	1069	1069	1115	1115
1024	1024	1070	1070	1116	1116
1025	1025	1071	1071	1117	1117
1026	1026	1072	1072	1118	1118
1027	1027	1073	1073	1119	1119
1028	1028	1074	1074	1120	1120
1029	1029	1075	1075	1121	1121
1030	1030	1076	1076	1122	1122
1031	1031	1077	1077	1123	1123
1032	1032	1078	1078	1124	1124
1033	1033	1079	1079	1125	1125
1034	1034	1080	1080	1126	1126
1035	1035	1081	1081	1127	1127
1036	1036	1082	1082	1128	1128
1037	1037	1083	1083	1129	1129
1038	1038	1084	1084	1130	1130
1039	1039	1085	1085	1131	1131
1040	1040	1086	1086	1132	1132
1041	1041	1087	1087	1133	1133
1042	1042	1088	1088	1134	1134
1043	1043	1089	1089	1135	1135
1044	1044	1090	1090	1136	1136
1045	1045	1091	1091	1137	1137

cdblw	mblw	cdblw	mblw	cdblw	mblw
1138	1138	1186	1186	1234	1234
1139	1139	1187	1187	1235	1235
1140	1140	1188	1188	1236	1236
1141	1141	1189	1189	1237	1237
1142	1142	1190	1190	1238	1242
1143	1143	1191	1191	1239	1243
1144	1144	1192	1192	1240	1244
1145	1145	1193	1193	1241	1245
1146	1146	1194	1194	1242	1246
1147	1147	1195	1195	1243	1247
1148	1148	1196	1196	1244	1248
1149	1149	1197	1197	1245	1249
1150	1150	1198	1198	1246	1250
1151	1151	1199	1199	1247	1251
1152	1152	1200	1200	1248	1252
1153	1153	1201	1201	1249	1253
1154	1154	1202	1202	1250	1254
1155	1155	1203	1203	1251	1255
1156	1156	1204	1204	1252	1256
1157	1157	1205	1205	1253	1257
1158	1158	1206	1206	1254	1258
1159	1159	1207	1207	1255	1259
1160	1160	1208	1208	1256	1260
1161	1161	1209	1209	1257	1261
1162	1162	1210	1210	1258	1262
1163	1163	1211	1211	1259	1263
1164	1164	1212	1212	1260	1264
1165	1165	1213	1213	1261	1265
1166	1166	1214	1214	1262	1266
1167	1167	1215	1215	1263	1267
1168	1168	1216	1216	1264	1268
1169	1169	1217	1217	1265	1269
1170	1170	1218	1218	1266	1270
1171	1171	1219	1219	1267	1271
1172	1172	1220	1220	1268	1272
1173	1173	1221	1221	1269	1273
1174	1174	1222	1222	1270	1274
1175	1175	1223	1223	1271	1275
1176	1176	1224	1224	1272	1276
1177	1177	1225	1225	1273	1277
1178	1178	1226	1226	1274	1278
1179	1179	1227	1227	1275	1279
1180	1180	1228	1228	1276	1280
1181	1181	1229	1229	1277	1281
1182	1182	1230	1230	1278	1282
1183	1183	1231	1231	1279	1283
1184	1184	1232	1232	1280	1284
1185	1185	1233	1233	1281	1285

cdblw	mblw	cdblw	mblw	cdblw	mblw
1282	1286	1330	1330	1378	1377
1283	1287	1331	1331	1379	1378
1284	1288	1332	1332	1380	1379
1285	1289	1333	1333	1381	1380
1286	1290	1334	1334	1382	1381
1287	1291	1335	1335	1383	1382
1288	1292	1336	1336	1384	1383
1289	1293	1337	1337	1385	1384
1290	1294	1338	1338	1386	1385
1291		1339	1339	1387	1386
1292		1340	1340	1388	1387
1293		1341	1341	1389	1388
1294		1342	1342	1390	1389
1295		1343	1343	1391	1390
1296		1344	1344	1392	1391
1297		1345	1345	1393	1392
1298		1346	1346	1394	1393
1299		1347	1347	1395	1394
1300		1348	1348	1396	1395
1301	1301	1349	1349	1397	1396
1302	1302	1350	1350	1398	1397
1303	1303	1351	1351	1399	1398
1304	1304	1352	1352	1400	1399
1305	1305	1353	1353	1401	1410.5
1306	1306	1354	1354	1402	1411.5
1307	1307	1355	1355	1403	1412.5
1308	1308	1356	1356	1404	1413.5
1309	1309	1357	1357	1405	1414.5
1310	1310	1358	1358	1406	1415.5
1311	1311	1359	1359	1407	1416.5
1312	1312	1360	1360	1408	1417.5
1313	1313	1361	1361	1409	1418.5
1314	1314	1362	1362	1410	1419.5
1315	1315	1363	1363	1411	1420.5
1316	1316	1364	1364	1412	1421.5
1317	1317	1365	1365	1413	1422.5
1318	1318	1366	1365	1414	1423.5
1319	1319	1367	1366	1415	1424.5
1320	1320	1368	1367	1416	1425.5
1321	1321	1369	1368	1417	1426.5
1322	1322	1370	1369	1418	1427.5
1323	1323	1371	1370	1419	1428.5
1324	1324	1372	1371	1420	1429.5
1325	1325	1373	1372	1421	1430.5
1326	1326	1374	1373	1422	1431.5
1327	1327	1375	1374	1423	1432.5
1328	1328	1376	1375	1424	1433.5
1329	1329	1377	1376	1425	1434.5

cdblw	mblw	cdblw	mblw	cdblw	mblw
1426	1435.5	1474	1476	1522	1524
1427	1436.5	1475	1477	1523	1533.5
1428	1437.5	1476	1478	1524	1534.5
1429	1438.5	1477	1479	1525	1535.5
1430	1439.5	1478	1480	1526	1536.5
1431	1440.5	1479	1481	1527	1537.5
1432	1441.5	1480	1482	1528	1538.5
1433	1442.5	1481	1483	1529	1539.5
1434	1443.5	1482	1484	1530	1540.5
1435	1444.5	1483	1485	1531	1541.5
1436	1445.5	1484	1486	1532	1542.5
1437	1446.5	1485	1487	1533	1543.5
1438	1447.5	1486	1488	1534	1544.5
1439	1448.5	1487	1489	1535	1545.5
1440	1449.5	1488	1490	1536	1546.5
1441	1450.5	1489	1491	1537	1547.5
1442	1451.5	1490	1492	1538	1548.5
1443	1452.5	1491	1493	1539	1549.5
1444	1453.5	1492	1494	1540	1550.5
1445	1454.5	1493	1495	1541	1551.5
1446	1455.5	1494	1496	1542	1552.5
1447	1456.5	1495	1497	1543	1553.5
1448	1457.5	1496	1498	1544	1554.5
1449	1458.5	1497	1499	1545	1555.5
1450	1459.5	1498	1500	1546	1556.5
1451	1460.5	1499	1501	1547	1557.5
1452	1461.5	1500	1502	1548	1558.5
1453	1462.5	1501	1503	1549	1559.5
1454	1463.5	1502	1504	1550	1560.5
1455	1464.5	1503	1505	1551	1561.5
1456	1465.5	1504	1506	1552	1562.5
1457	1466.5	1505	1507	1553	1563.5
1458	1467.5	1506	1508	1554	1564.5
1459	1468.5	1507	1509	1555	1565.5
1460	1469.5	1508	1510	1556	1566.5
1461	1470.5	1509	1511	1557	1567.5
1462	1471.5	1510	1512	1558	1568.5
1463	1472.5	1511	1513	1559	1569.5
1464	1473.5	1512	1514	1560	1570.5
1465	1474.5	1513	1515	1561	1571.5
1466	1475.5	1514	1516	1562	1572.5
1467	1476.5	1515	1517	1563	1573.5
1468	1470	1516	1518	1564	1574.5
1469	1471	1517	1519	1565	1575.5
1470	1472	1518	1520	1566	1576.5
1471	1473	1519	1521	1567	1577.5
1472	1474	1520	1522	1568	1578.5
1473	1475	1521	1523	1569	1579.5

cdblw	mblw	cdblw	mblw	cdblw	mblw
1570	1580.5	1618	1639	1666	1693
1571	1581.5	1619	1640	1667	1694
1572	1582.5	1620	1641	1668	1695
1573	1583.5	1621	1642	1669	1696
1574	1584.5	1622	1643	1670	1697
1575	1585.5	1623	1644	1671	1698
1576	1586.5	1624	1645	1672	1699
1577	1587.5	1625	1646	1673	1700
1578	1588.5	1626	1647	1674	1701
1579	1589.5	1627	1648	1675	1702
1580	1590.5	1628	1649	1676	1703
1581	1591.5	1629	1650	1677	1704
1582		1630	1651	1678	1705
1583		1631	1652	1679	1706
1584		1632	1653	1680	1707
1585		1633	1654	1681	1708
1586		1634	1655	1682	1709
1587		1635	1656	1683	1710
1588		1636	1657	1684	1711
1589	1610	1637	1658	1685	1712
1590	1611	1638	1659	1686	1713
1591	1612	1639	1660	1687	1714
1592	1613	1640	1661	1688	1715
1593	1614	1641	1662	1689	1716
1594	1615	1642	1663	1690	1717
1595	1616	1643	1664	1691	1718
1596	1617	1644	1665	1692	1719
1597	1618	1645	1666	1693	1720
1598	1619	1646	1667	1694	1721
1599	1620	1647	1668	1695	1722
1600	1621	1648	1669	1696	1723
1601	1622	1649	1670	1697	1724
1602	1623	1650	1671	1698	1725
1603	1624	1651	1672	1699	1726
1604	1625	1652	1673	1700	1727
1605	1626	1653	1674	1701	1728
1606	1627	1654	1675	1702	1729
1607	1628	1655	1676	1703	1730
1608	1629	1656	1677	1704	1731
1609	1630	1657	1678	1705	1738.5
1610	1631	1658	1679	1706	1739.5
1611	1632	1659	1680	1707	1740.5
1612	1633	1660	1681	1708	1741.5
1613	1634	1661	1682	1709	1742.5
1614	1635	1662	1683	1710	1743.5
1615	1636	1663	1690	1711	1744.5
1616	1637	1664	1691	1712	1761
1617	1638	1665	1692	1713	1762

cdblw	mblw	cdblw	mblw	cdblw	mblw
1714	1763	1762	1804	1808	1893
1715	1764	1763	1805	1809	1894
1716	1765	1764	1806	1810	1895
1717	1766	1765	1807	1811	1896
1718	1767	1766	1808	1812	1897
1719	1768	1767	1809	1813	1898
1720	1769	1768	1810	1814	1899
1721	1763	1769	1811	1815	1900
1722	1764	1770	1812	1816	1901
1723	1765	1771	1813	1817	1902
1724	1766	1772	1814	1818	1903
1725	1767	1773	1815	1819	1904
1726	1768	1774	1816	1820	1905
1727	1769	1775	1817	1821	1906
1728	1770	1776	1818	1822	1907
1729	1771	1777	1862	1823	1908
1730	1772	1778	1863	1824	1909
1731	1773	1779	1864	1825	1910
1732	1774	1780	1865	1826	1911
1733	1775	1781	1866	1827	1912
1734	1776	1782	1867	1828	1913
1735	1777	1783	1868	1829	1914
1736	1778	1784	1869	1830	1915
1737	1779	1785	1870	1831	1916
1738	1780	1786	1871	1832	1917
1739	1781	1787	1872	1833	1918
1740	1782	1788	1873	1834	1919
1741	1783	1789	1874	1835	1920
1742	1784	1790	1875	1836	1921
1743	1785	1791	1876	1837	1922
1744	1786	1792	1877	1838	1923
1745	1787	1793	1878	1839	1924
1746	1788	1794	1879	1840	1925
1747	1789	1795	1880	1841	1926
1748	1790	1796	1881	1842	1927
1749	1791	1797	1882	1843	1928
1750	1792	1798	1883	1844	1929
1751	1793	1799	1884	1845	1930
1752	1794	1800	1885	1846	1931
1753	1795	1801	1886	1847	1932
1754	1796	1802	1887	1848	1933
1755	1797	1803	1888	1849	1934
1756	1798	1804	1889	1850	1935
1757	1799	1805	1890	1851	1936
1758	1800	1806	1891	1852	1937
1759	1801	1807	1892		
1760	1802				
1761	1803				

cdblw	mblw	cdblw	mblw	cdblw	mblw
1853	1938	1898	2021	1943	2046
1854	1939	1899	2022	1944	2047
1855	1940	1900	2023	1945	2048
1856	1941	1901	2024	1946	2049
1857	1942	1902	2025	1947	2050
1858	1943	1903	2026	1948	2051
1859		1904	2027	1949	2052
1860		1905	2008	1950	2053
1861		1906	2009	1951	2054
1862		1907	2010	1952	2055
1863		1908	2011	1953	2056
1864		1909	2012	1954	2057
1865		1910	2013	1955	2058
1866	1989	1911	2014	1956	2059
1867	1990	1912	2015	1957	2060
1868	1991	1913	2016	1958	2061
1869	1992	1914	2017	1959	2062
1870	1993	1915	2018	1960	2063
1871	1994	1916	2019	1961	2064
1872	1995	1917	2020	1962	2065
1873	1996	1918	2021	1963	2066
1874	1997	1919	2022	1964	2067
1875	1998	1920	2023	1965	2068
1876	1999	1921	2024	1966	2069
1877	2000	1922	2025	1967	2070
1878	2001	1923	2026	1968	2071
1879	2002	1924	2027	1969	2070
1880	2003	1925	2028	1970	2071
1881	2004	1926	2029	1971	2072
1882	2005	1927	2030	1972	2073
1883	2006	1928	2031	1973	2074
1884	2007	1929	2032	1974	2075
1885	2008	1930	2033	1975	2076
1886	2009	1931	2034	1976	2077
1887	2010	1932	2035	1977	2078
1888	2011	1933	2036	1978	2079
1889	2012	1934	2037	1979	2080
1890	2013	1935	2038	1980	2081
1891	2014	1936	2039	1981	2082
1892	2015	1937	2040	1982	2083
1893	2016	1938	2041	1983	2084
1894	2017	1939	2042	1984	2085
1895	2018	1940	2043	1985	
1896	2019	1941	2044	1986	
1897	2020	1942	2045	1987	

cdblw	mblw	cdblw	mblw	cdblw	mblw
1988		2033	2131	2078	2176
1989		2034	2132	2079	2177
1990		2035	2133	2080	2178
1991		2036	2134	2081	2179
1992		2037	2135	2082	2180
1993		2038	2136	2083	
1994		2039	2137	2084	
1995		2040	2138	2085	
1996		2041	2139	2086	
1997		2042	2140	2087	
1998		2043	2141	2088	
1999		2044	2142	2089	
2000		2045	2143	2090	
2001		2046	2144	2091	
2002		2047	2145	2092	
2003		2048	2146	2093	
2004		2049	2147	2094	
2005	2106	2050	2148	2095	
2006	2107	2051	2149	2096	
2007	2108	2052	2150	2097	
2008	2109	2053	2151	2098	
2009	2110	2054	2152	2099	
2010	2111	2055	2153	2100	
2011	2112	2056	2154	2101	
2012	2110	2057	2155	2102	
2013	2111	2058	2156	2103	
2014	2112	2059	2157	2104	
2015	2113	2060	2158	2105	
2016	2114	2061	2159	2106	
2017	2115	2062	2160	2107	
2018	2116	2063	2161	2108	
2019	2117	2064	2162	2109	
2020	2118	2065	2163	2110	
2021	2119	2066	2164	2111	2208
2022	2120	2067	2165	2112	2209
2023	2121	2068	2166	2113	2210
2024	2122	2069	2167	2114	2211
2025	2123	2070	2168	2115	2212
2026	2124	2071	2169	2116	2213
2027	2125	2072	2170	2117	2214
2028	2126	2073	2171	2118	2215
2029	2127	2074	2172	2119	2216
2030	2128	2075	2173	2120	2217
2031	2129	2076	2174	2121	2218
2032	2130	2077	2175	2122	2219

cdblw	mblw
2123	2220
2124	2221
2125	2222
2126	2223
2127	2224
2128	2225
2129	2226
2130	2227
2131	2228
2132	2229
2133	2230
2134	2231
2135	2232
2136	2233
2137	2234
2138	2235
2139	2236
2140	2237
2141	2238
2142	2239
2143	2240
2144	2241
2145	2242
2146	2243
2147	2244
2148	2245
2149	2246
2150	2247

Appendix II. Fluid displacive, low viscosity resin embedding procedure for wet, unconsolidated sediment.

Resin is prepared using several chemicals in the following ratio:

vinylcyclohexene dioxide (VCD)	10.0 g;
diglycidol ether of polypropyleneglycol (DER 736)	6.0 g;
nonenyl succinic anhydride (NSA)	26.6 g;
dimethylaminoethanol (DMAE)	0.2 g.

Samples of wet sediment are placed into close-fitting, well-perforated aluminum foil containers and immersed in high-purity acetone within a glass desiccator containing silica gel. Acetone is replaced three times daily for five days. The chemical dries the sediment by replacing the aqueous pore fluids with the solvent. Samples must not be allowed to desiccate at any stage.

After the final soaking in acetone, this is removed and an acetone/resin mixture added. The first three additions are a mixture in the proportion 50:50, the second three in 25:75 and the third three in 10:90. The remaining six consisted of resin only. Each replacement is undertaken every 12 hours to prevent viscosity increase. Samples are left to soak for up to four week in the desiccator after the last addition of resin, ensuring that all pore spaces are filled.

Appendix III. Thin sections and sampling coring depths.

Coring depth	PTS
16.5-31.5 cm	
16.5-21 cm	63
20-24.5 cm	64
23.5-28 cm	65
27-31 cm	66
29.5-44.5 cm	
29.5-34 cm	67
33-37.5 cm	68
36.5-41 cm	69
40-44 cm	70
44.8-59.8 cm	
44.8-49 cm	71
48-52 cm	72
51-55 cm	73
54-58 cm	74
57-59.2 cm	74
57.5-72.5 cm	
57.5-62 cm	76
61-65.5 cm	77
64.5-69 cm	78
68-71.6 cm	79
71-78.5 cm	
71-75.5 cm	80
74.5-78 cm	81
77-79.8 cm	82
74-87 cm	
74-78 cm	83
77-81 cm	84
80-84 cm	85
83-87 cm	86

APPENDIX IV Detailed core description

On CD.

APPENDIX V Core images

On CD.

APPENDIX VI Coring depths of marker codes

On CD.

Appendix VII

XRF elemental intensities (1-cm) against composite depth below lake water (cdblw)

cdblw	Ca-cps	Fe-cps	Sr-cps	cdblw	Ca-cps	Fe-cps	Sr-cps	cdblw	Ca-cps	Fe-cps	Sr-cps
1000	1401	2049	69	1042	1891	3156	101	1084	1387	2965	109
1001	1898	2698	99	1043	2102	3277	98	1085	1356	2821	131
1002	2004	2959	86	1044	2631	3526	123	1086	1184	2550	100
1003	849	1445	44	1045	2159	3596	99	1087	1227	2785	108
1004	873	1254	48	1046	2417	3806	131	1088	1017	2459	107
1005	2298	2854	94	1047	1430	2991	84	1089	1222	2574	113
1006	2417	2994	104	1048	1687	3224	110	1090	1041	2562	90
1007	2057	2461	107	1049	1410	3280	95	1091			
1008	2028	2744	90	1050	1587	3473	113	1092			
1009	1658	2429	80	1051	1111	2927	81	1093			
1010	1420	2190	83	1052	1100	2706	75	1094			
1011	1874	2965	93	1053	1384	2466	107	1095			
1012	1901	2586	94	1054	1163	3037	86	1096			
1013	1672	2815	83	1055	1190	3634	79	1097			
1014	1296	2262	77	1056	1095	2989	103	1098			
1015	1233	2492	58	1057	1120	2878	92	1099			
1016	1071	1602	61	1058	1393	3214	101	1100			
1017	1786	2384	96	1059	2039	3036	127	1101	996	2400	89
1018	1612	2594	87	1060	1355	2982	88	1102	1282	3261	77
1019	1398	2095	83	1061	1225	3748	86	1103	1383	3004	95
1020	1354	2440	65	1062	1132	3231	75	1104	1258	2625	119
1021	2065	3109	86	1063	948	2953	86	1105	1294	2504	102
1022	1832	3085	82	1064	1048	3300	86	1106	1695	2269	134
1023	2151	3303	80	1065	955	2986	71	1107	1307	2784	108
1024	2181	3383	88	1066	1404	3503	92	1108	1219	2468	98
1025	1746	3361	75	1067	1285	3148	96	1109	1322	2425	112
1026	1279	2686	64	1068	955	2999	86	1110	1537	2745	136
1027	2080	3188	119	1069	1003	3235	81	1111	1505	2751	123
1028	1505	3344	80	1070	1155	2838	102	1112	1478	2688	139
1029	1581	2843	78	1071	1211	3166	107	1113	1589	2429	150
1030	1649	3275	80	1072	1027	2897	85	1114	1635	2636	136
1031	2274	3497	87	1073	1060	3053	98	1115	1376	2908	118
1032	1235	2740	60	1074	1061	3664	106	1116	1422	2924	109
1033	1511	3319	69	1075	851	2843	81	1117	1502	2630	118
1034	1586	2703	65	1076	1065	2344	102	1118	1633	2441	134
1035	1791	3644	82	1077	1330	2332	99	1119	1624	2253	152
1036	1841	3321	99	1078	1293	2679	142	1120	2051	2043	178
1037	1415	2839	83	1079	1164	2785	113	1121	1644	2016	139
1038	1500	2970	84	1080	1144	3005	96	1122	1715	2014	156
1039	1660	3325	94	1081	1105	3168	82	1123	1608	1640	167
1040	1762	3324	78	1082	1049	3059	86	1124	1767	1885	164
1041	2300	3339	127	1083	1178	2975	96	1125	1359	1953	147

cdblw	Ca-cps	Fe-cps	Sr-cps	cdblw	Ca-cps	Fe-cps	Sr-cps	cdblw	Ca-cps	Fe-cps	Sr-cps
1126	1363	1917	129	1171	1997	1213	139	1216	3267	735	176
1127	1422	1712	147	1172	1965	1143	168	1217	3277	1087	191
1128	1759	1878	172	1173	3214	922	176	1218	2695	1209	144
1129	2137	1666	200	1174	2880	939	162	1219	3064	929	170
1130	1985	1588	203	1175	2334	1055	165	1220	2526	1050	147
1131	1670	1791	173	1176	3269	910	190	1221	2696	1097	147
1132	1886	1660	182	1177	2832	1029	182	1222	2363	896	141
1133	1824	1455	171	1178	3116	828	194	1223	3197	827	177
1134	1850	1412	196	1179	3277	1021	178	1224	4297	951	206
1135	1678	1460	183	1180	4658	657	216	1225	3892	1032	190
1136	1856	1808	165	1181	3814	1014	171	1226	3564	1022	173
1137	1192	1264	109	1182	3171	911	165	1227	3956	1014	194
1138	1580	1681	164	1183	3613	893	153	1228	3961	966	198
1139	1458	1573	140	1184	3774	921	195	1229	4049	936	199
1140	1782	1326	187	1185	2324	968	113	1230	3900	745	180
1141	1462	1662	148	1186	2875	936	139	1231	4252	645	187
1142	1495	1530	129	1187	2387	1187	125	1232	3729	643	167
1143	2220	1118	195	1188	3090	1173	167	1233	3412	637	161
1144	2170	1477	180	1189	1745	1338	125	1234	2712	696	142
1145	1638	1581	153	1190	2135	1185	166	1235	1948	681	147
1146	1493	1837	146	1191	3192	1175	198	1236	2127	615	125
1147	1640	2318	142	1192	2775	1259	167	1237	1697	696	117
1148	1638	2319	130	1193	1781	1464	128	1238	2238	555	150
1149	1820	2135	131	1194	2123	1471	142	1239	3384	822	175
1150	2035	2134	156	1195	1651	1646	97	1240	2685	883	146
1151	2077	2095	156	1196	1376	1857	97	1241	2874	1090	156
1152	1672	1823	150	1197	2014	1724	135	1242	2881	1190	174
1153	2094	1833	166	1198	2877	1415	161	1243	2663	1073	148
1154	2216	1493	193	1199	2928	1643	143	1244	2890	1166	154
1155	1801	1426	139	1200	2605	1702	153	1245	2768	1161	153
1156	2652	1086	204	1201	2505	1795	160	1246	2603	1181	144
1157	2041	1366	130	1202	2439	1621	155	1247	2921	1003	183
1158	1745	1740	137	1203	2268	1671	118	1248	2958	1103	175
1159	1469	1884	116	1204	1812	1719	125	1249	2624	1115	181
1160	1574	1508	120	1205	1957	1614	140	1250	2675	1095	184
1161	1355	1563	113	1206	1966	1648	128	1251	2517	1023	178
1162	2168	1365	162	1207	1598	1540	112	1252	2950	1221	187
1163	2207	1339	155	1208	2010	1335	136	1253	2580	1046	158
1164	2602	1200	179	1209	2879	1197	178	1254	3178	1227	182
1165	2820	1304	213	1210	3034	1216	183	1255	2825	1266	157
1166	2587	1282	182	1211	3159	1055	176	1256	2709	1237	176
1167	2647	1143	192	1212	2401	1023	162	1257	2666	1235	163
1168	2313	1083	187	1213	2843	1018	166	1258	2420	1166	136
1169	2731	1170	158	1214	3214	938	182	1259	2646	1088	143
1170	2172	1252	125	1215	3110	824	180	1260	2673	1099	156

cdblw	Ca-cps	Fe-cps	Sr-cps
1261	3051	1020	168
1262	2788	1091	142
1263	2393	1044	155
1264	2468	968	156
1265	2823	1030	169
1266	2727	1043	174
1267	2661	1045	159
1268	2985	1054	181
1269	2746	986	171
1270	2144	849	143
1271	2113	839	155
1272	2234	763	174
1273	2867	755	189
1274	2922	848	178
1275	2941	874	161
1276	3038	779	177
1277	3794	731	199
1278	3685	723	177
1279	3317	757	188
1280	3375	746	188
1281	4337	663	212
1282	4493	675	215
1283	4237	765	214
1284	4001	683	230
1285	4140	636	238
1286	4325	618	245
1287	4037	627	234
1288	4111	684	217
1289	3577	805	219
1290	4313	860	238
1291			
1292			
1293			
1294			
1295			
1296			
1297			
1298			
1299			
1300			
1301	3199	805	192
1302	3585	850	205
1303	3602	757	217
1304	3305	745	196
1305	2939	926	184

cdblw	Ca-cps	Fe-cps	Sr-cps
1306	2897	1102	170
1307	2929	1122	165
1308	3423	1004	211
1309	3246	849	220
1310	2595	601	160
1311	2854	635	188
1312	3160	709	205
1313	2796	572	167
1314	2412	483	166
1315	2865	526	169
1316	2786	619	170
1317	2986	687	173
1318	2749	632	137
1319	2720	659	143
1320	2887	639	146
1321	2406	628	131
1322	2249	549	117
1323	2106	635	137
1324	2137	637	120
1325	2403	777	109
1326	2419	727	129
1327	2233	894	107
1328	2285	840	121
1329	2361	715	112
1330	2251	761	107
1331	2621	790	127
1332	2361	848	124
1333	2376	781	123
1334	2664	681	128
1335	2405	701	134
1336	2497	667	155
1337	2657	646	148
1338	2498	717	141
1339	2633	719	128
1340	2526	749	127
1341	2777	739	119
1342	2853	810	136
1343	2925	823	151
1344	2773	760	157
1345	2880	829	142
1346	3162	902	128
1347	3016	933	121
1348	2760	795	108
1349	3327	1069	137
1350	3415	966	135

cdblw	Ca-cps	Fe-cps	Sr-cps
1351	3112	856	126
1352	3259	782	149
1353	3194	736	143
1354	2900	780	127
1355	3092	742	153
1356	3198	670	135
1357	3239	701	136
1358	3209	752	136
1359	2928	784	138
1360	2973	774	126
1361	3474	725	128
1362	3474	689	132
1363	3336	702	140
1364	3555	663	120
1365	3709	732	153
1366	3188	794	139
1367	2990	817	155
1368	2972	874	160
1369	2949	864	141
1370	2961	871	163
1371	3098	734	164
1372	3082	744	159
1373	3118	793	158
1374	3290	790	184
1375	3649	884	189
1376	3472	809	172
1377	3208	799	164
1378	3392	888	157
1379	3203	897	177
1380	3317	893	176
1381	3391	917	174
1382	3207	895	170
1383	3561	999	161
1384	3076	937	141
1385	3435	899	155
1386	3418	1030	155
1387	3655	897	153
1388	3440	1001	170
1389	3264	1138	154
1390	3531	1153	162
1391	2168	766	137
1392	3042	1029	133
1393	3299	1137	139
1394	3510	1072	156
1395	3428	1097	157

cdblw	Ca-cps	Fe-cps	Sr-cps	cdblw	Ca-cps	Fe-cps	Sr-cps	cdblw	Ca-cps	Fe-cps	Sr-cps
1396	3419	1083	158	1441	3300	957	134	1486	3741	1193	153
1397	3443	1092	154	1442	3077	932	154	1487	3872	1092	136
1398	3212	1097	131	1443	3227	970	144	1488	4009	1081	121
1399	3138	1031	143	1444	3406	967	156	1489	3627	1093	124
1400	3395	1056	172	1445	3342	838	143	1490	3024	935	138
1401	3271	1057	170	1446	3797	858	153	1491	2879	949	123
1402	3356	1027	145	1447	3850	847	151	1492	2941	846	154
1403	3465	936	154	1448	3812	842	148	1493	2763	839	148
1404	3591	971	182	1449	4129	870	151	1494	2798	880	136
1405	3267	889	175	1450	3881	931	154	1495	2947	826	126
1406	3485	965	166	1451	3848	895	156	1496	2682	838	166
1407	3885	974	151	1452	3713	955	151	1497	2702	809	168
1408	3518	944	162	1453	4019	972	138	1498	2733	761	143
1409	3424	957	174	1454	4354	916	160	1499	2642	641	116
1410	3067	882	140	1455	3717	915	132	1500	3249	620	153
1411	3115	919	151	1456	3605	947	153	1501	3719	849	150
1412	3069	888	148	1457	3449	899	155	1502	3675	649	122
1413	3171	937	138	1458	3482	900	154	1503	3924	698	159
1414	3135	884	152	1459	3363	824	149	1504	3668	648	141
1415	3136	850	152	1460	3905	914	162	1505	3864	671	137
1416	3415	824	161	1461	4302	950	127	1506	3718	554	140
1417	3492	842	152	1462	4423	910	133	1507	3638	496	133
1418	3657	870	160	1463	4318	999	143	1508	4191	585	124
1419	3752	857	158	1464	4019	1133	167	1509	4552	442	130
1420	3783	870	140	1465	3792	1123	160	1510	3976	921	110
1421	3601	856	152	1466	3485	1121	141	1511	4307	502	116
1422	3546	817	161	1467	3135	1055	155	1512	5683	529	138
1423	3601	887	165	1468	3980	1028	148	1513	5095	427	142
1424	3366	769	151	1469	4258	1018	151	1514	5967	492	139
1425	3538	821	166	1470	4155	1023	150	1515	5157	624	121
1426	3502	856	164	1471	4095	991	166	1516	5025	691	125
1427	3396	822	172	1472	4155	1038	141	1517	5098	694	136
1428	3485	854	154	1473	3938	1114	145	1518	5715	579	131
1429	3476	867	153	1474	3827	1161	143	1519	6107	710	121
1430	3464	886	154	1475	3812	1259	153	1520	6135	677	116
1431	3649	962	165	1476	3839	1228	133	1521	6415	704	109
1432	3091	947	188	1477	4029	1285	153	1522	6398	447	136
1433	3074	915	177	1478	3868	1273	133	1523	4576	1046	117
1434	3245	1042	166	1479	3710	1358	133	1524	3976	990	95
1435	3289	989	185	1480	3609	1550	126	1525	3908	1051	95
1436	3066	973	154	1481	3437	1404	137	1526	3763	804	111
1437	3161	984	149	1482	3596	1155	144	1527	3058	669	95
1438	3090	878	155	1483	3856	1086	151	1528	3884	629	128
1439	3273	998	137	1484	4206	1100	146	1529	3829	1118	93
1440	3326	1018	138	1485	4115	1180	128	1530	3842	806	102

cdblw	Ca-cps	Fe-cps	Sr-cps	cdblw	Ca-cps	Fe-cps	Sr-cps	cdblw	Ca-cps	Fe-cps	Sr-cps
1531	3479	847	94	1576	4037	977	126	1621	7834	618	260
1532	3957	1199	95	1577	4812	895	120	1622	7917	848	219
1533	2999	662	98	1578	4749	703	135	1623	7452	721	228
1534	3428	1013	110	1579	4016	903	149	1624	6357	1044	210
1535	3715	559	96	1580	4677	711	133	1625	7634	1306	198
1536	4067	846	109	1581	3430	1400	167	1626	6304	782	218
1537	3993	889	117	1582				1627	5790	849	203
1538	3834	880	114	1583				1628	6383	1064	178
1539	3549	691	104	1584				1629	6877	1009	200
1540	3938	976	109	1585				1630	7199	1211	199
1541	2706	627	92	1586				1631	7645	1276	201
1542	4121	900	117	1587				1632	8906	1073	238
1543	4010	744	129	1588				1633	8388	1474	205
1544	4025	1038	103	1589	3581	1071	172	1634	6309	1942	176
1545	3772	746	100	1590	6486	691	221	1635	5345	2005	146
1546	3289	681	93	1591	6071	1456	185	1636	7450	1516	182
1547	2781	895	102	1592	6002	1073	156	1637	7500	1225	195
1548	4166	631	125	1593	6126	679	168	1638	8887	873	227
1549	4600	666	130	1594	6453	690	183	1639	7778	1412	215
1550	5185	736	116	1595	5588	894	176	1640	6306	1468	173
1551	3573	847	100	1596	7374	864	145	1641	8208	497	225
1552	4755	1085	103	1597	6680	948	135	1642	7992	515	256
1553	4585	1129	97	1598	6858	812	200	1643	9451	980	243
1554	3498	483	113	1599	6677	1210	183	1644	9161	1134	246
1555	3368	452	128	1600	6838	619	214	1645	8336	1327	243
1556	5084	722	129	1601	7665	830	199	1646	8234	1550	228
1557	4666	469	122	1602	6660	1422	185	1647	8465	1761	218
1558	4362	631	106	1603	9076	738	304	1648	8980	1591	199
1559	4660	627	125	1604	7995	1588	254	1649	9072	1026	204
1560	5568	440	152	1605	9261	876	233	1650	9206	895	211
1561	5312	609	129	1606	7736	1162	203	1651	8509	961	205
1562	6431	836	133	1607	7225	531	194	1652	9032	632	242
1563	6252	874	158	1608	7510	860	215	1653	8141	1303	193
1564	5889	746	146	1609	8295	1174	217	1654	8956	1517	190
1565	5387	818	141	1610	8966	1133	230	1655	8408	1029	200
1566	4084	1068	129	1611	7835	1494	204	1656			
1567	4481	748	137	1612	6881	715	185	1657			
1568	4692	1006	138	1613	5875	791	188	1658			
1569	4002	900	103	1614	6805	1185	163	1659			
1570	4491	773	126	1615	7321	683	228	1660			
1571	4243	1393	102	1616	6032	666	238	1661			
1572	5341	928	136	1617	5789	839	210	1662	6548	1152	212
1573	5206	796	140	1618	5685	1004	238	1663	7727	881	222
1574	4753	1227	102	1619	6728	916	243	1664	7324	1164	190
1575	4115	682	117	1620	7493	978	230	1665	6911	1188	176

cdblw	Ca-cps	Fe-cps	Sr-cps
1666	6744	1332	174
1667	7189	1072	185
1668	7534	1200	217
1669	7543	1369	210
1670	7197	866	228
1671	6713	950	207
1672	5760	1604	182
1673	6800	1264	177
1674	4125	1036	161
1675	3846	1255	187
1676	2148	827	120
1677	3628	932	181
1678	4503	1014	157
1679	6246	1097	184
1680	5702	1489	153
1681	5074	1199	197
1682	5038	1166	179
1683	6186	1159	176
1684	6413	1189	189
1685	7439	1058	188
1686	6411	749	199
1687	6488	707	181
1688	5886	868	187
1689	5951	677	162
1690	6517	682	198
1691	5522	593	202
1692	5784	508	220
1693	6490	818	203
1694	6317	917	195
1695	6419	825	213
1696	7118	643	237
1697	6912	821	197
1698	6585	693	195
1699	7787	873	193
1700	8155	833	214
1701	7232	1117	195
1702	7227	1556	166
1703	5721	830	213
1704	5723	1831	145
1705	3883	1924	156
1706	5073	1302	158
1707	5151	1501	140
1708	6449	621	196
1709	6233	880	204
1710	3825	794	158
1711	6600	528	228
1712	7901	685	206
1713	6425	1065	198
1714	6663	975	204
1715	6134	1072	197
1716	6766	701	208
1717	6856	700	174
1718	6669	561	183
1719	5990	418	168
1720	5639	500	182
1721	7882	623	204
1722	6935	1036	169
1723	4528	621	192
1724	3864	1397	170
1725	2897	729	140
1726	6171	288	228
1727	7855	826	188
1728	6901	563	209
1729	6083	873	167
1730	7799	506	235
1731	8936	699	224
1732	7953	982	193
1733	8096	522	248
1734	8309	870	209
1735	6285	1092	172
1736	5092	730	138
1737	7622	1096	197
1738	6053	889	193
1739	5765	2346	125
1740	3276	2238	125
1741	2952	2454	133
1742	2770	2286	107
1743	3807	1325	114
1744	5287	729	137
1745	5215	1117	158
1746	5303	1630	162
1747	4980	1608	147
1748	5556	1156	155
1749	7320	1591	145
1750	6432	2217	204
1751	2808	1815	137
1752	1737	1237	99
1753	1895	1277	122
1754	1644	1616	106
1755	2060	1347	137
1756	4228	1295	176
1757	5446	1349	193
1758	4120	1727	203
1759	4706	1253	182
1760	7052	973	234
1761	7688	956	234
1762	5696	1191	195
1763	6263	2027	183
1764	5842	1508	181
1765	5377	991	174
1766	8258	590	266
1767	8943	666	269
1768	8294	776	235
1769	8085	587	281
1770	6831	1062	194
1771	8684	554	236
1772	7717	457	238
1773	8361	439	257
1774	8031	1175	218
1775	6873	1052	223
1776	5470	1847	176
1777	3416	3567	84
1778	2658	2764	111
1779	3997	2039	195
1780	3088	1946	181
1781	1838	1151	78

Appendix VIII. LECO carbon analyser determined $CaC0_3$, OM, and biogenic opal (wt. %).

cmblw	$CaCO_3$	OM	Opal	cmblw	$CaCO_3$	OM	Opal
1500.0	48.7	31.1	20.2	1633.0	87.5	5.3	7.1
1503.0	50	24.7	25.3	1635.0	71.1	13.3	15.5
1506.0	47.3	26.6	26.1	1639.0	79.6	7.1	13.3
1509.0	53.3	22.6	24.1	1642.0	81.1	8.9	10.0
1513.0	62.6	15.0	22.4	1645.0	81.2	4.6	14.2
1516.0	60.2	17.8	22.0	1648.0	83.6	5.0	11.3
1520.0	63	12.1	24.9	1651.0	84.0	6.4	9.5
1524.5	55.2	23.6	21.2	1654.0	81.4	6.2	12.4
1527.5	54.6	21.0	24.5	1664	76.6	6.8	16.6
1530.5	56.6	23.0	20.4	1667	75.6	7.7	16.7
1533.5	50.0	22.2	27.9	1670	75.3	9.1	15.6
1537.5	59.3	17.4	23.3	1673	75.8	7.9	16.3
1539.5	52.1	18.9	29.1	1676	62.5	27.3	10.3
1542.5	61.6	30.7	7.7	1681	61.7	16.0	22.3
1545.5	41.7	24.1	34.3	1684	67.4	11.1	21.5
1548.5	46.1	16.8	37.2	1688.0	77.7	8.2	14.0
1551.5	54.8	16.2	29.0	1692	77.7	7.0	15.3
1554.5	50.0	31.7	18.3	1696.0	75.0	11.1	14.0
1557.5	45.3	18.9	35.8	1700	75.3	7.2	17.5
1560.5	61.6	12.1	26.2	1704.5	45.7	15.1	39.1
1563.5	63.5	13.4	23.1	1707.5	83.8	9.2	7.0
1566.5	58.5	16.1	25.4	1710.5	83.2	6.8	9.9
1569.5	48.3	24.3	27.4	1714.0	64.1	7.7	28.3
1572.5	64.1	15.5	20.3	1717.0	77.7	9.5	12.8
1575.5	62.3	19.4	18.3	1720.0	84.0	7.3	8.7
1578.5	57.6	12.7	29.6	1723.0	75.6	13.3	11.2
1581.5	52.8	17.0	30.2	1726.0	79.8	6.2	14.0
1585.0	55.3	16.7	28.0	1729.0	85.2	6.1	8.7
1588.0	48.4	20.9	30.6	1732.0	81.6	5.8	12.7
1591.0	68.0	14.0	18.0	1735.0	80.6	7.9	11.4
1594.0	65.6	21.2	13.3	1738.0	20.2	8.2	71.6
1597.0	72.4	10.7	16.9	1741.0	60.1	10.8	29.0
1600.0	75.9	16.0	8.2	1744.0	85.2	9.5	5.3
1603.0	84.5	7.6	8.0	1747.0	74.3	11.5	14.2
1606.0	81.2	9.9	8.9	1750.0	56.6	29.6	13.7
1609.0	83.0	11.4	5.7	1753.0	20.0	45.4	34.6
1612.0	75.6	11.8	12.6	1756.0	80.6	7.3	12.1
1615.0	75.4	9.7	14.9	1759.0	88.8	6.3	4.9
1618.0	68.4	9.1	22.5	1762.0	85.9	12.1	2.0
1621.0	73.6	9.1	17.4	1768.0	89.3	7.6	3.1
1624.0	78.1	8.8	13.2	1771.0	89.0	4.7	6.2
1627.0	67.5	11.7	20.8	1774.0	47.4	5.2	47.4
1630.0	86.5	5.6	8.0	1777.0	43.1	13.0	43.8

Appendix IX 2-mm sedimentation rate against cdblw

cdblw	mm/yr	cdblw	mm/yr	cdblw	mm/yr
1510.2	1.00	1518.8	0.67	1528.2	0.67
1510.4	0.67	1519	0.50	1528.4	0.67
1510.6	0.67	1519.2	0.67	1528.6	0.67
1510.8	0.67	1519.4	0.67	1528.8	0.67
1511	0.33	1519.6	1.00	1529	0.67
1511.2	0.67	1519.8	1.00	1529.2	0.67
1511.4	1.00	1520	1.00	1529.4	0.67
1511.6	0.67	1520.2	0.67	1529.6	0.50
1511.8	1.00	1520.4	0.67	1529.8	0.67
1512	1.00	1520.6	1.00	1530	1.00
1512.2	1.00	1520.8	0.67	1530.2	0.50
1512.4	2.00	1521	1.00	1530.4	0.67
1512.6	1.00	1521.2	0.67	1530.6	0.67
1512.8	1.00	1521.4	0.67	1530.8	0.67
1513	2.00	1521.6	1.00	1531	0.50
1513.2	0.67	1521.8	0.67	1531.2	0.50
1513.4	0.67	1522	1.00	1531.4	0.67
1513.6	1.00	1522.2	1.00	1531.6	0.50
1513.8	0.67	1522.4	1.00	1531.8	0.67
1514	0.67	1523.4	0.50	1532	0.40
1514.2	0.50	1523.6	0.33	1532.2	0.67
1514.4	1.00	1523.8	0.67	1532.4	0.40
1514.6	1.00	1524	0.40	1532.6	0.50
1514.8	2.00	1524.2	0.67	1532.8	0.40
1515	1.00	1524.4	0.50	1533	0.50
1515.2	1.00	1524.6	0.40	1533.2	0.50
1515.4	1.00	1524.8	0.50	1533.4	0.67
1515.6	1.00	1525	0.50	1533.6	0.67
1515.8	1.00	1525.2	1.00	1533.8	0.50
1516	0.67	1525.4	0.50	1534	0.50
1516.2	0.50	1525.6	0.67	1534.2	0.33
1516.4	0.50	1525.8	1.00	1534.4	0.50
1516.6	0.67	1526	0.67	1534.6	0.40
1516.8	0.67	1526.2	0.50	1534.8	0.40
1517	1.00	1526.4	0.50	1535	0.40
1517.2	2.00	1526.6	0.50	1535.2	0.50
1517.4	1.00	1526.8	0.50	1535.4	0.50
1517.6	0.67	1527	0.40	1535.6	0.50
1517.8	1.00	1527.2	0.50	1535.8	0.67
1518	2.00	1527.4	0.40	1536	0.50
1518.2	0.67	1527.6	0.67	1536.2	0.50
1518.4	2.00	1527.8	0.50	1536.4	0.50
1518.6	1.00	1528	0.50	1536.6	0.33

cdblw	mm/yr	cdblw	mm/yr	cdblw	mm/yr
1536.8	0.33	1553.8	0.50	1562.8	0.50
1537	0.67	1554	0.50	1563	0.33
1537.2	0.67	1554.2	0.67	1563.2	0.50
1537.4	0.40	1554.4	0.67	1563.4	0.50
1537.6	0.67	1554.6	0.50	1563.6	0.50
1537.8	0.50	1554.8	0.50	1563.8	0.50
1538	0.33	1555	0.67	1564	0.67
1538.2	0.50	1555.2	0.67	1564.2	0.40
1538.4	0.67	1555.4	0.50	1564.4	0.50
1538.6	0.50	1555.6	0.40	1564.6	0.50
1538.8	0.50	1555.8	0.67	1564.8	0.67
1539	0.40	1556	2.00	1565	0.50
1539.2	0.40	1556.2	1.00	1565.2	0.67
1539.4	0.50	1556.4	0.67	1565.4	1.00
1539.6	0.50	1556.6	0.67	1565.6	0.50
1539.8	0.67	1556.8	0.50	1565.8	0.50
1540	0.40	1557	0.67	1566	1.00
1540.2	0.50	1557.2	0.67	1566.2	0.40
1540.4	0.67	1557.4	0.67	1566.4	0.67
1540.6	0.50	1557.6	0.40	1566.6	0.50
1540.8	0.50	1557.8	0.67	1566.8	0.67
1541	0.50	1558	1.00	1567	0.50
1541.2	0.50	1558.2	1.00	1567.2	0.67
1541.4	0.50	1558.4	1.00	1567.4	0.67
1541.6	0.50	1558.6	1.00	1567.6	0.40
1541.8	0.67	1558.8	0.67	1567.8	0.50
1542	0.40	1559	0.67	1568	0.50
1542.2	0.50	1559.2	1.00	1568.2	0.67
1542.4	1.00	1559.4	0.67	1568.4	0.67
1542.6	0.67	1559.6	1.00	1568.6	0.29
1550.8	0.50	1559.8	1.00	1568.8	0.33
1551	0.67	1560	0.67	1569	0.50
1551.2	0.50	1560.2	0.33	1569.2	0.67
1551.4	1.00	1560.4	0.67	1569.4	0.50
1551.6	0.67	1560.6	0.50	1569.6	0.50
1551.8	0.67	1560.8	0.50	1569.8	0.50
1552	0.67	1561	0.67	1570	0.50
1552.2	0.50	1561.2	0.67	1570.2	0.50
1552.4	1.00	1561.4	0.67	1570.4	0.40
1552.6	0.50	1561.6	0.50	1570.6	0.40
1552.8	0.50	1561.8	0.50	1570.8	0.40
1553	1.00	1562	0.67	1571	0.50
1553.2	0.67	1562.2	0.50	1571.2	0.40
1553.4	0.67	1562.4	0.50	1571.4	0.50
1553.6	0.67	1562.6	0.33	1571.6	0.50

cdblw	mm/yr	cdblw	mm/yr	cdblw	mm/yr
1571.8	0.50	1580.8	1.00	1600.8	0.67
1572	0.50	1581	1.00	1601	0.67
1572.2	0.50	1581.2	1.00	1601.2	0.67
1572.4	0.67	1581.4	0.67	1601.4	1.00
1572.6	0.50	1592.6	0.67	1602.4	0.67
1572.8	0.50	1592.8	0.67	1602.6	0.50
1573	0.40	1593	0.67	1602.8	0.33
1573.2	0.40	1593.2	0.67	1616.6	1.00
1573.4	0.67	1593.4	1.00	1616.8	2.00
1573.6	0.67	1593.6	0.67	1617	1.00
1573.8	0.50	1593.8	0.67	1617.2	1.00
1574	0.50	1594	0.67	1617.4	2.00
1574.2	0.67	1594.2	0.67	1617.6	1.00
1574.4	1.00	1594.4	0.67	1617.8	2.00
1574.6	0.67	1594.6	0.67	1618	1.00
1574.8	0.67	1594.8	0.40	1618.2	1.00
1575	0.50	1595	0.40	1618.4	1.00
1575.2	0.40	1595.2	0.50	1618.6	1.00
1575.4	0.40	1595.4	0.67	1618.8	0.67
1575.6	0.67	1595.6	1.00	1619	0.67
1575.8	0.50	1595.8	0.67	1619.2	0.67
1576	0.67	1596	0.40	1619.4	0.67
1576.2	0.67	1596.2	1.00	1619.6	0.67
1576.4	0.67	1596.4	0.67	1619.8	0.67
1576.6	0.50	1596.6	0.50	1620	1.00
1576.8	0.67	1596.8	0.40	1620.2	0.67
1577	0.67	1597	0.50	1620.4	1.00
1577.2	0.67	1597.2	0.67	1620.6	1.00
1577.4	0.67	1597.4	1.00	1620.8	0.67
1577.6	0.67	1597.6	0.67	1621	0.67
1577.8	1.00	1597.8	0.67	1621.2	0.67
1578	0.67	1598	0.67	1621.4	0.67
1578.2	0.50	1598.2	0.67	1621.6	0.67
1578.4	1.00	1598.4	0.67	1621.8	1.00
1578.6	0.67	1598.6	0.67	1622	0.67
1578.8	1.00	1598.8	0.67	1622.2	0.67
1579	1.00	1599	0.67	1622.4	0.67
1579.2	1.00	1599.2	0.67	1622.6	1.00
1579.4	0.67	1599.4	0.67	1622.8	0.50
1579.6	2.00	1599.6	0.67	1623	1.00
1579.8	0.67	1599.8	0.67	1623.2	1.00
1580	0.67	1600	0.67	1623.4	0.67
1580.2	0.67	1600.2	0.50	1623.6	1.00
1580.4	1.00	1600.4	0.50	1623.8	1.00
1580.6	1.00	1600.6	0.67	1624	0.67

cdblw	mm/yr	cdblw	mm/yr	cdblw	mm/yr
1624.2	0.67	1633.2	0.67	1644.2	0.50
1624.4	1.00	1633.4	0.50	1644.4	0.67
1624.6	1.00	1633.6	0.67	1644.6	0.40
1624.8	0.67	1633.8	1.00	1644.8	0.50
1625	0.67	1634	0.67	1645	0.50
1625.2	1.00	1636.2	0.50	1645.2	0.50
1625.4	0.67	1636.4	0.50	1645.4	0.50
1625.6	1.00	1636.6	0.50	1645.6	0.50
1625.8	1.00	1636.8	0.50	1645.8	0.50
1626	1.00	1637	0.67	1646	0.50
1626.2	1.00	1637.2	0.67	1646.2	0.40
1626.4	0.67	1637.4	0.50	1646.4	0.40
1626.6	1.00	1637.6	0.50	1646.6	0.50
1626.8	1.00	1637.8	0.50	1646.8	0.50
1627	0.67	1638	0.50	1647	0.50
1627.2	0.67	1638.2	0.40	1647.2	0.50
1627.4	2.00	1638.4	0.40	1647.4	0.50
1627.6	1.00	1638.6	0.50	1647.6	0.50
1627.8	1.00	1638.8	1.00	1647.8	0.40
1628	0.67	1639	0.67	1648	0.40
1628.2	0.67	1639.2	0.50	1648.2	0.33
1628.4	1.00	1639.4	0.50	1648.4	0.50
1628.6	1.00	1639.6	0.50	1648.6	0.40
1628.8	0.67	1639.8	0.50	1648.8	0.50
1629	0.50	1640	0.40	1649	0.67
1629.2	0.67	1640.2	0.50	1649.2	0.50
1629.4	1.00	1640.4	0.50	1649.4	0.67
1629.6	0.67	1640.6	0.67	1649.6	0.50
1629.8	1.00	1640.8	0.67	1649.8	0.50
1630	0.50	1641	0.67	1650	0.50
1630.2	1.00	1641.2	0.67	1650.2	0.40
1630.4	0.67	1641.4	0.67	1650.4	0.50
1630.6	1.00	1641.6	1.00	1650.6	0.50
1630.8	0.67	1641.8	0.67	1650.8	0.67
1631	0.67	1642	0.67	1651	0.50
1631.2	0.67	1642.2	0.50	1651.2	0.29
1631.4	0.40	1642.4	0.50	1651.4	0.67
1631.6	0.40	1642.6	0.67	1651.6	0.50
1631.8	0.67	1642.8	0.40	1651.8	0.67
1632	0.40	1643	0.50	1652	0.50
1632.2	0.50	1643.2	0.50	1652.2	0.50
1632.4	0.50	1643.4	0.50	1652.4	0.50
1632.6	0.67	1643.6	0.40	1652.6	0.50
1632.8	0.67	1643.8	0.50	1652.8	0.50
1633	0.67	1644	0.67	1653	0.50

cdblw	mm/yr
1653.2	0.50
1653.4	0.67
1653.6	0.67
1653.8	0.50
1654	0.50
1654.2	0.67
1654.4	0.40
1654.6	0.50
1654.8	0.40
1655	0.50

Appendix X XRF elemental intensities (2-mm) against calendar yrs BP

cal yr BP	Ca-cps	Fe-cps	cal yr BP	Ca-cps	Fe-cps	cal yr BP	Ca-cps	Fe-cps
2480	1385	240	2584	2231	175	2722	1112	272
2482	1007	445	2587	2023	260	2727	1066	171
2485	1084	355	2591	1493	310	2730	1367	204
2488	1387	167	2594	1629	177	2734	1069	226
2491	1477	153	2597	1899	438	2738	825	140
2497	1568	160	2599	2029	286	2741	1253	279
2500	1610	174	2601	1919	217	2744	1202	242
2502	1827	129	2603	2038	181	2747	1338	170
2505	1938	117	2606	2223	154	2750	1372	196
2507	1996	190	2609	1891	232	2753	1098	259
2509	1958	202	2611	1681	552	2756	1229	288
2511	1655	262	2614	1803	317	2759	1034	349
2512	1712	243	2616	2099	161	2763	971	453
2514	1513	162	2619	2401	150	2766	1264	302
2516	1525	149	2622	2225	177	2768	1471	286
2517	1767	168	2624	1982	185	2772	1177	262
2520	1699	134	2627	2147	116	2775	1186	218
2523	1774	105	2629	2301	100	2778	1321	188
2525	1850	140	2631	2074	206	2781	1240	225
2528	1457	163	2633	2605	218	2785	840	348
2531	1676	154	2636	2237	354	2789	1201	339
2535	1972	159	2639	2243	335	2792	1018	278
2537	1855	224	2642	1269	472	2796	953	322
2539	1483	215	2645	1191	297	2799	1417	262
2540	1463	279	2649	1712	297	2804	1345	289
2542	1736	127	2655	1696	286	2807	1201	302
2544	1978	137	2658	1435	313	2812	1449	276
2546	1462	227	2663	1416	322	2816	1409	411
2548	1550	181	2666	1375	385	2821	1156	437
2550	1389	281	2670	1269	620	2825	1114	309
2553	1412	257	2675	1158	323	2829	696	229
2557	1709	190	2679	1091	275	2832	728	144
2561	1614	295	2683	1530	256	2835	1200	166
2564	1576	317	2685	1151	407	2839	1126	268
2567	1480	289	2689	1406	163	2843	966	300
2569	1397	247	2692	1610	159	2849	1418	188
2570	1884	118	2694	835	430	2853	1777	280
2572	1988	191	2697	1195	379	2858	967	286
2575	1902	201	2701	1150	264	2863	846	228
2577	2112	143	2705	1246	202	2868	644	200
2578	2010	147	2709	1114	242	2872	767	161
2581	1893	219	2713	963	228	2876	1190	141
2582	1939	247	2718	1210	250	2880	1312	180

cal yr BP	Ca-cps	Fe-cps	cal yr BP	Ca-cps	Fe-cps	cal yr BP	Ca-cps	Fe-cps
2883	1462	182	3050	1186	267	3181	1106	214
2887	1474	189	3053	1468	216	3185	1285	157
2891	1475	385	3056	1428	231	3188	1351	165
2895	1299	302	3059	1232	225	3191	1103	183
2901	1258	192	3061	1113	230	3195	1102	160
2907	1332	252	3064	1044	306	3199	926	150
2910	1368	227	3067	1005	246	3202	1054	120
2913	1284	514	3070	987	212	3205	1173	173
2918	1204	256	3072	982	212	3209	1298	140
2921	1419	233	3075	1073	185	3214	1258	113
2925	1179	201	3078	1314	199	3217	909	232
2931	1413	194	3081	605	364	3218	1754	121
2935	1355	201	3083	398	380	3220	1687	192
2938	1491	320	3086	617	264	3223	1652	356
2942	1154	268	3089	934	261	3226	1436	276
2946	1404	258	3092	1321	167	3230	1581	157
2951	1070	286	3094	1391	192	3233	1687	161
2956	1160	230	3097	1284	172	3236	1568	211
2960	1092	297	3100	1484	190	3239	1462	208
2964	929	212	3103	1150	204	3244	1627	105
2967	1134	238	3105	1150	238	3247	1536	113
2972	1296	229	3108	1326	243	3249	1401	146
2976	1244	284	3111	1467	352	3251	1199	128
2979	1399	244	3114	1181	176	3253	1596	142
2983	1215	333	3116	1427	208	3255	1793	164
2987	1282	308	3119	1553	180	3258	1406	236
2991	950	203	3122	1449	217	3261	1488	172
2995	676	245	3125	1342	215	3263	1682	169
2999	991	157	3127	1336	226	3266	1674	196
3003	1079	213	3130	1702	227	3268	1706	203
3006	1041	188	3134	1602	216	3270	1350	283
3011	997	219	3137	1420	241	3273	1439	299
3015	1229	276	3141	1330	230	3279	1293	166
3017	1477	296	3143	1188	439	3282	2042	110
3020	942	398	3146	784	229	3286	2322	154
3023	1495	161	3149	1164	212	3290	1769	178
3026	907	262	3152	1634	216	3293	2021	177
3028	995	237	3156	1245	195	3296	2211	180
3031	993	319	3158	1743	205	3299	2226	192
3034	1177	386	3162	1765	317	3303	2369	178
3037	1763	149	3166	1736	362	3307	2571	160
3039	1367	188	3168	1536	334	3310	2110	252
3042	1184	270	3171	1542	359	3314	2249	240
3045	1349	269	3174	1793	284	3318	2166	227
3048	1134	562	3177	1133	370	3324	2330	254

cal yr BP	Ca-cps	Fe-cps
3328	2005	223
3334	2203	243
3338	2418	193
3342	2358	187
3346	2244	262
3350	1935	367
3353	1789	190
3358	1654	183
3362	2021	250
3366	2026	236
3369	2023	494
3373	1620	696
3376	1656	369
3378	1389	248
3382	1583	123
3386	2012	220
3388	1488	253
3393	1200	394
3396	1219	819
3400	1435	221
3403	1457	171
3407	1527	195
3410	1364	250
3413	1144	428
3418	1560	283
3422	1573	198
3426	1750	288
3429	1314	519
3432	1282	356
3439	1199	209
3445	1806	299
3449	1501	335
3452	1413	485
3456	1511	269
3460	984	161
3464	1018	219
3468	1475	138
3472	1139	240
3477	1201	183
3482	1290	277
3487	1386	356
3491	1504	364
3496	1236	221
3500	1591	260
3504	1079	614
3508	1117	458
3512	1646	267
3516	1660	277
3519	1567	276
3523	1843	298
3527	1134	266
3532	1553	149
3537	1636	320
3540	1748	269
3543	1443	180
3547	1655	214
3551	1586	249
3554	2112	304
3556	973	748
3559	986	686
3562	1680	177
3566	1462	206
3571	805	477
3576	1251	226
3579	1487	157
3583	1792	169
3586	1187	265
3589	1306	255
3592	1520	264
3596	1530	286
3599	1595	462
3602	1760	295
3605	1963	184
3608	1702	308
3611	1519	412
3613	1753	236
3616	1574	187
3620	1930	165
3622	1697	148
3625	1952	141
3627	1410	424
3629	1416	238
3631	885	743
3634	1036	420
3635	1356	360
3638	1374	117
3641	1349	191
3644	1249	185
3646	1314	405
3648	1759	167
3650	1670	299
3652	1337	430
3654	1456	291
3657	1296	407
3767	1079	564
3770	1072	280
3773	2122	272
3776	1864	408
3778	2259	226
3781	2378	186
3784	2245	151
3787	2580	187
3790	1611	1137
3793	2346	307
3796	2355	297
3799	1746	603
3802	2233	227
3804	2091	228
3807	2358	313
3810	2369	271
3813	1565	376
3816	2029	197
3819	1516	228
3822	1984	246
3825	2387	251
3828	2455	174
3830	2262	220
3833	2750	158
3836	2287	369
3839	1976	318
3842	1975	92
3845	1512	146
3848	1538	325
3853	1376	888
3858	2579	133
3862	2310	141
3865	1421	140
3867	2425	127
3870	2195	645
3875	2187	358
3877	2505	344
3880	2447	382
3884	2650	446
3889	2672	277
3893	2384	237

cal yr BP	Ca-cps	Fe-cps
3896	2568	197
3898	1259	454
3901	2658	165
3904	1892	608
3907	2228	248
3910	2612	93
3913	2680	105
3916	2062	399
3919	2087	217
3922	2390	446
3925	2230	659
3928	2107	157
3931	2099	172
3934	1913	324
3937	2285	100
3941	2449	239
3945	1912	173
3948	2511	160
3951	2835	192
3954	2330	343
3957	2771	176
3959	2130	387
3962	2514	349
3964	2131	426
3967	2363	250
3969	2108	695
3972	1985	724
3976	3074	201
3982	3192	105
3987	2811	101
3991	2763	204
3996	3120	109
4000	3188	74
4005	2786	186
4009	2400	995
4014	2325	161
4018	2165	231
4023	3114	70
4027	3089	66
4032	2615	707
4036	2953	231
4041	2434	417
4043	2798	95
4046	2294	620
4048	2121	460
4050	1907	93
4053	2297	100
4057	2067	85
4060	1885	137
4063	1677	206
4064	2067	135
4066	1852	132
4067	1990	122
4069	2256	288
4070	2103	151
4072	2111	240
4074	1988	212
4078	2525	229
4082	2499	249
4090	2176	471
4098	2071	392
4106	2731	278
4114	2602	301
4122	2420	118
4130	2305	155
4138	2725	232
4146	2651	297
4154	2455	494
4162	2479	469
4170	2822	522
4178	2086	438
4186	1532	608
4194	1783	354
4200	2249	252
4206	1853	271
4212	2125	155
4218	2261	155
4224	2561	232
4230	2024	245
4236	2000	529
4242	1811	350
4247	1608	215
4251	1907	210
4256	2324	282
4259	2484	212
4262	1414	412
4265	1739	424
4268	1884	173
4271	2002	223
4275	1495	238
4278	2167	148
4282	2589	137
4285	2589	122
4289	1991	287
4292	1897	266
4296	1586	108
4299	1518	100
4301	998	245
4302	1595	79
4304	1815	181
4306	2116	430
4307	1720	326
4309	1952	270
4310	1494	507
4312	1497	427
4314	1473	262
4316	1938	211
4318	1625	414
4321	1751	329
4324	1271	252
4327	2162	135
4330	2496	289
4333	2766	313
4336	2465	261
4338	2430	315
4341	2394	209
4343	2051	164
4345	2265	117
4348	1695	130
4351	1439	222
4354	2174	89
4357	2435	260
4360	2514	373
4362	1788	216
4365	1954	313
4368	2725	187
4371	2770	299
4373	2475	400
4377	1466	360
4379	2506	151
4381	2281	241
4384	2037	210
4386	2412	226
4388	2084	417
4391	1897	427

cal yr BP	Ca-cps	Fe-cps
4394	1886	165
4396	2274	243
4398	2207	272
4401	2589	273
4404	2475	421
4406	2519	238
4409	1645	526
4411	2217	493
4413	1720	611
4415	2089	157
4417	2270	242
4420	2093	200
4422	1919	274
4424	1585	247
4427	1876	219
4430	1878	240
4431	2327	268
4433	2480	237
4435	2189	264
4438	1584	677
4441	2157	335
4443	2212	189
4445	2195	211
4448	2107	171
4452	1410	446
4455	2374	351
4457	2397	308
4460	1973	387
4462	2280	239
4466	2215	272
4468	2417	329
4471	2047	620
4473	2394	471
4476	2284	512
4479	1826	641
4482	2076	683
4487	2467	282
4492	2909	209
4495	2637	231
4500	2970	188
4504	2684	351
4508	2672	510
4511	2644	201
4514	2691	262
4517	2476	489
4520	2637	519
4524	2569	419
4527	2409	562
4529	1943	608
4532	1787	465
4536	2591	398
4540	2322	480
4544	1999	494
4548	2961	143
4551	2800	162
4554	1910	556
4558	1798	633
4562	1723	301
4566	2282	96
4570	2646	302
4575	2397	409
4580	2948	167
4584	2531	234
4586	2298	830
4589	1884	779
4593	2396	246
4597	2398	236
4601	2636	322
4605	2163	638
4610	1532	754
4614	1590	403
4618	2508	217
4621	1922	382
4624	2246	109
4627	2354	100
4630	2457	98
4633	2411	138
4635	2447	191
4638	2363	176
4641	2329	127
4645	2288	131
4649	2365	122
4652	2390	110
4657	2853	139
4661	2880	199
4665	3023	292
4669	2907	343
4674	2415	757
4678	2539	476
4681	2676	267
4685	3132	217
4688	2852	295
4693	2560	474
4697	2642	213
4701	2734	310
4705	2352	504
4709	2699	342
4713	2685	190
4717	2849	199
4721	2832	457
4726	2581	580
4731	1997	585
4735	2841	333
4739	2714	315
4743	2616	321
4747	2299	841
4751	2576	539
4755	2897	524
4760	3096	450
4765	2847	570
4771	2696	622
4775	2733	371
4780	2884	286
4784	2392	360
4787	2545	408
4791	2603	379
4794	2853	206
4798	2989	185
4802	3081	313
4806	2854	227
4811	2452	539
4815	2864	198
4819	3043	222
4822	2932	191
4826	2964	221
4833	2574	200
4836	2880	145
4840	2281	365
4843	2504	281
4847	2693	103
4851	2851	123
4855	2831	150
4859	2379	368
4863	2281	366
4867	2200	304

cal yr BP	Ca-cps	Fe-cps
4871	2847	315
4874	2582	520
4877	2352	497
4881	2875	231
4885	2983	380
4888	2685	884
4893	2594	337
4897	2756	512
4902	2685	294
4906	2677	281

Appendix XI Average varve thickness measurements against calendar yrs BP.

Cal. yr BP	Varve count	V tx (mm)	L tx (mm)	D tx (mm)	Cal. yr BP	Varve count	V tx (mm)	L tx (mm)	D tx (mm)	Cal. yr BP	Varve count	V tx (mm)	L tx (mm)	D tx (mm)
3300	1	0.50	0.31	0.18	3341	42	0.47	0.18	0.29	3382	83	0.47	0.30	0.17
3301	2	0.35	0.26	0.09	3342	43	0.59	0.24	0.35	3383	84	0.33	0.24	0.09
3302	3	0.35	0.16	0.19	3343	44	0.58	0.15	0.43	3384	85	0.44	0.18	0.27
3303	4	0.39	0.20	0.19	3344	45	0.49	0.12	0.37	3385	86	0.72	0.14	0.58
3304	5	0.40	0.23	0.17	3345	46	0.40	0.15	0.24	3386	87	0.39	0.16	0.23
3305	6	0.41	0.23	0.18	3346	47	0.55	0.30	0.25	3387	88	0.35	0.17	0.18
3306	7	0.43	0.22	0.21	3347	48	0.69	0.34	0.35	3388	89	0.30	0.16	0.14
3307	8	0.47	0.24	0.23	3348	49	0.82	0.44	0.39	3389	90	0.85	0.42	0.43
3308	9	0.62	0.40	0.22	3349	50	0.51	0.20	0.32	3390	91	1.13	0.24	0.90
3309	10	0.67	0.13	0.54	3350	51	0.51	0.11	0.40	3391	92	0.66	0.34	0.32
3310	11	0.27	0.11	0.15	3351	52	0.38	0.07	0.32	3392	93	1.27	0.33	0.94
3311	12	0.50	0.33	0.18	3352	53	0.35	0.05	0.30	3393	94	0.65	0.27	0.38
3312	13	0.40	0.20	0.20	3353	54	0.38	0.07	0.31	3394	95	0.45	0.09	0.36
3313	14	0.47	0.22	0.25	3354	55	0.33	0.06	0.27	3395	96	0.27	0.10	0.17
3314	15	0.30	0.12	0.18	3355	56	0.29	0.09	0.19	3396	97	0.41	0.08	0.33
3315	16	0.65	0.45	0.20	3356	57	0.31	0.11	0.20	3397	98	0.35	0.12	0.23
3316	17	0.37	0.15	0.22	3357	58	0.70	0.14	0.56	3398	99	0.43	0.14	0.29
3317	18	0.46	0.10	0.36	3358	59	0.89	0.15	0.74	3399	100	0.38	0.16	0.21
3318	19	0.26	0.09	0.17	3359	60	0.27	0.07	0.20	3400	101	0.38	0.18	0.20
3319	20	0.23	0.05	0.17	3360	61	0.30	0.07	0.23	3401	102	0.41	0.17	0.24
3320	21	0.22	0.09	0.13	3361	62	0.44	0.16	0.29	3402	103	0.33	0.10	0.23
3321	22	0.21	0.20	0.01	3362	63	0.75	0.17	0.58	3403	104	0.72	0.33	0.39
3322	23	0.26	0.23	0.02	3363	64	0.64	0.28	0.36	3404	105	0.54	0.15	0.39
3323	24	0.39	0.24	0.15	3364	65	0.60	0.31	0.29	3405	106	0.38	0.15	0.23
3324	25	0.55	0.30	0.25	3365	66	0.67	0.32	0.35	3406	107	1.00	0.22	0.78
3325	26	0.52	0.31	0.21	3366	67	0.63	0.35	0.28	3407	108	0.71	0.12	0.59
3326	27	0.33	0.09	0.24	3367	68	0.82	0.19	0.63	3408	109	0.54	0.27	0.27
3327	28	0.17	0.06	0.11	3368	69	0.41	0.18	0.23	3409	110	0.87	0.46	0.41
3328	29	0.17	0.06	0.12	3369	70	0.38	0.16	0.22	3410	111	0.67	0.21	0.46
3329	30	0.30	0.08	0.22	3370	71	0.33	0.16	0.17	3411	112	0.63	0.17	0.45
3330	31	0.32	0.18	0.14	3371	72	0.27	0.08	0.19	3412	113	0.68	0.29	0.39
3331	32	0.39	0.23	0.16	3372	73	0.36	0.14	0.22	3413	114	0.83	0.37	0.46
3332	33	0.44	0.29	0.16	3373	74	0.42	0.14	0.28	3414	115	0.87	0.48	0.39
3333	34	0.50	0.30	0.20	3374	75	0.47	0.17	0.31	3415	116	0.65	0.43	0.22
3334	35	0.50	0.32	0.18	3375	76	0.36	0.15	0.21	3416	117	0.58	0.36	0.22
3335	36	0.74	0.38	0.35	3376	77	0.50	0.11	0.39	3417	118	0.53	0.37	0.16
3336	37	0.36	0.11	0.24	3377	78	0.62	0.32	0.30	3418	119	0.35	0.13	0.21
3337	38	0.38	0.15	0.23	3378	79	0.55	0.20	0.34	3419	120	0.33	0.11	0.22
3338	39	0.60	0.23	0.37	3379	80	0.47	0.29	0.17	3420	121	0.43	0.18	0.26
3339	40	0.45	0.23	0.23	3380	81	0.61	0.45	0.16	3421	122	0.60	0.27	0.33
3340	41	0.55	0.23	0.32	3381	82	0.57	0.40	0.17	3422	123	0.62	0.31	0.32

Cal. yr BP	Varve count	V tx (mm)	L tx (mm	D tx (mm)
3423	124	0.47	0.17	0.29
3424	125	0.37	0.14	0.23
3425	126	0.42	0.16	0.26
3426	127	0.44	0.24	0.21
3427	128	1.04	0.10	0.94
3428	129	0.63	0.24	0.39
3429	130	0.67	0.36	0.31
3430	131	0.95	0.57	0.38
3431	132	0.91	0.39	0.52
3432	133	0.57	0.27	0.30
3433	134	0.80	0.22	0.57
3434	135	0.53	0.15	0.38
3435	136	0.90	0.07	0.83
3436	137	0.29	0.09	0.20
3437	138	0.39	0.17	0.23
3438	139	0.39	0.17	0.22
3439	140	0.50	0.19	0.31
3440	141	0.45	0.23	0.23
3441	142	0.35	0.16	0.19
3442	143	0.31	0.12	0.19
3443	144	0.36	0.10	0.25
3444	145	0.29	0.09	0.21
3445	146	0.55	0.19	0.37
3446	147	0.44	0.19	0.26
3447	148	0.53	0.17	0.36
3448	149	0.48	0.15	0.33
3449	150	0.35	0.13	0.23
3450	151	0.40	0.17	0.23
3451	152	0.40	0.21	0.18
3452	153	0.53	0.21	0.33
3453	154	0.45	0.21	0.24
3454	155	0.34	0.14	0.20
3455	156	0.47	0.22	0.26
3456	157	0.50	0.18	0.31
3457	158	0.44	0.12	0.31
3458	159	0.31	0.13	0.19
3459	160	0.29	0.10	0.19
3460	161	0.29	0.09	0.21
3461	162	0.33	0.13	0.21
3462	163	0.37	0.16	0.22
3463	164	0.62	0.22	0.40
3464	165	0.40	0.20	0.20
3465	166	0.40	0.11	0.29
3466	167	0.46	0.15	0.31
3467	168	0.49	0.26	0.22
3468	169	0.51	0.29	0.22
3469	170	0.52	0.21	0.31
3470	171	0.39	0.25	0.14
3471	172	0.32	0.17	0.15
3472	173	0.30	0.14	0.16
3473	174	0.30	0.12	0.18
3474	175	0.39	0.19	0.20
3475	176	0.46	0.18	0.28
3476	177	0.42	0.21	0.21
3477	178	0.42	0.17	0.25
3478	179	0.32	0.13	0.19
3479	180	0.33	0.11	0.22
3480	181	0.36	0.11	0.25
3481	182	0.29	0.11	0.17
3482	183	0.36	0.16	0.20
3483	184	0.65	0.16	0.49
3484	185	0.44	0.26	0.18
3485	186	0.38	0.23	0.15
3486	187	0.87	0.42	0.46
3487	188	0.35	0.13	0.22
3488	189	0.33	0.11	0.22
3489	190	0.32	0.15	0.17
3490	191	0.39	0.15	0.25
3491	192	0.42	0.10	0.31
3492	193	0.37	0.06	0.31
3493	194	0.28	0.09	0.20
3494	195	0.58	0.12	0.46
3495	196	0.50	0.19	0.31
3496	197	0.69	0.44	0.25
3497	198	0.83	0.36	0.47
3498	199	0.77	0.36	0.41
3499	200	0.81	0.17	0.64
3500	201	0.66	0.28	0.38
3501	202	0.59	0.33	0.26
3502	203	0.60	0.30	0.30
3503	204	0.50	0.19	0.32
3504	205	0.67	0.22	0.45
3505	206	0.66	0.37	0.29
3506	207	0.55	0.32	0.24
3507	208	0.59	0.33	0.26
3508	209	0.27	0.14	0.12
3509	210	0.39	0.13	0.25
3510	211	0.39	0.12	0.27
3511	212	0.47	0.26	0.21
3512	213	0.49	0.24	0.26
3513	214	0.58	0.21	0.37
3514	215	0.54	0.28	0.26
3515	216	0.60	0.27	0.34
3516	217	0.69	0.33	0.36
3517	218	0.69	0.47	0.22
3518	219	0.61	0.30	0.31
3519	220	0.54	0.28	0.26
3520	221	0.52	0.21	0.31
3521	222	0.53	0.25	0.28
3522	223	0.69	0.21	0.49
3523	224	0.51	0.21	0.30
3524	225	0.43	0.14	0.29
3525	226	0.53	0.20	0.33
3526	227	0.48	0.17	0.31
3527	228	0.53	0.20	0.33
3528	229	0.50	0.20	0.30
3529	230	0.51	0.22	0.29
3530	231	0.64	0.23	0.41
3531	232	0.79	0.44	0.36
3532	233	0.85	0.35	0.50
3533	234	0.56	0.35	0.20
3534	235	0.78	0.47	0.31
3535	236	0.69	0.30	0.39
3536	237	0.71	0.39	0.32
3537	238	1.00	0.30	0.70
3538	239	0.53	0.18	0.35
3539	240	0.94	0.22	0.72
3540	241	0.48	0.13	0.35
3541	242	0.45	0.20	0.25
3542	243	0.46	0.11	0.35
3543	244	0.41	0.13	0.27
3544	245	0.47	0.19	0.28
3545	246	0.66	0.35	0.31
3546	247	0.35	0.09	0.26
3547	248	0.49	0.16	0.33
3548	249	0.47	0.17	0.30
3549	250	0.50	0.23	0.27
3550	251	0.80	0.46	0.34
3551	252	0.49	0.22	0.27

Cal. yr BP	Varve count	V tx (mm)	L tx (mm)	D tx (mm)
3552	253	0.59	0.24	0.35
3553	254	0.71	0.33	0.38
3554	255	0.79	0.35	0.44
3555	256	1.20	0.19	1.01
3556	257	0.60	0.22	0.37
3557	258	0.50	0.24	0.26
3558	259	0.61	0.26	0.36
3559	260	0.54	0.23	0.31
3560	261	0.56	0.28	0.28
3561	262	0.58	0.26	0.32
3562	263	0.54	0.19	0.35
3563	264	0.59	0.27	0.32
3564	265	0.51	0.28	0.23
3565	266	0.73	0.43	0.30
3566	267	0.95	0.32	0.63
3567	268	0.32	0.12	0.20
3568	269	0.42	0.13	0.29
3569	270	0.56	0.33	0.23
3570	271	0.78	0.35	0.43
3571	272	0.97	0.27	0.70
3572	273	0.52	0.23	0.29
3573	274	0.66	0.29	0.37
3574	275	0.65	0.29	0.29
3575	276	0.49	0.25	0.24
3576	277	0.46	0.25	0.21
3577	278	0.51	0.28	0.23
3578	279	0.49	0.28	0.21
3579	280	0.78	0.45	0.33
3580	281	0.72	0.45	0.27
3581	282	1.14	0.81	0.33
3582	283	0.49	0.24	0.25
3583	284	0.57	0.32	0.26
3584	285	0.74	0.42	0.31
3585	286	1.20	0.44	0.76
3586	287	0.45	0.30	0.15
3587	288	0.67	0.23	0.44
3588	289	0.46	0.20	0.26
3589	290	0.56	0.25	0.30
3590	291	1.02	0.45	0.56
3591	292	0.69	0.47	0.21
3592	293	1.19	0.59	0.61
3593	294	0.65	0.37	0.28
3594	295	0.71	0.47	0.24
3595	296	1.05	0.47	0.58
3596	297	0.88	0.63	0.26
3597	298	0.95	0.46	0.49
3598	299	0.85	0.28	0.58
3599	300	0.70	0.28	0.42
3600	301	0.71	0.38	0.33
3601	302	0.99	0.64	0.35
3602	303	1.18	0.44	0.74
3603	304	0.47	0.14	0.33
3604	305	0.90	0.27	0.63
3605	306	0.61	0.18	0.44
3606	307	0.63	0.15	0.47
3607	308	0.64	0.39	0.25
3608	309	0.74	0.39	0.35
3609	310	0.79	0.47	0.31
3610	311	0.84	0.26	0.58
3611	312	0.80	0.24	0.55
3612	313	0.74	0.32	0.42
3613	314	0.77	0.31	0.46
3614	315	0.92	0.43	0.50
3615	316	1.15	0.41	0.74
3616	317	0.95	0.62	0.33
3617	318	1.07	0.64	0.43
3618	319	0.65	0.36	0.29
3619	320	0.99	0.65	0.34
3620	321	0.98	0.55	0.43
3621	322	0.72	0.41	0.31
3770	350	0.65	0.43	0.22
3771	351	0.69	0.27	0.42
3772	352	0.89	0.26	0.63
3773	353	0.58	0.20	0.38
3774	354	0.51	0.23	0.29
3775	355	1.13	0.26	0.87
3776	356	0.76	0.31	0.45
3777	357	1.28	0.73	0.55
3778	358	0.98	0.56	0.42
3779	359	1.03	0.52	0.51
3780	360	0.88	0.60	0.28
3781	361	0.90	0.51	0.39
3782	362	0.88	0.44	0.44
3783	363	0.84	0.57	0.27
3784	364	0.69	0.53	0.17
3785	365	0.62	0.31	0.31
3786	366	0.26	0.07	0.18
3787	367	0.35	0.13	0.21
3788	368	0.37	0.16	0.22
3789	369	0.54	0.35	0.19
3790	370	0.83	0.42	0.41
3791	371	0.93	0.59	0.33
3792	372	0.88	0.45	0.43
3793	373	0.66	0.33	0.33
3794	374	1.19	0.69	0.49
3795	375	0.88	0.61	0.26
3796	376	0.81	0.58	0.23
3797	377	0.94	0.67	0.27
3798	378	1.18	0.67	0.51
3799	379	0.82	0.67	0.15
3800	380	1.96	0.53	1.43
3801	381	0.77	0.45	0.31
3802	382	0.75	0.45	0.30
3803	383	1.08	0.85	0.23
3804	384	1.53	0.54	1.00
3805	385	1.16	0.75	0.41
3806	386	0.64	0.38	0.26
3807	387	0.49	0.23	0.27
3808	388	0.68	0.39	0.29
3809	389	0.82	0.50	0.32
3810	390	0.69	0.49	0.20
3811	391	0.43	0.21	0.21
3812	392	0.47	0.32	0.15
3813	393	0.63	0.34	0.30
3814	394	0.97	0.16	0.81
3815	395	0.57	0.40	0.18
3816	396	0.51	0.33	0.19
3817	397	0.50	0.15	0.36
3818	398	0.68	0.46	0.22
3819	399	0.67	0.32	0.35
3820	400	0.66	0.30	0.36
3821	401	0.41	0.24	0.17
3822	402	0.44	0.24	0.20
3823	403	0.73	0.45	0.29
3824	404	0.77	0.56	0.20
3825	405	0.61	0.25	0.35
3826	406	1.06	0.71	0.35
3827	407	1.16	0.32	0.84
3828	408	0.21	0.15	0.07

Cal. yr BP	Varve count	V tx (mm)	L tx (mm)	D tx (mm)
3829	409	0.45	0.15	0.30
3830	410	0.32	0.21	0.11
3831	411	0.22	0.06	0.16
3832	412	0.30	0.08	0.22
3833	413	0.24	0.06	0.18
3834	414	0.36	0.11	0.25
3835	415	0.23	0.08	0.15
3836	416	0.25	0.07	0.18
3837	417	0.30	0.12	0.18
3838	418	0.42	0.16	0.26
3839	419	0.43	0.23	0.20
3840	420	0.69	0.48	0.21
3841	421	1.04	0.67	0.37
3842	422	0.52	0.27	0.25
3843	423	0.35	0.20	0.15
3844	424	0.57	0.43	0.15
3845	425	0.75	0.58	0.16
3846	426	0.60	0.47	0.13
3847	427	0.48	0.39	0.10
3848	428	0.30	0.23	0.07
3849	429	0.65	0.54	0.12
3850	430	0.56	0.43	0.13
3851	431	0.47	0.35	0.11
3852	432	0.87	0.52	0.35
3853	433	1.07	0.72	0.35
3854	434	0.91	0.79	0.12
3855	435	0.39	0.21	0.18
3856	436	0.52	0.38	0.14
3857	437	0.60	0.46	0.14
3858	438	0.47	0.38	0.09
3859	439	0.52	0.38	0.14
3860	440	0.51	0.41	0.10
3861	441	0.54	0.42	0.11
3862	442	0.51	0.30	0.21
3863	443	0.58	0.23	0.35
3864	444	2.05	0.44	1.61
3865	445	0.44	0.31	0.13
3866	446	0.53	0.39	0.14
3867	447	0.92	0.35	0.57
3868	448	0.38	0.22	0.16
3869	449	0.58	0.42	0.16
3870	450	0.54	0.38	0.15
3871	451	0.42	0.25	0.16
3872	452	0.65	0.25	0.40
3873	453	0.51	0.38	0.13
3874	454	0.52	0.34	0.17
3875	455	0.67	0.53	0.14
3876	456	0.52	0.34	0.18
3877	457	0.34	0.25	0.09
3878	458	0.55	0.32	0.23
3879	459	0.52	0.29	0.23
3880	460	0.57	0.26	0.31
3881	461	0.59	0.10	0.49
3882	462	0.42	0.13	0.29
3883	463	1.02	0.49	0.53
3884	464	0.84	0.56	0.28
3885	465	0.81	0.22	0.60
3886	466	0.98	0.57	0.41
3887	467	1.58	0.62	0.97
3888	468	0.76	0.52	0.23
3889	469	0.55	0.29	0.26
3890	470	1.45	0.37	1.08
3891	471	0.82	0.55	0.26
3892	472	0.62	0.34	0.29
3893	473	0.78	0.55	0.23
3894	474	0.79	0.54	0.25
3895	475	0.59	0.47	0.12
3896	476	0.75	0.55	0.20
3897	477	0.57	0.48	0.09
3898	478	0.73	0.30	0.43
3899	479	0.59	0.38	0.22
3900	480	0.41	0.16	0.25
3901	481	0.76	0.37	0.40
3902	482	0.86	0.57	0.29
3903	483	0.91	0.65	0.26
3904	484	0.58	0.40	0.18
3905	485	0.41	0.19	0.22
3906	486	0.43	0.12	0.32
3907	487	0.55	0.16	0.39
3908	488	0.68	0.24	0.44
3909	489	0.76	0.32	0.44
3910	490	0.73	0.34	0.39
3911	491	0.61	0.30	0.31
3912	492	0.64	0.38	0.26
3913	493	0.69	0.45	0.24
3914	494	0.69	0.47	0.22
3915	495	0.63	0.38	0.25
3916	496	0.61	0.30	0.32
3917	497	0.76	0.43	0.32
3918	498	0.51	0.33	0.18
3919	499	0.77	0.42	0.35
3920	500	0.64	0.40	0.23
3921	501	0.62	0.38	0.23
3922	502	0.60	0.34	0.26
3923	503	0.56	0.32	0.25
3924	504	0.54	0.33	0.22
3925	505	0.45	0.23	0.22
3926	506	0.49	0.34	0.16
3927	507	0.67	0.39	0.28
3928	508	0.62	0.45	0.17
3929	509	0.83	0.45	0.37
3930	510	0.74	0.47	0.26
3931	511	0.89	0.63	0.26
3932	512	0.86	0.50	0.36
3933	513	0.61	0.42	0.19
3934	514	1.03	0.51	0.52
3935	515	0.99	0.63	0.36
3936	516	0.98	0.53	0.45
3937	517	0.83	0.63	0.20
3938	518	0.96	0.71	0.25
3939	519	0.72	0.44	0.27
3940	520	1.09	0.71	0.38
3941	521	1.50	1.02	0.48
3942	522	1.71	1.19	0.53
3943	523	1.74	1.22	0.52
3944	524	1.61	1.14	0.47
3945	525	1.34	0.96	0.38
3946	526	0.94	0.68	0.26
3947	527	0.61	0.45	0.16
3948	528	0.91	0.63	0.28
3949	529	1.23	0.75	0.48
3950	530	1.39	0.71	0.68
3951	531	1.40	0.59	0.80
3952	532	1.26	0.47	0.79
3953	533	0.97	0.40	0.57
3954	534	0.55	0.36	0.19
3955	535	0.30	0.19	0.11
3956	536	0.75	0.43	0.31
3957	537	0.54	0.20	0.34

Cal. yr BP	Varve count	V tx (mm)	L tx (mm)	D tx (mm)
3958	538	1.34	1.11	0.23
3959	539	0.57	0.35	0.22
3960	540	0.37	0.25	0.12
3961	541	0.48	0.35	0.14
3962	542	0.38	0.22	0.16
3963	543	0.59	0.23	0.35
3964	544	0.72	0.43	0.29
3965	545	0.65	0.49	0.16
3966	546	0.69	0.43	0.26
3967	547	0.46	0.25	0.22
3968	548	0.67	0.36	0.31
3969	549	0.73	0.49	0.24
3970	550	1.28	0.88	0.40
3971	551	0.78	0.61	0.17
3972	552	0.69	0.49	0.20
3973	553	0.93	0.74	0.19
3974	554	0.74	0.51	0.24
3975	555	0.50	0.40	0.10
3976	556	0.63	0.34	0.29
3977	557	0.72	0.44	0.28
3978	558	0.92	0.57	0.35
3979	559	1.16	0.86	0.30
3980	560	0.49	0.32	0.17
3981	561	1.12	0.79	0.33
3982	562	0.94	0.66	0.28
3983	563	0.90	0.58	0.31
3984	564	1.87	0.95	0.92
3985	565	0.85	0.69	0.17
3986	566	0.64	0.40	0.23
3987	567	1.66	0.88	0.78
3988	568	0.55	0.27	0.28
3989	569	0.40	0.21	0.19
3990	570	0.89	0.36	0.52
3991	571	0.80	0.47	0.33
3992	572	0.70	0.39	0.31
3993	573	0.88	0.30	0.58
3994	574	0.71	0.39	0.32
3995	575	0.66	0.52	0.14
3996	576	0.57	0.39	0.18
3997	577	0.68	0.48	0.20
3998	578	1.23	0.82	0.42
3999	579	1.12	0.79	0.33
4000	580	0.78	0.61	0.17
4001	581	0.74	0.60	0.15
4002	582	0.89	0.75	0.13
4003	583	0.74	0.61	0.13
4004	584	0.80	0.64	0.16
4005	585	0.98	0.70	0.28
4006	586	1.11	0.83	0.28
4007	587	1.05	0.87	0.18
4008	588	0.91	0.80	0.11
4009	589	0.91	0.74	0.17
4010	590	0.92	0.80	0.12
4011	591	0.82	0.60	0.22
4012	592	0.93	0.44	0.49
4013	593	0.60	0.53	0.07
4014	594	0.44	0.33	0.11
4015	595	0.32	0.24	0.08
4016	596	0.47	0.26	0.21
4017	597	0.54	0.46	0.08
4018	598	0.53	0.41	0.12
4019	599	0.68	0.54	0.14
4020	600	0.77	0.67	0.09
4021	601	0.89	0.42	0.47
4022	602	0.82	0.63	0.19
4023	603	0.98	0.74	0.24
4024	604	1.10	0.66	0.43
4025	605	0.56	0.30	0.27
4026	606	0.34	0.18	0.16
4027	607	0.50	0.36	0.14
4028	608	0.70	0.51	0.19
4029	609	0.43	0.12	0.31
4030	610	0.31	0.05	0.26
4031	611	0.64	0.40	0.25
4032	612	0.42	0.32	0.10
4033	613	0.36	0.08	0.28
4034	614	0.34	0.22	0.11
4035	615	0.49	0.40	0.10
4036	616	0.56	0.38	0.18
4037	617	0.85	0.66	0.19
4038	618	1.32	0.75	0.57
4039	619	0.41	0.30	0.11
4040	620	0.43	0.35	0.08
4041	621	0.45	0.37	0.09
4042	622	0.50	0.20	0.30
4043	623	0.58	0.11	0.47
4044	624	0.55	0.18	0.36
4045	625	0.46	0.18	0.28
4046	626	0.71	0.50	0.20
4047	627	0.34	0.13	0.21
4048	628	0.45	0.31	0.14
4049	629	0.46	0.36	0.10
4050	630	0.45	0.35	0.10
4051	631	0.53	0.16	0.36
4052	632	0.69	0.40	0.28
4053	633	0.54	0.37	0.18
4054	634	0.38	0.30	0.08
4055	635	0.55	0.48	0.07
4056	636	0.43	0.34	0.09
4057	637	0.70	0.51	0.19
4058	638	0.29	0.14	0.14
4059	639	0.29	0.13	0.15
4060	640	0.37	0.24	0.13
4061	641	0.42	0.10	0.32
4062	642	0.60	0.41	0.19
4063	643	0.58	0.46	0.12
4064	644	0.40	0.27	0.13
4065	645	0.61	0.53	0.08
4066	646	0.57	0.51	0.06
4067	647	0.34	0.19	0.15
4068	648	1.62	0.47	1.15
4069	649	1.28	0.34	0.94
4070	650	0.38	0.16	0.21
4071	651	0.55	0.43	0.12
4072	652	0.43	0.31	0.13
4073	653	0.30	0.10	0.20
4074	654	0.42	0.29	0.13
4075	655	0.50	0.34	0.16
4076	656	0.85	0.27	0.58
4077	657	0.27	0.12	0.15
4078	658	0.62	0.49	0.13
4079	659	0.47	0.35	0.13
4080	660	0.45	0.34	0.11
4081	661	0.31	0.13	0.18
4082	662	0.48	0.37	0.11
4083	663	0.40	0.28	0.12
4084	664	0.32	0.18	0.14
4085	665	0.27	0.18	0.08
4086	666	0.40	0.24	0.16

Cal. yr BP	Varve count	V tx (mm)	L tx (mm)	D tx (mm)
4087	667	0.47	0.30	0.17
4088	668	0.60	0.20	0.40
4089	669	1.91	0.83	1.08
4090	670	1.50	0.67	0.82
4091	671	0.50	0.32	0.18
4092	672	0.63	0.42	0.21
4093	673	0.91	0.10	0.82
4094	674	1.08	0.67	0.40
4095	675	0.48	0.28	0.20
4096	676	0.32	0.22	0.10
4097	677	0.47	0.34	0.13
4098	678	0.39	0.27	0.12
4099	679	0.38	0.27	0.11
4100	680	0.25	0.09	0.17
4101	681	0.39	0.14	0.25
4102	682	0.63	0.46	0.17
4103	683	0.50	0.34	0.17
4104	684	0.22	0.10	0.12
4105	685	0.22	0.05	0.17
4106	686	0.31	0.14	0.17
4107	687	0.43	0.06	0.37
4108	688	0.49	0.08	0.41
4109	689	0.47	0.17	0.29
4110	690	0.40	0.21	0.18
4111	691	0.39	0.25	0.13
4112	692	0.58	0.19	0.39
4113	693	0.55	0.13	0.42
4114	694	0.35	0.12	0.24
4115	695	0.41	0.23	0.18
4116	696	0.45	0.22	0.23
4117	697	0.41	0.19	0.22
4118	698	0.19	0.07	0.13
4119	699	0.64	0.46	0.18
4120	700	0.27	0.14	0.13
4121	701	0.39	0.13	0.26
4122	702	0.50	0.23	0.27
4123	703	0.54	0.40	0.14
4124	704	0.61	0.22	0.39
4125	705	0.46	0.28	0.19
4126	706	0.42	0.17	0.25
4127	707	0.49	0.29	0.20
4128	708	0.39	0.23	0.16
4129	709	0.37	0.22	0.15
4130	710	0.65	0.40	0.24
4131	711	0.44	0.28	0.16
4132	712	0.46	0.38	0.09
4133	713	0.38	0.29	0.09
4134	714	0.50	0.32	0.18
4135	715	0.37	0.26	0.11
4136	716	0.29	0.21	0.07
4137	717	0.39	0.17	0.22
4138	718	0.37	0.30	0.07
4139	719	0.30	0.22	0.08
4140	720	0.29	0.20	0.09
4141	721	0.22	0.13	0.09
4142	722	0.45	0.30	0.15
4143	723	0.38	0.24	0.13
4144	724	0.26	0.13	0.13
4145	725	0.38	0.24	0.14
4146	726	0.40	0.26	0.13
4147	727	0.49	0.13	0.36
4148	728	0.34	0.12	0.22
4149	729	0.63	0.35	0.28
4150	730	1.35	0.11	1.24
4151	731	0.42	0.26	0.16
4152	732	0.80	0.65	0.16
4153	733	0.76	0.40	0.36
4154	734	0.93	0.81	0.13
4155	735	0.52	0.35	0.18
4156	736	0.47	0.31	0.16
4157	737	0.40	0.28	0.12
4158	738	0.48	0.38	0.11
4159	739	0.29	0.13	0.16
4160	740	0.40	0.28	0.12
4161	741	0.36	0.27	0.09
4162	742	0.24	0.10	0.14
4163	743	0.24	0.12	0.13
4164	744	0.29	0.19	0.09
4165	745	0.22	0.13	0.10
4166	746	0.41	0.24	0.17
4167	747	0.45	0.33	0.12
4168	748	0.53	0.21	0.32
4169	749	0.63	0.35	0.28
4170	750	0.62	0.46	0.15
4171	751	0.51	0.21	0.30
4172	752	0.58	0.05	0.52
4173	753	0.37	0.20	0.17
4174	754	0.45	0.28	0.17
4175	755	0.41	0.30	0.11
4176	756	0.26	0.12	0.14
4177	757	0.37	0.20	0.17
4178	758	0.31	0.13	0.18
4179	759	0.21	0.11	0.11
4180	760	0.41	0.27	0.15
4181	761	0.39	0.23	0.16
4182	762	0.33	0.15	0.17
4183	763	0.39	0.28	0.11
4184	764	0.61	0.42	0.20
4185	765	0.39	0.26	0.13
4186	766	0.48	0.28	0.21
4187	767	0.51	0.34	0.18
4188	768	0.34	0.12	0.21
4189	769	0.31	0.17	0.14
4190	770	0.43	0.24	0.19
4191	771	0.41	0.28	0.12
4192	772	0.62	0.41	0.21
4193	773	0.73	0.33	0.40
4194	774	0.66	0.14	0.51
4195	775	0.84	0.37	0.47
4196	776	0.72	0.24	0.48
4197	777	0.66	0.35	0.31
4198	778	0.71	0.16	0.55
4199	779	0.52	0.11	0.41
4200	780	0.47	0.16	0.31
4201	781	0.66	0.38	0.28
4202	782	0.71	0.30	0.41
4203	783	0.78	0.45	0.33
4204	784	0.91	0.13	0.77
4205	785	1.30	1.00	0.30
4206	786	0.59	0.37	0.22
4207	787	0.93	0.36	0.58
4208	788	0.73	0.38	0.34
4209	789	0.60	0.37	0.23
4210	790	2.66	0.67	1.99
4211	791	1.17	0.63	0.54
4212	792	0.59	0.33	0.26
4213	793	0.79	0.66	0.13
4214	794	0.56	0.28	0.29
4215	795	0.50	0.31	0.19

Cal. yr BP	Varve count	V tx (mm)	L tx (mm)	D tx (mm)
4216	796	0.50	0.29	0.21
4217	797	0.60	0.38	0.22
4218	798	0.53	0.35	0.19
4219	799	0.47	0.18	0.29
4220	800	0.42	0.13	0.29
4221	801	0.55	0.33	0.22
4222	802	0.84	0.42	0.43
4223	803	0.74	0.38	0.36
4224	804	0.99	0.13	0.86
4225	805	0.66	0.43	0.22
4226	806	0.39	0.11	0.28
4227	807	0.92	0.24	0.68
4228	808	0.67	0.49	0.18
4229	809	0.55	0.23	0.32
4230	810	0.96	0.59	0.37
4231	811	0.84	0.58	0.26
4232	812	0.62	0.40	0.22
4233	813	0.68	0.44	0.24
4234	814	0.73	0.49	0.24
4235	815	0.83	0.51	0.32
4236	816	0.91	0.44	0.46
4237	817	0.65	0.30	0.36
4238	818	0.76	0.52	0.24
4239	819	0.74	0.42	0.33
4240	820	1.64	0.40	1.24
4241	821	1.46	1.04	0.42
4242	822	1.33	0.50	0.83
4243	823	1.09	0.65	0.45
4244	824	1.03	0.40	0.63
4245	825	0.71	0.31	0.40
4246	826	1.21	0.46	0.75
4247	827	1.35	0.59	0.76
4248	828	0.55	0.23	0.32
4249	829	1.46	0.71	0.75
4250	830	1.99	0.91	1.08
4251	831	2.11	1.65	0.45
4252	832	0.45	0.32	0.13
4253	833	0.70	0.43	0.27
4254	834	0.38	0.28	0.10
4255	835	0.49	0.27	0.22
4256	836	0.57	0.29	0.28
4257	837	0.35	0.19	0.16
4258	838	0.37	0.25	0.12
4259	839	0.25	0.16	0.10
4260	840	0.58	0.39	0.19
4261	841	0.65	0.44	0.21
4262	842	0.56	0.30	0.27
4263	843	0.64	0.41	0.23
4264	844	1.33	1.16	0.17
4265	845	0.75	0.48	0.27
4266	846	0.62	0.40	0.23
4267	847	0.78	0.47	0.31
4268	848	0.84	0.49	0.35
4269	849	0.80	0.49	0.31
4270	850	0.43	0.28	0.15
4271	851	0.60	0.19	0.40
4272	852	1.93	1.09	0.84
4273	853	2.32	0.69	1.64
4274	854	1.52	0.80	0.73
4275	855	1.41	0.69	0.72
4276	856	1.78	0.79	0.99
4277	857	1.16	0.59	0.56
4278	858	1.44	0.65	0.79
4279	859	1.27	0.47	0.81
4280	860	1.37	0.88	0.49
4281	861	1.87	1.22	0.65
4282	862	1.41	0.90	0.52
4283	863	1.71	1.23	0.48
4284	864	2.81	1.12	1.68

APPENDIX XII Low resolution BSEI photomosaics

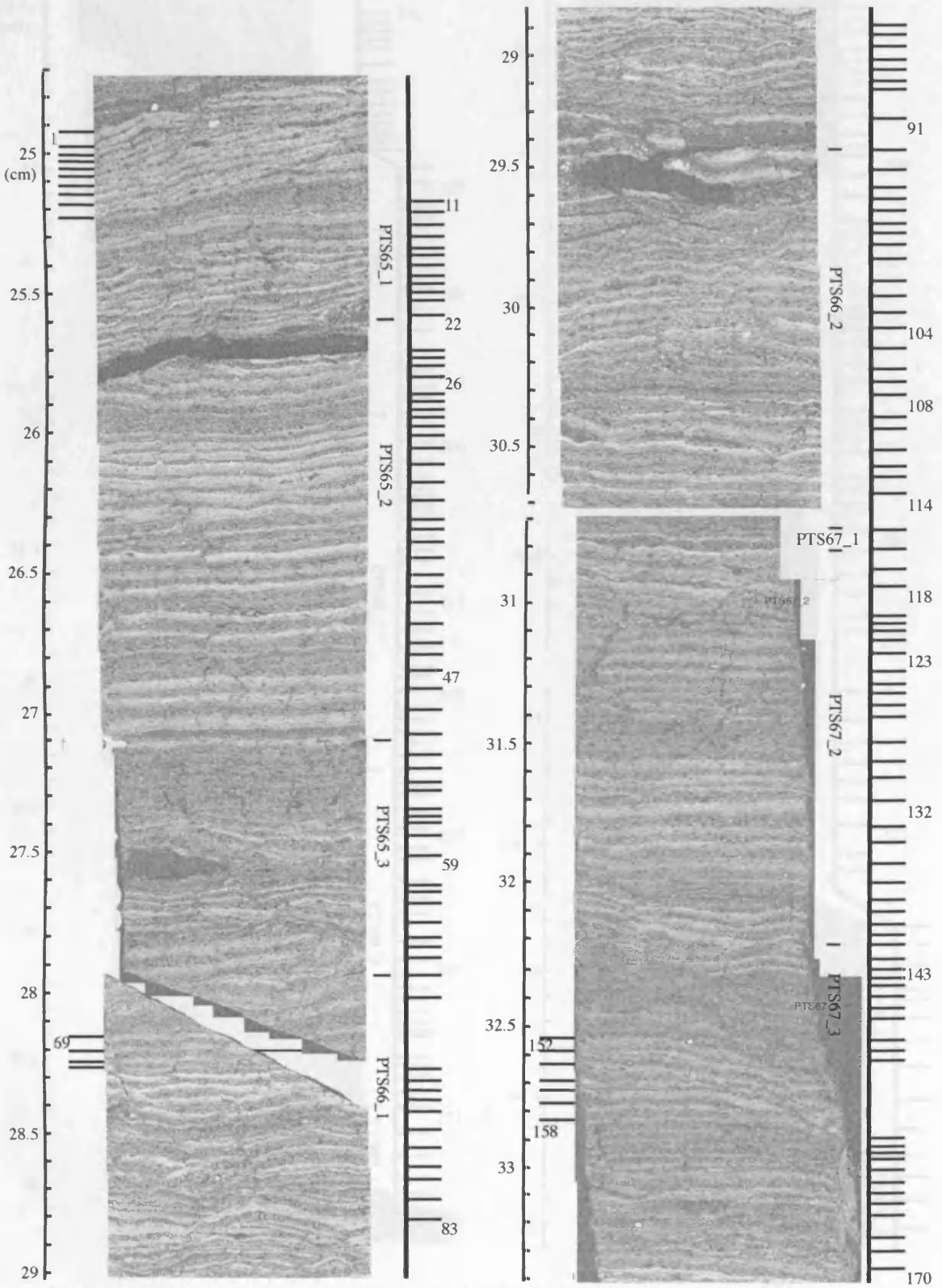

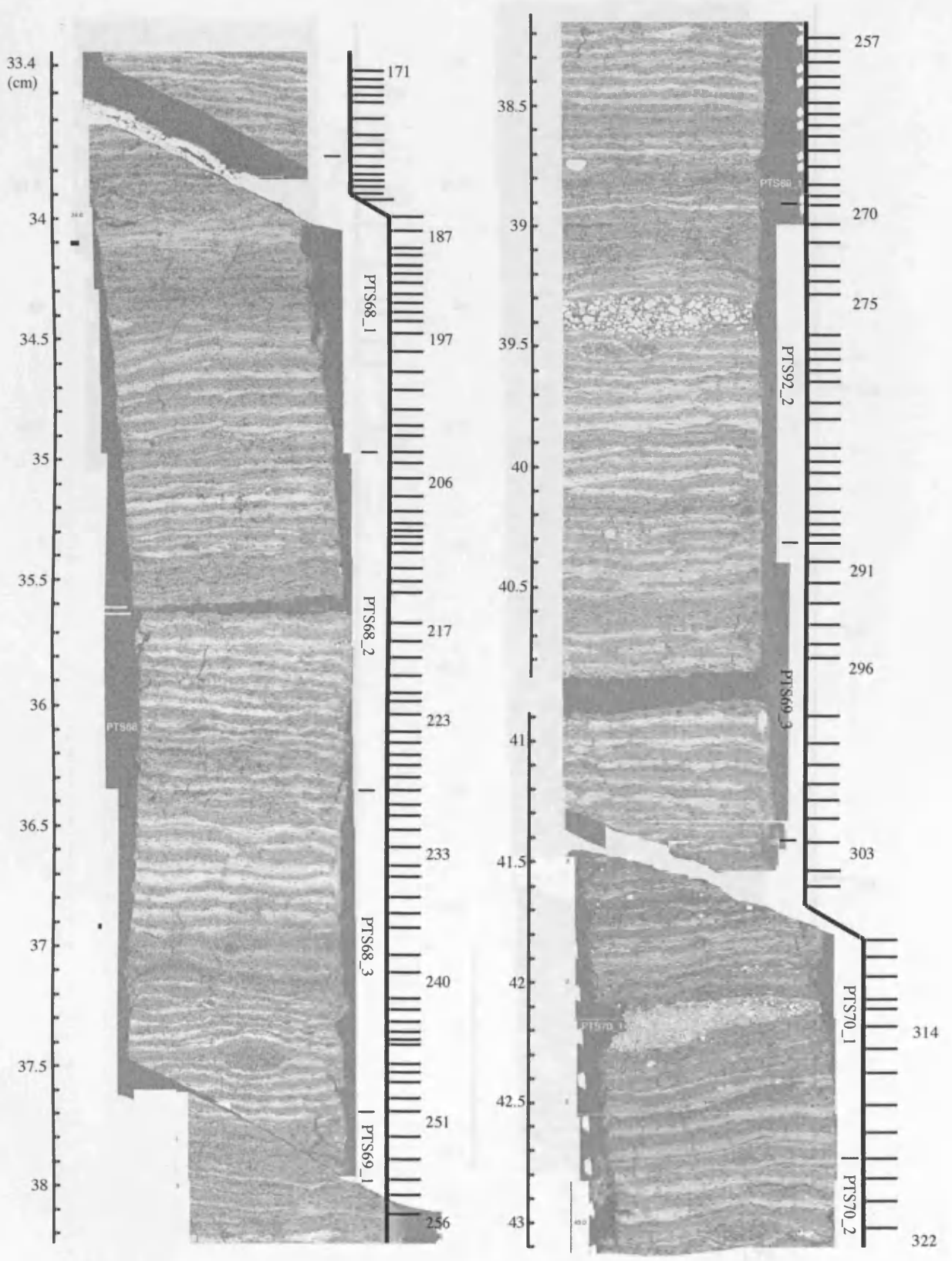
33.4
(cm)
34
34.5
35
35.5
36
36.5
37
37.5
38
171
187
197
206
217
223
233
240
251
256
PTS68_1
PTS68_2
PTS68_3
PTS69_1
38.5
39
39.5
40
40.5
41
41.5
42
42.5
43
257
270
275
291
296
303
314
322
PTS92_2
PTS69_3
PTS70_1
PTS70_2

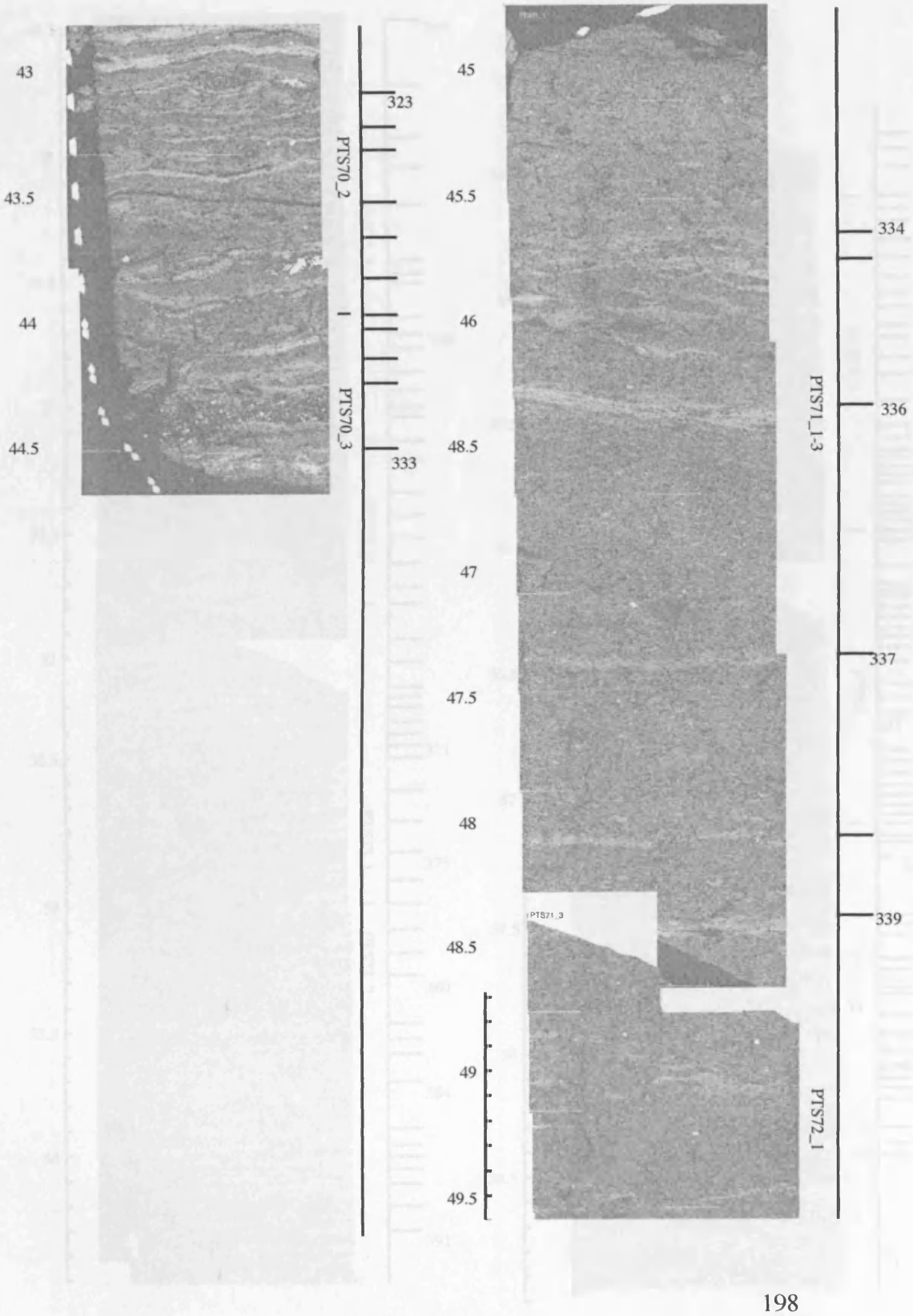
43
43.5
44
44.5
323
PTS70_2
PTS70_3
333
45
45.5
46
48.5
47
47.5
48
48.5
49
49.5
PTS71_3
334
PTS71_1-3
336
337
339
PTS72_1

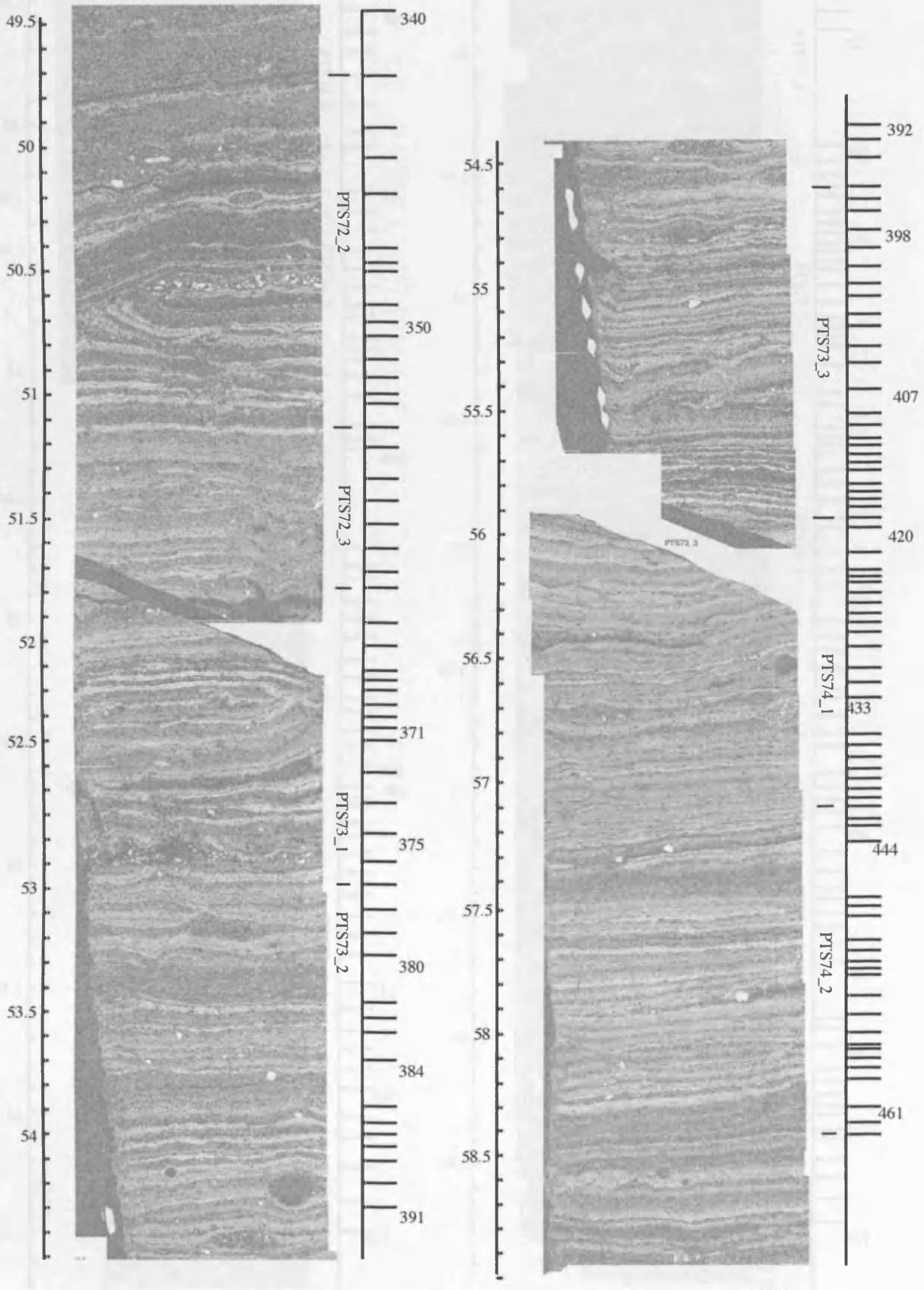
49.5
50
50.5
51
51.5
52
52.5
53
53.5
54
340
350
371
375
380
384
391
PTS72_2
PTS72_3
PTS73_1
PTS73_2
54.5
55
55.5
56
56.5
57
57.5
58
58.5
392
398
407
420
433
444
461
PTS73_3
PTS74_1
PTS74_2

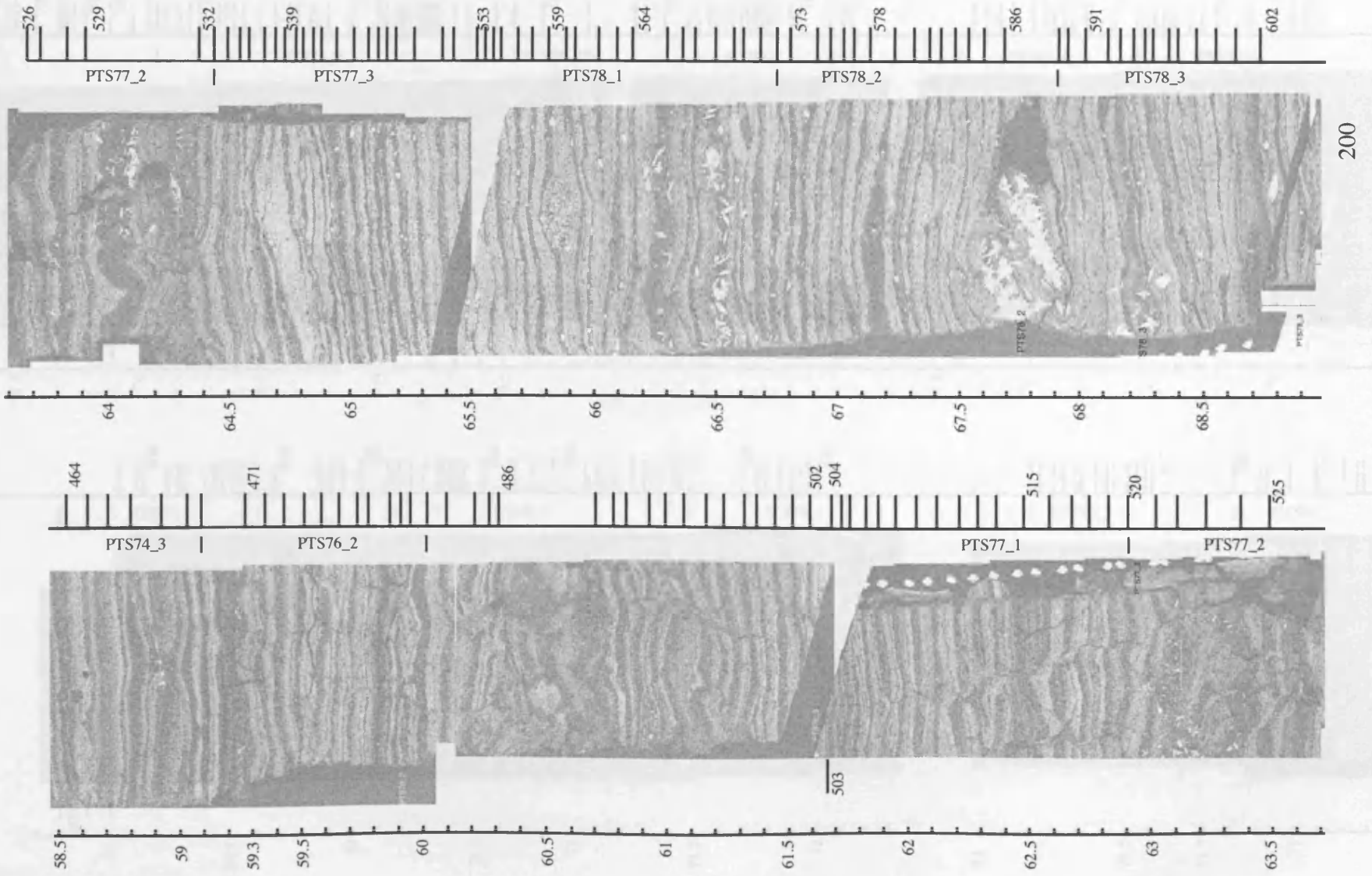
526
529
532
539
553
559
564
573
578
586
591
602
PTS77_2
PTS77_3
PTS78_1
PTS78_2
PTS78_3
64
64.5
65
65.5
66
66.5
67
67.5
68
68.5
464
471
486
502
504
515
520
525
PTS74_3
PTS76_2
PTS77_1
PTS77_2
503
58.5
59
59.3
59.5
60
60.5
61
61.5
62
62.5
63
63.5

200

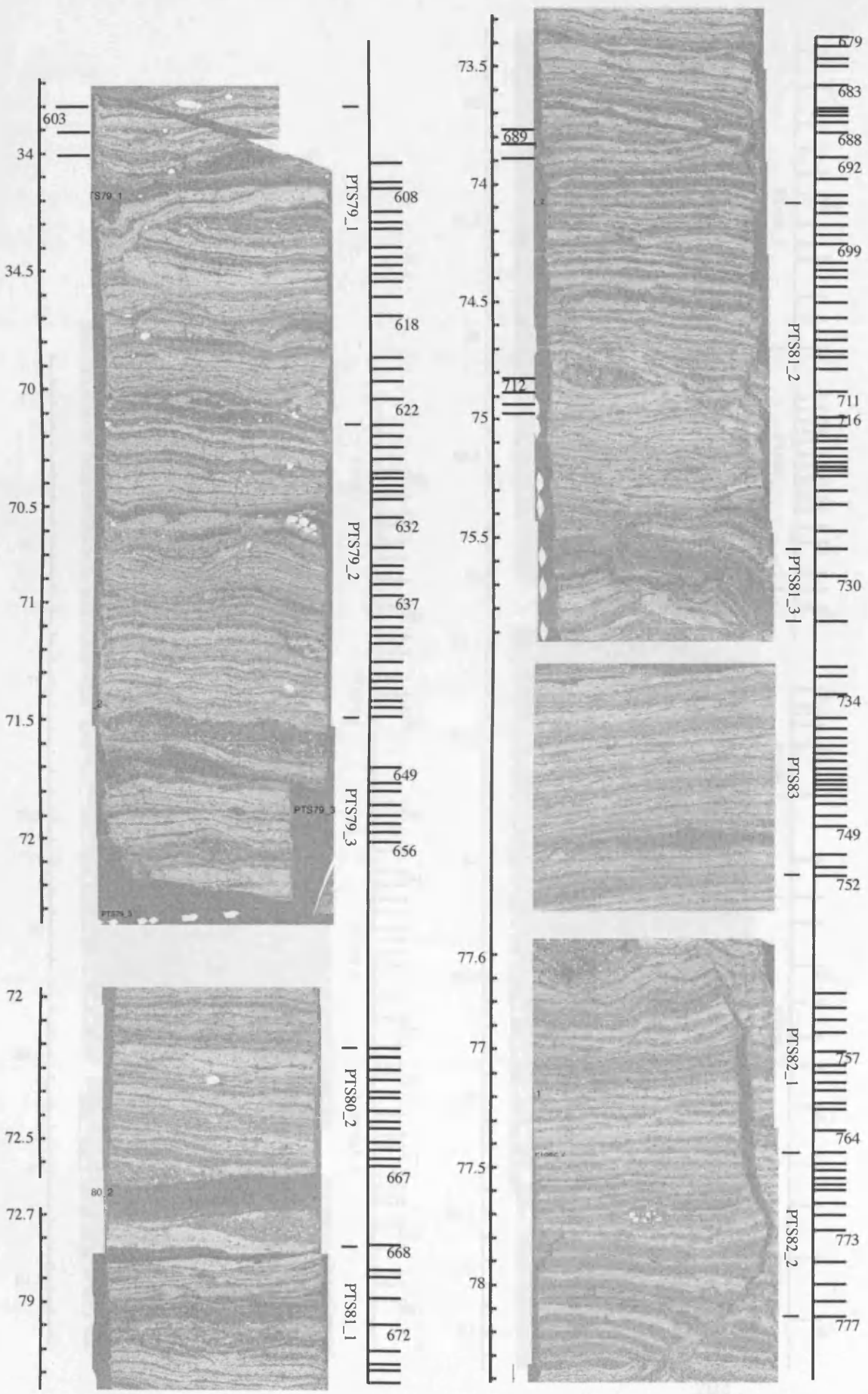
603
34
34.5
70
70.5
71
71.5
72
PTS79_1
PTS79_2
PTS79_3
608
618
622
632
637
649
656
72
72.5
72.7
79
PTS80_2
PTS81_1
667
668
672
73.5
74
74.5
75
75.5
689
712
PTS81_2
PTS81_3
679
683
688
692
699
711
716
730
734
77.6
77
77.5
78
PTS83
PTS82_1
PTS82_2
749
752
757
764
773
777

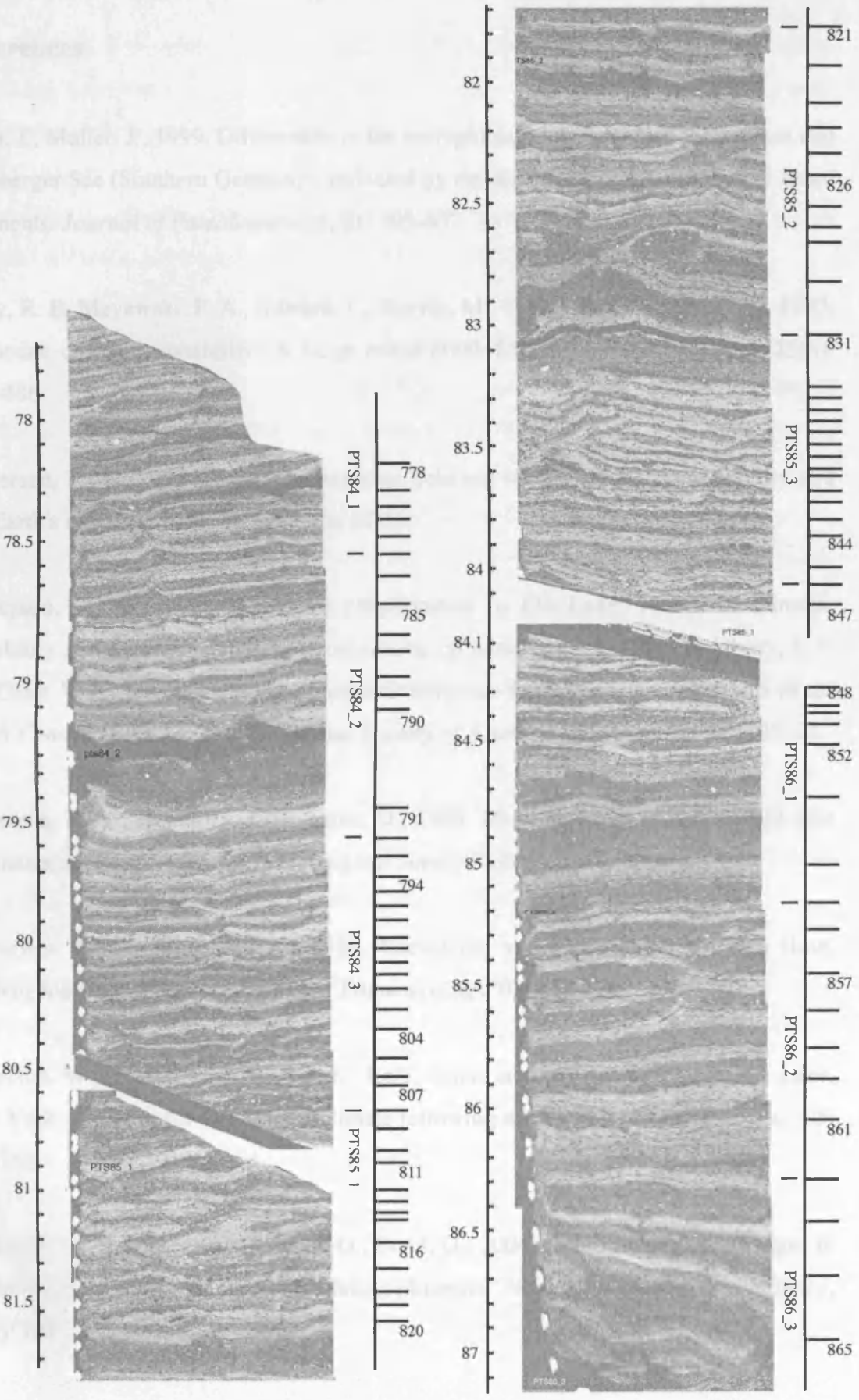
78
78.5
79
79.5
80
80.5
81
81.5
PTS84_1
778
785
PTS84_2
790
791
794
PTS84_3
804
807
PTS85_1
811
816
820
82
82.5
83
83.5
84
PTS85_2
821
826
831
PTS85_3
844
847
84.1
84.5
85
85.5
86
86.5
87
PTS86_1
848
852
PTS86_2
857
861
PTS86_3
865

References

Alefs, J., Muller, J., 1999. Differences in the eutrophication dynamics of Ammersee and starnberger See (Southern Germany), reflected by the diatom succession in varved-dated sediments. *Journal of Paleolimnology*, 21: 395-407.

Alley, R. B. Mayewski, P. A., Sowers, T., Stuiver, M., Taylor, K. C., Clark, P. U., 1997. Holocene climatic instability: A large event 8000–8400 years ago. Geology 25(6): 482–486.

Anderson, R. Y., 1992. Possible connection between surface winds, solar activity and the Earth's magnetic field. *Nature*, 358: 51-53.

Anderson, R. Y., 1993. The varve chronometer in Elk Lake: record of climatic variability and evidence for solar/geomagnetic-climate connection. *In*: Bradbury, J. P. and Dean, W. E. (eds), Elk Lake, Minnesota: *Evidence for Rapid Climate Change in the North-Central United States*. Geological Society of America Special paper, 276: 45–68.

Anderson, R. Y., Bradbury, J. P., Love, D., 1985. Meromictic lakes and varved lake sediments in North America. *US Geological Survey Bulletin*, 1607, 19p.

Anderson. R. Y., Dean, W. E., 1988. Lacustrine varve formation through time. *Palaeogeography, Palaeoclimatology, Palaeoecology*, 62: 215-235.

Anderson, W. T., Mullins, H. T., Ito, E., 1997. Stable isotope record from Seneca Lake, New York: evidence for a cold paleoclimate following the Younger Dryas. *Geology*, 25: 135-138.

Andresen, C. .S, Björck, S., Bennike, O., Bond, G., 2004. Holocene climate changes in southern Greenland: evidence from lake sediments. *Journal of Quaternary Science*, 19(8): 783-795.

Anneville, O., Gammeter, S., and Straile, D., 2005. Phosphorus decrease and climate variability: mediators of synchrony in phytoplankton changes among European peri-alpine lakes. Freshwater Biology (2005) 50, 1731–1746.

Appenzeller, C., Stocker, T. F., Anklin, M., 1998. North Atlantic Oscillation dynamics recorded in Greenland ice cores. *Science,* 282, 446-449.

Baier, J., Lücke, A., Negendank, J. F. W., Schleser, G. H., Zolitschka, B., 2004. Diatom and geochemical evidence of mid- to late Holocene climatic changes at Lake Holzmaar, West-Eifel (Germany). *Quaternary International,* 113: 81-96.

Bailie, M. G., 1995. Dendrochronology and the chronology of the Irish Bronze Age. *In:* Wassell, J., Shee Twohig, E. (eds.), *Ireland in the Bronze Age.* The Stationery Office: Dublin; 30-37.

Baldwin, M. P., Dunkerton, T. J., 2001. Stratospheric harbingers of anomalous weather regimes. *Science,* 294: 581-584.

Barber, K. E., Chambers, F. .M, Maddy, D., 2003. Holocene palaeoclimates from peat stratigraphy: macrofossil proxy climate records from three oceanic raised peat bogs in England and Ireland. *Quaternary Science Reviews,* 22: 521-539.

Bar-Matthews, M., Ayalon, A., Kaufman, A., Wasserburg, G. J., 1999. The eastern Mediterranean paleoclimate as a reflection of regional events: Soreq cave, Israel. *Earth and Planetary Science Letters,* 166: 85-95.

Battarbee, R. W., 1981. Diatom and Chrysophyceae microstratigraphy of the annually laminated sediments of a small meromictic lake. *Striae,* 14: 105-109.

Beer, J., Baumgartner, S., Dittrich-Hannen, B., Hauenstein, J., Kubik, P., Lukasczyk, C., Mende, W., Stellmacher, R., Suter, M., 1994. Solar variability traced by cosmogenic

isotopes. *In:* Pap, J. M., C. Fröhlich, H. S. Hudson & S. K. Solanki (eds), *The Sun as a Variable Star: Solar and Stellar Irradiance*. Cambridge University Press, Cambridge, UK, 291–300.

Behling, H., Hooghiemstra, H., 2001. Neotropical savanna environments in space and time: Late Quaternary inter-hemispheric comparisons. *In*: Markgraf, V. (ed.), *Inter-Hemispheric Climate Linkages*. Academic Press, Burlington, MA, pp. 307– 323.

Behling, H., 2002. Carbon storage increases by major forest ecosystems in tropical South America since the Last Glacial Maximum and the early Holocene. *Global and Planetary Change,* 33, 107– 116.

Benner, T. C., 1999. Central England temperatures: long-term variability and teleconnections. *International Journal of Climatology,* 19: 391–403.

Bennett, K. D., 1983. Devensian Late Glacial and Flandrian vegetational history at Hockham Mere, Norfolk, England, I. Pollen percentages and concentrations. *New Phytologist,* 95: 457-487.

Bennett, K. D., 1986. Competitive interactions among forest tree populations in Norfolk, England, during the last 10,000 years. *New Phytologist,* 103: 603-620.

Bennett, K. D., 1988. Holocene pollen stratigraphy of central East Anglia, England, and comparison of pollen zones across the British Isles. *New Phytologist,* 109. No.2: 237-253.

Bennett, K. D., Simonson, W. D., Peglar, S. M., 1990. Fire and man in postglacial woodlands of eastern England. *Journal of Archaeological Sciences,* 17: 635-642.

Bennion, H., 1994. A diatom-phosphorus transfer function for shallow, eutrophic ponds in southeast England. *Hydrobiologia,* 275/276: 391-410.

Benson-Evans, K., Antoine. R., Antoine, S., 1999. Studies of the water quality and algae of Llangorse Lake. *Aquatic conservation: marine and freshwater ecosystems,* 9: 425-439

Berger and Loutre, 1991. Insolation values for the climate of the last 10 million years. *Quaternary Science Reviews,* 10: 297-317.

Berglund, B. E., 1986. Handbook of Holocene palaeoecology and palaeohydrology. *Wiley*, Chichester: 869p.

Bergquist, .A. M., Carpenter, S. R., 1986. Grazing of phytoplankton: Effects on species growth rates, phosphorus limitation, chlorophyll, and primary production. *Ecology,* 67: 1351-1360.

Bianchi, G., McCave, I. N., 1999. Holocene periodicity in North Atlantic climate and deep-ocean flow south of Iceland. *Nature*. 397: 515-527.

Birks, H. J. B., 1994. The importance of pollen and diatom taxonomic precision in quantitative palaeoenvironmental reconstructions. *Reviews of Palaeobotany and Palynology*, 83: 107-117.

Bjune, A. E., Bakke, J., Nesje, A. and Birks, H. J. B., 2005. Holocene mean July temperature and winter precipitation in western Norway inferred from palynological and glaciological lake-sediment proxies. *The Holocene* 15(2): 177-189.

Boberg, F., Lundstedt, H., 2002. Solar wind variations related to fluctuations of the North Atlantic Oscillation. *Geophysical Research Letters,* 29: 10.1029/2002GL014903.

Bond, G., Showers, W., Cheseby, M, Lotti, R., Almasi, P., deMenocal, P, Priore, P., Cullen, H., Hajdas, I., Bonani, G., 1997. A pervasive millennial-scale cycle in North Atlantic Holocene and glacial climates. *Science,* 278: 1257-1266.

Bond, G, Kromer, B., Beer, J., Muscheler, R., Evans, M. N., Showers, W., Hoffmann, S., Lotti-Bond, R., Hajdas, I., Bonani, G., 2001. Persistent Solar influence on North Atlantic climate during the Holocene. *Science,* 294: 2130-2136.

Booth, S. J., 1982. The sand and gravel resources of the country around Whittlesey, Cambridgeshire. *Mineral Assessment Report of the Institute of Geological Sciences,* No. 93.

Boreham, S., Horne, D. C., 1999. The role of thermokarst and solution in the formation of Quidenham Mere, Norfolk, compared with some other Breckland meres. *Quaternary Research Association, Quaternary Newsletter,* 87: 16-27.

Borgmark, A., 2005. Holocene climate variability and periodicities in south-central Sweden, as interpreted from peat humification analysis. The Holocene. 15(3): 387-395.

Bradbury J. P., 1988. A climatic-limnologic model of diatom succession for paleolimnological interpretation of varved sediments at Elk Lake, Minnesota. *Journal of Paleolimnology,* 1: 115-131.

Bradbury, J. P., Dean, W.E., Anderson, R.Y., 1993. Holocene climatic and limnologic history of the north-central United States as recorded in the varved sediments of Elk Lake, Minnesota: a synthesis. *Geological Society of America Special Paper*, 276, 309–328

Bradbury, P., Cumming, B., Laird, K., 2002. A 1500-yr record of climatic and environmental change in Elk Lake, Minnesota III: measures of past primary productivity. *Journal of Paleolimnology,* 27: 321-340.

Bradbury, J. P., Colman, S. M., Dean, W. E., 2004. Limnological and climatic environments at Upper Klamath Lake, Oregon during the past 45 000 years. *Journal of Paleolimnology,* 31: 167–188.

Broecker, WS. 1997. Thermohaline circulation, the Achilles Heel of our climate system: will man-made CO_2 upset the current balance? *Science,* 278:1582–8.

Brüchmann, C., Negendank, J. F. W., 2004. Indication of climatically induced natural eutrophication during the Holocene period, based on annually laminated sediment from Lake Holzmaar, Germany. *Quaternary International,* 123-125, 117-134.

Brunskill, G. J., 1969. Fayetteville Green Lake, New York. II: Precipitation and sedimentation of calcite in a meromictic lake with laminated sediments. *Limnology and Oceanography*, 14: 1423-1428.

Brunskill, G. J., Ludlam, S. D. 1969. Fayetteville Green Lake, New York. I. Physical and chemical limnology. *Limnology and Oceanography,* 14: 817-829.

Bucha, V., Bucha Jr., V., 1998. Geomagnetic forcing of changes in climate and in the atmospheric circulation. *Journal of Atmospheric and Terrestrial Physics,* 60: 145-169.

Card V. M., 1997. Varve-counting by the annual pattern of diatoms accumulated in the sediment of Big Watab Lake, Minnesota, AD 1837-1990. *Boreas,* 26: 103-112.

Carlow, K. S., Harrison, R. G., Kirkby, J., 2002. Cosmic Rays, Clouds, and Climate. *Science,* 298: 1732-1737.

Chaing, J. C. H., Kushnir Y., Zebiak, S. E., 2000. Interdecadal changes in eastern Pacific ITZC variability and its influence on the Atlantic ITCZ. *Geophysical Research Letters*, 27: 3687-3690.

Chondrogianni, C., Ariztegui, D., Ohlendorf, C., Lister, G. S., 1996. Pleistocene and Holocene sedimentation Albano and Lake Nemi (central Italy). *Memorie dell'Istituto Italiano di Idrobiologia,* 55: 23-38.

Clement, A. C., Seager, R., Cane, M. A., 2000. Suppression of El Nino during the mid-Holocene by changes in the Earth's orbit. *Paleoceanography,* 15 (6): 731-737.

Cook, E. R., D'Arrigol, R. D., Briffa, K. R., 1998. A reconstruction of the North Atlantic Oscillation using tree-ring chronologies from North America and Europe. *The Holocene,* 8: 9–17.

Cook, E., R., D'Arrigo, R. D., 2002. A well-verified, multiproxy reconstruction of the winter North Atlantic Oscillation Index since A.D. 1400. *Journal of Climate,* 15: 1754-1764.

Cooper, M. C., O'Sullivan P. E., Shine, A. J., 2000. Climate and solar variability recorded in Holocene laminated sediments - a preliminary assessment. *Quaternary International,* 68-71: 363-371.

Conrad, V., 1946. Usual formulas of continentality and their limits of validity. *Transactions of the American Geophysical Union,* 27: 663-664.

Crumpton, W. G., Wetzel, R. G., 1982. Effects of differential growth and mortality in the seasonal succession of phytoplankton populations in Lawrence Lake, Michigan. *Ecology,* 63: 1729-1739.

Cushing, E. J., 1967. Late Wisconsin pollen stratigraphy and the glacial sequence in Minnesota, in Cushing, E. J., and Wright, H. E., Jr. eds. *Quaternary paleocecology*: New Haven, Connecticut, Yale University Press: 59-88.

Czaja, A., A. W. Robertson, T. Huck, 2002. The role of Atlantic ocean-atmosphere coupling in affecting North Atlantic Oscillation variability. *In*: Hurrell, J. W., Kushnir, Y., Ottersen, G., Visbeck , M. (eds.), *The North Atlantic Oscillation: climatic significance and environmental impact,* AGU Geophysical Monograph Series, 134, 147-172.

Dalfes, H.N., Kukla, G., Wiess, H., 1994. Third millennium BC climate change and old world collapse. *NATO ASI Series 1: Global Environmental Change*, vol. 49, Springer, Berlin.

Davies, J. C.,1986. Statistics and data analysis in geology. Second edition, *Wiley*, New York. 646p.

Davis, B. A. S., Brewerb, S., Stevenson, A. C., Guiot, J., and Data Contributors, 2003. The temperature of Europe during the Holocene reconstructed from pollen data. *Quaternary Science Reviews,* 22: 1701-1716.

Davis, M.B., Moeller, R. E., Ford, J., 1984. Sediment focusing and pollen influx. *In:* Haworth, E. Y., Lund, J. W. G. (eds.), *Lake sediments and environmental history.* University of Minnesota Press, USA: 261-293.

Dean, J. M., Kemp, A. E. S., Bull, D., Pike, J, Petterson, G., Zolitschka, B., 1999. Taking varves to bits: Scanning electron microscopy in the study of laminated sediments and varves. *Journal of Paleolimnology,* 22: 121-136.

Dean J. M., Kemp A. E. S., and Pearce R. B. 2001. Palaeo-flux records from electron microscope studies of Holocene laminated sediments, Saanich Inlet, British Columbia. *Marine Geology,* 174, Issue: 1-4: 139-158.

Dean, W. E., 1974. Determination of carbonate and organic matter in calcareous sediments and sedimentary rocks by loss-on-ignition: comparisons with other methods. *Journal of Sedimentary Petrology,* 44: 242-248.

Dean, W. E., 1999. The carbon cycle and biogeochemical dynamics in lake sediments. *Journal of Paleolimnology,* 21: 375–393.

Dean, W. E., 2002. A 1500-yr record of climatic and environmental change in Elk Lake, Clearwater Country, Minnesota II: geochemistry, mineralogy, and stable isotopes. *Journal of Paleolimnology,* 27: 301-319.

Dean, W. E., Bradbury, J. P., Anderson, R. Y., Barnosky, C. W., 1984. The variability of Holocene climate change: evidence from varved lake sediments. *Science,* 226: 1191-1194.

Dean W.E., Megard R.O. 1993. Environment of deposition of $CaCO_3$ in Elk Lake, Minnesota. *In*: Bradbury J.P. and Dean W.E. (eds), *Elk Lake, Minnesota: Evidence for Rapid Climate Change in the North-Central United States.* Geological Society of America, Special Paper, 276: 97–113.

Dean, W. E., Anderson, R., Bradbury, J. P., Anderson, D., 2002. A 1500-year record of climatic and environmental change in Elk Lake, Minnesota I: Varve thickness and gray-scale density. *Journal of Paleolimnology,* 27: 287–299.

Deevey, E. S., Foster Flint, R., 1957. Postglacial Hypsithermal Interval. *Science,* 125: 182-184.

deMenocal, P., Oritz, J., Guilderson, T., Sarnthein, M., 2000. Coherent high- and low-latitude climate variability during the Holocene warm period. *Science,* 288: 2198-2202.

Denton, G. H., Karlén, W., 1973. Holocene climatic variations: their pattern and possible cause. *Quaternary Research,* 3: 155-205.

Deser, T., Blackmon, L., 1993. Surface climate variations over the North Atlantic Ocean during the winter, 1900-89. *Journal of Climate,* 6: 1743-1753.

Digerfeldt, G., 1988. Reconstruction and regional correlation of Holocene lake-level fluctuations in Lake Bysjon, South Sweden. *Boreas,* 17: 165–182.

Dittrich, M., Koschel, R., 2002. Interactions between calcite precipitation (natural and artificial) and phosphorus cycle in the hard water lake. *Hydrobiologica,* 469: 49-57.

Dittrich, M, Kurz, P. Wehrli, B., 2004. The role of autotrophic picocyanobacteria in calcite precipitation in an Oligotrophic Lake. *Geomicrobiology Journal,* 21: 45–53.

Edmonds, C. N., 1983. Towards the prediction of subsidence risk upon the Chalk outcrop. *Quarterly Journal of Engineering Geology,* 16: 261-266.

Felis, T., Pätzold, J., Loya, Y., Fine, M, Nawar, A., H., and Wefer, G., 2000. A coral oxygen isotope record from the northern Red Sea documenting NAO, ENSO, and North Pacific teleconnections on Middle East climate variability since the year 1750. *Paleoceanography,* 15: 679-694.

Ferreira, D., Frankignoul, C., Marshall, J., 2001. Coupled ocean-atmosphere dynamics in a simple mid-latitude climate model. *Journal of Climate,* 14: 3704-3723.

Folk, R. L., 1974. The natural history of crystalline calcium carbonate: effects of magnesium content and salinity. *Journal of Sediment Petrology,* 44: 40-53.

Foster. S. S. D., Milton, V. A., 1974. The permeability and storage of an unconfined chalk aquifer. *Hydrological Sciences Bulletin,* 19: 485-500.

Foster. S. S. D., Robertson, A. S., 1977. Evaluation of a semi-confined Chalk aquifer in East Anglia. *Proceedings of the Institution of Civil Engineers,* Part 2, 63: 803-817.

Foy, R.H., Gibson C.E., 1993. The influence of irradiance, photoperiod and temperature on the growth kinetics of three planktonic diatoms. *European Journal of Phycology,* 28: 203-212.

Fritz, S. C., 1989. Lake Development and Limnological Response to Prehistoric and

Historic Land-Use in Diss, Norfolk, U.K. *Journal of Ecology,* 77. No. 1: 182-202.

Fromentin, J. M., Pankquem, B. 1996. Calanus and environment in the eastern North Atlantic: influence of the NAO on *C. finmarchicus* and *C. gelgolandicus. Marine Ecology Progress Series,* 134: 111-118.

Gasse, F., 2000. Hydrological changes in the African tropics since the Last Glacial Maximum. *Quaternary Science Reviews,* 19: 189-211.

Gibbard, P. L., Bryant, I. D., Hall, A. R., 1986. A Hoxnian interglacial doline infilling at Slade Oak Lane, Denham, Buckinghamshire, England. *Geological Magazine,* 123 (1): 27-43.

Goldstein, J. I., Newbury, D. E., Echlin, P., Joy, D. C., Fiori, C., Lifshin, E., 1981. Scanning Electron Microscopy and X-ray Microanalysis. *Plenum,* New York.

Goodman, J., Marshall. J., 1999. A model of decadal middle-latitude atmosphere-ocean coupled modes. *Journal of Climate,* 12, No. 2: 621-641.

Goslar, T., Pazdur, M. F., Walanus, A., 1989. Chronology of lower part of annually laminated sediments of the Gosciaz Lake. *Zeszyty Naukowe Politech. Slaskiej, Seria: Matematika-Fizyka,* 57: 11-20.

Gozzard, J. R., 1982. The sand and gravel resources of the country around Chatteris, Cambridgeshire. *Mineral Assessment Report of the Institute of Geological Sciences,* No. 124.

Greatbach, R. J., 2000. The North Atlantic Oscillation. *Stochastic and Environmental Risk Assessment,* 14: 213-242.

Groleau, A., Vincon-Leite, B., Tassin, B., Sarazin, G., Quiblier–Lloberas, C., 1999.

Calcite precipitation and interaction with phosphorus cycle in Lake Bourget, France. *In:* Armannsson, H. (ed.), *Geochemistry of the Earth's Surface.* Balkema, Rotterdam: 565–568.

Gruber, N., Wehrli B., Wüest, A., 2000. The role of biogeochemical cycling for the formation and preservation of varved sediments in Soppensee (Switzerland). *Journal of Paleolimnology,* 24, 277-291

Hall, R. I., Smol, J. P., 1992. A weighted-average regression and calibration model for inferring total phosphorus concentration from diatoms in British Columbia (Canada) Lake. *Freshwater Biology,* 27: 417-434.

Hammarlund, D., Björck, S., Buchardt, B., Israelson, C., Thomsen, C. T., 2003. Rapid hydrological change during the Holocene revealed by stable isotope records of lacustrine carbonates from Lake Igelsjön, southern Sweden. *Quaternary Science Reviews,* 22: 353-370.

Harrison, S.P., Digerfeldt, G., 1993. European lakes as palaeohydrological and palaeoclimatic indicators. *Quaternary Science Reviews,* 12: 233–248.

Hartley, A. M., House, W. A., Callow, M. E., Leadbeater, B. S. C., 1995. The role of a green alga in the precipitation of calcite and the co-precipitation of phosphate in freshwater. *International Reviews ges. Hydrobiolofia,* 80: 385-401.

Hartley, D. E., Villarin, J. T., Black, R. X., and Davis, C. A., 1998. A new perspective on the dynamical link between the stratosphere and troposphere. *Nature,* 391: 471-474.

Haug, G. H., K. A. Hughen, D. M. Sigman, L. C. Peterson, and U. Röhl, 2001. Southward migration of the intertropical convergence zone through the Holocene, Science, 293: 1304–1308.

Hausmann, S., Lotter A.F. 2001. Numerical *Cyclotella comensis* taxonomy and its importance for quantitative temperature reconstruction. *Freshwater Biology,* 46, 1323-1333.

Heiri, O., Lotter, A. F., Hausmann, S., Kienast, F., 2003. A chironomid-based Holocene summer air temperature reconstruction from the Swiss Alps. *The Holocene,* 13(4): 477-484.

Hodell, D. A., Brenner, M., J., Curtis, H., Guilderson, T., 2001. Solar forcing of drought frequency in the Maya Lowlands. *Science,* 292:1367-1370.

Hoerling, M. P. , Hurrell, J. W., Xu, T., 2001. Tropical Origins for Recent North Atlantic Climate Change. *Science.* 292: 90-92.

Holmer, M., Storkholm, P., 2001. Sulphate reduction and sulphur cycling in lake sediments: a review. *Freshwater Biology,* 46: 431-451.

Horne, D. C., 1999. Biostratigraphhy and palaeolimnology of late-glacial and Holocene lake marls at Quidenham Mere, Norfolk. Unpublished PhD thesis, University of Cambridge.

House, W. A., 1987. Inhibition of calcite crystal growth by inorganic phosphate. *Journal of Colloid and Interface Science,* 119: 505-511.

House, W. A., 1990. The prediction of phosphate co-precipitation with calcite in freshwater. *Water Research,* 24: 1017-1023.

Hughes, P. D. M., Mauquoy, D., Barber, K. E., Langdon, P. G., 2000. Mire-development pathways and palaeoclimatic record from a full Holocene peat archive at Walton Moss, Cumbria, England. *The Holocene,* 10: 465-479.

Hurrell, J. W., 1995. Decadal trends in the North Atlantic Oscillation, regional temperatures and precipitation. *Science,* 269: 676-679.

Hurrell, J. W., 2000. The North Atlantic Oscillation. *National Academy of Sciences. 12th Annual Symposium, Frontiers of Sciences.* http://www.cgd.ucar.edu/~jhurrell/white.html

Hurrell, J.W., van Loon, H., 1997. Decadal variations in climate associated with the North Atlantic Oscillation. *Climatic Change,* 36: 301–326.

Hurrell, J. W., Y. Kushnir, Ottersen, G. Visbeck, M. (eds), 2003. The North Atlantic Oscillation: Climate Significance and Environmental Impact, *Geophysical monograph,* 134, American Geophysical Union, pp 279.

Ineson, J., 1962. A hydrogeological study of the permeability of the Chalk. *Journal of the Institution of Water Engineers,* 16: 449-463.

Interlandi S. J., Kilham S. S., Theriot E. C., 1999. Responses of phytoplankton to varying resource availability in large lakes of the greater Yellowstone ecosystem. *Limnology and Oceanography,* 44, No. 3, part 1: 668-682.

Itkonen, A., Salonen, V. P., 1994. The response of sedimentation in three varved lacustrine sequences to air temperatures, precipitation and human impact. *Journal of Paleolimnology,* 11:323–332.

Jansen, J. H. F., Van der Gaast, S. J., Koster, B., Vaars, A. J., 1998. CORTEX, a shipboard XRF-scanner for element analyses in split sediment cores. *Marine Geology,* 151: 143–153.

Jenkins, G. M., Watts, D. G., 1968. Spectral analysis and its applications. *Holden-Day,* San Francisco, 525 pp.

Jennings, A. E., Knudsen, K. L., Hald, M., Hansen, C. V., Andrews, J. T., 2002. A mid-Holocene shift in Arctic sea-ice variability on the East Greenland Shelf. *The Holocene.* 12: 49–58.

Jones, P. D., Jonsson, T., Wheeler, D., 1997. Extension to the North Atlantic Oscillation using early instrumental pressure observations from Gibraltar and south-west Iceland. *International Journal of Climatology,* 17: 1433-1450.

Keigwin, L. D., Pickart, R. S., 1999. Slope Water Current over the Laurentian Fan on Interannual to Millennial Time Scales. *Science,* 286: 520-523.

Kelts, K., Hsü, K. L., 1978. Freshwater carbonate sedimentation. *In*: Lerman A. (ed.) *Lakes: geology, chemistry, physics.* Springer-Verlag, New York: 295-323.

Kelts, K., Talbot, M. R., 1990. Lacustrine carbonates as geochemical archives of environmental change and biotic-abiotic interactions. *In:* Tilzer, M. M., Serruya, C. (eds.), *Large Lakes: Ecological Structure and Function.* Springer-Verlag, New York: 288-315.

Kemp, A. E. S., Pearce, R. B., Pike, J., Marshall, J. E. A., 1998. Microfabric and micro-compositional studies of Pliocene and Quaternary sapropels from the eastern Mediterranean. *In: Proceedings of ODP, Scientific Results, Leg 160*: 333-348.

Kemp, A. E. S., Pearce, R. B., Koizumi, I., Pike, J., Rance, S. J., 1999. The role of mat forming diatoms in formation of the Mediterranean sapropels. *Nature,* 398: 57-61.

Kettlewell, P. S., Sothern, R. B., Koukkari, W. L., 1999. U.K. wheat quality and economic value are dependent on the North Atlantic Oscillation. *Journal of Cereal Science,* 29: 205-209.

Kilham S. S., 1984. Silicon and phosphorus growth kinetics and competitive interactions between *Stephanodiscus minutus* and *Synedra* sp. *Int. Ver. Theor. Angew. Limnol. Verh.*, 22: 435-439.

Kilham S. S., 1990. The ecology of *Melosira* species in the Great Lakes of Africa, *In*: Tilzer, M. M., Serruya, C. (eds.), *Large lakes, ecological structure and function.* Springer-Verlag. 414-427.

Kilham S. S., Theriot E. C., Fritz S. C., 1996. Linking planktonic diatoms and climate change in the large lakes of the Yellowstone ecosystem using resource theory. *Limnology and Oceanography*, 41, No. 5, Freshwater Ecosystems and Climate Change in North America: 1052-1062.

Klemer, A., Barko, J., 1991. Effects of mixing and silica enrichment on phytoplankton seasonal succession. *Hydrbiologia,* 210 (3): 171-181.

Koç, N., Jansen, E., 1994. Response of the high-latitude northern hemisphere to orbital climate forcing: evidence from the Nordic Seas. *Geology,* 22, 523–526.

Kodera, K., 2002. Solar cycle modulation of the North Atlantic Oscillation: Implication in the spatial structure of the NAO. *Geophysical Research Letters,* 29: 10.1029/2001GL014557.

Koschel, R., 1997. Structure and function of pelagic calcite precipitation in lake ecosystems. *Verh. Internat. Verein. Limnol.*, 26: 343-349.

Koslowski, G., Loewe, P., 1994. The western Baltic ice season in terms of mass-related severity index: 1879-1992. Part I: temporal variability and association with the North Atlantic Oscillation. *Tellus,* 46A: 66-74.

Koslowski, G., Glaserr, R., 1999. Variations in reconstructed ice winter severity in the western Baltic from 1501-1995 and their implications for the North Atlantic Oscillation. *Climate Change,* 41: 175-191.

Kullenberg B., 1947. The piston core sampler. *Svenaka Hydro-Biol. Komm. Skr.* 3: 1-46.

Lamb, A. L., Leng, M. J., Lamb, H. F., Mohammed, M. U., 2000. A 9000-year oxygen and carbon isotope record of hydrological change in a small Ethiopian crater lake. *The Holocene,* 10(2): 167-177.

Lamb, H., 1995. Climate, History and the Modern World. *Routledge*, London, New York, 2nd Edition.

Lamb, P. J., Peppler, R. A., 1987. North Atlantic Oscillation: Concept and an Application. *Bulletin American Meteorological Society,* 68(10): 1218-1225.

Landscheidt, T., 1990. Relationship between rainfall in the northern hemisphere and impulses of the torque in the Sun's motion. *In*: Schatten, K. H., Arking, A. (eds.): *Climate impact of solar variability.* Greenbelt, NASA: 259-266.

Lehman, J. T., 1975. Reconstructing the rate of accumulation of lake sediment: The effect of sediment focusing. *Quaternary Research,* 5: 541-550.

Livingstone, D. A., 1955. A lightweight piston sampler for lake deposits. *Ecology,* 36: 137-139.

Livingstone, D. M., Hajdas, I., 2001. Climatically relevant periodicities in the thicknesses of biogenic carbonate varves in Soppensee, Switzerland (9740–6870 calendar yr BP). *Journal of Paleolimnology,* 25: 17–24.

Lotter, A. F., 1989. Evidence of annual layering in Holocene sediments of Soppensee, Switzerland. *Aquatic Sciences,* 51: 19-30.

Lotter, A. F., 1998. The recent eutrophication of Baldeggersee (Switzerland) as assessed by fossil diatom assemblages. *The Holocene,* 8, 4: 395–405.

Lotter, A. F., Birks, H. J. B., 1997. The separation of the influence of nutrients and climate on the varve time-series of Baldeggersee, Switzerland. *Aquatic Sciences,* 59: 362-375.

Lotter, A. F., Sturm, M., Teranes, J. L., Wehrli, B., 1997a. Varve formation since 1885 and high-resolution varve analyses in hypertrophic Baldeggersee (Switzerland). *Aquatic Sciences,* 59: 304–325.

Lotter, A. F., Merkt, J., Sturm, M., 1997b. Differential sedimentation *versus* coring artefacts: a comparison of two widely used piston-coring methods. *Journal of Paleolimnology,* 18: 75-85.

Lotter, A. F., Birks, J. B., Hofmann, W., Marchetto, A., 1998. Modern diatom, caldocera, chironomid, and chrysophyte cyst assemblages as quantitative indicators for the reconstruction of past environmental conditions in the Alps. II: Nutrients. *Journal of Paleolimnology,* 19: 395-420.

Lotter, A. F., Lemcke, G., 1999. Methods for preparing and counting biochemical varves. *Boreas,* 28: 243-252.

Ludlam, S.D., 1967. Sedimentation in Cayuga Lake, New York. *Limnology and Oceanography,* 12, 618–632.

Ludlam, S. D., 1969. Fayetteville Green Lake, New York. III: The Laminated Sediments. *Limnology and Oceanography,* 14, (6): 848-857.

Luterbacher, J., Schmutz, C., Gyalistras, D., Xoplaki, E., Wanner, H., 1999. Reconstructions of monthly NAO and EU indices back to AS 1675. *Geophysical Research Letters,* 26: 2745-2748.

Mackereth, I. J. H., 1958. A portable piston sampler for lake deposits. *Limnology & Oceanography,* 3: 181-191.

Macklin, M. G., and Lewin, J., 2003. River sediments, great floods and centennial-scale Holocene climate change. Journal of Quaternary Science, 18(2): 101–105.

Mann, M. E., Lees, J. M., 1996. Robust estimation of background noise and signal detection in climatic time series. *Climatic change,* 33: 409-445.

Mann, M. E., 2002. Large-scale climate variability and connections with the Middle East in past centuries. *Climatic Change,* 55: 287–314.

Marchant, R., Hooghiemstra, H., 2004. Rapid environmental change in African and South American tropics around 4000 years before present: a review. *Earth-Science Reviews,* 66: 217-260.

Marsh, N. D., Svensmark, H., 2000. Low cloud properties influenced by cosmic rays. *Physics Review Letters,* 25: 5004.

Marshall, J., Johnson, H., Goodman, J., 2001. Interaction of the North Atlantic Oscillation with ocean circulation. *Journal of Climate,* 14 (7): 1399-1421.

Mayewski, P. A., Rohling, E. E., Stager, J. C., Karlén, W, Maasch, K. A., Meeker, L. D., Meyerson, E. A., Gasse, F., van Kreveld, S. Holmgren, K., Lee-Thorp, J. Rosqvist, G. Rack, F. Staubwasser, M. Schneider, R. R., Steig, E. J., 2004. Holocene climate variability. *Quaternary Research,* 62: 243-255.

McCoy, F. W., 1985. Mid-core flow-in: Implications for stretched stratigraphic sections in piston cores. *Journal of Sediment Petrology,* 55: 608–610.

McDermott, F., Mattey, D. P., Hawkesworth, C., 2001. Centennial-scale Holocene climate variability revealed by a high-resolution speleothem $\delta^{18}O$ record from SW Ireland. *Science,* 294: 1328-1331.

Megard, R. O., 1968. Planktonic photosynthesis and the environment of calcite carbonate deposition in lakes. *Limnology Research Center, University of Minnesota,* Interim Report. 2.

Megard, R. O., Bradbury, J. P., Dean, W. E., 1993. Climatic and limnologic setting of Elk Lake. *In:* Bradbury J. P. & W. E. Dean (eds.). *Elk Lake, Minnesota: Evidence for Rapid Climate Change in the North-Central United States.* Geological Society of America, Special Paper, 276: 19-36.

Meyers, P. A., 2002. Evidence of mid-Holocene climate instability from variations in carbon burial in Seneca Lake, New York. *Journal of Paleolimnology,* 28: 237-244.

Morel, E. H., 1980. The use of a numerical-model in the management of the chalk aquifer in the Upper Thames Basin. *Quarterly Journal of Engineering Geology,* 13: 153-165.

Moros, M., Emeis, K., Risebrobakken, B. Snowball, I. Kuijpers, A., McManus, J., Jansen, E., 2004. Sea surface temperatures and ice rafting in the Holocene North Atlantic: climate influences on northern Europe and Greenland. *Quaternary Science Reviews,* 23: 2113–2126.

Moses, T., Kiladis, G. N., Diaz, H. F., Barry, R. G. 1987. Characteristics and frequency of reversals in mean sea level pressure in the North Atlantic sector and their relationship to long-term temperature trends. *Journal of Climatology,* 7: 13–30.

Müller, B., Wang, Y., Dittrich, M., Wehrli, B., 2003. Influence of organic carbon decomposition on calcite dissolution in surficial sediments of a freshwater lake. *Water Research,* 37: 4524-4532.

Mullins, H. T., 1998. Environmental change controls of lacustrine carbonate, Cayuga Lake, New York. *Geology,* 26: 443-446.

Muñoz, A., Ojeda, J., Sánchez-Valverde, B., 2002. Sunspot-like and ENSO/NAO-like periodicities in lacustrine laminated sediments of the Pliocene Villarroya Basin (La Rioja, Spain). *Journal of Paleolimnology,* 27: 453-463.

Nesje, A., Matthews, J. A., Dahl, S. O., Berrisford, M. S., Andersson, C., 2001. Holocene glacier fluctuations of Flatebreen and winter-precipitation changes in the Jostedalsbreen region, western Norway, based on glaciolacustrine sediment records. *The Holocene,* 11(3): 267–280.

Niggemann, S., Mangini, A., Mudelsee, M., Richter, D. K., Wurth, G., 2003. Sub-Milankovitch climatic cycles in Holocene stalagmites from Sauerland, Germany. *Earth and Planetary Science Letters,* 216: 539-547.

Nõges, T., 1997. Zooplankton-phytoplankton interactions in lakes Võrtsjärv, Peuipis (Estonia) and Yaskhan (Turkmenia). *Hydrobiologia,* 342/343: 175-184.

Noren, A. J. Bierman, P. R., Steig, E. J. Lini, A. and Southon, J., 2002. Millennial-scale storminess variability in the northeastern United States during the Holocene epoch. Nature. 419, 24: 821-824.

Nuhfer, E. B., Anderson, R. Y., Bradbury, J. P., Dean, W. E., 1993. Modern sedimentation in Elk Lake, Clearwater County, Minnesota. *In:* Bradbury J. P., Dean, W. E. (eds.), *Elk Lake, Minnesota: Evidence for Rapid Climate Change in the North-*

Central United States. Geological Society of America Special Paper 276: 76-96.

O'Brien, S. R., Mayewski, P. A., Meeker, L. D., Meese, D. A., Twickler, M. S., Whitlow, S. I., 1995. Complexity of Holocene Climate as Reconstructed from a Greenland Ice Core. *Science,* 270: 1962-1964.

Osborn, T. J., Briffa, K. R., Tett, S. .F, B., Jones, P. D., and Trigo, R. M., 1999. Evaluation of the North Atlantic oscillation as simulated by a climate model. *Climate Dynamic,* 15: 685-702.

O'Sullivan, P. E., 1983. Annually-laminated lake sediments and the study of Quaternary environmental changes - a review. *Quaternary Science Reviews,* 1: 245–313.

Ottersen, G., Planque, B., Belgrano, A., Post, E., Reid, P. C., Stenseth, N. C., 2002. Ecololgical effects of the North Atlantic Oscillation. Oecologia, 128:1-14.

Owen, M., Robinson, V. K., 1978. Characteristics and yield in fissured chalk. *Proceedings of the Conference on Thames Groundwater Scheme. Institution of Civil Engineers*: 33-49.

Padisák, J., Krienitz, L., Scheffler, W., Koschel, R., Kristiansen, J., Grigorszky, I., 1998. Phytoplankton succession in the oligotrophic Lake Stechlin (Germany) in 1994 and 1995. *Hydrobiologia,* 369/370: 179-197.

Padisák, J., Scheffler, W., Sipos, C., Kasprzak, P., Koschel, R., Krienitz, L., 2003. Spatial and temporal pattern of development and decline of the spring diatom populations in Lake Stechlin in 1999. *Arch. Hydrobiol. Spec. Issues Advancec. Limnol.,* 58: 135-155.

Pantaléon-Cano, J., Yll, E.-I., Pe´rez-Obiol, R., and Roure, J. M., 2003. Palynological evidence for vegetational history in semi-arid areas of the western Mediterranean

(Almerl a, Spain). *The Holocene.* 13(1): 109–119.

Peglar, S. M., Fritz, S C., Alapieti, T., Saarnisto, M., Birks, H. J .B., 1984. Composition and formation of laminated sediments in Diss Mere, Norfolk, England. *Boreas,* 13: 13-28.

Peglar, S. M., Fritz, S C., Birks, H. J .B., 1989. Vegetation and land-use history at Diss, Norfolk, U.K. *Journal of Ecology,* 77: 203-222.

Peglar, S. M., 1993a. The development of the cultural landscape around Diss Mere, Norfolk, UK, during the past 7000 years. *Review of Palaeobotany and Palynology,* 76: 1-47.

Peglar, S. M., 1993b. The mid-Holocene *Ulmus* decline at Diss Mere, Norfolk, U.K.: a year-by-year pollen stratigraphy from annual laminations. *The Holocene,* 3: 1-13.

Peltier, J. D., 1998. The power spectral density of atmospheric temperature from time scales of 10^{-2} to 10^{6} yr. *Earth and Planetary Science Letters,* 158: 157-164.

Peng, S, Robinson, W. A., Li, S., 2002. North Atlantic SST forcing of the NAO and relationships with intrinsic hemispheric variability. *Geophysical Research Letters,* 29 (8): 10.1029/2001GL014043.

Perlwitz, J., & Graf, H-F., 1995. The statistical connection between troposphere and stratospheric circulation of the Northern Hemisphere in winter. *Journal of Climate,* 8: 2281-2295.

Perry, A., 2000. The North Atlantic Oscillation: an enigmatic seesaw. *Progress in Physical Geography,* 24, 2: 289-294.

Pike, J., Kemp, A.E.S., 1996. Preparation and analysis techniques for studies of laminated sediments. *In:* Kemp, A. E. S. (ed.), *Paleoclimatology and Palaeoceanography from laminated sediments.* Geological Society Special Publication (London), 116: 37-48.

Porter, K. G., 1973. Selective grazing and differential digestion of algae by zooplankton. *Nature,* 244: 179-180.

Porter, K. G., Saunders, P. A., Haberyan, K. A., Macubbin, A. E., Jacobsen, T. R., Hodson, R. E., 1996. Annual cycle of autotrophic and heterotrophic production in a small, monomictic Piedmont lake (Lake Oglethorpe): analog for the effects of climatic warming on dimictic lakes. *Limnology and Oceanography,* 41: 1041-1051.

Priestley, M. B., 1981. Spectral analysis and times series. *In:* Priestley, M. B. (ed), *Multivariate series, prediction and control.* Academic Press (London): 654-890.

Ramisch, F., Dittrich, M., Mattenberger, C., Wehrli, B., Wüest, A., 1999. Calcite dissolution in two deep eutrophic lakes. *Geochemica et Cosmochimica Acta,* 63: 3349-3356.

Reavie, E. D., Hall, R. I., Smol, J. P., 1995. An expanded weighted-averaging model for inferring past total phosphorus concentrations from diatom assemblages in eutrophic British Columbia (Canada) lakes. *Journal of Paleolimnology,* 14: 49-67.

Reed, J. M., Stevenson, A. C., and Juggins, S., 2001. A multi-proxy record of Holocene climatic change in southwestern Spain: the Laguna de Medina, Ca´diz. *The Holocene* 11(6): 707–719.

Reimer, P. J., Baillie, M. G. L., Bard, E., Bayliss, A., Beck, J. W., Bertrand, C., Blackwell, P. G., Buck, C. E., Burr, G., Cutler, K. B., Damon, P. E., Edwards, R. L., Fairbanks, R. G., Friedrich, M., Guilderson, T. P., Hughen, K. A., Kromer, B.,

McCormac, F. G., Manning, S., Bronk Ramsey, C., Reimer, R. W., Remmele, S., Southon, J. R., Stuiver, M. S., Talamo, S., Taylor, F. W., van der Plicht, J., and Weyhenmeyer, C. E., 2004. IntCal04 Terrestrial radiocarbon age calibration, 26 - 0 ka BP. Radiocarbon 46:1029-1058.

Renberg, I., Segerström, U., Wallin, J-E., 1984. Climatic reflection in varved lake sediments. *In*: Mörner, N-A., Karlén, W. (eds), *Climatic changes on a yearly to millennial basis*. Reidel: 249-256.

Reynolds, C. S., 1973. The phytoplankton of Cross Mere, Shropshire. *Journal of British Phycology,* 8: 153-162.

Reynolds, C. S., 1976. Succession and vertical distribution of phytoplankton in response to thermal stratification in a lowland mere, with special reference to nutrient availability. *The Journal of Ecology,* 64: 529-551.

Reynolds, C. S., 1980. Phytoplankton assemblages and their periodicity in stratifying lake systems. *Holarctic Ecology*, 3, 141-159.

Reynolds C. S. 1984. *The ecology of freshwater phytoplankton.* Cambridge University Press, pp 384.

Reynolds, C. S., Bellinger, E. G., 1992. Patterns of abundance and dominance of the phytoplankton of Rostherne Mere, England: evidence from an 18-year data set. *Aquatic Sciences,* 54: 10-36.

Rhoades, R., Sinacori, M. N., 1941. Pattern of ground-water flow and solution. *Journal of Geology,* 4: 785-794.

Rioual, P., 2000. Reconstruction of palaeoclimatic and palaeolimnological changes during the last interglacial from sedimentary diatom assemblages in the French Massif Central. *Unpublished PhD Thesis*, University of London.

Rioual, P., Andrieu-Ponel, V., Rietti-Shati, M., Battarbee, R. R., de Beaulieu, J., Cheddadi, R., Reille, M., Svobodova, H., Shemesh, A., 2001. High-resolution record of climate stability in France during the last interglacial period. *Nature,* 413: 293-296.

Risebrobakken, B., Jansen, E., Andersson, C., Mjelde, E., Hevroy, K., 2003. A high-resolution study of Holocene paleoclimatic and paleoceanographic changes in the Nordic Seas. *Paleoceanography,* 18: 1017–1031.

Robock, A., Mao, J. P., 1992. Winter warming from large volcanic eruptions. *Geophysical Research Letters,* 119: 2405-2408.

Rodwell, M. J., Rowell, D. P., Folland, C. K., 1999. Oceanic forcing of the wintertime North Atlantic Oscillation and European climate. *Nature,* 398: 320-323.

Rogers, J. C., 1984. The association between the North Atlantic Oscillation and the Southern Oscillation in the Northern Hemisphere. *Monthly Weather Review,* 112: 1999–2015.

Rogers, J. C., 1990. Patterns of low-frequency monthly sea level pressure variability (1899–1986) and associated wave cyclone frequencies. *Journal of Climate,* 3: 1364–79.

Röhl, U., Abrams, L. J., 2000. High-resolution, downhole, and nondestructive core measurements from Sites 999 and 1001 in the Caribbean Sea: application to the late Paleocene Thermal Maximum. *In:* Leckie, R.M., Sigurdsson, H., Acton, G.D., Draper, G. (eds.), *Proceedings of the Ocean Drilling Program, Scientific Results,* 165: 191–203.

Ruddiman, W.F., Cameron, D., Clement, B.M., 1987. Sediment disturbance and

correlation of offset holes drilled with the hydraulic piston corer: Leg 94. *In*: Ruddiman, W.F., *et al.*, *Deep Sea Drilling Project Initial Reports,* 94 (Pt. 2): 615-634.

Saravanan, R., Chang, P., 2000. Interaction between tropical Atlantic variability and El Niño-Southern Oscillation. *Journal of Climate,* 13: 2177-2194.

Schimmelmann, A., Lange, C. B., Berger, W.H., 1990. Climatically controlled marker layers in Santa Barbara Basin sediments and fine-scale core-to-core correlation. *Limnology and Oceanography,* 35: 165-173.

Schlegel, I., Koschel, R., Krienitz, L., 1998. On the occurrence of *Phacotus lenticularis* (Chlorophyta) in lakes of different trophic state. *Hydrobiologia,* 370: 353-361.

Schneider, U., Schonwiese, C-D., 1989. Some statistical characteristics of the El Niño/Southern Oscillation and North Atlantic Oscillation indices. *Atmosfera,* 2, 167–80.

Schnurrenberger, D., Russell, J., Kelts, K., 2003. Classification of lacustrine sediments based on sedimentary components. *Journal of Paleolimnology,* 29: 141–154.

Shapiro J., Pfannkuch, H. O., 1973. The Minneapolis chain of lakes, a study of urban drainage and its effects 1971-1973. Limnological Research Centre, University of Minnesota, Minneapolis, *Interim Report No. 9,* 119 pp.

Shindell, D. T., Miller, R. L., Schmidt, G. A., and Pandolfo, L., 1999. Simulation of recent northern winter climate trends by greenhouse-gas forcing. *Nature.* 399: 452-455.

Shindell, D. T., Schmidt, G. A., Mann, M. E., Rind, D., Waple, A., 2001. Solar forcing of regional climate change during the Maunder Minimum. *Science,* 294: 2149-2152.

Silliman, J. E., Meyers, P. A., Bourbonniere, R. A., 1996. Record of postglacial organic matter delivery and burial in sediments of Lake Ontario. *Organic Geochemistry,* 24: 463-472.

Simola H., 1977. Diatom succession in the formation of annually laminated sediment in Lovojäri, a small eutrophic lake. *Annales Botanici Fennici,* 14: 143-148.

Simola H., 1979. Micro-stratigraphy of sediment laminations deposited in a chemically stratifying eutrophic lake during the years 1913-1976. *Holarctic Ecology,* 2: 160-168.

Simola H., 1984. Population dynamics of plankton diatoms in a 69-year sequence of annually laminated sediment. *Oikos,* 43: 30-40.

Smol, J. P., 1988. Chrysophycean microfossils in paleolimnological studies. *Palaeogeography, Palaeoclimatology, Palaeoecology,* 62: 287–297.

Sommer, U., 1986. Phytoplankton competition along a gradient of dilution rates. *Oecologia,* 68: 503-506.

Sparks, B. W., 1971. *Rocks and Relief.* Longman, London.

Sprowl, D. R., 1993. On the precision of the Elk Lake varve chronology. *In:* Bradbury, J. P., Dean, W. E. (eds), *Elk Lake, Minnesota: Evidence for rapid climate change in the North-Central United States.* Geological Society of America Special Paper 276: 69-74.

Stabel, H. H., 1986. Calcite precipitation in Lake Constance: chemical equilibrium, sedimentation, and nucleation by algae. *Limnology and Oceanography,* 31:1081-1093.

Starmach, K., 1985. *Chrysophyceae und Haptophyceae.* Gustav Fischer Verlag, Stuttgart-New York.

Staubwasser, M., Sirocko, F., Grootes, P. M., Segl, M., 2003. Climate change at the 4.2 ka BP termination of the Indus valley civilization and Holocene: south Asian monsoon variability. *Geophysical Research Letters,* 30 (8): 14-25.

Stein, R., Dittmers, K., Fahl, K., Kraus, M., Matthiessen. J., Niessen. F., Pirrung. M., Polyakova, Y., Schoster, F., Steinke, T., Fütterer, D. K., 2004. Arctic (palaeo) river discharge and environmental change: evidence from the Holocene Kara Sea sedimentary record. *Quaternary Science Reviews*. 23: 1485-1511.

Stockton, C. W., Glueck, M. F., 1999. Long-term variability of the North Atlantic Oscillation (NAO). *In:* Preprint of the *American Meteorological Society*. 10th Symposium on Global Change Studies, Dallas, Texas: 290-293.

Stoermer, E. F., 1978. Phytoplankton as indicators of water quality in the Laurentian Great Lakes. *Transactions of the American Microscopic Society,* 97: 2-16.

Stoermer, E.F., Yang, J.J., 1970. Distribution and relative abundance of dominant plankton diatoms in Lake Michigan, *Great Lakes Research*, Division 16, Michigan, USA: 64pp.

Stoermer, E. F., Ladewski, T. B., 1976. Apparent optimal temperatures for the occurrence of some common phytoplankton species in southern Lake Michigan. *Great Lakes Research,* Division 16, Publication No. 18.

Stoermer E. F., Wolin J. A., Schelske C. L., 1993. Paleolimnological comparison of the Laurentian Great Lakes based on diatoms. *Limnology and Oceanography,* 38: 1311-1316.

Stoermer E. F., Emmert G., Julius M. L., Schelske C. L., 1996. Paleolimnological evidence of rapid recent change in Lake Erie's trophic status. *Canadian Journal of Aquatic Science,* 53: 1451-1458.

Straile, D., 2000. Meteorological forcing of plankton dynamics in a large and deep continental European lake. Oecologia 122: 44–50

Straile, D., and Adrian, R., 2000. The North Atlantic Oscillation and plankton dynamics in two European lakes – two variations on a general theme. *Global Change Biology*. 6: 663-670.

Straile, D., Jöhnk, K., Rossknecht, H., *2003*. Complex effects of winter warming on the physicochemical characteristics of a deep lake. *Limnology & Oceanography*. 48(4): 1432–1438.

Stuvier, M., Reimer, P. J., Braziunas, T. F., 1998. High precision radiocarbon age calibration for terrestrial and marine samples. *Radiocarbon*, 40: 1127-1151.

Sutton, R. T., and Allen, M. R., 1997. Decadal predictability of North Atlantic sea surface temperature and climate. Nature, 388: 563-567.

Sutton, R. T., Norton, W. A., Jewson, S. P., 2001. The North Atlantic Oscillation – what role for the Ocean? *Atmospheric Science Letters,* 1: 89-100.

Sutton, R. T., Hodson, D. L. R., 2003. Influence of the ocean on North Atlantic climate variability 1971-1999. *Journal of Climate,* 16 (20): 3296–3313.

Svensmark, H., 1998. Influence of cosmic rays on Earth's climate. *Physics Review Letters*, 81: 5027-5030.

Svensmark, H., Friis-Christensen, E., 1997. Variation of cosmic ray flux and cloud coverage: A missing link in solar-terrestrial relationships. *Journal of Atmospheric and Solar Terrestrial Physics,* 59: 1225-1232.

Tallantire, P. A., 1953. Studies in the post-glacial history of British vegetation: XIII. Lopham Little Fen, a late-glacial site in central East Anglia. *Journal of Ecology,* 41: 361-373.

Tallantire, P. A., 1954. Old Buckenham Mere data for the study of Post-Glacial history. XIII. *New Phytologist,* 53: 131-139.

Thejll, P., Christiansen, B., Gleisner, H., 2003. On correlations between the North Atlantic Oscillation, geopotential heights, and geomagnetic activity. *Geophysical Research Letters,* 30: 10.1029/2002GL016598.

Thomas, T. M., 1954. Swallow holes in the Millstone Grit and Carboniferous Limestone of the South Wales coalfield. *The Geographical Journal,* 120. No. 4: 468-475.

Tilman D., 1981. Tests of resource competition theory using four species of Lake Michigan algae. *Ecology,* 62: 802-815.

Ting, M., Lau, N-C., 1993. A diagnostic and modelling study of the monthly mean wintertime anomalies appearing in a 100-year GCM experiment. *Journal of Atmospheric Science,* 50: 2845-2867.

Turner, J., 1962. The *Tilia* decline: an anthropogenic interpretation. *New Phytologist,* 61: 321-341.

Ulbrich, U., Christof, M., 1999. A shift of the NAO and increasing storm track activity over Europe due to anthropogenic greenhouse gas forcing. *Climate Dynamics,* 15(7): 551-559.

van Dam, H., Mertens, A., Sinkeldam, J., 1994. A coded checklist and ecological indicator values of freshwater diatoms from the Netherlands. *Netherlands Journal of Aquatic Ecology,* 28 (1): 117-133.

Van Loon, H., Labitzke, K., 2000. The influence of the 11-year solar cycle on the stratosphere below 30-km: A review. *Space Science Review,* 94: 259-278.

Venzke, S., Allen, M. R., Sutton R. T., Rowell, D. P., 1999. The atmospheric response over the North Atlantic to decadal changes in sea surface temperatures. *Journal of Climate,* 12: 2562-2584.

Verschuren, D., Laird, K. R. and Cumming, B. F., 2000. Rainfall and drought in equatorial east Africa during the past 1,100 years. Nature. 403: 410-414.

Vincens, A., 1993. Nouvelle séquence pollinique du Lac Tanganyika: 30,000 ans d'histoire botanique et climatique du Bassin Nord. *Review of Palaeobotany and Palynology,* 78, 381–394.

Vinson, D. K., Rushforth, S. R., 1989. Diatom species composition along a thermal gradient in the Portneuf River, Idaho, USA. *Hydrobiologia,* 185: 41-54.

Visbeck, M., Chassignet, E. P., Curry, R. G., Delworth, T. L., Dickson, R. R., Krahmann, G., 2002. The ocean's response to North Atlantic Oscillation variability. *In:* Hurrell, J. W., Kushnir, Y., Ottersen, G., Visbeck, M. (eds.), *The North Atlantic Oscillation: climatic significance and environmental impact.* AGU Geophysical Monograph Series, 134: 147-172.

Vos, H., Sanchez, A., Zolitschka, B., Brauer, A., Negendank, J. F. W., 1997. Solar activity variations recorded in varved sediments from the crater lake of Holzmaar – a maar lake in the West Eifel Volcanic Field, Germany. *Surveys in Geophysics,* 18: 163-182.

Wallace, J., Gutzler, D., 1981. Teleconnections in the geopotential height field during the Northern Hemisphere winter. *Monthly Weather Review,* 109: 784-812.

Wanner, H., Brönnimann, S., Casty, C., Gyalistras, D., Luterbacher, J., Schmutz, C., Stephenson, D. B., Xoplaki, E., 2001. North Atlantic Oscillation – concepts and studies. *Survey of Geophysicis,* 22: 321-381.

Wehrli, B., Lotter, A .F., Schaller, T., Sturm, M., 1997. High-resolution varve studies in Baldeggersee (Switzerland): Project overview and limnological background data. *Aquatic Sciences,* 59: 285-294.

West, R. G., 1991. The origin of Grunty Fen and other landforms in southern Fenland, Cambridgeshire. *Geological Magazine,* 128 (3): 257-262.

Weyhenmeyer, G. A., Blenckner, T., Pettersson, K., 1999. Changes of the plankton spring outburst related to the North Atlantic Oscillation. Limnology and Oceanography. 44 (7): 1788-1792.

Whitlock, C., and Bartlein, P. J., 1993. Vegetation history of Elk Lake. in Bradbury J.P. and W. E. Dean (eds.). Elk Lake, Minnesota: Evidence for Rapid Climate Change in the North-Central United States: Boulder, Colorado, Geological Society of America Special Paper 276: 251-274.

Wiseman, B., Frere, J., Hatchett, C., 1798. Account of a substance found in a clay-pit; and of the effect of the mere of Diss, upon various substances immersed in it. *Philosophical Transactions of the Royal Society of London,* 88: 567-581.

Woodland, A. W., 1946. Water supply from underground sources of Cambridge-Ipswich District. Geological Survey. GB. 10, *Wartime pamphlet,* 20:1-86.

Woodland, A. W., 1970. The buried tunnel-valleys of East Anglia. *Proceedings of the Yorkshire Geological Society,* 37: 521-578.

Wunsam S., Schmidt R., 1995. A diatom-phosphorus transfer function for Alpine and pre-Alpine lakes. *Memorie dell'Istituto Italiano di Idrobiologia,* 53: 85-99.

Wunsam S., Schmidt R., Klee R., 1995. *Cyclotella*-taxa (Bacillariophyceae) in lakes of the Alpine region and their relationship to environmental variables. *Aquatic Sciences,* 57 (4): 360-383.

Wurth, G., Niggemann, S., Richter, D. K., Mangini, A., 2004. The Younger Dryas and Holocene climate record of a stalagmite from Hölloch Cave (Bavarian Alps, Germany). *Journal of Quaternary Science,* 19(3): 291-298.

Xie, S-P., Tanimoto, Y., 1998. A pan-Atlantic decadal climate oscillation. *Geophysical Research Letters,* 25: 2185-2188.

Yates, K. K., Robbins, L. L., 1998. Production of carbonate sediments by a unicellular green alga. *American Mineralogist,* 83(11-12): 1503-1509.

Yu, Z., Ito, E., 2002. The 400-Year Wet-Dry Climate Cycle in Interior North America and Its Solar Connection. PACLIM Conference Proceedings.

Zolitschka, B., 1992. Climatic change evidence and lacustrine varves from maar lakes, Germany. *Climate Dynamics,* 6: 229-232.

Zolitschka, B., 1996. High-resolution lacustrine sediments and their potential for palaeoclimatic reconstruction. *In:* Jones, P. D., Bradbury, R. S., Jouzel, J. (eds), *Climatic variations and forcing mechanisms of the last 2000 years.* NATO ASI Series, 141.

Zolitschka, B., 1998. A 14,000-year sediment yield record from western Germany based on annually laminated lake sediments. *Geomorphology,* 22:1-17.

Zolitschka, B., Negendank, J. F. W., 1996. Sedimentology, dating and palaeoclimatic interpretation of a 76.3 ka record from Lago Grande Di Monticchio, Southern Italy. *Quaternary Science Reviews,* 15: 101-112.

Zolitschka, B., Negendank, J. F. W., 1999. High-resolution records from European Lakes. *Quarternary Science Reviews,* 18: 885-888.

Zolitschka, B., Brauer, A., Negendank, J. F. W., Stockhausen, H., Lang, A., 2000. Annually dated late Weichselian continental palaeoclimate record from the Eifel, Germany. *Geology,* 28 (9): 783-786.